The marine flatworm *Macrostomum lignano* as a model to study immunity, the microbiome and the effects of environmental pollutants

Dissertation

zur Erlangung des Doktorgrades

der Mathematisch-Naturwissenschaftlichen Fakultät

der Christian-Albrechts-Universität zu Kiel

vorgelegt von

Yuanyuan Ma

aus China

Kiel, December 2019

Prüfer:

Prof. Dr. Thomas Roeder

Prof. Dr. Holger Heine

Termin der Disputation: 18.03.2020

Declaration

I, Yuanyuan Ma, here declare that my doctoral thesis entitled "The marine flatworm *Macrostomum lignano* as a model to study immunity, the microbiome and the effects of environmental pollutants" and the work presented in it are my own work apart from supervisor's guidance and design of the paper. This dissertation has not been submitted for the award of doctoral degree to another examining body and was prepared according to the Rules of Good Scientific Practice of the German Research Foundation.

Erklärung

Hiermit erkläre ich, Yuanyuan Ma, dass diese Dissertation mit dem Titel: " The marine flatworm *Macrostomum lignano* as a model to study immunity, the microbiome and the effects of environmental pollutants", sowie die darin beschriebenen Arbeiten, abgesehen von der Beratung durch meinen akademischen Lehrer, nach Inhalt und Form meine eigene Arbeit ist. Diese.Arbeit wurde weder im Ganzen noch zum Teil an anderer Stelle im Rahmen eines Promotionsvorhabens eingereicht. Sie wurde nach den Regeln guter wissenschaftlicher Praxis der Deutschen Forschungsgemeinschaft angefertigt.

Kiel, December 2019

Yuanyuan Ma

Publications

Ausdieser Arbeit sind folgende Publikationen entstanden:

Ma, Y., Rivera-Ingraham, G., Nommick, A., Bickmeyer, U., and Roeder, T. (2019). Copper and Cadmium administration induce toxicity and oxidative stress in the marine flatworm *Macrostomum lignano*. *Aquatic Toxicology*, 221(2020):105428.

Congresses

2-5 July 2019 Costa Del Science, Seville, Spain.

17-18 November 2019 11th International Meeting of *Macrostomum lignano*. Lund, Sweden.

List of abbreviations

aa	amino acids
AIF	apoptosis-inducing factor 1
AMP	antimicrobial peptide
AP-1	activator protein 1
ASW	artificial seawater
casp3	caspase 3
CBP	CREB-binding protein
Cd^{2+}	cdmium ion
cox5b	cytochrome c oxidase subunit 5B
CTAK1	cdc25C-associated kinase 1
CTL	C-type lectin
Cu^{2+}	copper ion
d	day
DAF pathway	dauer larva formation abnormal (daf), an insulin-like receptor pathway
DAMPs	damage-associated molecular patterns
DNA	deoxyribonucleotideic acid
dNTPs	deoxyribonucleotide
EtOH	ethanol
FBNs	fibrinogen-like domain immune lectins
g	gram
GALES	galectins
GFP	green flourescence protein
GNBPs	gram-negative binding proteins
gstp1	glutathione S-transferase pi 1
GTP	guanosine-5'-triphosphate
h	hour

HIF	hypoxia-inducible factor
IL-1	interleukin-1
IMW	immature worms
IRAK	receptor-associated serine/threonine kinase
IRF	interferon regulatory factor
JNK	c-Jun N-terminal kinases
kb	kilobase pairs
L	Liter
LPV	*Vibrio* (*Listonella*) *anguillarum*, *Planococcus citreus* and *Vibrio alginolyticus*
mdr1	multiple drug resistance-associated protein1
mdr5	multiple drug resistance-associated protein5
mdr7	multidrug resistance-associated protein 7 isoform X4,X5
mg	milligram
Mg^{2+}	magnesium ion
mg2a	GM2 ganglioside activator
mgst1	microsomal glutathione S-transferase1
min	minute
ml	milliliter
mM	millimolar
mRNA	messenger RNA
MyD88	myeloid differentiation factor 88
NCBI	national center for biotechnology information
NF-κB	nuclear factor kappa B
ng	nanogram
NLRs	nucleotide-binding and oligomerization domain (NOD)-like receptors
P38 MAPK	P38 mitogen-activated protein kinase
PAMPs	pathogen-associated molecular patterns
PBS	phosphate buffered saline

pg	picogram
PGRPs	peptidoglycan recognition proteins
PPRs	patern recognition receptors
prdx1	peroxiredoxin 1
prdx6	peroxiredoxin 6
qRT-PCR	quantitative real-time polymerase chain reaction
RCM	recolonized medium
RLRs	retinoic acid-inducble gene I-like receptors
RNA	ribonucleic acid
RNI	reactive nitrogen intermediates
ROS	reactive oxygen species
rpl12	ribosomal protein L12
Rpl32	60S ribosomal protein L32
rpm	rounds per minute
RT	room temperature
RT-PCR	reverse transcription PCR
SCRs	scavenger receptors
Sec	second
SMW	starved mature worms
sod2	superoxide dismutase 2, mitochondrial
SYK	C-type Lectin
TAK1	transforming-growth-factor-β-activated kinase1
TEPs	thioester-containing proteins
TGFβ	a transforming growth factor-β-like
TLRs	toll-like receptors
TRAF	tumor necrosis factor receptor-associated factor
Mg	microgram
Ml	microliter
µM	micromolar

Contents

List of tables

List of figures

Zusammenfassung

In der vorliegenden Arbeit, wurde der marine Plattwurm *Macrostomum lignano* als Modellorganismus verwendet, um insbesondere die Stressantwort auf unterschiedliche toxische Substanzen zu untersuchen und die Aktivierung des Immunsystems genauer zu betrachten. Bei all diesen unterschiedlichen Fragestellungen spielt das Mikrobiom des marinen Plattwurms eine große Rolle. Umweltschadstoffe können sich im Wasser akkumulieren und so für die dort lebenden Organismen toxische Konzentrationen erreichen und diese damit langanhaltend schädigen. In *M. lignano* konnte ich zeigen, dass die Verwendung toxischer Substanzen die Lebensspanne der Tiere reduziert, die Mobilität stark einschränkt und zu einer intensiv gesteigerten Konzentration an Reaktiven Sauerstoffspezies, sowohl in den Mitochondrien als auch in der zellularen Matrix, der Tiere führt. Im Vergleich zu den Kontrolltieren, nimmt die Apoptoserate in den behandelten Tieren mit zunehmender Konzentration der Substanzen zu. Des weiteren sind die Tiere unterschiedlich sensitiv in Bezug auf die verschiedenen toxischen Substanzen. In der vorliegenden Arbeit wurde gezeigt, dass die Würmer eine höhere Suszeptibilität gegenüber Kupfer-Ionen (Cu) haben als gegenüber Cadmium-Ionen (Cd), denn selbst geringe Kupferkonzentrationen von 10 µM haben einen tödlichen Effekt. Die Analyse der Sequenzierungsdaten zeigte, dass eine Reihe von Antioxidantien nach einer Konfrontation mit Metallionen herunterreguliert waren, darunter waren z. B. *prdx6*, *prdx1*, *sod2* und *mgst1*. Eine Ausnahme zeigte das Antiredox-Enzym *Gstp1,* welches in seiner Expression signifikant verstärkt exprimiert wurde. Ergänzend wurden die ABC Transporter genauer untersucht, insbesondere *mdr1*, *mdr5* und *mdr7*, welche eine gesteigerte Expression unter den induzierten Stressbedingungen zeigten.

Toxisch aktive Substanzen haben nicht nur einen direkten Einfluss auf die Aktivität der Würmer, sondern beeinflussen nachweisbar das Mikrobiom der Tiere. Das

Mikrobiom von *M. lignano* unter Laborbedingungen lässt sich deutlich von dem des Mediums abgrenzen. Daraus lässt sich schließen, dass spezifische Mechanismen vorhanden sein müssen, die das Mikrobiom der Tiere verändern. So zeigte sich in hungernden Tieren eine Verschiebung in der bakteriellen Zusammensetzung in denen *Stramenopiles* und *Cytophagales* die am häufigsten auftretenden Bakterienordnungen sind. Außerdem ändert sich die bakterielle Zusammensetzung des Mikrobioms in Abhängigkeit der zugeführten Metallionen. *Alteronomadaceae* waren signifikant in Cu-behandelten Tieren angereichert; *Oceanospirillales* und *Burkholderiales* waren in Cd-induzierten Tieren vermehrt vorhanden; *Rhodobacterales* waren gehäuft in Atr-, Del- and ABD-behandelten Würmern nachweisbar und *Kiloniellales* und *Flavobacteriales* wurden vermehrt in Bis-induzierten Tieren nachgewiesen.

Eine weitere Untersuchung galt der Aktivierung des Immunsystems durch Infektion mit pathogenen Bakterien. Diese Form des biotischen Stresses führte dazu, dass die Wundheilung der infizierten Würmer gestört war. Die Transkriptomanalyse der infizierten Würmer zeigte eine deutlich veränderte Regulation mehrerer tausend Gene, welche unterschiedlichen Gengruppierungen zugeordnet werden konnten. Anhand dieser Analyse war es möglich die Struktur des Immunsystems von *M. lignano* aufzuklären. So sind der NF-κB (Imd-) Signalweg, der JNK-Signalweg und die p38 MAPK an der Immunregulation dieser Organismen beteiligt. Gene wie *Actin, Rac1*, *Rho*, *Rsk*, *S6K*, *FGFR*, *GNBP3*, *k-Ras* und *Shp2* wurden stark reguliert und zeigen eine Beteiligung an intrazellulären Prozessen wie Migration, Differenzierung, Mustergebung, Zellproliferation und Morphogenese.

Die Ergebnisse dieser Arbeit geben generelle Einblicke in die Reaktion von *M. lignano* auf unterschiedlichste Stressoren und stellen somit eine Basis für weitere Untersuchungsmethoden dar, die *M. lignano* als Modellorganismus für marine Wirbellose auszeichnen.

Summary

In the current work, I used the marine planarian model organisms *Macrostomum lignano* to study various aspects of its stress response, ranging from the reaction to toxicants to elucidating its immune system. In all these aspects, the microbiome of this marine flatworm played an important role. Pollutants can accumulate in waters and generate toxicity when concentrations reach certain values on the organism. In *M. lignano*, I could demonstrate that they reduce the animals' lifespan, physical activities, and increase the reactive oxygen species formation in both the mitochondrial and the cellular matrix. Compared to the non-drug confronted animals, the numbers of cell deaths significantly increased at higher drug concentrations. Animals displayed differential sensitivity to various drugs. In the present study, worms were more susceptive to copper (Cu) than to cadmium (Cd), with only a trace amount (10 µM) can cause poisonous effects. Various antioxidant enzymes, including *prdx6*, *prdx1*, *sod2*, and *mgst1*, were down-regulated in response to metal ion confrontation. *Gstp1* was the only anti-redox enzyme coding gene that was significantly up-regulated regarding its expression. Moreover, we quantified transcript levels of ABC transporter genes, namely of *mdr1*, *mdr5*, and *mdr7*. They showed either no change or increased transcript levels under drug stress.

Toxicologically active compounds not only directly affect physiological functions of worms, but they also influence their corresponding microbiome. *M. lignano* has a native microbiome under normal lab conditions, which is distinct from the bacterial community associated with its substrates. This points to specific mechanisms that shape the microbiome of the host. In starved animals, a different microbiome could be observed with *Stramenopiles* and *Cytophagales* becoming the most abundant bacterial groups. Furthermore, drug-treated animals changed their microbial abundance distribution. *Alteronomadaceae* were significantly up-regulated in Cu-treated animals; *Oceanospirillales* and *Burkholderiales* were increased in Cd-induced animals; *Rhodobacterales* accumulated in Atr-, Del- and ABD-treated animals; *Kiloniellales* and *Flavobacteriales* were found at higher concentrations in Bis-treated animals.

Pathogenic bacteria on the other hand act as a biotic stress, which led to dysfunctioning of the animals' ability to repair wounds. This process of infection-induced the transcription of thousands of unigenes, which could be classified into different gene ontologies. The worms' innate immune system seems to be composed mainly of three immune-related pathways. The apparently most important pathways include NF-κB, IMD, JNK, and p38 MAPK. Genes like *Actin, Rac1*, *Rho*, *Rsk*, *S6K*, *FGFR*, *GNBP3*, *k-Ras*, and *Shp2*, were regulated and are involved in processes such as migration, differentiation, patterning, cell proliferation or morphogenesis. The results of this study provide basic insights into the reaction of *M. lignano* to different stressors and might help to develop this marine flatworm into a valuable model organism for invertebrate marine organisms.

1 Introduction

1.1 Marine water pollutant

Water pollution is a main part of the overall environmental pollution (Krishna, Manickam, Shah, & Davergave, 2017). It is one of the most serious global challenges, which influence most organisms all over the world. Major pollutants result from human activities, such as industrial effluents, pesticides, fertilizers etc. (Hu, 2016). Pollutants can be classified into organic and inorganic compounds. Organic pollutants are carbon chemical pollutants that are mostly resistant to environmental degradation through photolytic, biological and chemical processes (Ritter, Solomon, Forget, Stemeroff, & O'Leary, 1995). Herbicides and pesticides are common organic pollutants, which more than 500 structures in more than 54,000 formulations registered as commercial products (Ashton & Crafts, 1973; Faust & Aly, 1964). Usually, low amounts of pesticides are present in the water, while some frequently introduced compounds and accidental events can cause higher concentrations, such as observed in response to the discharge of wastewaters without any purification processes. Atrazine (2-chloro-4-ethylamino-6-isopropyl-amino-s-triazine), which was a widely employed herbicide since 1959 (Goldman, 1994), with between 70,000 and 90,000 tons/year applied, represents a typical pesticide (Steinberg, Lorenz, & Spieser, 1995). It is often reported that contaminations of atrazine in streams occur with concentrations as high as 1000 µg/l (Christopher, 1992; Davies, Cook, & Barton, 1994; DeNoyelles, Kettle, & Sinn, 1982). Deltamethrin ((S) α-cyano-3-phenoxybenzyl- (1R) -cis-3- (2.2-dibromovinyl) -2,2-dimethylcyclopropane carboxylate) is another example of an environmentally relevant pesticide. It was preferably used due to its potent insecticidal properties in pest-control programs (Yousef, Awad, & Mohamed, 2006) and also in malaria control projects in developing countries (Ansari & Razdan, 2001; Jana-Kara et al., 1995). In some water samples, the concentration of deltamethrin was as high as 320 ng/L (Maguire, Germain, Tkacz, & Forrest, 1989), which is enough to accelerate the metabolism of fishes, e.g. that of carp (*Cyprinus carpio* L.) (Viran, Erkoç, Polat, & Koçak, 2003). It is even been reported that local deltamethrin contamination has led to the death of about 30 tons of eels (*Anguilla anguilla*) within a short time (Nemcsók et al., 1999). Once toxic compounds are present in freshwater aquatic environments, they are ultimately poured into the oceans and cause poisonous stress within larger aquatic communities.

Inorganic pollutants include toxic metals and different types of nutrients and salts, which generally occur in the form of dissolved anions and cations (Goldscheider, 2010). In general, according to their biological function, metals (metal ions) are classified as nonessential and essential ones. For the nonessential metals, such as lead (Pb), cadmium (Cd), tin (Si), mercury (Hg), and aluminum (Al), no biological function is observed and there positive correlations between their toxicity and their concentration are apparent (Sfakianakis, Renieri, Kentouri, & Tsatsakis, 2015). On the other hand, essential metals, e.g. chromium (Cr), copper (Cu), iron (Fe), cobalt (Co), nickel (Ni), molybdenum (Mo), and zinc (Zn), are vital for multiple biological reactions, but at high concentrations they induce negative, toxic effects (Sfakianakis et al., 2015). Animals are usually sensitive to metals, where slightly higher accumulations than optimal levels may lead to toxicity (Kennedy, 2011). The most commonly detected metals in waters are Co, Hg, Cd, Cu, Mo, Zn, Si, Ni and Cr (X. Wu et al., 2016). Under normal conditions, both essential and nonessential metals are present in water samples in trace amounts, and the typical (uncontaminated) values of Cd and Cu range from 0.02-0.41 nM and 2.8-8.5 nM, respectively (Prego & Cobelo-Garcıa, 2004). Environmental levels sometimes overpass these levels. For example, Polak-Juszcak recorded much higher concentrations of Cd (2500 µM) and Cu (150 µM) in coastal sediments of the Baltic Sea (Polak-Juszczak, 2013). The Cu values were even more concentrated in the sediments of the Portuguese Atlantic coast (300 µM). From the data reported by the International Atomic Energy Agency, the maximum levels of Cd and Cu in 433 marine sediments were 6 µM and 375 µM, respectively (Wyse, Azemard, & De Mora, 2004), which are 300,000 folds and 130,000 folds more than those observed in pristine regions for Cd and Cu. Some events such as tanker sinks may cause extremely high concentrations of cadmium and copper released to the sea locally, with up to 25 kg of Cd, 170 kg of Cu being released into the ocean water during a short period time (Prego & Cobelo-Garcıa, 2004).

1.2 Toxic effects induced by pollutants

The pollutants present in waters, including pesticides, herbicides, metals and other chemicals, resulting in serious risks for numerous aquatic creatures. Different species exhibit different sensitivities to various compounds. In addition, toxicant effects are also concentration and time-dependent. The poisonous effect on animals often includes behavior disorders, which further influence the fitness and survival of organisms in the living ecosystems. Frequently confrontation with the toxicants may even give rise to significant mortality.

Contaminations often induce oxidative stress and result processes such as lipid peroxidation and induction of antioxidant enzymes, such as catalase (CAT), antioxidants superoxide dismutase (SOD), glutathione S-transferases (GST), and glutathione reductase (GR) etc. (Claudianos et al., 2006). It has been shown that CAT, SOD and GR were induced in atrazine-exposed fish (*Channa punctatus*) (Nwani et al., 2010). Another study reported that zebrafish (*Danio rerio*) embryos will eliminate the elevation of the detoxication enzymes activity within 24-48 h after atrazine exposure (Wiegand, Pflugmacher, Giese, Frank, & Steinberg, 2000). These toxic effects even can be observed in mammals, e.g. in rats (Piper et al., 1998). Multiple biochemical analyses about pesticide intoxications have shown that the polyphenol oxidase enzymatic ability was competitively inhibited, which reduced the ability to degrade these compounds, therewith enhancing the toxicity (Fattouch et al., 2010).

Compared with the complex constitution and structure of organic toxicants, the poisonous effects of inorganic contaminants are easier to understand. For many vital biological targets, their structure and function could be altered by metal ions (Santini et al., 2013; Wang et al., 2015). In addition, post-translational modifications of proteins, production or scavenging can also be influenced by the overload with metal ions. During normal metabolic processes, there are inevitably occurring by-products, notably redox-active species (RAS). RAS allows the reduction of hydrogen peroxide (H_2O_2) to the hydroxyl radical (·OH) or molecular oxygen to the superoxide anion (O2·-). The O2·- and H2O2 are not only the major forms of reactive oxygen species (ROS), but are also produced via different routes (Ju et al., 2016). Fan et al. reported that ROS triggered bursts that lead to mitochondria dysfunction (Fan et al., 2018). Nevertheless, the reactive activity of ROS indicates its potential dangerousness (D'Autréaux & Toledano, 2007). Earlier studies suggested that oxidative damage caused by ROS plays a critical role in metal poisoning. Excessive metal can result in peroxidative harm to membrane lipids through oxygen and lipid radicals to peroxy radicals (Powell, 2000), and can stimulate peroxidation of lysosomal membranes (Bremner, 1998; Sokol, Deverbaux, Mierau, Hambidge, & Shikes, 1990). Metal overload can decrease the activity of cytochrome c oxidase and damage liver mitochondrial respiration (Myers, Prendergast, Holman, Kuntz, & Larusso, 1993). Moreover, metal confronted rats induce oxidative injury (e.g., reduced levels of α-tocopherol and hepatic GSH) (Ohhira et al., 1995; Sansinanea, Cerone, Streitenberger, Garcia, & Auza, 1998; Sokol et al., 1990; S. Zhang, Noordin, Rahman, & Haron, 2000). Both organic and inorganic drugs often exhibit bioaccumulation or biomagnification, meaning that the impacts of contaminations become more persistent and more severe (Mishra et al., 2019).

1.3 The role of the microbiota in responses to stressors

Toxicants are not only directly altering the physiological performance of organisms but also interfere with their co-existing bacteria. Associated bacteria are important for animals because they play roles in the survival and fitness of their hosts (McFall-Ngai et al., 2013). Many animal traits, *e.g.* behavior, growth, fecundity, and lifespan etc., could be shaped by bacterial symbionts (Collins, Surette, & Bercik, 2012; Sommer & Bäckhed, 2013). Symbioses can be facultative or obligate. In obligate mutualistic interactions, there is a rigorous interdependency between host and bacteria (Douglas, 2010). By supplying essential metabolic compounds and food, the relevant microbiome could directly accelerate host growth (Storelli et al., 2018). On the contrary, the host provides shelter and necessary nutrients and also improves the bacterial metabolic capabilities (Wilson et al., 2010). The relationship in the facultative symbiosis is much more flexible. Both partners of facultative symbiosis can survive without each other (Storelli et al., 2018). For the species with complicated lifestyles, the flexibility and adaptability of facultative nutritional mutualism could improve their ecological success (Cho & Blaser, 2012; Ley, 2010). However, some extreme stress events can lead to dysbiosis or damage to the interactions and relationships (Holmes, Li, Athanasiou, Ashrafian, & Nicholson, 2011). These stressors include infections, antibiotics, environmental toxins, climate changes among others (Apprill, 2017). The impact of drug treatments on the nature of these symbioses of marine meiofaunal organisms is still obscure.

1.4 Biotic (pathogen) effects

Environmental conditions are complex, the stressors may not only be environmental toxicants but also be microorganisms, e.g. pathogen bacteria. On peculiar host, response is inflammation that usually occurs in response to infection and tissue damage. The capacity and mechanisms to eliminate inflammation during tissue repair have fascinated researchers for a long time (Elliott & Sánchez Alvarado, 2013; Galliot, 2012; Poss, 2010). Tissue damage can trigger a complex set of responses that also healing of wounds and fighting invading bacteria. By coordinating cellular and mechanical responses, it lowers the injury, the surface area of wounds, and coordinates the functional integration between pre-existing and new structures (King & Newmark, 2012; Levin, 2007). New structural regeneration (tissue repair) is closely related to the proliferation and differentiation of stem cells. At the same time, the animal's natural immune system, facing the inflammatory response, is another important regulator of wound repair (Eming, Hammerschmidt, Krieg, & Roers, 2009; Godwin & Brockes, 2006; Godwin, Pinto, & Rosenthal, 2013; Godwin & Rosenthal, 2014; Murawala, Tanaka, & Currie, 2012). As a protective factor, the immune system usually works as a defense system. Actually, organisms can drive both tissue repair and damage-induced immune responses. The proper synchronization between injury and immune response plays an important role in animals during the repair process, such as, the repair of injured and inflamed skin of mammal and the regeneration of infected structure of amphibian extremities (Bely & Nyberg, 2010; Bosch, 2013; Bosch et al., 2009; Nonaka & Kimura, 2006). Earlier studies showed that an intact planarian flatworm, including its complex brain, can be regenerated within 7-10 days (Aboobaker, 2011; Elliott & Sánchez Alvarado, 2013; Gentile, Cebrià, & Bartscherer, 2011). Little wound infection is observed in regenerated planarians, indicative of an effective immune system (Abnave et al., 2014; Peiris, Hoyer, & Oviedo, 2014).

Earlier studies showed that the amount of mucus covering the worm body was significantly increased after injury, and it was speculated that the mucus has antimicrobial properties (Pedersen, 1959, 1963). Moreover, some reticular cells with putative phagocytic activity were observed in planarians, which could take up bacteria (Morita, 1991; Morita & Best, 1974). In the genome of the freshwater planaria *Dugesia japonica*, many genes potentially related to innate immunity were found (L. Zhou et al., 2012) (Table 1 The comparison of innate immune system-related genes of *M. lignano*, *Homo sapiens,* and other invertebrates). Interestingly, Abnave reported that planarians have a stronger resistance to pathogenic infections than observed in *Drosophila melanogaster*, *Caenorhabditis elegans* or even in *Homo sapiens* (Abnave et al., 2014). Gutiérrez-Gutiérrez et al. demonstrated that planarians have homologs for human immune-related genes, whereas these homologs were not found either *in Drosophila melanogaster* or in *C. elegans* (Gutiérrez-Gutiérrez, Felix, & González-Estévez, 2017).

Table 1 The comparison of innate immune system-related genes of *M. lignano*, *Homo sapiens,* and other invertebrates

Phylum	Order/Species	Common name	Pattern recognition receptors (PRRs)	Main signaling cascades	Gene involved	Reference
Nematoda	*Caenorhabditis elegans*	Roundworms	TLRs with MyD88; NLRs	DBL; MAPK; Toll-like; P38 MAPK; TGFβ; DAF-2/DAF-16	ATF-7; PMK-1	Andrew and Nicholas, 1976; Bargmann and Mori, 1997; Hodgkin et al., 2000; Schulenbrug et al., 2004; Sun et al., 2019; Troemel, 1999; Wang et al.,2018.
Phatyhelminthes	*Dugesia japonica*	Flatworms	TNFR	RIG-I-Like Receptor Signaling Pathway	RIG-I; TRAF3; TRAF6; P38; 14-3-3 family; namely; Dj14-3-3 α; Dj14-3-3 ζ	Alvarado et al.,1999; Pang et al., 2016.
	Schmidtea mediterranea	Flatworms	SYK;CTAK1;TRAF6	MORN2;p38 MAPK	TAK1; SYK	Maciel et al., 2019.
	Macrostomum lignano	Flatworms	TRAF 2; TRAF 5; TRAF 6	NF-Kappa B Pathway; IMD; JNK and p38 MAPK	RIG; Lap2; AP-1/ Jra; NF-KB; JNK; GADD45	In Present study
	Cestoda	Tapeworms	Unreported	Unreported	Unreported	Unreported
	Trematoda	Flukes	Unreported	Unreported	Unreported	Unreported
Arthropoda	*Drosophila melanogaster*	Flies	PGRPs; TEPs; GNBPs; SCRs; CTL; GALES; TLR; FBNs	IMD/Relish; Toll/DifToll; IMD; JAK/STAT(19-21)	STAT; AP-1 NF-κB; Drosomycin; Diptericin; AttacinA; cAMPs	Dostert et al., 2005; Kim et al., 2007; Tanji et al., 2007
Arthropoda	*Fenneropenaeus chinensis*	Shrimp	TLRs	Toll-like; IMD	AMPs; Cru1, Cru 3, ALF 6, ALF 8, Lys2, proPO	Yang et al., 2008; Lan et al., 2013; Li et al., 2013
Molluscs	*Saccostrea glomerata*	Oyster	PPRs; TLR; PAMPs; DAMPs	Toll-like signalling;apoptosis pathways to a complex antioxidant defence mechanism.	TRAF ; TAK1 ;RIG-1;AIF; AP-1 (activator protein 1); NF-κB; IRF; HIF; CBP; RNI; AMP	Ertl et al., 2016.
Cnidaria	Hydra	Hydra	TLRs with MyD88;	JNK;NF-κB	IL-1; IRAK; IRAK; JNK; NF-κB; AMP	Bosch, 2013.

			NLRs			
Vertabrata	*Homo sapiens*	Human	TLRs; RLRs; NLRs; RIG like receptor	Toll;P38 MAPK;MyD88-dependent & independent pathway	NF-kB; CD14; MyD88; TIRAP; TRAF6; IRAKs;TAB1; TBK1; IRF3	Ausubel, 2005;; Adachi et al., 2007; Shang et al., 2019.

1.5 Advantages of *M. lignano* as a model organism

In this project, the typical planarian *M. lignano* was used to explore the components of the innate immune system, the wounding repair, and the response to toxicants. *M. lignano* not only has the distinctive features of strong regenerative capacities of any damaged tissue (Elliott & Sánchez Alvarado, 2013), but also benefits from their other features, such as small size, transparent body, ease of cultivation and short generation time (Lengerer et al., 2014; Mouton et al., 2009; Mouton, Wudarski, Grudniewska, & Berezikov, 2018; Pfister et al., 2007; Schärer, Sandner, & Michiels, 2005). As a flatworm that lives freely in the intertidal zone and estuary, *M. lignano* is often exposed to highly variable environments, such as salinity changes caused by sudden heavy rainfall, daily tidal scouring and temperature changes, among others. Coastal ecosystems are also frequently influenced by different effluents, pesticides, and fertilizers from human industrial and agriculture activities, which inevitably increases the risk of stress induction. Therefore, *M. lignano* is an ideal model for studying physiological adaptations to many different environmental stressors (Rivera-Ingraham, Bickmeyer, & Abele, 2013).

1.6 Aims of the study

In this study, a series of different aspects of the model planarian *M. lignano* was quantified in order to evaluate its suitability for general biological studies, but also for more applied studies including toxicological ones. First, the usefulness and the responses of *M. lignano* towards different toxicants should be evaluated and used to quantify the corresponding effects. Furthermore, the composition of the native microbiota and its response to different toxicologically active pollutants should be analyzed.

As a last aspect, the worm's natural immune response was studied by transcriptomic analyses to disentangle immune and wound healing responses. This attempt was made to understand the architecture of a very basal immune system.

2 Materials and Methods

2.1 Materials

2.1.1 *Macrostomum lignano*

M. lignano n. sp. belongs to the largest genus of Macrostomorpha, the sub-taxon of the Platyhelminthes, Rhabditophora. It is part of the clade Macrostomorpha, which contains over 100 marine, fresh-water, and brackish water species, some of them with worldwide distribution (Ladurner, Schärer, Salvenmoser, & Rieger, 2005). *M. lignano* has become a new model organism in developmental, evolutionary, tissue homeostasis, regeneration and stem cell studies (Mouton et al., 2018; Rieger, 2001; Wudarski, Ustyantsev, Glazenburg, & Berezikov, 2019). It is a hermaphrodite, of smaller size, with only about 25,000 cells constituting all major bilaterian organ systems (Ladurner et al., 2005). Due to the advantages of the flatworm, it represents an ideal model organism for toxicity assays and biomarker screenings.

2.1.2 Guillard's f/2 Medium

35g marine salt (Tropic marine – zoo und Angel Knudzen, Kiel) were dissolved in 950 ml H_2O. After autoclaving (20min / 121℃), cooling and filtration, artificial seawater (ASW) was stored at 4 ℃. Before using ASW, 1ml sterile $Na_2SiO_3{\cdot}9H_2O$ (30 g/l) and 20ml Guillard's 50× medium (Sigma G0154) were added to 1L medium.

2.1.3 Storage algae medium

0.9 g agar powder was stirring and dissolved into 100ml f/2 medium and autoclaved. Under a clean bench, 5ml of the medium was poured into 60 mm petri dishes. After solidification, the medium was smeared paraffin to avoid over consuming under luminous (Lumilux Bidux T8) conditions. The algae need to growth 3-5 weeks and it can be kept several months.

2.1.4 Large scale algae culture

15ml of Guillard's f/2 into the storage algae medium were added, followed by carefully scraping the algae from the surface of the solid medium. Using a 1ml pipette to separate algae, they were washed with 40ml ASW and let them stand for 2 hours to allow their precipitation. The upper liquid was discarded and the sediment washed with Guillard's f/2 again. Afterward, concentrated algae liquor was obtained. This was transferred to 800 ml f/2 medium and cultured with constant air-supply.

2.1.5 Bacterial strains

2 gram-negative and 1 gram-positive marine bacterial strains were used. These are *Vibrio alginolyticus*, *Vibrio* (*Listonella*) *anguillarum* and *Planococcus citreus*. And all of them were obtained from the German Collection of Microorganisms (DSM, Deutsche Sammlung von Mikroorganismen, Braunschweig, Germany).

2.1.6 Solutions

Phosphate Buffered Saline (PBS) 9.07g NaCl, 0.21g KH_2PO_4, 0.49g $Na_2HPO_4{\cdot}2H_2O$. pH was added to distilled water and the pH was adjusted to 7.4 and the solution was filled up to 1L. The solution was then autoclaved.

Phosphate Buffered Saline Tween-20 (PBST): 0.2% (v/v) or 2% (v/v) of Tween-20 was added to PBS solution for the preparation of 0.2% or 2% PBST.

Paraformaldehyde in PBS (4% PFA): 2 g paraformaldehyde powder were dissolved with 50 ml PBS solution under continuous stirring at 45 °C. The fixing solution was aliquoted and stored at -20 °C. Before using, the storage solution needed to be warmed until it became clear.

2.1.7 Antibodies

Rabbit monoclonal phospho-histone H3 antibody was from Sigma-Aldrich, Steinheim, Germany. Goat anti-Rabbit antibody was also from Sigma-Aldrich, Steinheim, Germany.

2.1.8 Oligonucleotides

Table 2 Primer pairs used for the present study

Gene Name	GenBank No.	Sequence (5'->3') Forward/Reverse	length	Tm(°C)	Reference
Actin/beta Actin/F Actin	BOX15_Mlig021739g1	TCCTCAGTCAAGGTGAGGGT/TCAGCGAGGCCAGAATTGAG	168	60	present study
AP-1/Jra	BOX15_Mlig030395g2	TCAGACGCCGACAACTTTCC/GTCGCCACCGAGGATATGAC	189	60	present study
Bcl-XL	BOX15_Mlig019434g3	ATCTGGTGGCAAAAGTGGCA/TCACTAGCAGCGAAGTCAGG	198	60	present study
casp3	RNA1310_1479.1	GCCAGAAGACTCCAGCCCC/CTGCGTCTCTCCCTGGCAG	208	62	A.Rivera-Ingraham et al., 2016
casp8	BOX15_Mlig011129g1	TGGTCCTGAGCAACGAGAAC/CTATGAAGCCGAGACGCTGT	193	60	present study
C-JUN/JunD	BOX15_Mlig030395g2	TCAGACGCCGACAACTTTCC/GTCGCCACCGAGGATATGAC	189	60	present study
cox5b	RNA1310_41945	CGCCTGCTAGACCGGTTCC/CTGACGGTACCAGCACGGG	112	60	A.Rivera-Ingraham et al., 2016
EGFR	BOX15_Mlig016186g5	CAATCAGCCAGTGAGTTGCG/TGTAGACGCGGTGATTCCAG	117	60	present study
ERK5	BOX15_Mlig013187g1	AGATTGTGGAGTTCGCCTGC/GTTCGTCTGCCCTGTTTGTTC	91	60	present study
FGFR	BOX15_Mlig000537g2	TCAGCACCTCTCCGACTTTG/TCGACCAGCGAATGCTTGAG	147	60	present study
GADD45	BOX15_Mlig017197g3	ATCCGCCAGACAAAACCAAC/TTGAGCGTGACTTGCTGAGA	97	60	present study
GNBP3	BOX15_Mlig024988g3	ATTCAGGATGTCCACGCCAG/CGAGTACGGCAACGACTTTC	118	60	present study
gstp1	RNA1310_29579.1	TTCGGTGCCAGGAAGAATCT/CCCATTTAAAGATGCGGCGA	89	60	A.Rivera-Ingraham et al., 2016
IRAK1/4	BOX15_Mlig000935g1	CAGCTCGAAGACGACCAAGA/GCATTTACCGTTCCAACCGAC	101	60	present study
K-Ras/p53	BOX15_Mlig010610g1	GCCGCATCGCATCTTTCTTC/ATAAGACGCCACCCGTGTTC	158	60	present study

lap2	BOX15_Mlig024044g1	CTCTCTGATGCGGCGTTTCT/CTAACGTCGGACAGCAAAGG	160	60	present study
mdr1	LFJF01003519.1	CCCTGCTGAGGAAGTCCAAG/AACTCCCTGCGAATGGTCTG	100	60	present study
mdr5	LFJF01002971.1	GGTAGATGTCGCTGTCTTGGT/ATGCGACTGAGATCGGAGAG	99	60	present study
mdr7	LFJF01001259.1	AGCCATCTCGTAGAACACGG/TCGGCTGAATACGGTGATGG	121	60	present study
mg2a	RNA1310_42438	CATCACCCTGCCCGAGATTC/TCTTCAATGCGACCCTCAAGC	132	62	A.Rivera-Ingraham et al., 2016
mgst1	RNA1310_49001.2	ATGTGCTGCCGTTTGTACTG/CCTACTGGCGGCAAAGATTC	98	60	A.Rivera-Ingraham et al., 2016
MKK4	BOX15_Mlig013576g6	GCTGTACCGGGTGGTGTATC/GTTTCCAGCGATGCCAAAGT	198	60	present study
p65/NF-kB	BOX15_Mlig024864g2	GAACGTCCCTGCCAATCAAC/GCGTTCCCCCAAGTTCCTTT	102	60	present study
prdx1	RNA1310_28865.2	CGCGGCCTGTTCATCATCAA/GCTTGTCGGTGAACTGGAAG	124	60	A.Rivera-Ingraham et al., 2016
prdx6	RNA1310_35269	ACCAGGCCTTGTGATCTTCA/TGTCAATCTGAAGCCGGAGT	229	60	A.Rivera-Ingraham et al., 2016
Rac1	BOX15_Mlig011074g1	GACGCCATAGTTCTGCTGGT/TTAAGTCCAGCGTCTGCTCC	187	60	present study
Rho	BOX15_Mlig027552g2	GACGTGGGTGTCAGTGTAGG/ATTGCATTGAGCCTGTGGGA	81	60	present study
RIG-1	BOX15_Mlig021912g1	GCACTACCTGCGACTGAAGA/CTCCTTGGCATCCTCTGGTC	139	60	present study
rpl12	RNA1310_36703	GACAAGGTTAACGACGGCTC/TATAGCAGCCGGTGTGTCAA	81	60	A.Rivera-Ingraham et al., 2016
RSK	BOX15_Mlig005353g2	AACTGCGGGTGCTGAGTG/ATACAGATGACCCGTGGCTG	135	60	present study
S6k	BOX15_Mlig026841g1	GCCGCAGAATGTGTTGGTG/TTAACGGCATTGTGTACCGC	134	60	present study
SHP2	BOX15_Mlig029219g1	GAGCTGGGACGAAGCAAGAA/ACTGTCTCAGTGGCTCCAAC	116	60	present study
sod2	RNA1310_30405	AAGAACGTTCGCCCAGACTA/AGCTTAACTCCGCCACTCTT	101	60	A.Rivera-Ingraham et al., 2016
SOS	BOX15_Mlig030586g1	CGGCAGTTGTTGAATCGTGG/CCAGCAGCAGTCGTCAGTAT	151	60	present study

TAK1	BOX15_Mlig002175g3	CCCACTTGATCTGACGGCT/GCACCGGAGATTCCAAGCAT	125	60	present study
TRAF2	BOX15_Mlig010026g1	ATTCCAATCACGAGACCGCC/GCTTTCCCGTAGACTTTGCC	160	60	present study
TRAF5	BOX15_Mlig028646g2	TGGACTCGAAGCTCAAGCAG/TTGAACTGCTCGAAGACGCT	160	60	present study
TRAF6	BOX15_Mlig033058g1	CTCTTCAACGCCCGACAGA/TAGCAGGTAGCTCGGCTCA	185	60	present study

2.1.9 Enzymes

Table 3 Enzymes used in the present study

Enzyme	Company
DNase (RNase free 1U/µl)	Invitrogen，Darmstadt，Germany
LA taq	Thermo Scientific, Germany
RNase inhibitor (40U/µl)	Invitrogen, Darmstadt, Germany
Superscript IV TM Reverse Transcriptase	Invitrogen, Darmstadt, Germany
2x qPCRBIOSyGreen Mix Hi-ROX	PCR Biosystems, London, UK
Taq DNA Polymerase (5 U/µl)	Invitrogen, Darmstadt, Germany
T4 DNA Ligase	Thermo Scientific, Germany

2.1.10 Chemicals

Table 3 Chemicals used in the present study

Chemical	Company
Agar-Agar	Carl Roth, Karlsruhe, Germany
Agarose	Biozym, Oldendorf, Germany
dNTPs	Promega, Mannheim, Germany
Ethanol	Carl Roth, Karlsruhe, Germany
GeneRuler TM 100bp DNA Marker	Fermentas, St.Leon-Roth, Germany
GeneRuler TM 1kb DNA Marker	Fermentas, St.Leon-Roth, Germany
HPLC water	Carl Roth, Karlsruhe, Germany
Magnesium chloride hexahydrate	Carl Roth, Karlsruhe, Germany
SYBR® Green	Invitrogen, Darmstadt, Germany
TritonX-100	Sigma-Aldrich, Steinheim, Germany
Tween-20	Carl Roth, Karlsruhe, Germany

2.1.11 Equipment

Table 4 The enzymes used in the present study

Equipment	Company
Agarose Gel electrophoresis unit	Biometra GmbH, Göttingen, Germany
Centrifuge 5415D	Eppendorf, Hamburg, Germany
Centrifuge 5417R	Eppendorf, Hamburg, Germany
EV 245 Electrophoresis power supply	Consort, Belgium
Leica TCS SP1 confocal Microsystems	Leica, Heidelberg, Germany
NanoDrop (ND-1000UV)	Peqlab, Erlangen, Germany
Olympus SZX12 microscope	Olympus GmbH, Hamburg, Germany
Imager.Z1, Zeiss	Zeiss, Oberkochen, Germany
Omni Bead Ruptor 24	Omni International Inc, Kennesaw, USA
PCR amplification	Bio-RadLaboratories GmbH, München
StepOnePlus™ System	Applied Biosystems, Life Technologies
Vortex-2 Genie	Scientific Industries, INC., Bohemia, N.Y., USA
Waterbath WNB 10	memert GmbH+Co.KG, Schwabach, Germany

2.2 Methods

2.2.1 Animal culturing and experimental treatments

Macrostomum lignano lived in ASW and was fed with the diatom (*Nitszchia curvilineata*) for 3 weeks. Both animals and diatoms were maintained at 20 °C with 12/12 hours (h) dark/light cycles. Adults and 1-2 days hatched worms were mostly used. In order to avoid developmental effects, all experimental mature animals employed in our study were young adults with not more than 1 month of age.

2.2.2 Lifespan measurement

Experiments employed 20 adult animals with 5 replicates giving in total of 100 worms. Worms were kept in 24-well plates without any food supply. To reduce any other effects, such as water evaporation, degradation of product from dead animals etc., animals were translocated to new metal confronted medium every 3 days.

2.2.3 Animal survival test

Experiments employed 20 adult animals and previously starved in the ASW for 48 h were used. $CuSO_4$ and $CdSO_4$ stock concentrations were 0.26 M and 3.67M, respectively. $CuSO_4$ was diluted as follows: 1:1500; 1:3000; 1:6000; 1:12000; 1:15000; 1:17000; 1:20000; 1:25000. $CdSO_4$ was gradient diluted as follows: 1:500; 1:1000; 1:2000; 1:3000; 1:4000; 1:5000; 1:8000; 1:11000. Animals were transferred to the above liquids and incubated until death. The survival rate was measured every 5 min at higher metal concentrations and every 20 min at lower concentrations.

2.2.4 Hatching rate measurement

Adult animals were firstly washed with clean medium and then transferred to new plates, where animals laid eggs without food supply. Twenty freshly laid eggs (< 1.5 h) were kept in the selected concentrations of heavy metals until the end of the experiment (7 days). The whole experiment were repeated 5 times.

2.2.5 Total RNA extracting

Adult worms from the original culture medium were transferred to sterile artificial seawater (ASW) for 48 h while minimizing any other disturbance. *M. lignano* was treated with different experimental concentrations of $CuSO_4$ and $CdSO_4$ for 24-48 h. Each group employed 150 animals and their total RNA was extracted using NucleoSpin®RNA kit (Macherey-Nagel, Düren, Germany) following the manufacturer's description. 1 µl of each sample was run in a 1% agarose gel for quality control, while the RNA concentration was measured Nano Drop.

2.2.6 Genomic DNA (gDNA) digestion

If gDNA contaminations were detected in samples during the process of RNA quality control, a gDNA digestion was performed. 1 µg of RNA was mixed with 1 µl 10× reaction buffer containing $MgCl_2$, 1 U of DNase I (RNase-free), 0.25 µl of RNase inhibitor and HPLC water was added up to a total volume of 10 µl. The mixture liquid was incubated for 30 min at 37 °C, and then it was incubated at 65 °C for another 10 min with 1 µl of 50 mM EDTA to prevent RNA hydrolysis.

2.2.7 First-Strand cDNA synthesis

0.5 µl dNTPs mix (10 mM), 0.5 µl Oligo-dT7 (10 pmol/µl), 250 to 500 ng of total RNA were added and HPLC water added up to 6.75 µl. The total liquid was incubated at 65 °C for 5 min and ice shocked for at least 1 min. The following components were added to the mixture: 2 µl 5 ×First strand buffer, 0.5 µl DTT (0.1 M), 0.25 µl RNase Inhibitor (10 U) and 0.5 µl Superscript III Reverse Transcriptase (100 U). Reaction liquid was gently mixed and kept at room temperature for 5 min, then incubated at 50 °C for 1 h. Finally, the reaction was terminated at 70 °C for 15 min to inactivate the transcriptase. The specimens were stored at -20 °C.

2.2.8 qRT-PCR

The StepOnePlus™ Real-Time PCR System was used for the primer efficiency tests and quantitative expression analysis of the target genes. For the primer efficiency check, the template cDNA was used in a series of 2-fold dilutions from 50 ng/µl to the 3.125 ng/µl. For determination of the gene transcriptome levels, all cDNAs were normalized to 20 ng/µl. Then 1 µl template cDNA, 5 µl 2x qPCRBIOSyGreen Mix, 3 µl HPLC H_2O, Hi-ROX, 0.5 µl anti-sense primer (5 µM) and 0.5 µl sense primer (5 µM) were mixed. The amplification program was set as below: 95 °C, 10 min, (95 °C, 15 seconds (sec); 60 °C, 20 sec;17 °C, 35 sec) 40 cycles, (95 °C, 5 min; 60 °C + 0.3 °C until 95 °C), 95 °C, 15 sec.

The primer efficiencies were calculated referring to published protocols (Pfaffl, 2001). *Rpl12* (ribosomal protein L12) considered as a reference gene for all of the assays

(Rivera-Ingraham, Nommick, Blondeau-Bidet, Ladurner, & Lignot, 2016). Five biological replicates were performed and all primers used in the present study were listed in (Table 2).

2.2.9 Animal activity

The animal activity procedure was performed as described by Rivera-Ingraham et al. (Rivera-Ingraham et al., 2016). Briefly, 5 animals that had been previously confronted with different metal conditions were stained with 0.33 µM Mitotracker Deep Red 633 (Ex: 633nm; Em: 660 nm) for at least 1 h. Animals were observed individually in a ≈ 200 µm deep slide with 3 µl medium, covered by a coverslip. This ensured that animals could only move in the X-Y plane while staying under focus and permanently in the field of vision of the microscope objective. Animals were scanned for 2 min with at least 1800 frames at a frequency of 67 msec using an Olympus SZX microscope coupled with a CellSens camera. Pictures were stacked using ImageJ (NIH, Rasband WS) and then imported into Imaris, with which behavioral parameters were analyzed using the “Imaris Track” module (Bitplane).

2.2.10 Fluorescence intensities

Metal induced animals were relaxed in artificial seawater containing 7.14% $MgCl_2$ for 5 min, followed by 15 min in pure 7.14% $MgCl_2$. Animals were fixed for 2 h at room temperature in 4% paraformaldehyde (PFA) in 0.1 M PBS. Then stained for 0.5-1 h with different fluorescence probes (Table 5) and imaged using a Zeiss Axio Imager Z1 microscope equipped with an apotome (Zeiss Oberkochem, Germany). Images were converted to 8 bits. In order to standardize all measurements, only the head region of each worm was considered for analysis (Fig. 1) (Rivera-Ingraham et al., 2013). In the present study, all experiments were performed using 10 animals per treatment with 3 replicates, resulting in 27-30 animals in total. To avoid inevitable interferences with and among various dyes, all dyes we stained separately and fixed with the same exposure time. The median and maximum value of the signal was analyzed using ImageJ software.

Table 5 The fluorescent dye used in the present study

Dye Catalog	Excitation/Emission wavelength λ(nm)	Final conc. Used (μM)	Staining time (min)	Speculation Number	N repetition (total N /treatment)	Intensity Calculation
Cell ROS green in DMSO	508/525	5	30	10	3 (27-30)	None
C-H2DFFDA in Ethanol	492/495	11	30	10	3 (27-30)	Maximum and mean intensity
Dihydroethidium (DHE) in DMSO	518/605	4	30	10	3 (27-30)	Maximum and mean intensity
Ethidium Homodimer iii in DMSO	530/620	5	30	10	3 (12-19)	Dead cell number
MitoTracker Deep Red 633 in DMSO	644/665	0.33	60	10	3 (27-30)	Maximum and mean intensity
MitoSOX in DMSO	510/580	5	30	10	3 (27-30)	Maximum and mean intensity

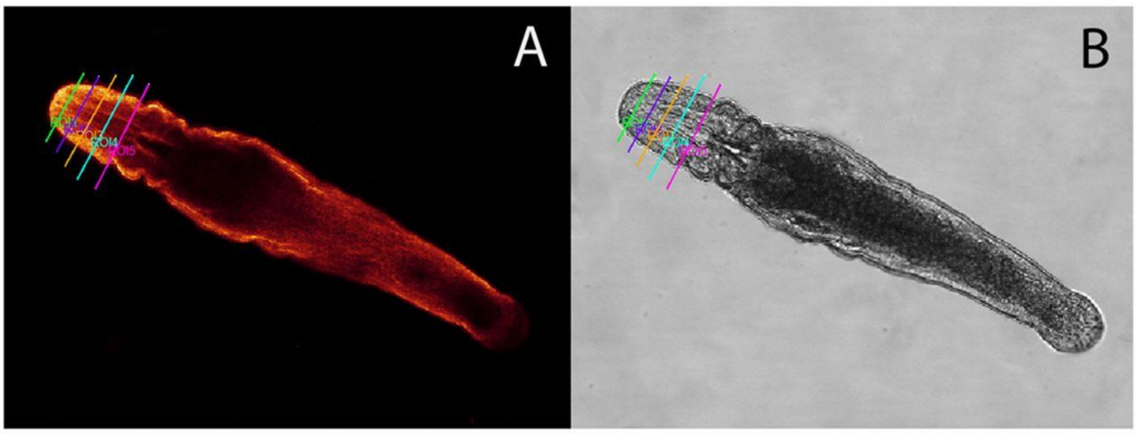

Fig. 1 The area of fluorescent intensity quantification analysis. Referring to the protocol of Rivera-Ingraham et al., a total of 5 transects in the anterior part of each animal were considered as the region of interest (ROI) (Rivera-Ingraham et al., 2013). It located in the region with the strongest fluorescence signal and vertical to the longitudinal axis of the animal. (A) An individual stained with MitoTracker Deep Red 633. (B) Transmission picture of the same animal.

2.2.11 Phospho-histone H3 labeling

Worms were collected from the experimental medium. After $MgCl_2$ anesthesia and PFA fixation, samples were washed multiple times with PBS-T (0.1%). Samples were transferred to 0.1 N HCl for 10 min on ice and followed by a 1h denaturation in 2 N HCl at 37 °C. Worms were treated with 0.22 µg/ml Protease XIV at 37 °C for 30 min and blocking was performed with BSA-T for 30 min. A 3 × 5 min wash in PBS-T was done to remove acids completely. Samples were incubated with primary antibodies (rabbit anti- phosphorylated histone H3, Roche) overnight at 4 °C, at a 1:150 dilution ratio in PBS-BSA-T. After washing with PBS-T (3 × 5 min), specimens were incubated with a secondary antibody (goat-anti-rabbit IGG - Cy3-conjugated (Jackson ImmunoResearch)), 1:150 dilution at RT in darkness for 1 h and washed again with PBS-T for 3 × 5 min. Specimens were mounted in Vectashield (Vector Laboratories) and observed with AxioVision SE64 fluorescent microscope.

2.2.12 Number of dead cells

In order to assess levels of cell death, worms were incubated with ethidium homodimer III (30 min, 5 µM). Every treatment group contained 7 animals with 3 replicates, in total 21 animals. To quantify the number of positive cells at different treatments, pictures were taken using an AxioVision 4.9.1. Resulting pictures were combined in Z-stacks, and the ethidium positive cells were counted in each layer.

2.2.13 Statistical analysis

In all experiments, Prism version 7.0 was mainly used for statistical analyses. Unpaired two-tailed Student's t-test was used in comparison between 2 groups. For multiple comparisons needed, one-way ANOVA followed by a Tukey post-hoc test proceeded. Two-way ANOVA was performed when 2 different categorical independent variables on 1 continuous dependent variable had to be analyzed. All histograms were represented as means ± S.D. The survival curves of lifespan were conducted with the log-rank (Mantel-Cox) test. Statistical analysis of significant difference was defined as n.s. (not significant), *$p < 0.05$, **$p < 0.01$, ***$p < 0.001$ and ****$p < 0.0001$.

2.2.13 Antibiotic Treatment for both algae and worms

The antibiotic treatment was performed according to the method for germ-free (GF) *Nematostella* (Domin et al., 2018). Antibiotics (Anti) were solved in sterile Guillard's f/2 medium, which included 50 µg/ml ampicillin, 50 µg/ml streptomycin, 50 µg/ml neomycin, 50 µg/ml rifampicin, and 50 µg/ml spectinomycin. The algae were treated with Guillard's f/2 for 1 month and the medium was replaced by fresh medium at 2-day intervals. The newly hatching juveniles were washed in the sterile Guillard's f/2 medium for 2 days. Then the animals were transferred into the sterile algae medium for 3-4 weeks until animals have grown up. The medium was renewed every 2 days. After 4 weeks of treatment, the germ-free (GF) animals were cultured in sterile Guillard's f/2 medium for 3 days to get rid of antibiotics effects. For the GF worm, no bacterial colonization was discovered after plating homogenized worms on Marine-agar plates (MA). Moreover, no cultivatable bacterium were detected by PCR. We used the specific 16s rRNA gene primers (forward primer 27F (AGAGTTTGATCMTGGCTCAG) / reverse primer 338R (TGCTGCCTCCCGTAGGAGT)) for PCR and only a very weak band was detected in the PCR product.

2.2.14 Recolonization

For recolonization treatment, the 3 weeks culturing medium were filtered with a 0.8 µm filter and re-suspended with Guillard's f/2medium to the final OD_{600} of 0.045. It was the normal value under the lab conditions. For the control group, a 0.2 µm filter was used and the final OD_{600} was 0. Worms were grown in the 24-well plates that each well was filled with 1 ml of filtered homogenates. The GF worms recolonized with bacterium were named as "recolonization" worms (RC).

2.2.15 Worm Lifespans

50 worms (10 per replicate) were used in animal lifespan tests. In the drug-free medium, the worms can survive for 50 days. To reduce contamination and other factors interference, e.g. evaporation, elements released from dead animals, we changed the medium every day.

2.2.16 Feces output measurements

Feces was quantified in 12-well plates in groups employing 3 animals and 5 replicates. All animals were cultured in sterile and non-sterile medium for 10 days and the medium was renewed every day.

2.2.17 Gut pH staining

The pH measurements were performed by the indicator dyes, m-cresol purple (657890, Sigma-Aldrich) and bromocresol purple (B5880, Sigma-Aldrich). Undertreatment of drugs and fed conditions, animals were stained by the 0.1 % final concentration for each dye under the in ratio 1:1 for 4 hours. Before taking photographs, they were anesthetized with 7.14% $MgCl_2$ for 15 min.

2.2.18 Bacterial qPCR

Real-Time PCR (qPCR) System was used to determine the bacterial load. The same worm DNA samples for Miseq sequencing were used as qPCR template. For normalization, the template DNA was diluted to 5 ng/µl. Then 5µl of 2x qPCR BIOSyGreen Mix Hi-ROX (London, UK), 0.5 µl of sense primer (5 µM), 0.5 µl of anti-sense primer (5 µM), 1 µl of template cDNA and 3 µl of HPLC H_2O were mixed for one reaction. The amplification was run as the following PCR program: 1 cycle (95 °C, 10 min), 40 cycles (95 °C, 15 sec; 60 °C, 20 sec; 17 °C, 35 sec). The reaction was performed using the StepOnePlus™. The primer set for 16S as follows: 8Fm (5′-AGAGTTTGATCMTGGCTCAG-3′); Bact515F (5′-TTACCGCGGCKGCTGGCAC-3′) (Pais et al., 2018). In this case, *rpl12* of *M. lignano* was served as a reference gene (Rivera-Ingraham et al., 2016).

2.2.19 *M. lignano* and substrate DNA extraction for Miseq genotyping

Animals were treated by 2 methods: (1) for the direct approach, worms were cultured on the algae lawns for 4 weeks, followed by fast washing 5 times with sterile Guillard's F/2 medium, and then their DNA was extracted; (2) the indirect approach; worms underwent 2-5 days starvation or 2-5 days drug treatment before DNA extraction. 5 mature or 10 immature animals from culture medium were carefully cleaned. These samples together with 20 days culturing algae and its living substrates prepared for comparing nature microbiome of "lab–enriched worms". All groups were analyzed in 5 replicates. Total DNA extractions were done with the DNeasy ®Blood &Tissue kits (Qiagen, Hilden, Germany). DNA was eluted in 50 µl elution buffer and frozen at -20 °C until sequencing. The specimens were sequenced on an Illumina MiSeq platform at the Kiel Institute for Clinical Molecular Biology. Substrate samples, from which worms were successfully isolated, were homogenized in liquid nitrogen and their DNA was then purified as described earlier.

We considered 6 different drugs for which no mortality rates had been observed in 24h preliminary experiments: $CdSO_4$ (Sigma 481882), $CuSO_4$ (Sigma PHR 1477), 220 µM atrazine (Atr) (Sigma 45330), 700 µM deltamethrin (Del) (Sigma 45423) and 2000 µM suberoyl bis-hydroxamic acid (Bis) (Sigma 390585), 60 µg/ml ampicillin (Sigma 59349). Animals were exposed to the environment for 2-5 days in all cases. To test the effects of drug dose on worm microbiome, 3 different concentrations of each metal were used: 10 µM, 12 µM, 15 µM for $CuSO_4$; 730 µM, 460 µM, 330 µM for $CdSO_4$.

We used the 16S rRNA gene primers 27F / 338R (AGAGTTTGATCMTGGCTCAG / TGCTGCCTCCCGTAGGAGT) to test the quality of DNA samples in a 20 µl duplex PCR reactions with Phusion High Fidelity DNA Polymerase (Thermo Fisher Scientific, Waltham, USA). The parameters of PCR programme as follows: an initial denaturation step at 98 °C for 3 min, followed by 35 cycles (98 °C for 10 s, 58 °C for 30 s and 72 °C for 1 min), and then a final elongation step at 72 °C for 5 min. After checking the PCR products by 2% agarose gel, the positively tested DNA samples having clear and right bands were used to sequence the bacterial V2 region through the MiSeq platform (Illumina).

Clean bench and other required equipment were sterilized using 70% ethanol or followed by 20 min UV irradiation prior to DNA isolation. With the exception of the centrifugation step, almost all steps of the DNA isolation protocol were accomplished under a clean bench to avoid any contamination with microorganisms in the laboratory environment. Similarly, PCRs were set-up under the aseptic conditions, including positive and negative controls. We used sterile deionized water instead of template DNA in the negative control and therefore no amplification products were produced.

2.2.20 Analysis of Bacterial Communities

The raw sequences were analyzed by the QIIME 2 package (Caporaso et al., 2010). Assembly of paired-end reads and identification of chimeric sequences were performed by SeqPrep and Chimera Slayer, respectively (Haas et al., 2011). For operational taxonomic unit (OUT) picking, we used the protocol of pick_open_reference_otus.py with a threshold of 97% identity per OTU. And annotation was executed with the UCLUST algorithm (RRID: SCR_011921; Edgar, 2010) against the GreenGenes database v13.8 (RRID: SCR_002830; DeSantis et al. implemented in QIIME (DeSantis et al., 2006).

To avoid false-positive OTUs from sequencing errors, OTUs with at least 50 reads were kept in the dataset (Faith et al., 2013). Normalized 10,000 reads were chosen during the analysis. For the calculation of Alpha-diversity, we used the Chao1 metric implemented in QIIME (10 replicates of rarefication per sample). To depict Beta-diversity in the analysis of a principal component analysis (PCA), Bray–Curtis and unweighted or weighted UniFrac metrics (100 jackknifed replicates) were used. The ADONIS method was used for the analysis of clustering.

2.2.21 Bacterial culture and experimental bacterial treatments

Vibrio alginolyticus, *Vibrio anguillarum*, and *Planococcus citreus* were all cultured overnight in pH 7.5 marine medium (1% w/v NaCl, 1% w/v tryptone, 0.4% w/v $MgCl_2 \cdot 6H_2O$, 0.1% w/v KCl). Our experiments were carried out with pretested concentrations of bacterial mixtures, which did not induce significant mortality rates for 24 hours. We finally chose an OD_{600} of 1 for each bacterium and mixed them together with a ratio of 1:1:1. For the treatment group, we added 7.5% (v/v) above bacterial mix to the f/2 medium. For the control groups, we added the same volume of the bacterial-free medium instead.

2.2.22 Generate wounding worms

I wanted to test the pathogenic effects on wounding animals. I, therefore, generated injured animals to mimic this pathogenic effect. In order to reduce the infection from the gut microbiome, 100 worms were kept in the sterile f/2 medium for 1-2 days to empty their guts and washed them with sterile f/2 medium for 3 times (2h each) and then consecutively treated them with bacterial mixes for 24 hours. All groups, including only cutting groups, non-cutting groups, and LPV cutting groups, were repeated four times for RNA sequencing and 5 times for qPCR. Animals were starved during the whole experiment.

2.2.23 Pathogenic induced survival analysis

Experiments used 20 mature animals and were repeated 5 times, in total 100 worms were employed. Worms were kept in 24-well plates without any food supply. To lower the influences from other factors', such as water evaporation, degradation of product from dead animals etc., the medium was renewed every 2 days. Worms colonized with the bacteria mix (*Vibrio alginolyticus*, *V. anguillarum* and *Planococcus* *citreus*) were kept under normal rearing conditions (20°C). Dead worms were counted within the 24h intervals.

2.2.24 Reproductive capability

Population size was measured with 10 mature worms starting populations after 16 days under standard laboratory conditions. Worms were kept in 24-well plates with fresh food supply and changed fresh medium every 2 days. Five replicates were analyzed for each group.

2.2.25 RNA sequencing preparation

Each group consisted of 150 animals and their total RNA was isolated using NucleoSpin®RNA (Macherey-Nagel, Düren, Germany) following the manufacturer's guidelines. The quality of the processed RNA samples was checked by running samples on an agarose gel and concentrations were measured by the Qubit RNA BR Assay kit (ThermoFisher).

2.2.26 Construction of cDNA libraries and Illumina HiSeq 4000 sequencing

RNA samples were sent for analysis to the Institute of Clinical Molecular Biology (IKMB, Kiel, Germany) for mRNA-seq library preparation and sequencing with the Illumina HiSeq 4000 (Illumina, Inc., San Diego, CA, USA) next-generation platform. mRNA-seq library were prepared by the Illumina's library construction manuscript. Raw-reads FASTQ files were produced and were differentiated by barcodes for further analysis (http://bioinfogp.cnb.csic.es/tools/venny/).

2.2.27 Assembly of transcriptomes and functional classification

Prior to performing transcriptome assemblies, paired-end raw reads were processed to remove the adaptor sequences (excluding nucleotides number of the adaptor less than 35) and low-quality sequences (Phred quality score <20). The microbes contaminated reads were also deleted by using Trimmomatic packages (Bolger, Lohse, & Usadel, 2014).The FastQC package was applied to test the quality of generated trimmed and filtered reads.

2.2.28 Annotation of Unigenes

The complete unigene transcripts were considered as queries (BLASTX; E-value < 10-5), matched with protein databases as PANM (http://malacol.or.kr/blast/) (Kang et al., 2015), Kyoto Encyclopedia of Genes and Genomes (KEGG), Unigene, Gene Ontology (GO), and Eukaryotic Cluster of Orthologous Groups (KOG) to obtain the amount of significant hits to published protein sequences in these databases. The count of unigene was visualized by using Venny 2.0.

2.2.29 Phalloidin and DAPI staining

Worms were collected from the culturing medium and were washed twice with f/2 medium. Then relaxed in 1:1 7.14% $MgCl_2$: artificial seawater for 5 minutes, followed by 15 minutes in pure 7.14% $MgCl_2$. Then fixed 1 hr at RT in 4% PFA in 0.1 M PBS. Samples were washed several times with PBS-T (0.1%). Protease treatment (0.22 µg/ml Protease XIV (30 min, 37°C) was followed by incubation for 10 minutes in 0.1 N HCl on ice and further denaturation in 2 N HCl (1 h, 37°C). A 3 × 5 minutes wash with PBS-T to remove acids completely and staining with 1:150 phalloidin for 30 minutes and 1:2000 DAPI at RT were done in darkness. Specimens were washed again with PBS-T for 3 × 10 minutes and mounted in Vectashield (Vector Laboratories). Animals were observed with AxioVision SE64 fluorescent microscope.

2.2.30 Phospho histone H3 staining

Worms were anesthetization in 1:1 7.14% $MgCl_2$: artificial seawater (ASW) for 5 minutes and 15 minutes in pure 7.14% $MgCl_2$. Then fixed with 4% PFA in 0.1 M PBS for 3 hours at room temperature (RT). Samples were washed with 1× PBS-Tween (PBS-T, 0.1%) for 5 minutes and 3 times repeated. Then they were blocked with 5%

blocking solution (NGS) (dissolved in 0.1% PBS-T) at RT for 1 hour. Samples were incubated with phosphor histone-H3-Serine 10-antibody (from rabbit) (1:100 in blocking solution) at 4°C overnight. Followed with multiple washes with PBS-T (3×5 minutes), samples incubated with goat-anti-rabbit (Alexa Fluor® 488) (1:150) antibodies at 4 °C in darkness and kept overnight. DAPI diluted 1:2000 was simultaneously stained with the secondary antibody. After multiple PBS-T (3 × 10 minutes PBS-T) washing, animals were embedded in a 50% glycerol solution. Pictures were taken by using the Zeiss microscope (Germany). Assembly and editing was performed with Imager.Z1, Zeiss Software (Zeiss, Oberkochen, Germany).

3 Results

3.1 Administration of organic and inorganic compounds induce toxicity and oxidative stress in the marine flatworm *M. lignano*

3.1.1 Toxicity induced by organic compounds

3.1.1.1 Organic compounds toxicity reduced worms' lifespan

Administration of the tested organic compounds significantly reduced lifespan. *M. lignano* was treated with four organic chemicals with pretested concentrations, which had no significant effect on mortality during a two h observation period. Animals exposed to bromophenol blue (Bro) and suberoyl bis-hydroxamic acid (Bis) merely survive two to three days, which is dramatically shorter than observed for untreated controls (Fig. 2, Bro_60 µM vs. Ctr, $p < 0.0001$; Bis_2000µM vs. Ctr, $p < 0.0001$). Toxicity of deltamethrin (Del) and curcumin (Cur) treatment were milder than compared to the two other compounds, but the lifespans were still significantly decreased to 7 days and 10 days, respectively (Fig. 2, Del_700 µM vs. Ctr, $p < 0.0001$; Cur_680µM vs. Ctr, $p < 0.0001$).

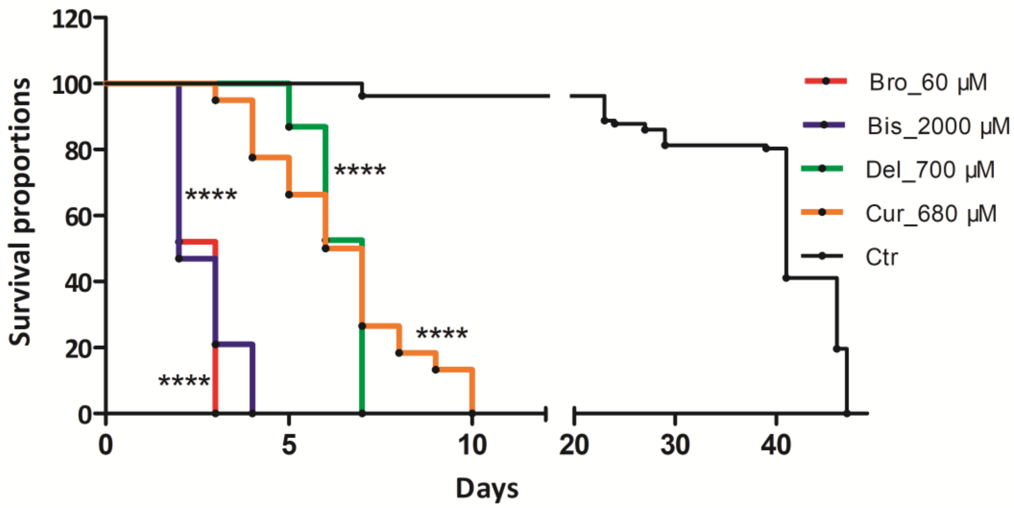

Fig. 2 Survival curves in response to organic compound exposure. Animals were treated with four organic chemicals with previously tested concentrations. The concentrations were 60 µM for Bro, 2000 µM for Bis, 700 µM for Del and 680 µM for Cur. The control groups were without any drug

treatment. Experiments employed 10 adult animals per treatment with 10 replicates and survival was recorded every 24 hours. The median survival rate of controls was 46 days. The median survival rate of treated animals was three drugs for Bro, two for Bis, seven for Del, and for Cur 10 days. Asterisks denote significant differences from non-drug control (Log-rank (Mantel-Cox) Test, ****, $p < 0.00001$). The color highlights the different types of drug stresses.

3.1.1.2 Worm remained their body shape under short-term organic toxicity

Relative body volume over time was analyzed for animals under different conditions of organic chemical exposure (Fig. 3). Animals maintained the osmotic condition of their internal fluids during the 24h observation period.

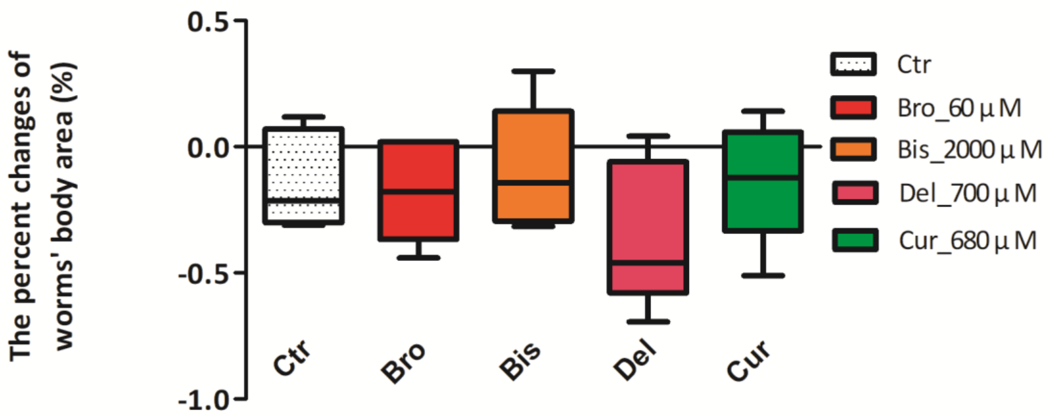

Fig. 3 Body area changes in response to organic compounds. Drug treatment did not significantly change the body area of the animals. All treatment groups were compared with the control group and statistics were performed by using one-way ANOVA with Turkey Post-hoc test, n.s. indicates no significant changes.

3.1.1.3 Organic compound toxicity lowers the worm's activity

Animals subjected to the toxicants, Bro, Bis, Del and Cur, showed significantly lower movement activities. All compound-induced groups significantly reduced their average speed as well as their maximum speed (Fig. 4 A and B). The average speed of the treated groups was in the range of 1100-1400 µm/s, which was at least 500 µm/s slower than in the control group (~ 1900 µm/s) (Fig. 4 A). The maximum speed of treated animals was 2500-3500 µm/s, which was also slower than in the control group (Fig. 4 B). Cur and Del treated animals remained at ~2100 µm/s and ~1600 µm/s, no significant speed changes within the observed duration. Bis-exposure animals dropped their maximum speed from 2600µm/s to 1600µm/s, which was opposite from the control group that organisms increase from the lowest point ~1300 µm/s to ~2900 µm/s (Fig. 5A). Interestingly, the speed of Bro treated animals kept growth, which indicated the animals might be stimulated to move. But the increases of Bro groups slower than the control groups (Fig. 5A). Prior to 40s, the drug-induced animals have faster speed than the control groups, especially for the Bis and Cur groups. However, the speed increased if the control group chase up all treatment groups after the 40s (Fig. 5A).

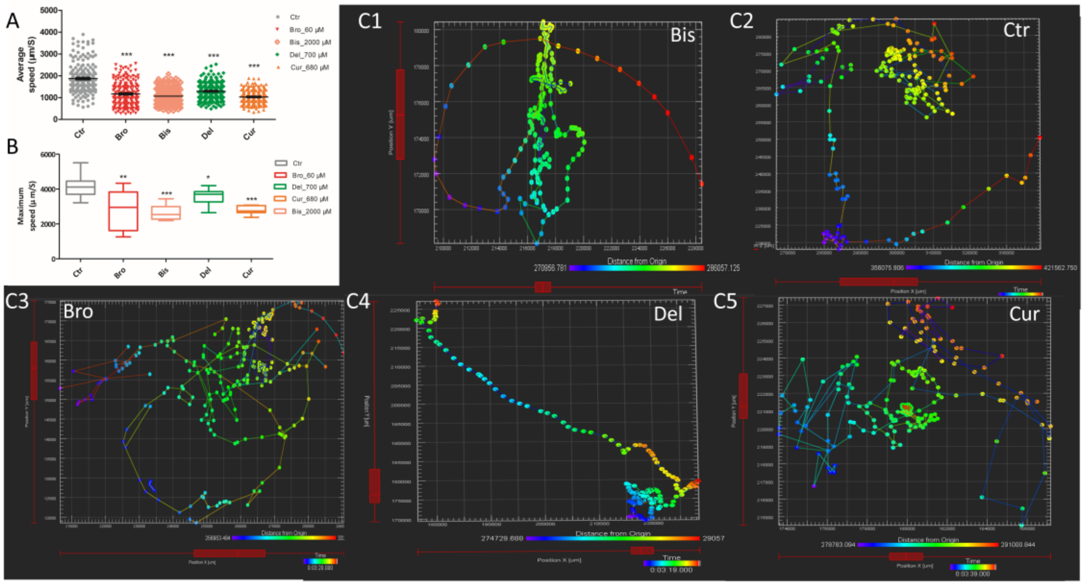

Fig. 4 Locomotor behavior of organic chemical treated animals. Animals were treated with four organic chemicals, which showed no significant mortality during a two hour observation period; namely 60 µM Bro, 2000 µM Bis, 700 µM Del and 680 µM Cur. The control groups were without any drug treatment. Five animals per treatment were stained with Mitotracker Deep Red 633 at a concentration of 0.33 µM for at least 1 h before the analysis. Animals were observed individually and scanned for 3.20 min with at least 1000 frames at a frequency of 67 msec using an Olympus SZX microscope coupled with a CellSens camera. The total stacked pictures were shown above. The average speed of control groups was roughly 1900 µm/s, while it was greatly reduced to ~ 1100-1400 µm/s in the treatments (A, $p<0.001$). The maximum speeds of treatment groups were 2500-3500 µm/s, which was also 500 µm/s slower than the control group (B). The tracking locus of 5 individuals in their corresponding conditions was shown in C1-C5. Asterisks denote significant differences from non-drug control (Unpaired t-test, ***, $p < 0.001$). The color highlights the different concentrations of compounds.

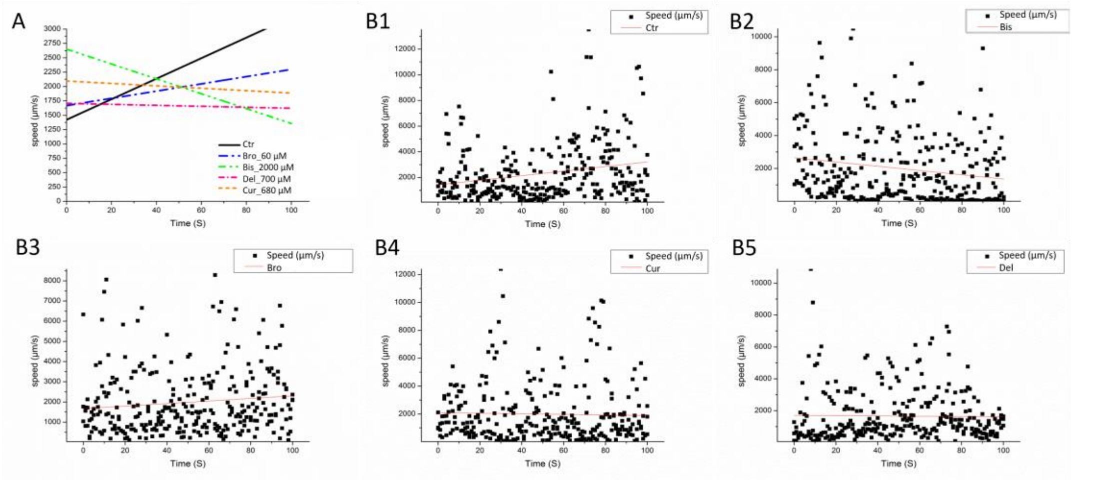

Fig. 5 Changes in the movement speed of organic chemical treated animals. A shows the speed linear fit cure of all drug-treated groups during 100 seconds of observation time. By using Imaris, the average speed was monitored every 0.5 seconds in total 200 points were collected in each treatment. B1-B5 shown the speed of five different individuals. Each chemical condition with 5 replicates.

3.1.1.4 Organic toxicity affects mitochondrial parameters

As a whole, $O_2^{\cdot-}$ formation showed no significant changes in response to chemical treatment, as indicated by the 2-OH-E+: DHE ratio results (Fig. 6 A). While a decrease happens in Bis treated animals (Fig. 6 A, Ctr vs. Bis, $p < 0.01$). We found a significant increase in expression of hydrogen peroxide/ peroxidase (HRP) in three induced toxicities (Fig. 6 B, Ctr vs. Bis, $p < 0.01$; Ctr vs. Del, $p < 0.05$; Ctr vs. Cur, $p < 0.05$). No strong differences were detected by mitotracker deep red staining (Fig.6 C).

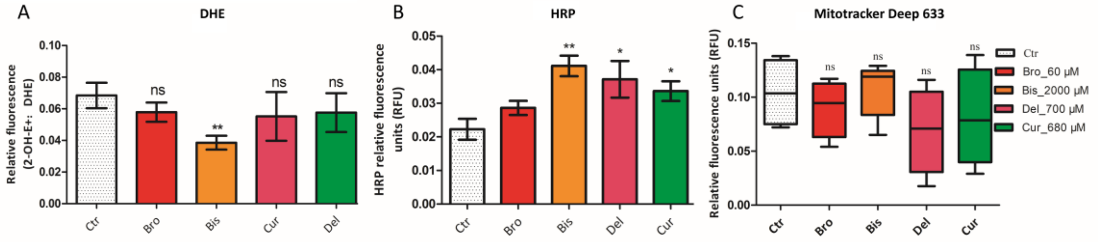

Fig. 6 Fluorescent intensities showing reactive oxygen species of organic compound treated animals. For detecting the response to organic compounds, 24 h treated animals were incubated for 30 min with three types of fluorescent probes and then imaged. In order to avoid any signal from the gut, the fluorescence intensity, in the present study, was only measured in the head regions (before eyes),

which is according to Rivera-Ingraham et al (2013) (Fig. 1). To reduce the interferences between dyes and to lower the exposure time, the dyes were used separately. A shows Dihydroethidium (DHE) staining results. DHE fluorescent intensity indicates $O_2{\cdot}^-$ formation. B shows the expression of hydrogen peroxide/ peroxidase (HRP) in 3 environmental toxicities. C shows mitotracker deep red staining. Asterisks denote significant differences from non-drug control (one-way ANOVA with Turkey Post-hoc test, *p < 0.05, **p < 0.01, and ns no significant difference).

3.1.1.5 Organic toxicity decreased the number of dead cells

Ethidium homodimer staining was used to monitor dead cells. As expected, exposure to poisonous compounds dramatically increased dead cell numbers. Bro and Bis had 40-48 dead cells in the observation area, which was two times higher than in the controls group (Fig. 7). Treatment with Cur and Del also led to higher cell death rates (Fig. 7).

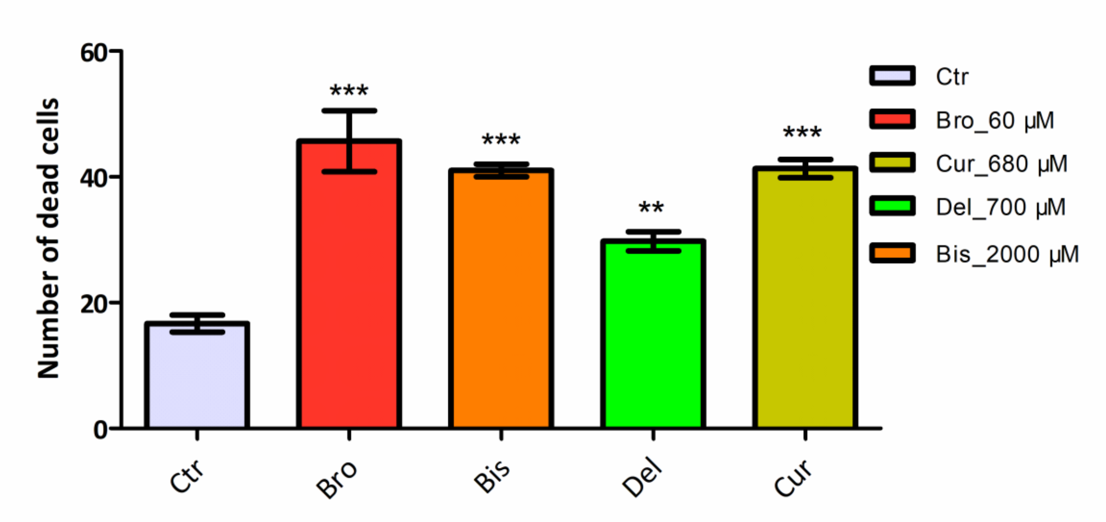

Fig. 7 Dead cell numbers in response to organic compounds. The counting regions included the anterior (before “eyes”) and posterior region (after female opening). Region of interest (ROI) was 260 pixels × 200 pixels (high × wide). 24 h treated animals were incubated for 30 min with 5 µM ethidium homodimer III and afterward the dead cells were detected with red fluorescence. Pictures were taken by combining seven Z-stacks. Every treatment group contained seven animals with two replicates. By using AxioVision 4.9.1, the death positive cells were counted in each layer. Asterisks denote significant differences from the non-drug control (Unpaired t-test, **p < 0.01;***, p < 0.001). The scale bar indicates 100 µm.

3.1.2 Inorganic toxicity effects

3.1.2.1 $CdSO_4$ and $CuSO_4$ treatments affect worm survival

Metals accumulate in aquatic animals and become toxic when concentrations reach certain thresholds. The toxicity may vary considerably between different metal cations. To identify the concentrations of Cd^{2+} and Cu^{2+} that are not directly toxic, eight different concentrations were tested. Survival curves revealed that animals can survive more than 100 minutes only when $CdSO_4$ concentrations are lower than 1000 µM (Fig. 8 A). However, worms were even more susceptible to $CuSO_4$, where $CuSO_4$ concentrations above 25 µM were lethal (Fig. 8 B).

Furthermore, hatching rates of newly laid eggs also showed a disparate tolerance towards Cu and Cd. The hatching rate of *M. lignano* dramatically decreased when $CdSO_4$ concentrations were above 500 µM (Fig. 8 A2). $CuSO_4$, on the other hand, showed a massive reduction in hatching rates at ~14 µM (Fig. 8 B2).

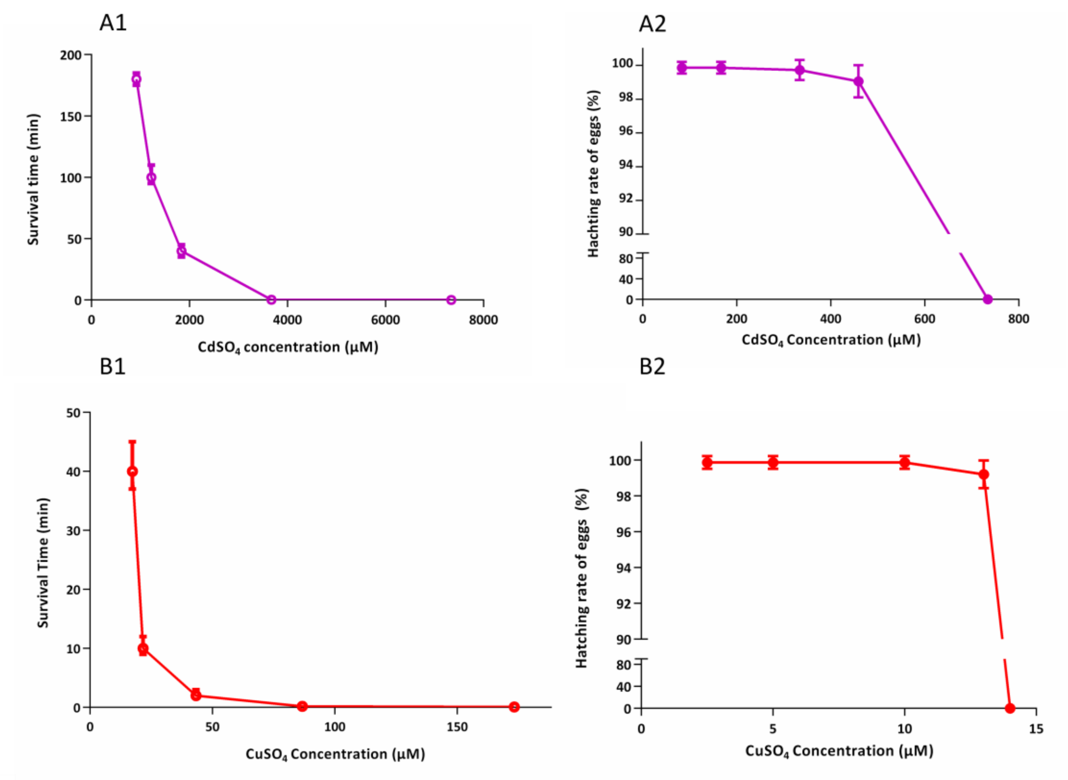

Fig. 8 $CdSO_4$ and $CuSO_4$ treatments affect the survival of worms and impact the hatching rate of the eggs. Adult worms were treated with eight different concentrations of $CdSO_4$ and $CuSO_4$. The tested concentration of $CdSO_4$ ranged from 7340 µM to 333.6 µM (A1) and concentrations of $CuSO_4$ ranged from 173.3 µM to 10.4 µM (B1). Animal survival was measured every 5 min and for lower concentrations, they were measured every 20 min. Hatching rate of Cd and Cu induced groups was measured as total offspring of twenty worms after seven days (A2 and B2). Animals were starved during the whole procedure.

3.1.2.2 Lifespan

M. lignano can survive for about 50 days without food supply. When animals suffer from a toxic environment, lifespan is greatly reduced. As expected, lifespan showed a negative correlation with the presence of heavy metals. Worms confronted with 730 µM $CdSO_4$ were able to survive only four days, which was significantly less than in the control group (Fig. 9 A, $p < 0.0001$). Animals exposed to lower $CdSO_4$ concentrations (460 µM and 330 µM), showed slightly longer lifespans, which were up to eight days (Fig. 9, $CdSO_4$_460 µM vs. $CdSO_4$_730 µM, $p < 0.0001$; $CdSO_4$_330 µM vs. $CdSO_4$_730 µM, $p < 0.0001$). Worms treated with $CuSO_4$ also showed the same trend, lifespan dramatically decreased at slightly higher concentrations of 14 µM and 12 µM, respectively (Fig. 9 B). In addition, most animals died very quickly at 10 µM $CuSO_4$, while a small fraction of worms can live almost as long as control animals (Fig. 9 B).

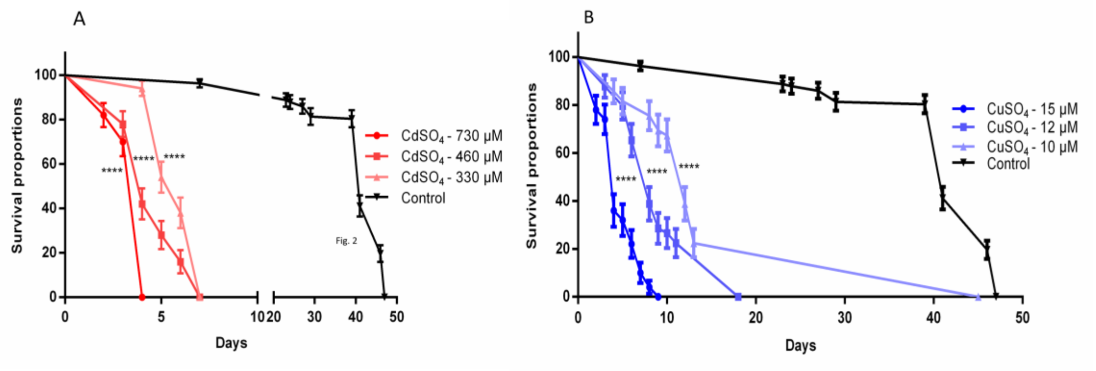

Fig. 9 Survival curves of Cu^{2+} and Cd^{2+} treated animals. Animals were treated with three concentrations of $CdSO_4$ (A; 730 µM, 460µM, 330µM) and $CuSO_4$ (B; 15 µM, 12 µM, 10 µM). Experiments employed 20 adult animals per treatment with 5 replicates and survival was measured every 24h hours. The median survival rate of the control group was 41 days. The median survival rate of tested $CdSO_4$ stress from higher to lower concentrations were four days, four days and six days, respectively. This decreased median rate also found in tested $CuSO_4$ groups, which was four days, eight days and twelve days, respectively. Asterisks denote significant differences from non-drug

control (Log-rank (Mantel-Cox) Test, ****, p < 0.00001). Colors highlight the different concentrations of metal stress.

3.1.2.3 Locomotor activity

Treatment with metal ions, especially exposure to higher concentrations, had a significant impact on animal behavior (Fig. 10). Animals exposed to all tested cadmium and to the two higher concentrations of copper showed significantly lower movement activities than untreated controls. The average speed of control animals was about 80 µm/s, while it was greatly reduced to below ~ 25 µm/s under cadmium treatments (Fig. 10, $p < 0.05$). This obvious decrease was also found in response to copper treatment. Only the lowest copper concentration had no statistically significant effect (Fig. 10, control vs. $CuSO_4$_15µM, p=0.0128; control vs. $CuSO_4$_10µM, p=0.0222).

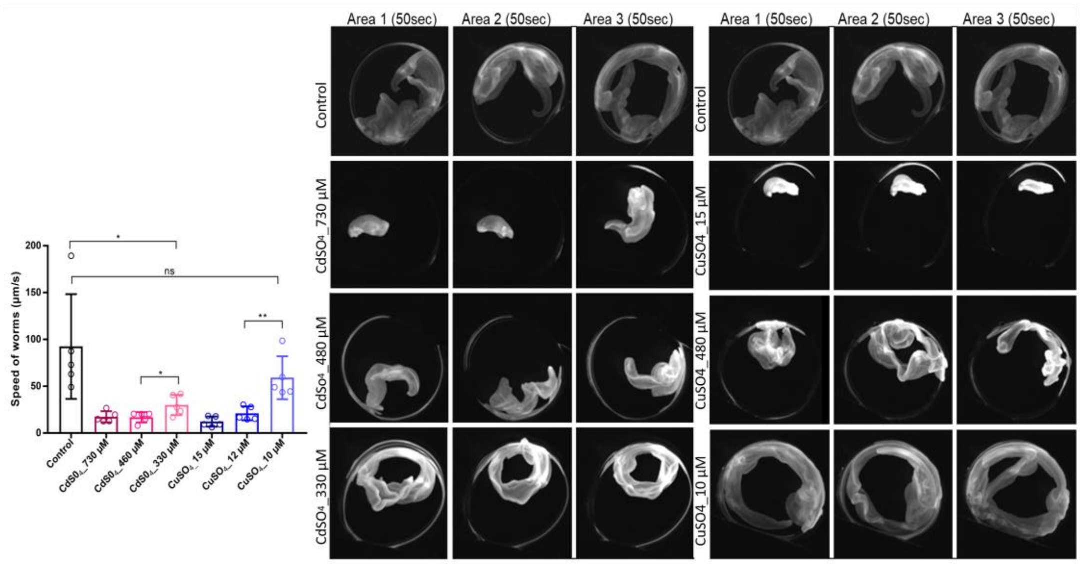

Fig. 10 Physical activities of Cu^{2+} and Cd^{2+} treated animals. Animals were treated with three different concentrations of $CdSO_4$ (730 µM_24h, 460 µM_48h, 330µM_48h) and $CuSO_4$ (15 µM_24h, 12 µM_48h, 10 µM_48h), respectively. Five animals that had previously been exposed to different conditions were stained with Mitotracker Deep Red 633 at a concentration of 0.33 µM for at least 1 h before the analysis and were kept in this medium until the end of the experiment. Animals were observed individually and scanned for 2 min with at least 1800 frames at a frequency of 67 msec. The 50 sec stacked pictures are shown (right). The average speed of the control groups was roughly 80 µm/s, while it was greatly reduced to below ~ 25 µm/s in the cadmium treatments ($p < 0.05$). This obvious decrease was also found in response to copper treatment (left). Only the lowest copper concentration had no statistically significant effect. Asterisks denote significant differences from

non-drug control (Unpaired t-test, *, $p < 0.005$). The color highlights the different concentrations of metal stress.

3.1.2.4 Reactive oxygen species formation

The O_2^- formation arises with increasing metal ion concentrations, as indicated by the 2-OH-E+: DHE ratio results ($p < 0.001$) (Fig. 11 A1 and A2). Furthermore, in accordance with the results obtained when plotting the 2-OH-E+: DHE ratios, mitochondrial O_2^- formation (MitoSOX staining) also suggested a remarkable increase with heavy metal treatment ($p < 0.001$) (Fig. 11 B1 and B2). These results are further supported by staining with C-H2DFFDA, which detects ROS formation aside from $O_2\cdot$ (-), such as H_2O_2, HOO·, and $ONOO^-$ (Fig. 11 C1 and C2). The upregulation of ROS levels after metal-treatment is consistent with the results obtained from hyperoxic exposure (Rivera-Ingraham et al., 2013).

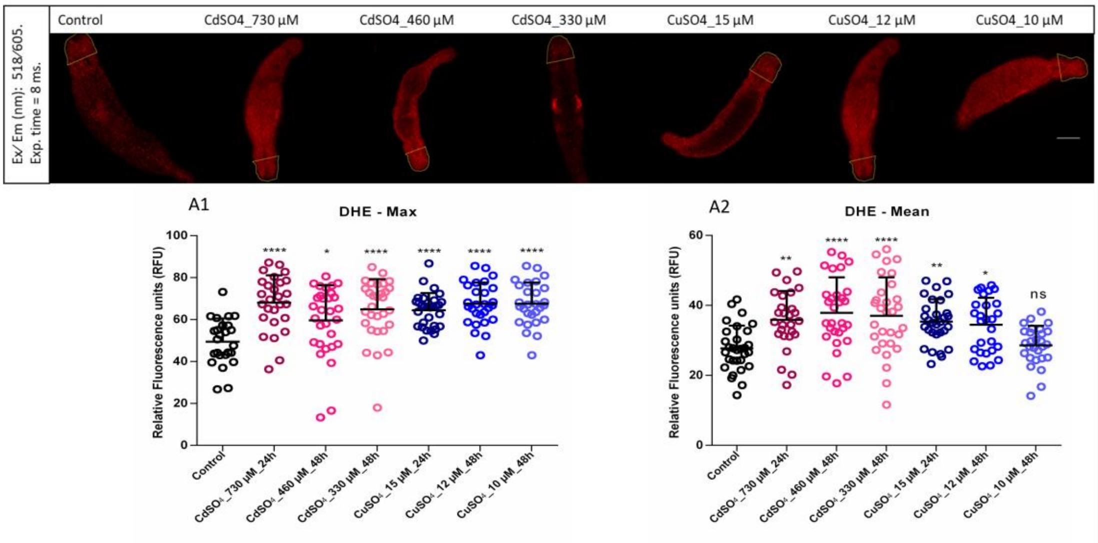
Control
CdSO4_730 µM
CdSO4_460 µM
CdSO4_330 µM
CuSO4_15 µM
CuSO4_12 µM
CuSO4_10 µM
Ex/Em (nm): 518/605.
Exp. time = 8 ms.
A1
DHE - Max
A2
DHE - Mean
Relative Fluorescence units (RFU)
Control
CdSO4_730 µM_24h
CdSO4_460 µM_48h
CdSO4_330 µM_48h
CuSO4_15 µM_24h
CuSO4_12 µM_48h
CuSO4_10 µM_48h
ns

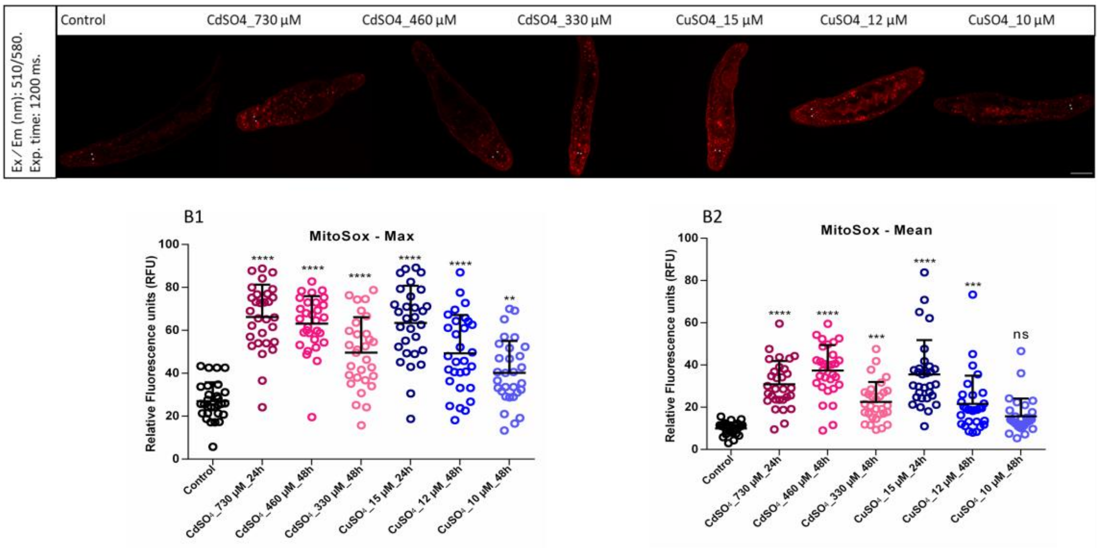
Control
CdSO4_730 µM
CdSO4_460 µM
CdSO4_330 µM
CuSO4_15 µM
CuSO4_12 µM
CuSO4_10 µM
Ex/Em (nm): 510/580.
Exp. time: 1200 ms.
B1
MitoSox - Max
B2
MitoSox - Mean
Relative Fluorescence units (RFU)
Control
CdSO4_730 µM_24h
CdSO4_460 µM_48h
CdSO4_330 µM_48h
CuSO4_15 µM_24h
CuSO4_12 µM_48h
CuSO4_10 µM_48h
ns

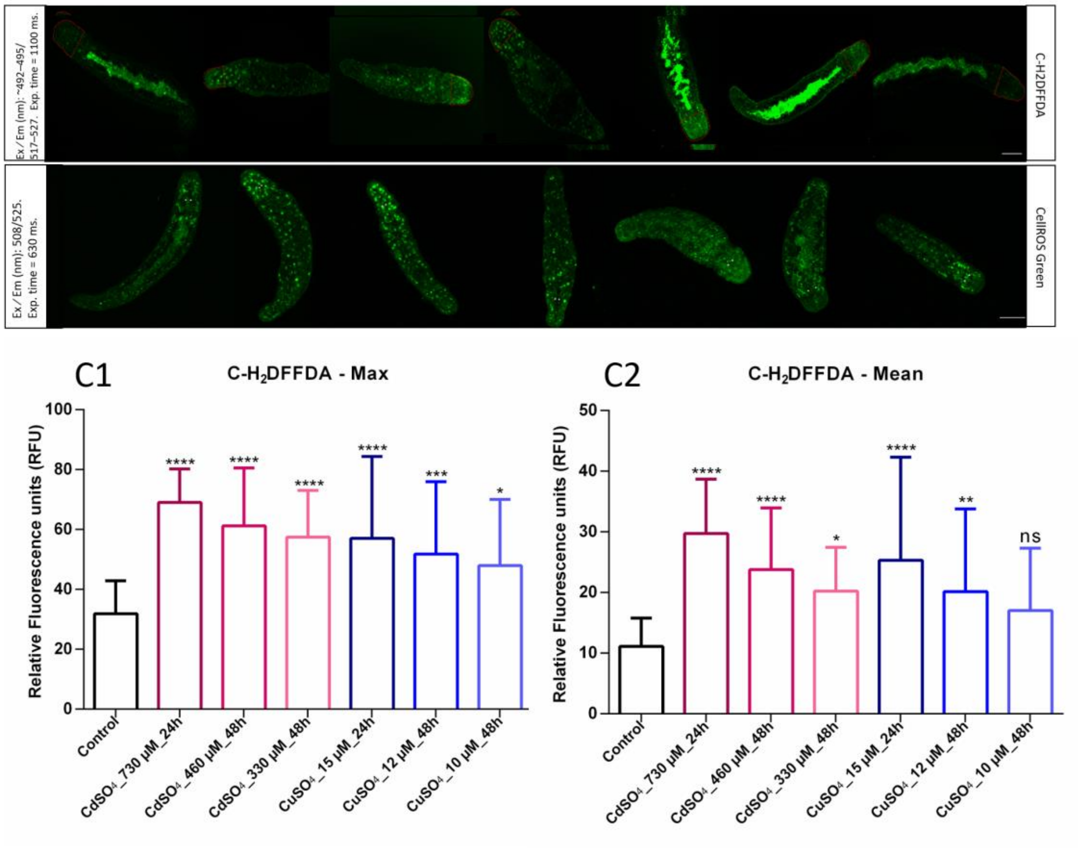

Fig. 11 Fluorescence intensity of reactive oxygen species indicating dyes of Cu^{2+} and Cd^{2+} treated animals. For monitoring the heavy metal response, treated animals were incubated for 30 min at four types of fluorescence probes and then imaged using the Zeiss Axio Imager Z1 microscope. The fluorescence intensities were analysed only at the head regions, which is described in Fig. 1, were considered. A1, A2, B1 and B2 show DHE, MitoSOX staining results, which indicating superoxide (O_2·-) formation increases with increasing metal ion concentrations. C1 and C2 show C-H2DFFDA staining results, indicating other ROS formations asides from O_2- such as hydrogen peroxide (H_2O_2), HOO- and ONOO-. Asterisks denote significant differences from non-drug control (one-way ANOVA with Turkey Post-hoc test, *P < 0.05, **P < 0.01, ***P < 0.001 and ****P < 0.0001).

3.1.2.5 Mitochondrial density

A notable increase was observed in the mitochondrial (mt) density of animals that were exposed to higher concentrations of heavy metal ions during a period of 24-48 h (Fig. 12 A1 and A2, $p < 0.001$). The mt density of copper treated animals increased by ~1.4-fold considering the maximum values and by ~1.1-fold when mean values were regarded (Fig. 12 A1, $p < 0.001$). In cadmium treated animals these differences are higher, reaching up to ~1.8-fold (Fig. 12 A1, $p < 0.001$). The fluorescence intensity results suggest that higher concentrations of metal ions led to increased mitochondrial densities.

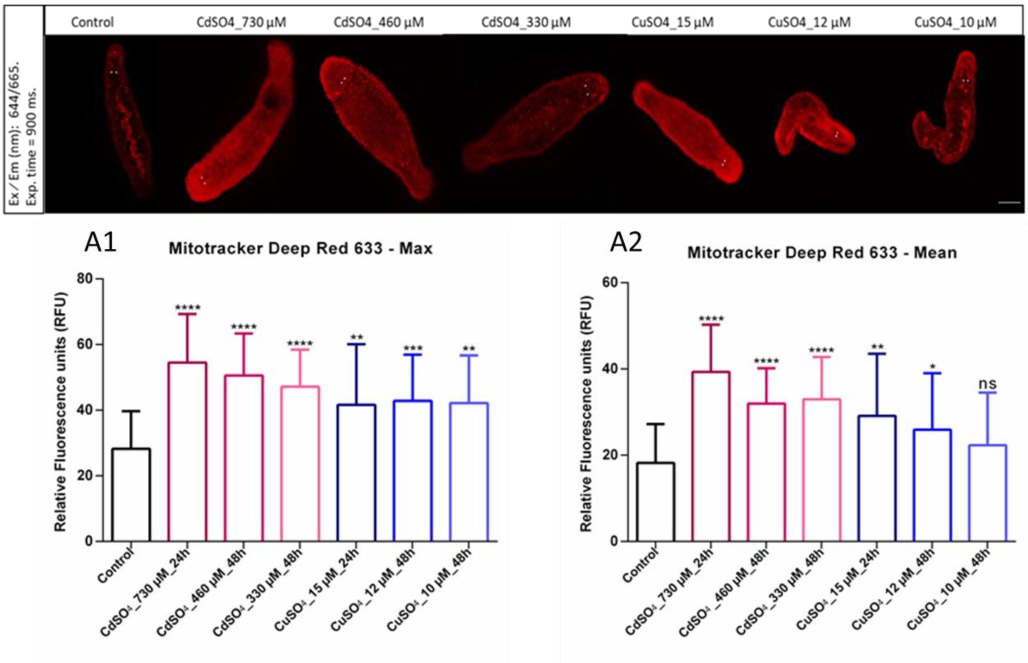

Fig. 12 Mitochondrial markers in Cu^{2+} and Cd^{2+} treated animals. A1 and A2 show the maximum and average mitochondrial (mt) density of animals that were exposed to the tested concentrations of heavy metal ions over a period of 24-48 hours. Mitochondrial intensities were indicated by mitotracker deep red 633 (mitotracker), treated animals were soaked in 0.33 µM mitotracker for 1 hour. Asterisks denote significant differences from non-drug control (one-way ANOVA with Turkey Post-hoc test, *$p < 0.05$, **$p < 0.01$, ***$p < 0.001$ and ****$p < 0.0001$).

3.1.2.6 Cell mitosis

In order to test the effect of heavy metal ions on cell proliferation, we used the anti-phosphorylated histone 3 antibody to evaluate the number of mitotically active cells. Values were significantly reduced in the 730 µM and 460 µM $CdSO_4$ treatment groups, while an apparent increase was observed at 330 µM $CdSO_4$ (Fig. 13). No significant increases or decreases of mitotically active cell numbers were found for either of the Cu^{2+}-induced treatment groups.

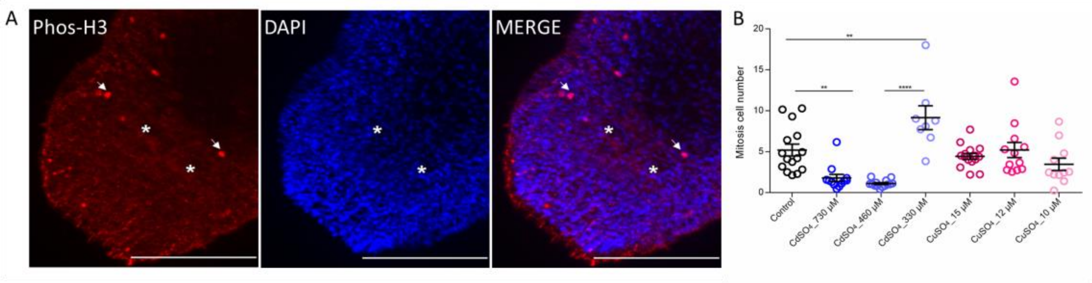

Fig. 13 Mitosis cell numbers of Cu^{2+} and Cd^{2+} treated animals. The treated worms were used for immunostaining with histone H3 phosphorylation to visualize mitotic cells. The white arrows shown in the pictures indicate mitotic cells (A). Mitotically active cell numbers in both treatment groups were shown in B. Pictures were taken by combining 7 Z-stacks and each group employ 6 animals and three biological replicates were performed, 8-17 animals in total. Animals were observed with AxioVision 4.9.1 fluorescent microscope and positive cells were counted by each layer. Asterisks denote significant differences from non-drug control (Unpaired t-test, $^{**}p < 0.01$, $^{****}p < 0.0001$). The scale bar indicates 100 μm.

3.1.2.7 Cell death quantification

Compared with unexposed animals, the number of dead cells significantly increased in the 330 μM Cd^{2+} group, whereas no changes were observed for the other concentrations. Copper ion cytotoxicity was observed at higher concentrations. The dead cell numbers highly increased in 15 μM and 12 μM Cu^{2+}-treated groups (Fig. 14).

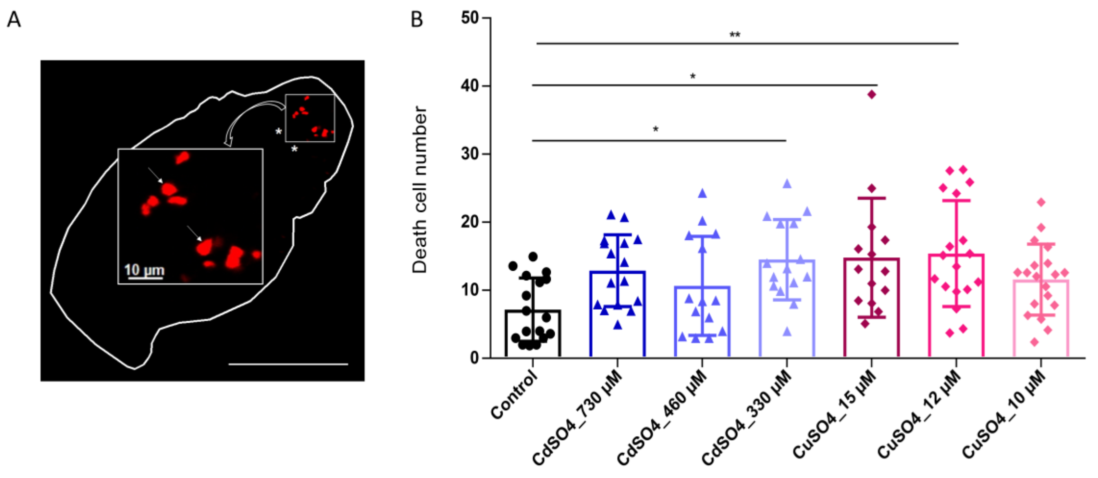

Fig. 14 Numbers of dead cells of Cu^{2+} and Cd^{2+} treated animals. A showed the labelling of dead cell and B presented their numbers under metal treatment conditions. Cu^{2+} and Cd^{2+} treated animals were incubated for 30 min at 5 µM ethidium homodimer III and afterwards the dead cells were stained with red fluorescence. Pictures were taken by combining 7 Z-stacks. Every treatment group contains 7 animals with 3 replicates, in total 13-19 animals. By using AxioVision 4.9.1, the dead positive cells were counted by each layer. Asterisks denote significant differences from non-drug control (Unpaired t-test, $*p < 0.05$, $**p < 0.01$). The scale bar indicates 100 µm.

3.1.2.8 Gene expression quantification of antioxidant enzymes and multidrug resistance transporter genes

The transcription of genes coding for major antioxidant enzymes were significantly reduced in response to heavy metal confrontation. These tested enzymes include peroxiredoxin (prdx6), glutathione-s-transferase pi-1 (gstp1), peroxiredoxin 1 (prdx1), mitochondrial superoxide dismutase (sod2), and microsomal glutathione-s-transferase (mgst1). The gstp1 was the only anti-redox coding gene that showed a significant increase in expression (Fig. 15 A). Gene expression was also reduced for caspase 3 (casp3), coding for an enzyme directly involved in programmed cell death. The mitochondrial cytochrome c oxidase subunit b (cox5b) showed a decreased transcription in all tested metal groups.

The multi-drug-resistant transporter genes (*mdr*, adenosine triphosphate-binding cassette transporter) play a crucial role in protecting cells from xenobiotics, chemicals, and drugs (Mease, Sane, Podila, & Taub, 2012; Uhr et al., 2008). I therefore quantified transcript levels of three typical ABC transporter cassette family members, namely *mdr1*, *mdr5*, and *mdr7*. As *mdr5* showed no or reduced transcript levels in response to metal confrontation, *mdr1* and *mdr7* contrarily presented either no change or increased transcript levels (Fig. 15B).

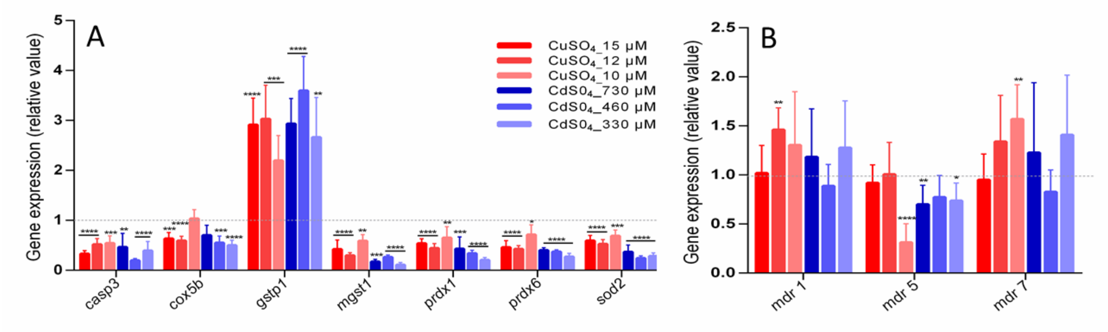

Fig. 15 Quantitative gene expression analysis of *M. lignano* under different metal confrontations. A The expression of genes coding for antioxidant enzymes; B multi-drug-resistance transporter genes. Groups with significant statistical differences with non-drug treatment control (value=1, dash line), and the groups shared with the same differences values are labeled with a line and shown together. A total of 5 biological replicates were performed. Both parametric Unpaired t-test and paired t-test statistics were used.

3.2 The native microbiome of *Macrostomum lignano*

3.2.1 Lab-reared *M. lignano* carries a distinct microbiome

M. lignano primarily grows in the high-tide interstitial space in the sand of beaches of the Northern Adriatic Sea. In the lab, they have been grown for more than four years now. Animals were grown in Guillard's F/2 (Sigma G0154) medium and fed with diatom *Nitszchia curvilineata*. We named our specimens "lab-reared worms". The different samples were characterized as follows: 1) worms cultured on the algae medium for at least 3 weeks were denoted as "mature worms" (MWs); 2) mature worms with 5 days starvation were denoted as "starvation mature worms" (SMWs); 3) worms collected directly after hatching within 1-2 days were denoted as "immature worms" (IMWs); 4) medium after 3 weeks colonization with the worms denoted as "pre-colonized medium" (PCM); 5) the algae medium preparing for worms inoculate were denoted as “Algae”. The bacterial microbiomes were defined for all samples referring to the V2 region of the 16S ribosomal DNA.

We found an abundant microbiome of *M. lignano* under lab conditions, 55 bacterial families were identified in our studies (Table). Algae without any contact with worms had a specific microbial community (Fig. 16 A). It contains more Hyhomicrobiaceae and unknown bacteria (Fig. 16 B, $p < 0.0001$). After colonization with worms, *Rhodobacteracea*, *Phyllobacteriaceae*, *Alteromonadaceae*, *Hyphomonadaceae*, *Flavobacteraceae*, *Flammeovirgaceae*, and other bacteria family (consists of bacterial taxa which abundances below 0.01) all significantly increased in the PCM (Fig. 16 A and B, Algae vs. PCM, $P < 0.0001$). Bacterial distributions of SMWs were different from MWs and IMWs. With *Hyphomonadaceae*, *Flavobacteriaceae* and unknown bacterium being significantly reduced, *Alteromonadaceae* became the dominated bacteria in SWMs (Fig. 16 15 A and C). This indicates that the prior two bacterial families might be transit bacteria and *Alteromonadaceae* being the resident bacterial family in lab-enriched worms. IMWs and MWs had a similar bacterial abundance distribution, which *Hyphomonadaceae* and *Flavobacteriaceae* being the dominate bacteria (Fig. 16 B and C). *Rhodobacteraceae* bacterial taxa were more abundant in all examined IMWs than to MWs (Fig. 16 C).

Shannon index analyses verified that worm contacted samples have more bacterial diversity than pure Algae samples (Algae vs. PCM; Algae vs. IMWs/MWs; $p < 0.0001$). SMWs lost bacterial diversity (SMWs vs. MWs; SMWs vs. IMWs; $p < 0.0001$) (Fig. 17 A). Species diversity in each community was also tested by alpha diversity, namely by Simpson’s index (Table 6).

Both weighted and unweighted Unifrac distance analyses verified the presence of a worm-specific microbiome. The first and second axis separates all worms from algae and pre-colonized medium (PCM) samples, which indicates that worm associated microbiomes are distinct from that of the living environment (Fig. 17 B, Algae/PCM vs. SMWs/IMWs/MWs; P ≤ 0.0003; Table 7 and Table 8). Irrespective of their developmental stage IMWs and MWs cluster closely together (p = 0.9627).

As no dominant microbial taxa of *M. lignano* have been reported up to now, we could not speculate if the high abundance of those bacterial families is also seen in the other *M. lignano* strains. Actually, the microbiome of worms is constantly changing according to their living environments. Members of dominant taxonomic groups may play a central role in the interaction with *M. lignano* and these bacteria can be easily obtained by lately hatching worms from the environment.

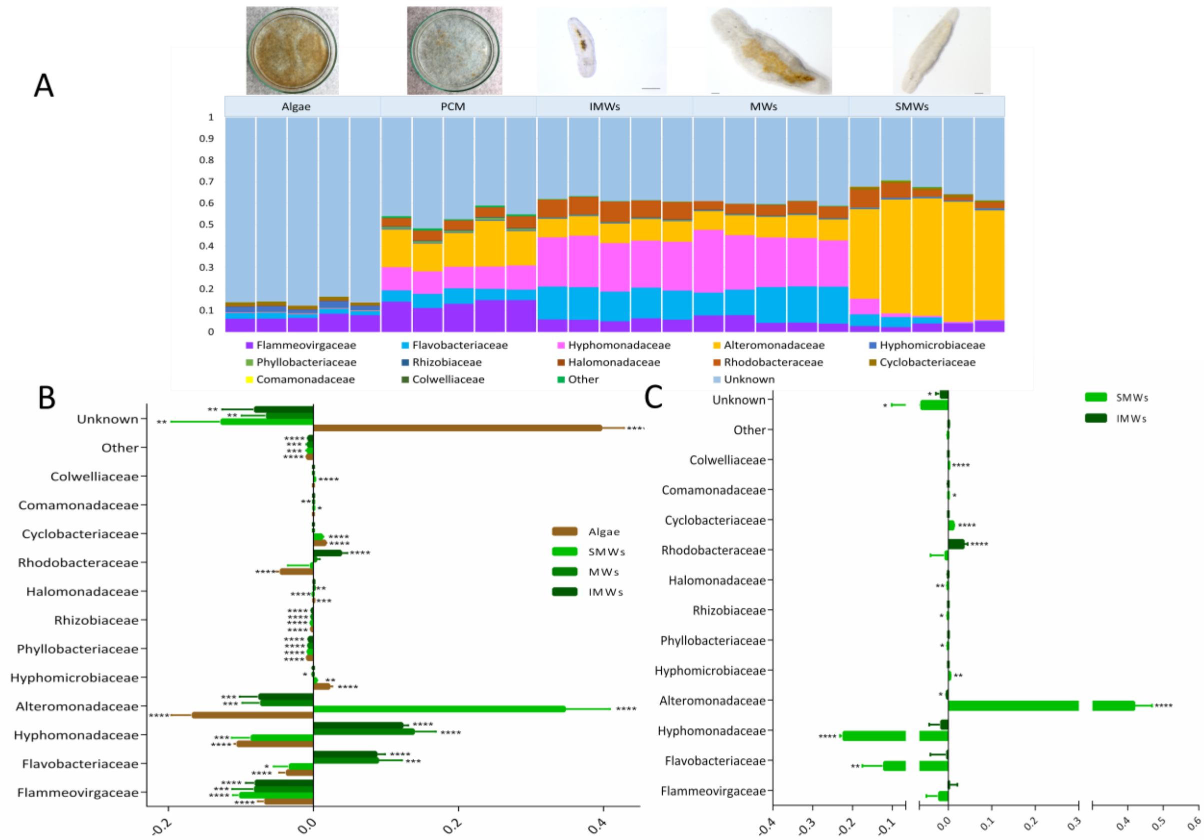

Fig. 16 Bacterial abundance and diversity of worms and of their medium. In A, the different microbial colonizer taxa are listed as bar charts with color coded assignments. For each type of sample (Algae, PCM, IMWs, MWs, SMWs) five biological replicates are shown. In B, comparison of the major bacteria family constitution of IMWs, MWs, and SMWs with PCM is shown. In C, comparison of the major bacterial constitutions of SMWs and IMWs with MWs. Asterisks denote significant differences from PCM control (one-way ANOVA with Turkey Post-hoc test, * p < 0.05, ** p < 0.01, and ns no significant difference). Algae: algae medium; PCM, pre-colonized medium; SMWs, the starved mature worms; MWs, mature worms; IMWs, immature worms.

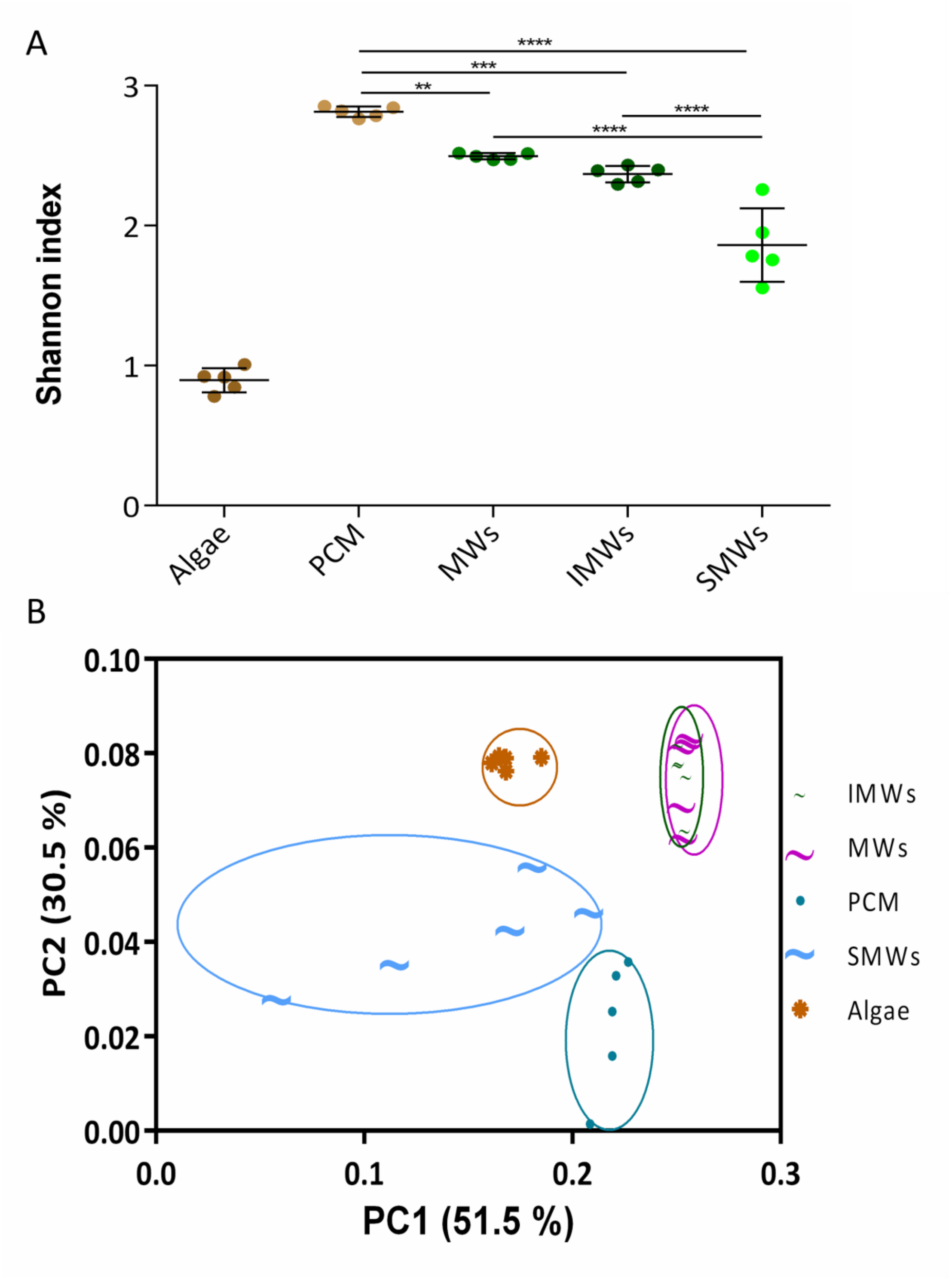

Fig. 17 Shannon index and principle components analysis. In A, Shannon index analysis indicating bacterial diversity among different samples. B shows the principal components analysis based on the weighted Unifrac distances analyses. Asterisks denote significant differences from PCM control (one-way ANOVA with Turkey Post-hoc test, *, $p < 0.05$, **, $p < 0.01$, and ns no significant difference).

3.2.2 The presence of a native microbiome speeds up *M. lignano*'s feces production

To infer the potential effects of the native microbial on worms, we generated germ-free animals through antibiotic treatments and recolonized adult animals with their native bacterial community. We found that the microbiota did not significantly affect the worm's development. All experimental juveniles, grown either in sterile (SM) or re-colonization medium (RCM), developed into an adult after 6-7 days. Population sizes were measured with 10 mature worms after 16 days under standard laboratory conditions (RT, 20 ℃). Our observations revealed that germ-free worms had higher population sizes than those that had been reconstituted (Fig. 18 A, $p < 0.001$). The presence of bacteria sped up the decomposition of the culture medium, which stressed worms to starvation resulting in decreased population size. When the culture medium was frequently refreshed, the population size was then compared to that found in sterile conditions (Fig. 18 A). We subsequently tested the feces output of mature worms. Re-colonization (RC) animals obtained more integrated and brunet feces than to the germ-free (GF) animals (Fig. 18 B, $p < 0.0001$). While GF animals harvested more separated, transparent and smaller-sized feces (Fig. 18 B, $p < 0.0001$). The total feces output of RC animals were larger than of GF animals. In conclusion, the bacteria effect on *M. lignano* is complex. On the one hand, it causes the fast degradation of medium which minimize population sizes. On the other hand, the worms' gut content evacuation is sped up.

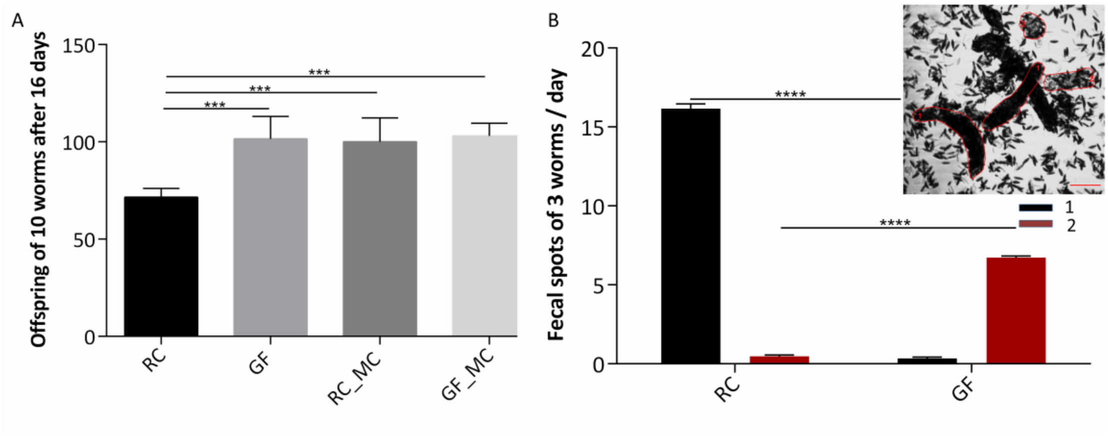

Fig. 18 Offspring and feces output of re-colonized (RC) worms and germ-free (GF) worms. In A, population size was measured with 10 mature worms after 16 days under standard laboratory conditions (RT, 20 °C). Recolonization groups harvest lower number of offspring than the GF group, while the offspring number was back to the normal one after constantly changing the medium. In B, quantification of the fecal spots in Re-colonization (RC) animals and GF animals. RC_MC, re-colonized medium with constantly medium change; GF_MC, germ-free medium with constantly medium change. Unpaired two-tailed Student's t-test, statistical analysis of significant differences were defined as ***, $p < 0.001$ and ****, $p < 0.0001$.

3.2.3 *M. lignano* carries a drug-sensitive microbiome

In order to examine whether the worms' microbiome can be altered by their corresponding substrates, the bacterial communities of drug-exposed *M. lignano* were isolated. As an estuarine coast flatworm, *M. lignano* continuously cope with various poisonous chemicals in their living water. These factors may come from the non-purified waters from the sewage or from poisoning wastewater from agriculture.

3.2.3.1 Treatment with two metals affect the microbiome of *M.lignano*

Each metal, Cu^{2+} and Cd^{2+}, was used in three different concentrations and exposure was for 48h to examine dose effect on microbial compositions. Apart from the non-drug treatment control, we include ampicillin (Amp) and deltamethrin (Del).

The observed microbiome of *M. lignano* showed decreased bacterial diversity in response to drug treatment. The quantities of *Alteromonadaceae*, which account for 9.6% in mature worms and 51.4 % in starved worms, increased to over 70% in all 3 concentrations of Cu^{2+}- and ampicillin-treated samples (Fig. 19 A). Another bacterial family, *Alcanivoracaceae*, was greatly up-regulated and became the dominant bacteria in all Cd^{2+}- induced groups (Fig. 16 A and B). Under Cu^{2+} and Cd^{2+} conditions, the operational taxonomic unit (OTUs) significantly decreased (Fig. 19 C and Table 9, MWs vs. $CuSO_4$_14 µM; MWs vs. $CuSO_4$_12 µM; MWs vs. $CuSO_4$_10 µM; MWs vs. $CdSO_4$_730 µM; MWs vs. $CdSO_4$_460 µM; MWs vs. $CdSO_4$_330 µM, $p < 0.0001$). The bacterial community of deltamethrin treated animals were much more stable, which presents similar OTUs with MWs (Fig. 19 C). Except for two lower concentrations of Cu^{2+}-treated groups, all the other drug treatment groups showed a significantly dropped community diversity (MWs vs. $CuSO_4$_14 µM; $p=0.0023$; MWs vs. $CdSO_4$_730 µM; MWs vs. $CdSO_4$_460 µM; MWs vs. $CdSO_4$_330 µM; $p < 0.0001$) (Fig. 19 D and Table 10).

These differences are illustrated by the Weighted UniFrac analysis (Fig. 19 E, Table 11, MWs vs. Amp; MWs vs. Del; MWs vs. all $CuSO_4$ groups; MWs vs. all $CdSO_4$ groups; $p \leq 0.001$). The first axis separates MWs from metal treated groups, while the second axis separated the Cd^{2+} and Del samples from Cu^{2+} and Amp treated groups (Fig. 19 E, MWs vs. all $CdSO_4$ groups; MWs vs. all $CuSO_4$ groups; $CdSO_4$ groups vs. $CuSO_4$ groups, $P \leq 0.001$). Bacterial communities from the same drug treatment clustered closely together. These differences were also verified by Unweighted UniFrac analysis and the ADONIS assessment, where worm specimens formed distinct clusters ($p \leq 0.001$) (Table 12 and Table 13).

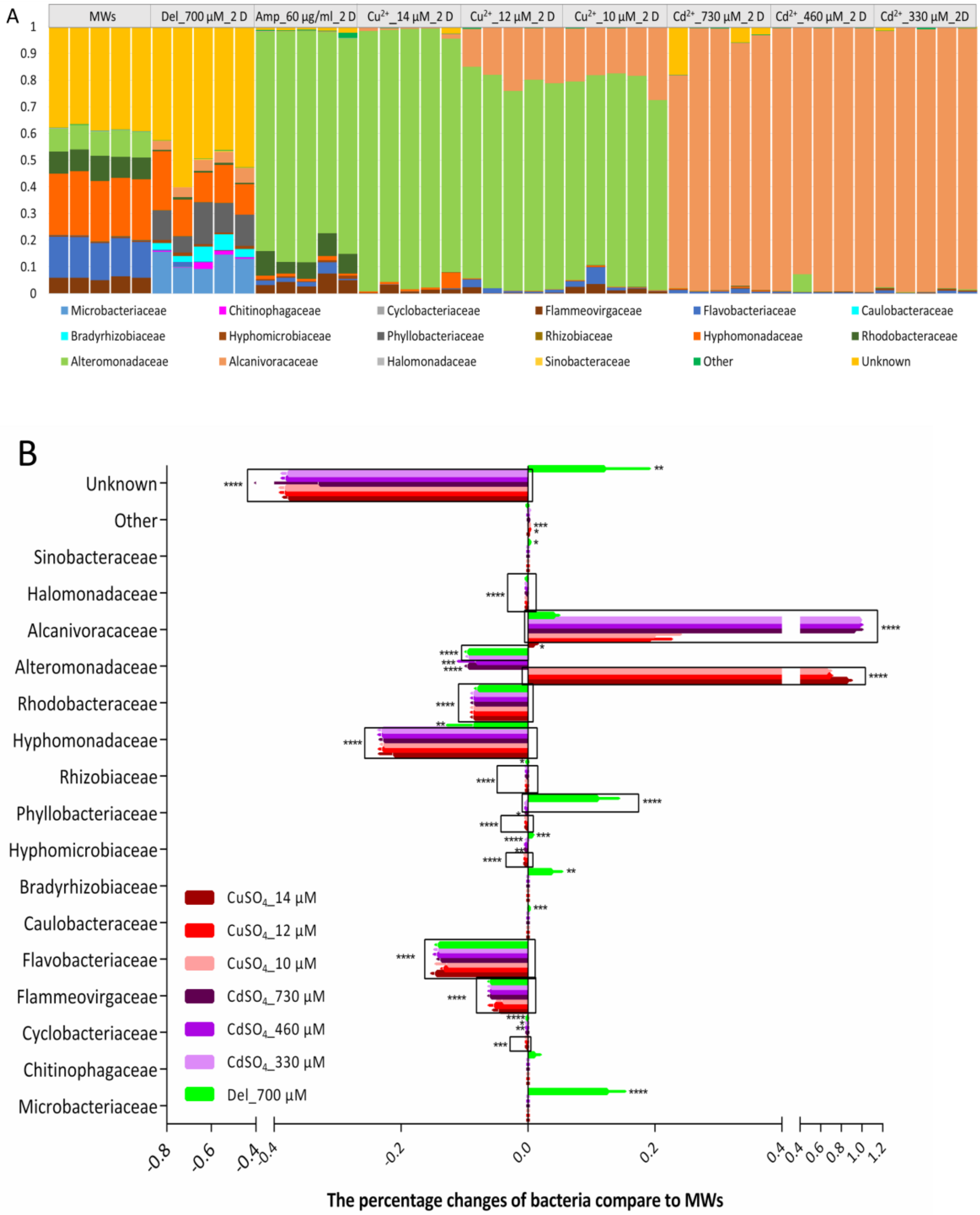
A
MWs
Del_700 µM_2 D
Amp_60 µg/ml_2 D
Cu2+_14 µM_2 D
Cu2+_12 µM_2 D
Cu2+_10 µM_2 D
Cd2+_730 µM_2 D
Cd2+_460 µM_2 D
Cd2+_330 µM_2D
Microbacteriaceae
Chitinophagaceae
Cyclobacteriaceae
Flammeovirgaceae
Flavobacteriaceae
Caulobacteraceae
Bradyrhizobiaceae
Hyphomicrobiaceae
Phyllobacteriaceae
Rhizobiaceae
Hyphomonadaceae
Rhodobacteraceae
Alteromonadaceae
Alcanivoracaceae
Halomonadaceae
Sinobacteraceae
Other
Unknown
B
CuSO4_14 µM
CuSO4_12 µM
CuSO4_10 µM
CdSO4_730 µM
CdSO4_460 µM
CdSO4_330 µM
Del_700 µM
The percentage changes of bacteria compare to MWs

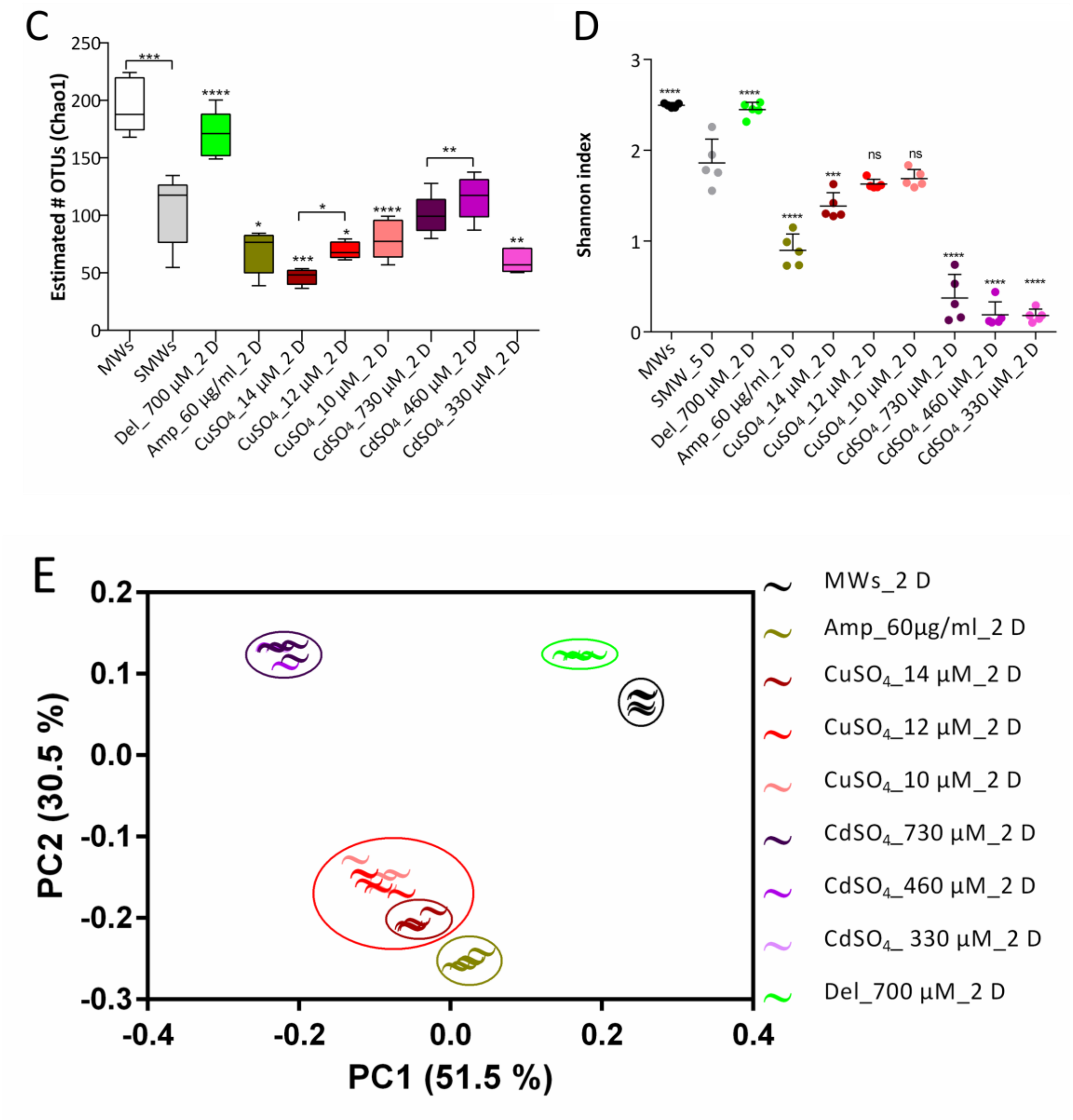

Fig. 19 Bacterial abundances and diversity of metal-confronted worms. Apart from MWs, we include ampicillin (Amp) and deltamethrin (Del) stresses as antibiotic and organic controls. In A, the different microbial colonizer taxa are listed as bar charts with color coded assignments. For each type of sample (MWs, Del, Amp, Cu^{2+}_14 μM, Cu^{2+}_12 μM, Cu^{2+}_10 μM, Cd^{2+}_730 μM, Cd^{2+}_460 μM, Cd^{2+}_330 μM) two days treatment and five biological replicates are shown. In B, compare the major bacterial family constitution of drug treatment groups with MWs. In C and D, estimated OTUs and calculated the Shannon index in all groups. In E, PC diagram based on the Weighted UniFrac analysis. Asterisks denote significant differences from MWs control (one-way ANOVA with Turkey Post-hoc test, **, p < 0.01, ***, p < 0.001 and ****, p < 0.0001).

3.2.3.2 Xenobiotic treatment affects the microbiome of *M.lignao*

The microbial composition of lab-enriched *M. lignano* was studied in response to xenobiotic treatments. To better understand the environmental effects on worms, I prepared a xenobiotic mix, which adjust 220 µM of atrazine (Atr), suberoyl bis-hydroxamic acid (Bis) and deltamethrin (Del), and mixture in ratio 1:1:1 (denoted as 'ABD'). The exposure time was determined to refer to their toxicity. Worms were exposed for five days in Atr and Del containing medium, while two days incubation was chosen for Bis and ABD. Worms were starved during all processes.

Worms exposed to organic chemicals showed a different community composition in comparison to SWMs. Two bacteria families, *Rhodobacteraceae* and *Hyphomonadaceae*, increased in all drug treatment groups (Fig. 20 A and B), while *Flammeovirgaceae* reduced in all xenobiotic samples (Fig. 20 A and B). Animals exposed to Atr and Del showed a similar microbial distribution, with *Alteromonadaceae* (49.2% and 62.4%) and *Rhodobacteraceae* (33.4% and 16.4%) being the most abundant families (Fig. 19 A and B). Bis and ABD groups exhibited a comparable pattern, *Flavobacteriaceae* and *Rhodobacteraceae* became the dominate bacteria, which account for 32.6% and 21.6%, 10.8% and 60.2%, respectively (Fig. 20 A and B). OTUs and bacterial diversity of xenobiotic treatment groups decreased compared with MWs, while there was no apparent difference with SMWs (Fig. 20 C, Table 14). Compared with SMWs, Del containing groups increased their community diversity (Fig. 20 D) and all the other treatment groups have no apparent difference in bacterial diversity (Fig. 20 D, Table 15).

According to the Weighted UniFrac analysis, the first and second principal components explained 57.5% variance (Fig. 20 E, Table 16). SMWs separated from all remaining groups and xenobiotic groups separated from each other. Major microbial composition of ABD group was close to Bis sample, but separated from Atr, Del and SMWs groups (Fig. 20 E). This result supported by unweighted Unifrac distances and multivariate analysis of variance (ADONIS) (Anderson, 2001; Oksanen et al., 2014) on Bray-Curtis (SMWs vs. xenobiotic treatment; $p \leq 0.001$) (Table 17).

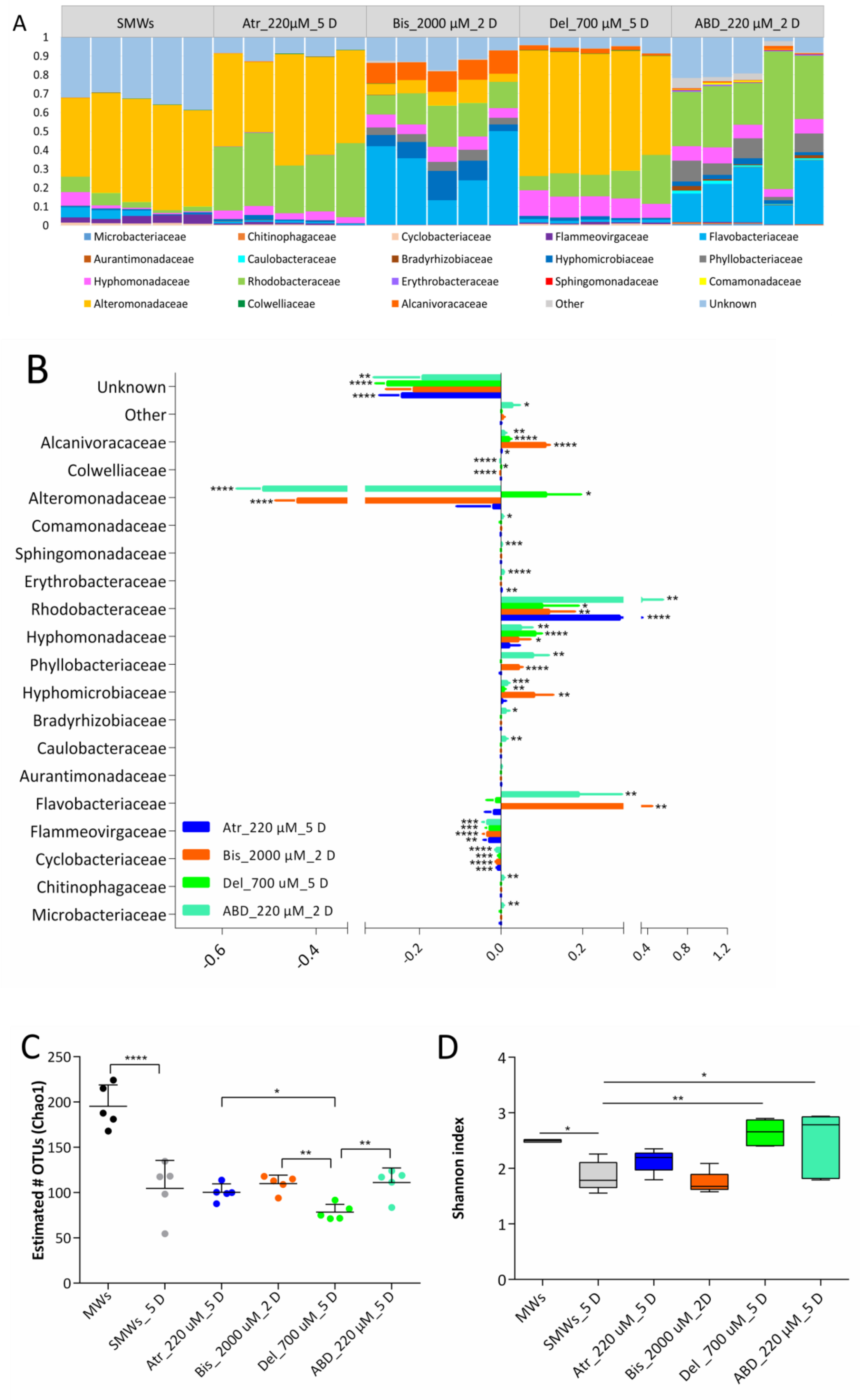
A
SMWs
Atr_220µM_5 D
Bis_2000 µM_2 D
Del_700 µM_5 D
ABD_220 µM_2 D
Microbacteriaceae
Chitinophagaceae
Cyclobacteriaceae
Flammeovirgaceae
Flavobacteriaceae
Aurantimonadaceae
Caulobacteraceae
Bradyrhizobiaceae
Hyphomicrobiaceae
Phyllobacteriaceae
Hyphomonadaceae
Rhodobacteraceae
Erythrobacteraceae
Sphingomonadaceae
Comamonadaceae
Alteromonadaceae
Colwelliaceae
Alcanivoracaceae
Other
Unknown
B
Atr_220 µM_5 D
Bis_2000 µM_2 D
Del_700 uM_5 D
ABD_220 µM_2 D
C
Estimated # OTUs (Chao1)
MWs
SMWs_5 D
Atr_220 uM_5 D
Bis_2000 uM_2 D
Del_700 uM_5 D
ABD_220 uM_5 D
D
Shannon index
Atr_220 uM_5 D
Bis_2000 uM_2D
Del_700 uM_5 D
ABD_220 uM_5 D

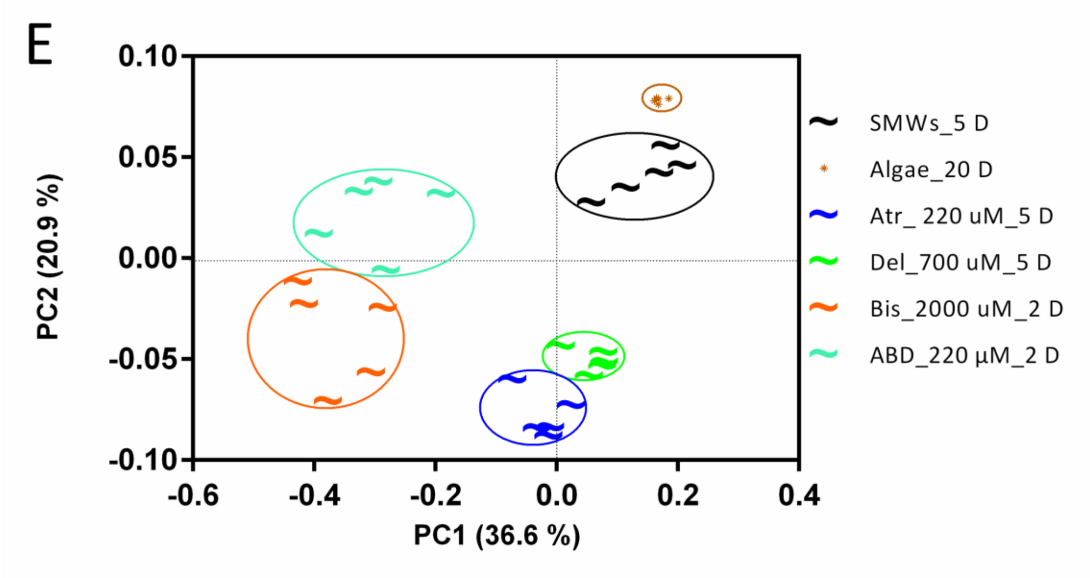

Fig. 20 Bacterial abundances and diversities in worms of three types of confrontations with organic compounds. In A, the different microbial colonizer taxa are listed as bar charts with color coded assignments. For each type of sample (SMWs, Atr_220µM, Bis_2000µM, Del_700µM, ABD_220µM) with two to five days of treatment and five biological replicates are shown. In B, comparison of the major bacteria family constitution of Atr, Bis, Del, and ABD with SMWs. In C and D, estimated OTUs and Shannon index in all groups. In E, PC diagram based on the weighted UniFrac analysis. MWs, mature worms; Atr, atrazine; Bis, suberoyl bis-hydroxamic acid; Del, deltamethrin; ABD, Atr, Bis and Del mixture under ration 1:1:1. Asterisks denote significant differences from SMWs control (one-way ANOVA with Turkey Post-hoc test, * $p < 0.05$, ** $p < 0.01$ and **** $p < 0.0001$).

3.2.4 The effects of the microbiota for the worm's fitness

To evaluate if the native microbiome only has an influnces on the worm's fitness, I performed lifespan experiments under compound stress. Three groups were generated: 1) animals with a one-week pre-antibiotic treatment considered as "germ-free" (GF); 2) GF animals were treated with $CdSO_4$ considered as "GF and $CdSO_4$" (GF_$CdSO_4$); 3) GF animals were simultaneously contacted with recolonization medium and $CdSO_4$. It considered as "RC and $CdSO_4$" induced groups ("RC_$CdSO_4$"); 4) GF animals primarily lived in the re-colonization medium for five days and further introduced $CdSO_4$. It was considered as "pre-recolonization and $CdSO_4$" induced groups ("PreRC_$CdSO_4$").

Without treatment, both GF and RC worms can live roughly 50 days under starvation (Fig. 21 A and B lifespan, SM vs. RC, $p = 0.0586$). When confronted with $CdSO_4$, worms exhibit a different survival capability. "PreRC_$CdSO_4$" animals, where worms obtained a stable intestinal and surface microbiome, significantly increased the lifespan of *M. lignano* that had been confronted with lower $CdSO_4$ concentrations. The survival curve analysis showed a lifespan extension of 1-2 days (Fig. 21 C, in both cases $CdSO_4$_460 µM and 330 µM, $p < 0.0001$). However, the bacterial recolonization could not enhance the lifespan in the highest tested concentration (730 µM). We observed that the GF_$CdSO_4$ animals lived much longer than RC_$CdSO_4$ animals (Fig. 21 A and B, GF_$CdSO_4$_730 µM vs. RC_$CdSO_4$_730 µM, $p < 0.0005$; GF_$CdSO_4$_460 µM vs. RC_$CdSO_4$_460 µM, $p < 0.0001$; GF_$CdSO_4$_330 µM vs. RC_$CdSO_4$_330 µM, $p < 0.0001$). But pre-colonization with native microbiome may possibly benefit the animals' survival under these conditions. Total feces output analysis suggested that recolonized worms accelerate the speed of gastrointestinal evacuation.

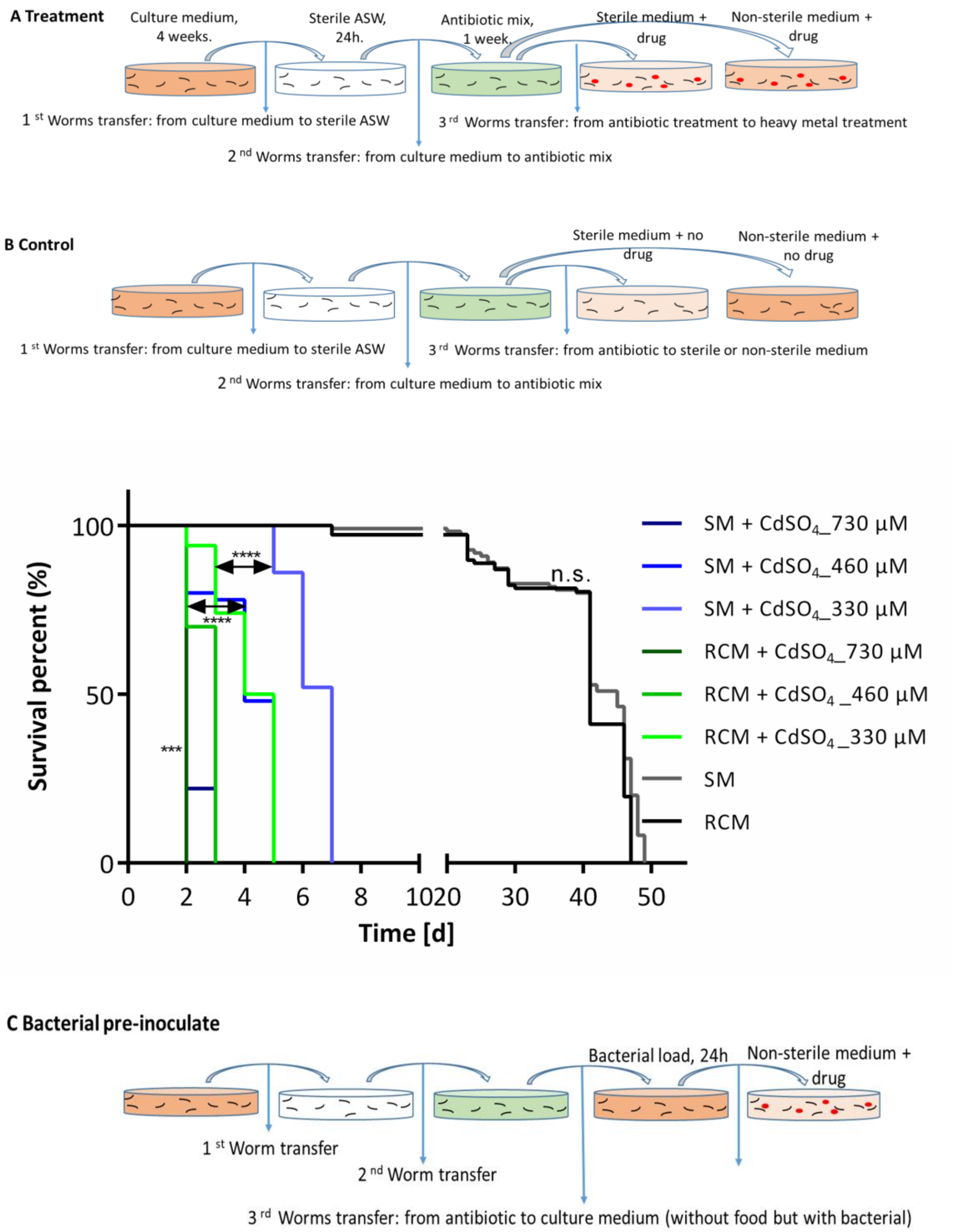
A Treatment
Culture medium, 4 weeks.
Sterile ASW, 24h.
Antibiotic mix, 1 week.
Sterile medium + drug
Non-sterile medium + drug
1 st Worms transfer: from culture medium to sterile ASW
3 rd Worms transfer: from antibiotic treatment to heavy metal treatment
2 nd Worms transfer: from culture medium to antibiotic mix
B Control
Sterile medium + no drug
Non-sterile medium + no drug
1 st Worms transfer: from culture medium to sterile ASW
3 rd Worms transfer: from antibiotic to sterile or non-sterile medium
2 nd Worms transfer: from culture medium to antibiotic mix
Survival percent (%)
100
50
0
****
****
***
n.s.
0
2
4
6
8
1020
30
40
50
Time [d]
SM + CdSO4_730 µM
SM + CdSO4_460 µM
SM + CdSO4_330 µM
RCM + CdSO4_730 µM
RCM + CdSO4 _460 µM
RCM + CdSO4 _330 µM
SM
RCM
C Bacterial pre-inoculate
Bacterial load, 24h
Non-sterile medium + drug
1 st Worm transfer
2 nd Worm transfer
3 rd Worms transfer: from antibiotic to culture medium (without food but with bacterial)

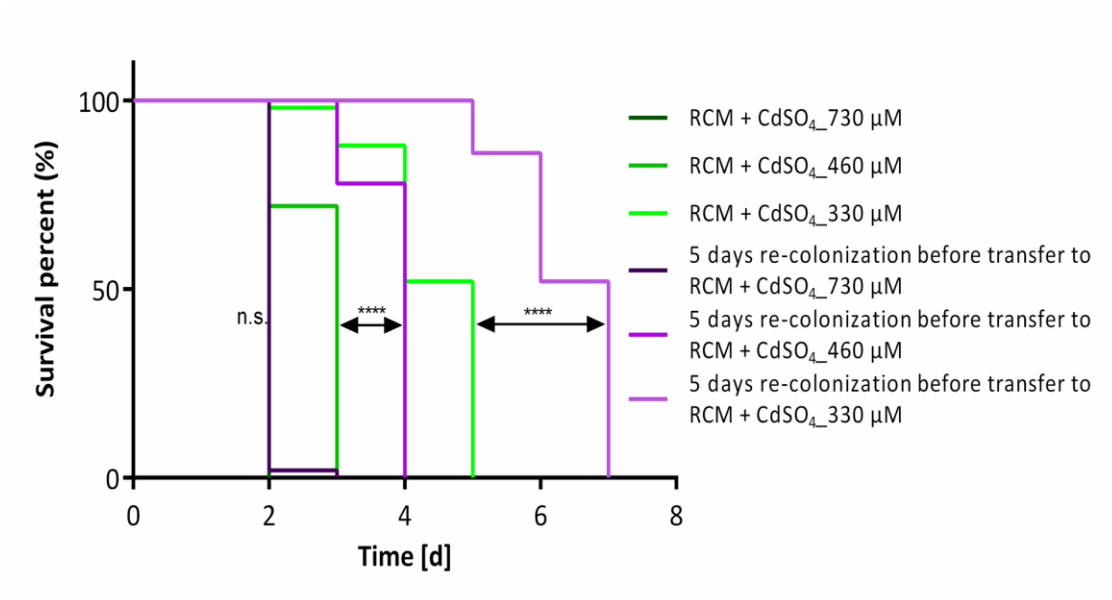

Fig. 21 Survival analyses of Cd^{2+} treated animals. A, B and C show the experimental design. In A, animals incubated with antibiotics for one week were transfered back to sterile (SM) and non-sterile medium (NSM) with drug treatment. B shows the respective control. C, prior to the drug treatment the animals were pre-recolonized (PreRC) with their native microbiome. In the treatment group animals incubated with 3 different concentrations of Cd^{2+}, while SM and NSM control groups without any drugs. SM, sterile medium; RC recolonized worms; GF, germ-free worms; PreRC, pre-recolonization. Asterisks denote significant differences from non-drug control (Log-rank (Mantel-Cox) Test, ****, $p < 0.0001$).

3.2.5 Bacterial load relative to toxicological treatment

The total bacterial DNA loads of worms were measured using real-time quantitative PCR, which is based on the amplification of universal segments of the 16S rRNA genes. As expected, the bacterial load was significantly reduced after five days of starvation (Fig. 22, MW vs. SMWs_5 d, $p < 0.0005$). In all heavy metal treatment groups, substantially increased bacterial DNA loads were detected only in two higher concentrations of the $CdSO_4$ treated groups (Fig. 22, $CdSO_4$_730 µM vs. SMWs_5 d, $p < 0.0001$; $CdSO_4$_460 µM vs. SMWs_5 d, $p < 0.0001$). Bacterial loads in the xenobiotic treatment groups were not significantly changed in general, except for Bis treated groups (Fig. 22, Bis_2000 µM_5 d vs. SMWs_5 d, $p < 0.0001$; ABD_220 µM_2 d vs. SMWs_5 d, $p < 0.0001$). The worms' bacterial loads differ from each other in different environments.

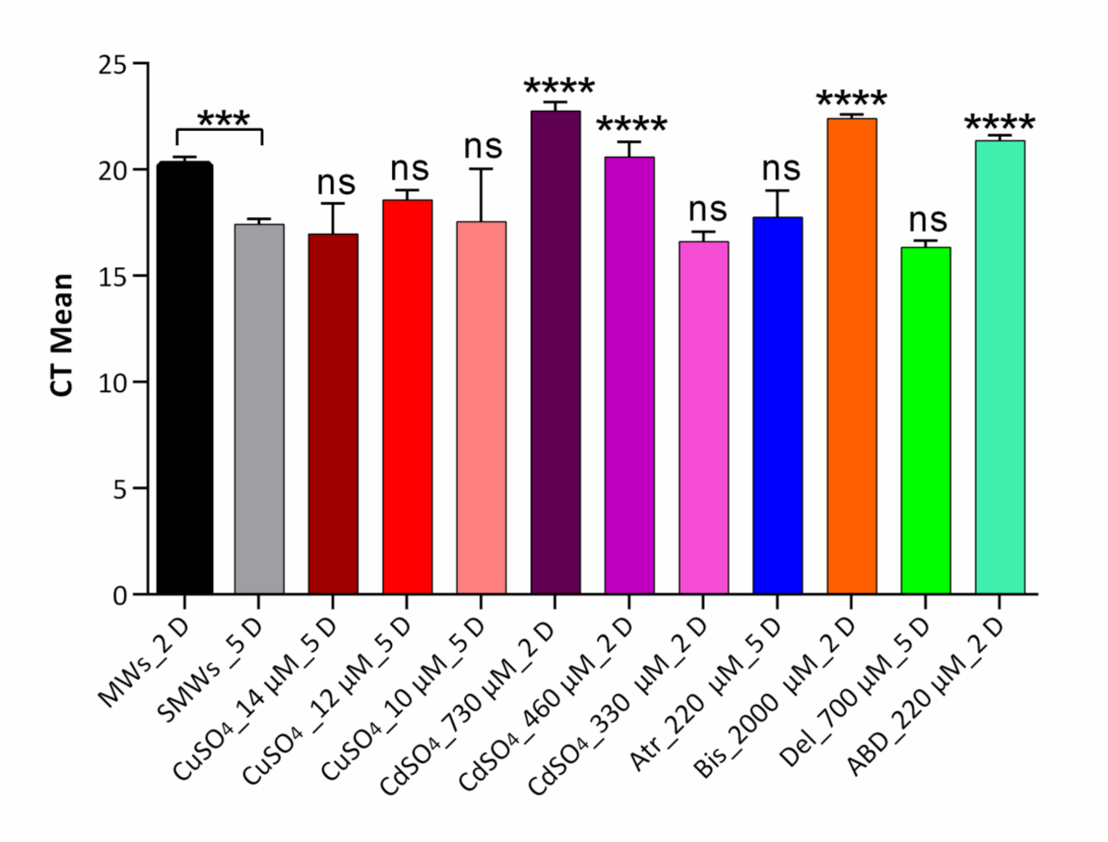

Fig. 22 Bacterial loads in response to treatment. qPCR was performed by using universal bacterial V2 primer 27F/338R. MWs, mature worms; Atr, atrazine; Bis, suberoyl bis-hydroxamic acid; Del, deltamethrin; ABD, Atr, Bis and Del mixture under ration 1:1:1. Asterisks denote significant differences from 5 days starvation mature worms (MW – 5 d starvation) (***, $p < 0.0005$; ****, $p < 0.0001$).

3.3 Deep sequencing-based transcriptome profiling analysis of pathogen-challenged bacteria reveals insight into the immune and wound repair response in *M. lignano*

3.3.1 *Vibrio (Listonella) anguillarum*, *Planococcus citreus* and *Vibrio alginolyticus* (LPV) reduced the worms' lifespan and its wound repair

We established an assay that generates wounded worms and examining five points for the animal's posterior regeneration (cut off from female opening) (Fig. 23 A). Without bacterial contact and food supply, the wounded *M. lignano* can survive for about 50 days (Fig. 23 B). When animals suffer from pathogenic bacteria, the lifespan is greatly reduced. The LPV-induced animals were able to survive eight days, which was significantly shorter than in the LPV-free group (Fig. 23 B, Cut_LPV vs. Cut_LPV free, $p < 0.0001$). Under LPV infection, the lifespan of non-cutted worms was two days longer than that of the cutted worms (Fig. 23 B, Uncut_LPV vs. Cut_LPV, $p < 0.0001$). However, the lifespan still dramatically decreased compared with LPV-free groups (Fig. 23 B, Uncut_LPV vs. Cut_LPV free, $p < 0.0001$).

LPV presenting was not only a disadvantage to the animals' survival but also influenced their wounding repair. Under both LPV-confronted and LPV-free conditions, wounded animals can quickly repair the affected tissues (Fig. 23 C). Without pathogenic bacteria, animals were capable of regrowth a functional female opening after 2 days, which is 1 day earlier than seen in the LPV-induced groups. During the observation, the LPV-free injured animals kept dividing, differentiating and regenerating the tail plate cells. In the end, generating male opening holes and completed a functional tail plate in four days (Fig. 23 C). However, the LPV-induced confronted animals stopped repairing the wounding tail plates in the first 24 hours. An apparently shrink of the body size has been found in LPV confront animals after the 3rd day (Fig. 23 D). In addition, animals lost their reproductive ability. During three weeks of observation, hardly any offspring of survivors of LPV-induced wounding animals was found, whereas a 100% hatching rate was obtained in the wounding groups (Fig. 23 E).

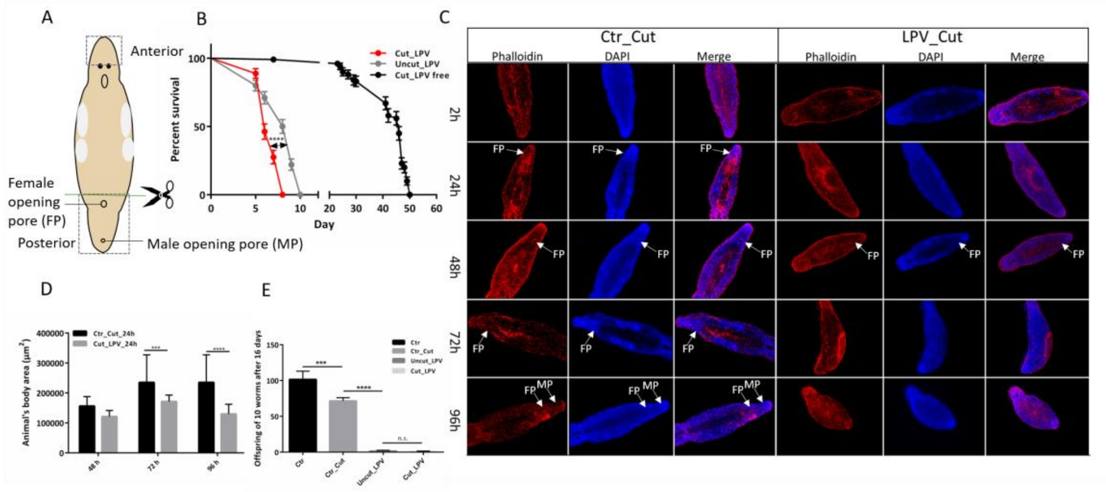

Fig. 23 LPV confronted animals have a shortened lifespan, an unsuccessful wounding repair, reduced body size, and lower reproductive capacity. A Schematic diagram of generating wounding *M. lignano*. Animals were amputated before the female opening pore (FP). B Survival curves of LPV infected wounding (Cut_LPV, red line) and non-wounding (Uncut_LPV, grey line) *M. lignano* in comparison with the control wounding group (Ctr_Cut, black line). C Phenotypes of the worms infected with LPV. White arrows show the female opening (FP)and male opening (MP). D Animal's body area changes after 48h, 72h, and 96h treatment. E LPV infected animals decreased the number of offspring during 16 days. Two-tailed Student t-test was performed. 5 repeats and mean ± SD are shown. * $p < 0.05$, ** $p < 0.01$, *** $p < 0.001$ and **** $p < 0.0001$.

3.3.1 Changes of proliferation in the LPV treatment group

The worms' wounding response requires neoblasts, a proliferating cell population containing pluripotent stem cells (Wagner, Wang, & Reddien, 2011). Accordingly, numerous wounding repair failures were explained by proliferation defects (Scimone, Cote, & Reddien, 2017). Based on our observations, a failure of wounding repair was detected in LPV-confronted animals. We, therefore, tested general proliferation dysfunction in wounded animals. Large (>50 μm^2) and clustered cell types were identified as type I (donated as "I"); separated and smallest (10-50 μm^2) cell types were identified as type III (donated as "III"); single and middle-size (<10 μm^2) cell types were grouped as type II (donated as "II") (Fig. 24 and Fig. 25). The distribution of proliferating cells in wounding *M. lignano* follows several phases. There is an initial "wound response", proliferation occurs rapidly in the anterior region (0-2 h post-wounding). During this phase, type I cells are mainly expressed and centralized before the “eyes” region (Fig. 26). Subsequently, additional events presented that collectively comprise the “tail regenerative response” (~24-72h post-wounding, Fig. 25). This phase includes persistent neoblast proliferation and accumulation at wounds and sustained generating of new tissues during small injury repair and tissue turnover. During this phase, type I cells are present near to the wounded tail plate (Fig. 24). Soon after these 2 phases, the large accumulated proliferation cells were reduced/disappeared and instead with smaller separated proliferation cells and cell types mainly presented as type II (Fig. 24). Interestingly, type III cells, which are generally distributed in the main body part, rarely exist in the wounding tail plate (Fig. 25).

In both, anterior and posterior regions, in general, the LPV-treated animal expresses more type I cells, while LPV-free animals have more type II cells. LPV-free animals accumulated type I cells in the anterior region in the first 2 h after amputation (Fig. 25 A2, Ctr_Cut_2h vs. Cut_LPV_2h, $p=0.0389$). While in the following time (48-96h), LPV confronted animals have more type I cells (Fig. 25 A2, Ctr_Cut_48h vs. Cut_LPV_48h, $p=0.003$; Ctr_Cut_72h vs. Cut_LPV_72h, $p < 0.0001$; Ctr_Cut_96h vs. Cut_LPV_96h, $p < 0.0001$). Type I proliferating cells also found in the posterior region of LPV-induced animals (Fig. 25 B2, Ctr_Cut_24h vs. Cut_LPV_24h, $p=0.0264$; Ctr_Cut_48h vs. Cut_LPV_48h, $p=0.0292$; Ctr_Cut_72h vs. Cut_LPV_72h, $p=0.0096$). There was an opposite expression of type II cells in both anterior and posterior regions during the 48-96 h period (Fig. 25 A2 and B2, Ctr_Cut_48h vs. Cut_LPV_48h, $p < 0.0001$; Ctr_Cut_72h vs. Cut_LPV_72h, $p < 0.0001$; B2, Ctr_Cut_48h vs. Cut_LPV_48h, $p < 0.0001$; Ctr_Cut_72h vs. Cut_LPV_72h, $p < 0.0001$). As the LPV-treated animals were unable to repairing the wounded region, thus, newly generated tissues of the control groups may not exist in the pathogen-induced groups. Therefore, besides the anterior and posterior regions, we additional add the female pore area as a normalizing region, which regenerated in both groups, to clarify the status of proliferating cells. Besides 72h post wounding, where more type I cells were found in the LPV-treated groups, proliferation type I cells in all the other groups were not significantly changed (Fig. 25 B3, Ctr_Cut_96h vs. Cut_LPV_96 h, p=0.0195). Control groups possessed more type II cells around female openings 2 h after amputation, while after 24 h, LPV-treated groups exceed this value compared with the control groups (Fig. 25 B3, Ctr_Cut_2h vs. Cut_LPV_2h, p=0.0026; Ctr_Cut_24h vs. Cut_LPV_24h, p=0.0005). 72h and 96h groups had comparable numbers of type II cells (Fig. 25, Ctr_Cut_72h vs. Cut_LPV_72h, p=0.02526; Ctr_Cut_96h vs. Cut_LPV_96h, p=0.2401).

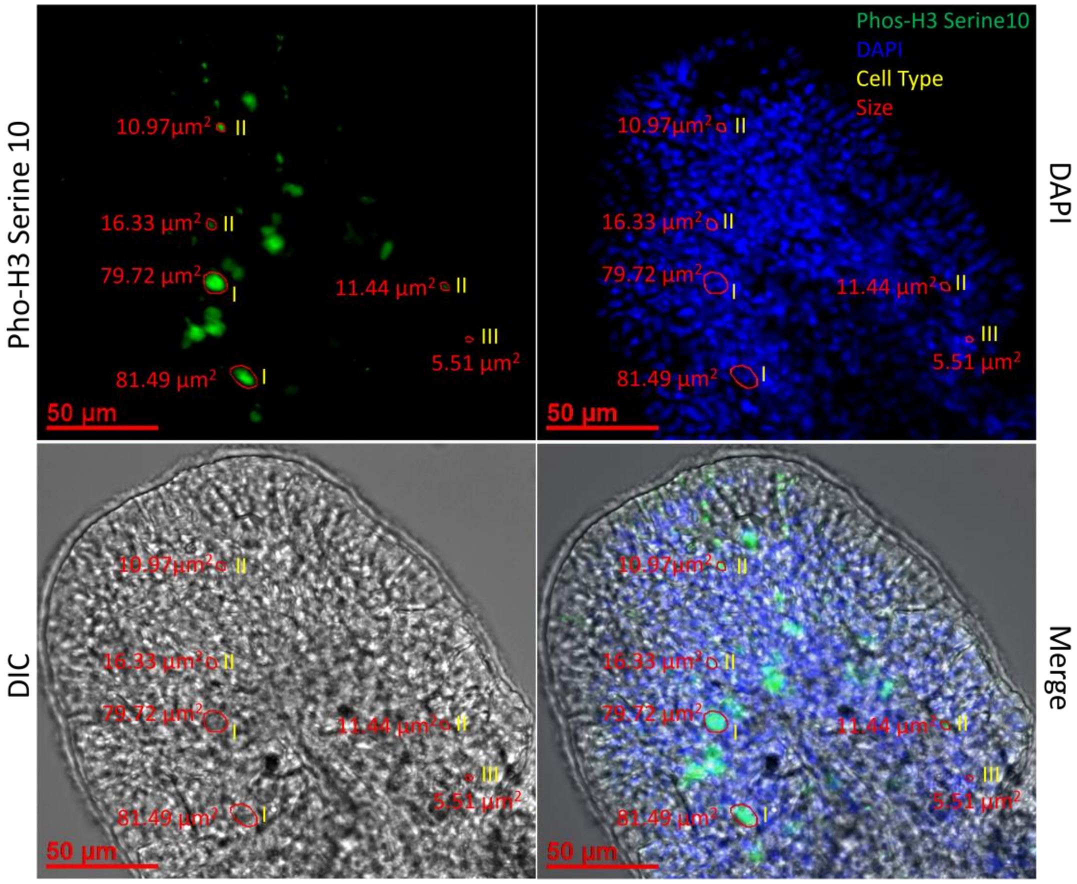

Fig. 24 Types of proliferative cells in *M. lignano*. Three types of proliferating cells can be distinguished. Large (>50 µm^2) and clustered cell types were identified as type I (named "I"); single and middle-size (<10 µm^2) cell types were grouped as type II (named "II"); separated and smaller (10-50 µm^2) cell types were identified as type III (named "III").

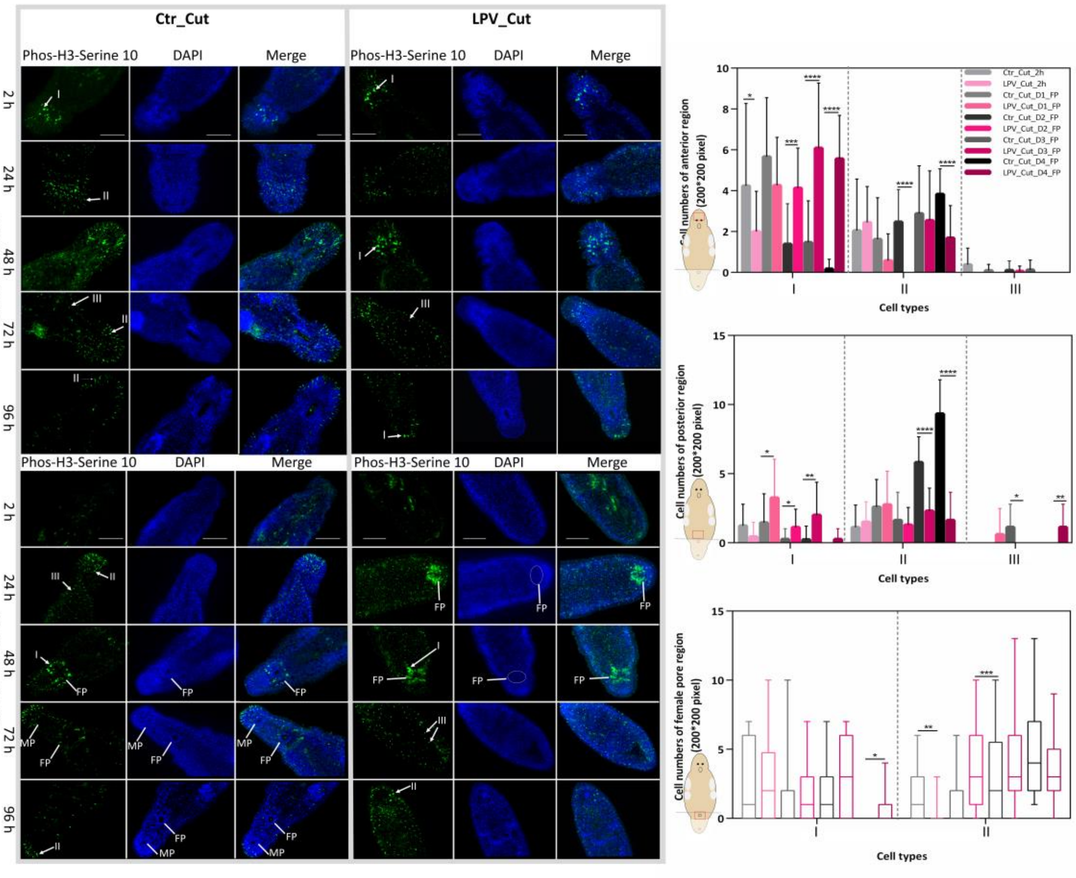

Fig. 25 Changes of the numbers of proliferative cells in Cut_LPV and Ctr_Cut animals. Using immunohistochemistry with phosphorylated histone 3 serine 10 antibodies (Phos-H3-Serine-10) the proliferation cells were labelled (green). Cell numbers were quantified in three categories (Fig. 24). A1 and A2 show the distribution and quantity of proliferative cells in the worms' anterior part and. B1 and B2 show worms' posterior proliferation cell distribution and quantity. B3 Proliferation cell numbers of female opening pore (FP). * $p < 0.05$, ** $p < 0.01$, *** $p < 0.001$ and **** $p < 0.0001$.

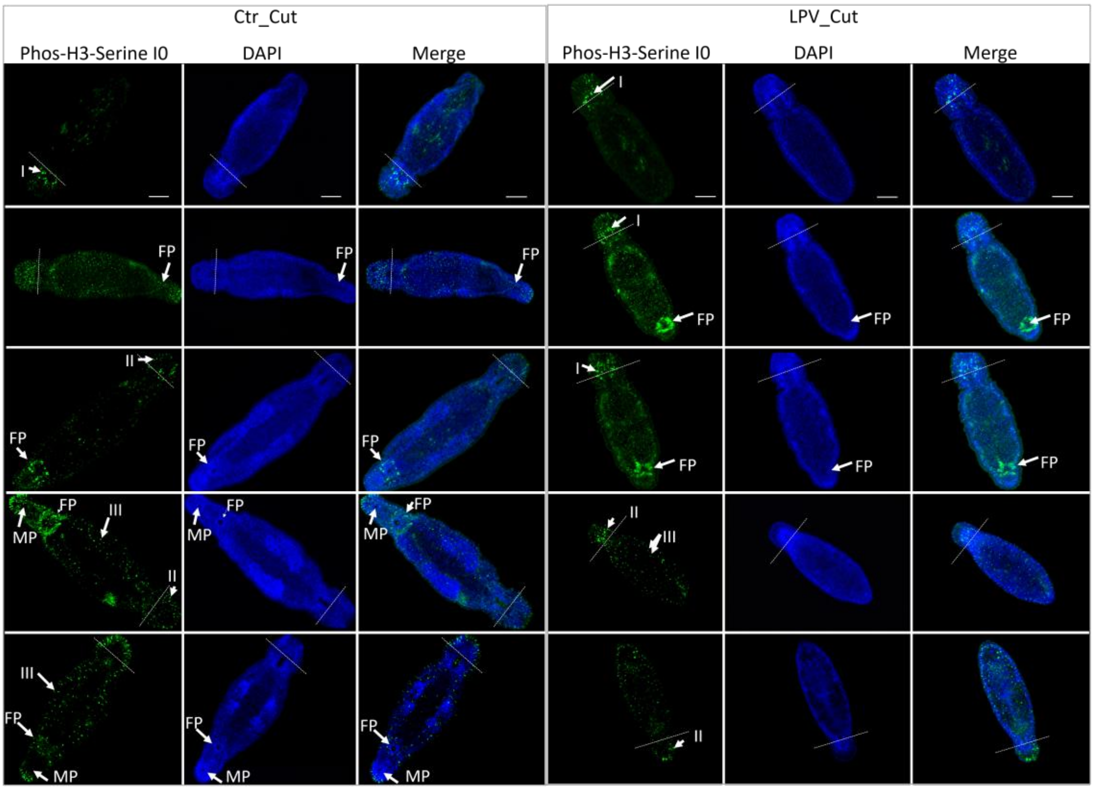

Fig. 26 Overview of the proliferative cell distribution of Cut_LPV and Ctr_Cut *M. lignano*. The dashed line marks the 'eyes' position. 2h post-wounding, type I cells mainly expression and centralized before "eyes". 24h post wounding, type I cells expressed in both anterior and posterior region. ~48-72h post-wounding, type I cells expressed the wounded tail plate. 96h post-wounding, the large accumulated proliferation cells disappear and instead with smaller separated proliferation cells and cell types mainly presented as type II. Cell type III, generally distribution in the main body part.

3.3.2 Functional identification and classification of transcriptionally regulated genes in response to LPV infections

To gain insights into transcriptional changes in *M. lignano* infected by *Vibrio anguillarum* (*L. anguillarum*), *Planococcus citreus* and *Vibrio alginolyticus* (LPV), I conducted pairwise comparisons between libraries to identify the differentially expressed transcripts (DETs) (Table 18 and Table 19). The following types of samples were analyzed: 1) worms isolated without cutting the tail plate denoted as 'noncutting control' (Ctr); 2) cutted worms without LPV treatment denoted 'cutting control' (Ctr_Cut); 3) cutting worms with LPV treatment denoted 'Cutting with LPV' (Cut_ LPV)).

Relative to the certain control, transcripts with greater than 2-fold change and p-value less than 0.001 were considered as differentially expressed. The complete list of DETs with FPKM (fragments per kilobase of transcript per million) values revealed that many unigenes exhibited remarkable changes in mRNA levels in the treatment groups.

Compared with Ctr_Cut, there were 2,472 (1,389 up-regulated and 1,083 down-regulated) transcripts that were significantly changed in Cut_LPV groups (Fig. 27 A). The Venn diagram analysis revealed that 2,323 (76.4%) transcripts were specifically differentially expressed after the infections, while 569 (18.7%) other transcripts were exclusively regulated in the wounded animals (Fig. 27 B). The hierarchical clustering of DETs showed a discrete expression trends relevant to the bacterial infection. I assume that immunity-related genes might be contained in these consistent up-regulation genes after bacterial infection.

To elucidate potential functions of all identified DETs and the pathways involved, the Gene Ontology (GO) enrichment and KEGG analyses were performed further proceed for DETS (Ashburner et al., 2000; Kanehisa & Goto, 2000). GO assignment determined all unigenes functional classifications. In the gene repertoire, more DETs from the LPV induced transcriptome were assigned as binding and catalytic activities in the sorting of molecular function (Fig. 29). Meanwhile, DETs were also enriched in the following GO terms: membrane, membrane part, cell and cell part processes in cellular component, cellular process and metabolic process in biological process (Fig. 29). Enriched GO terms were also analyzed by functional classification based on the organismal systems, genetic information processing, environmental information processing, metabolism and cellular processes (Fig. 29). KEGG classification was performed to analyze putative functions of the PLV induced DETs, which mainly focus into the 20 most enriched pathways (Fig. 30). An obviously functional associated disparity was found among the major functional gene groups. A large proportion of up-regulated genes encoded enzymes involved in the biosynthesis of secondary metabolites, glycan degradation, MAPK signaling pathway, pathogen interaction and pyruvate/tryptophan metabolism (Fig. 31). Other functional gene groups were associated with xenobiotic biosynthesis and metabolism, such as aminoacyl-tRNA biosynthesis, glycerol phospholipid metabolism, amino acid metabolism, ABC transporters etc. (Fig. 31). Based on the principal component (PCA) analysis, the first and second principal components explained 88.52% variance. Ctr_Cut groups were separated from Cut_LPV groups. The hierarchical relationship analysis (metal and ABD treatment data unpublished yet) found a clear cluster among pathogen-induced worms, which is separated from the Ctr_Cut groups (Fig. 32).

In summary, these results suggested that overall gene expression profiles varied between Cut_LPV and Ctr_Cut. For in-depth analysis and BLAST search for the RNA-seq data, we were able to detect numerous infection-related genes. This result showed that *M. lignano* is well suited for a number of different research fields, including basic immune responses and regeneration.

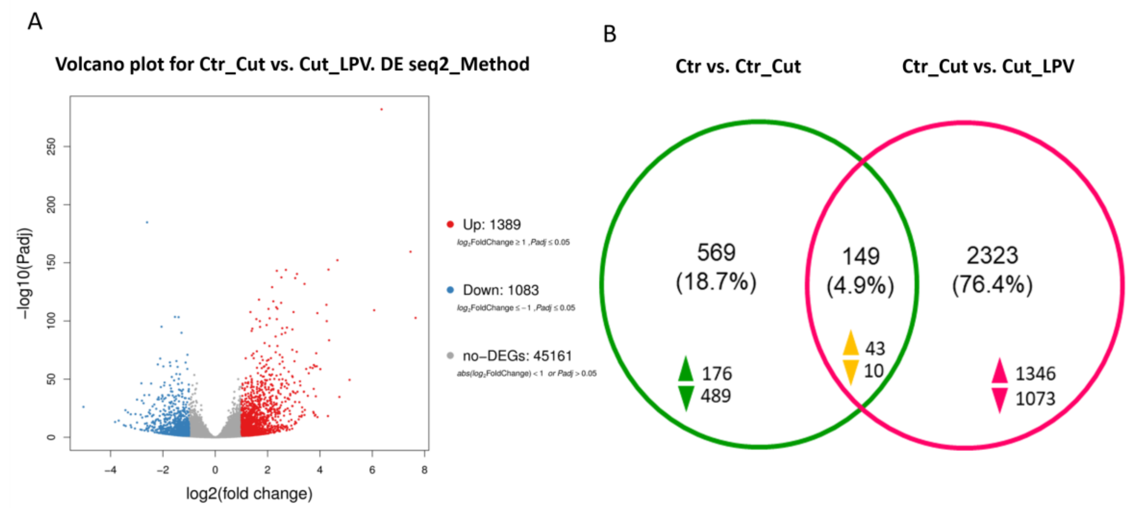

Fig. 27 Analysis of differentially expressed genes (DEGs) between wounded and infected worms (Table). A. Volcano plot for differential expression genes. B Venn diagram showing the shared and unique DETs among noncutting control (Ctr), cutting control (Ctr_Cut) and LPV infected wounding groups (LPV_Cut). The overlapping regions represent genes that are concomitantly regulated in two samples. The directions of transcript level changes are indicated by upward and downward-pointing arrows.

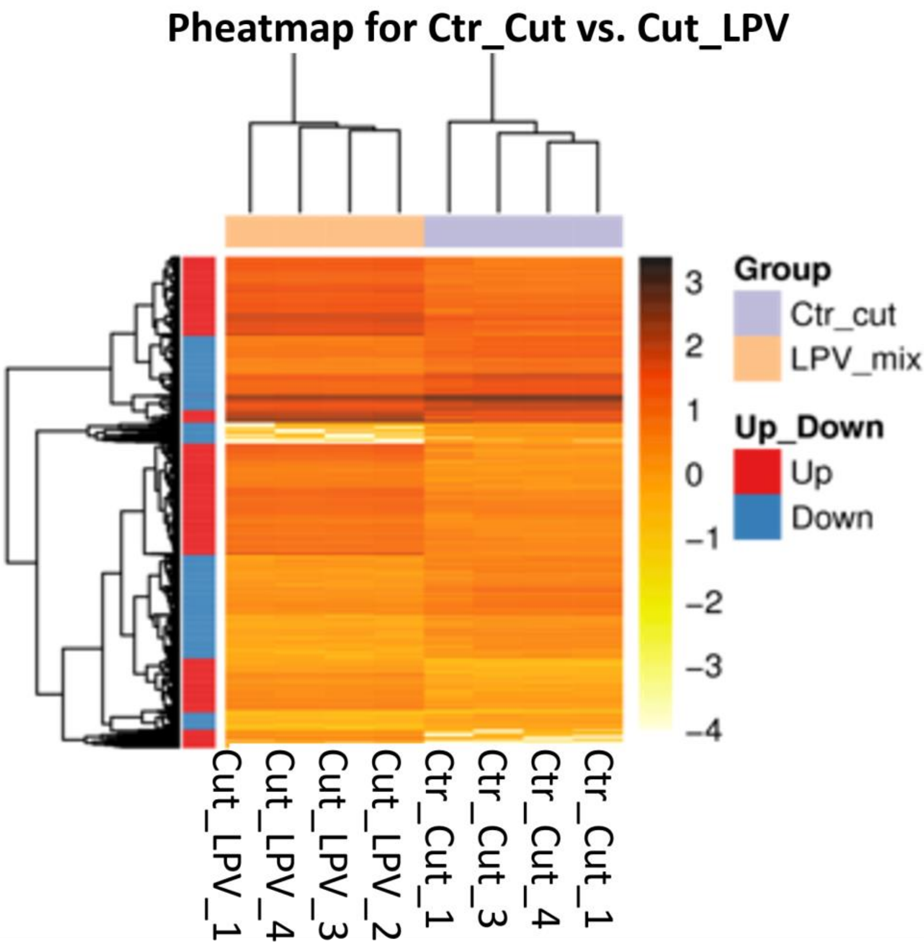

Fig. 28 Heat map clustering of sample replicates showing hierarchical relationships based on overall expression similarity of the transcriptome data from wounded (cut) and infected (LPV) worms.

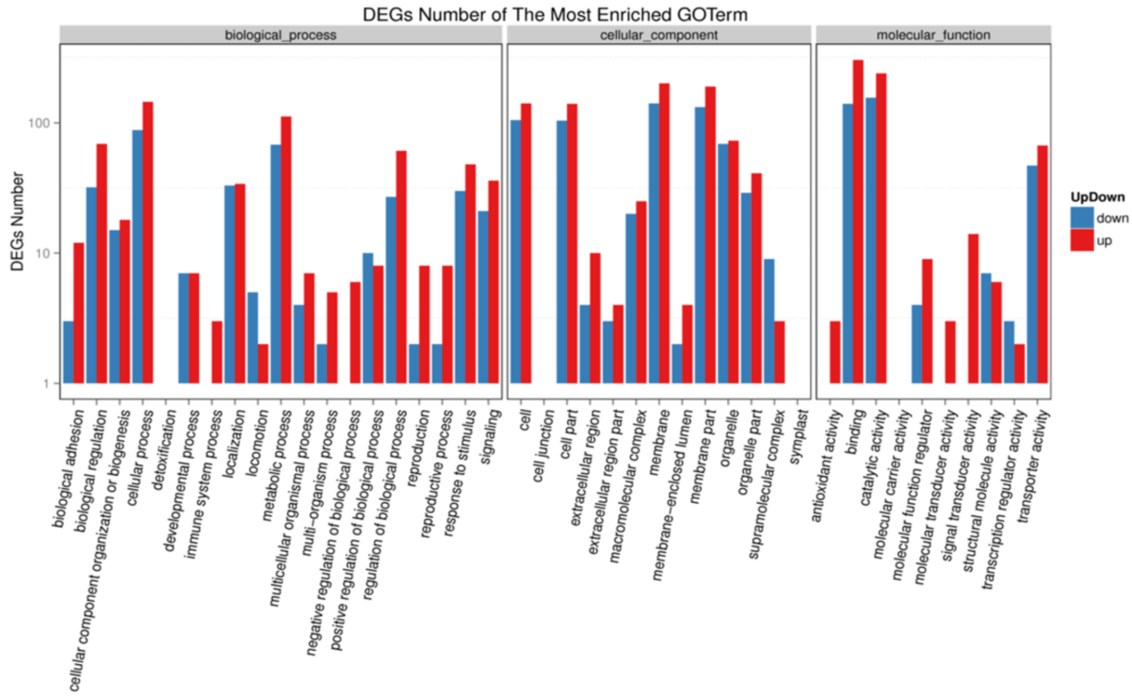

Fig. 29 Gene Ontology (GO) functional classification on DEGs for injured and infected worm. Y-axis indicates the number of DEGs. X-axis represents GO terms. All GO terms are grouped into three major functional categories, namely biological process, cellular component, and molecular function. P-values ≤ 0.05 were considered significantly enriched GO.

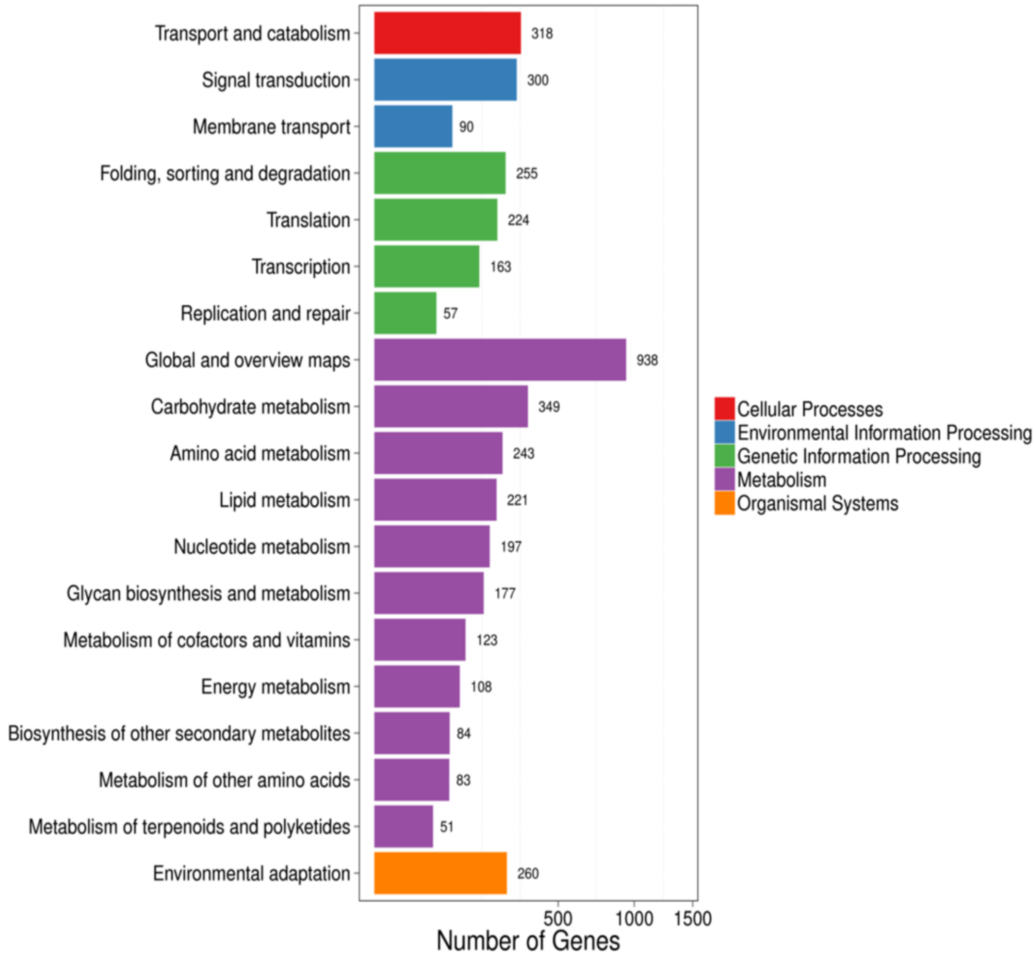

Fig. 30 Kyoto Encyclopedia of Gene and Genomes (KEGG) categories of non-redundant consensus sequences of injured and infected worms. All non-redundant consensus sequences were annotated using KEGG Automatic Annotation Server for pathway information, and about 4,241 consensus sequences were annotated and grouped into 5 functional classes, namely cellular processes, environmental information processing, genetic information processing, metabolism, and organismal systems.

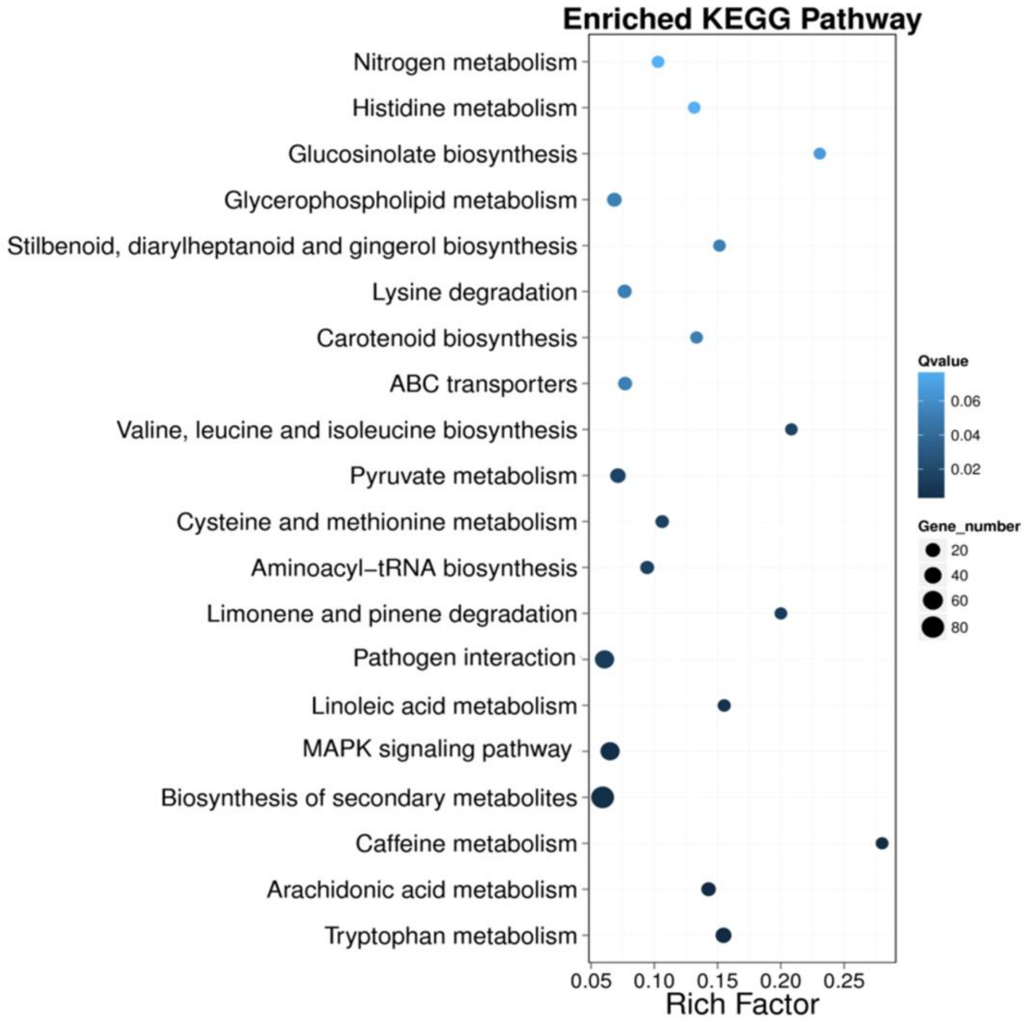

Fig. 31 Enrichment analysis for KEGG pathways database of DEGs. The top 20 regulated pathway were represented by comparing LPV_Cut and Ctr_Cut are shown.

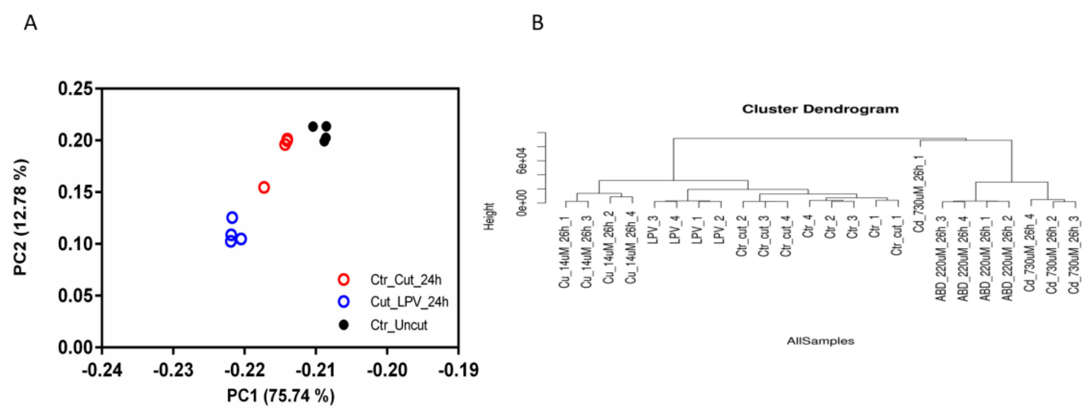

Fig. 32 DEGs clusters and hierarchical relationships of infected and injured worms. A Principal component analysis showing clustering of sample replicates and relative variance among samples across PC1 and PC2. B Hierarchical relationship analysis compared DEGs in the transcriptomes and

found clear clusters among LPV_Cut, Ctr_Cut and Ctr (uncut worms). Cu, $CuSO_4$; Cd, $CdSO_4$; PLV, *Vibrio (Listonella) anguillarum*, *Planococcus citreus* and *Vibrio alginolyticus* bacterial mix under the ration 1:1:1. ABD, Atr, Bis and Del mixture under ration 1:1:1.

3.3.3 Annotation of immune-related genes and pathways of *M. lignano*

Multiple pathways are involved in the response to pathogens in *M. lignano*. Animals react to PLV infection by at least three genetic pathways, which can be summarized into two major groups. The first group consists of the (1) NF-Kappa B and IMD signaling pathways, which are necessary for innate immunity in many organisms; (2) JNK and p38 MAP kinase pathways comprising many pathogen-responsive genes (Fig. 33). The signaling between local and systemic immune pathways might be relevant for the host to protect from pathogen bacterium breach the epithelial barrier (Tang, Kambris, Lemaitre, & Hashimoto, 2008).

3.3.4 The NF-Kappa B pathway

In flies and mammals, Toll/IL-1 (TIR) and tumor necrosis factor (TNF) receptors are both responsible for the detection of exogenous and endogenous pathogen-associated molecular patterns. Following stimulation, TLR receptors (except TLR3) recruit Myd88 through their cytoplasmic receptor (TIR) domain (Martin & Wesche, 2002). In *M. lignano*, IL-1R and TNF-R1 were both found similarly as activation phosphorylase through recruiting interleukin1 and 4 receptor-associated kinase (IRAKs 1/4) and tumor necrosis factor receptor-associated factor (TRAF) 2, 5, 6 (Fig. 28, A1 and A2). This receptor complex generates a transient signaling platform for the recruitment of the transforming growth factor-beta activating Kinase 1 (TAK1) (Fernando, Kounatidis, & Ligoxygakis, 2014). The TAK1 complex mediates phosphorylation of the IκB kinase α (IKBα). In turn, the catalytic IKBα phosphorylated the IκB and leading to NF-κB activation (Zandi, Rothwarf, Delhase, Hayakawa, & Karin, 1997). Recent biochemical evidence had indicated that TRAF6 possesses ubiquitin ligase activity (Lamothe et al., 2007) and it could initiate auto-ubiquitination in *M. lignano*.

3.3.5 The IMD signaling pathway

Binding of PGN to its cognate receptors leads to the recruitment of the caspase 8 homolog Dredd to generate signaling complexes that start the IMD pathway. Dredd becomes activated through the E3-ligase inhibitor of apoptosis 2 (lap2) (Meinander et al., 2012) which associates with the Effete (R. Zhou et al., 2005). Once activated, Dredd cleaves IMD, removing a 30-aa N-terminal fragment, and creates a novel binding site for lap2, which could ubiquitinate IMD (Paquette et al., 2010). This leads to the recruitment and activation of the Tab2/Tak1 complex, which is responsible for the phosphorylation and activation of the JNKK complex. In *Drosophila*, Tab2/Tak1 could active Relish by the phosphorylation of multiple sites at Ankyrin (Silverman et al., 2000). I found a regulated expression of Ankyrin in *M. lignano* but not for Relish. Like in mammals, the worm's IMD pathway bifurcates into the JNK signaling pathway (Delaney et al., 2006). *M. lignano* activator protein1 (AP-1) transcriptional complex includes Jra to initiate gene expression of wound repair and stress defense response. Lap2 and AP-1/ Jra were significantly up-regulated in both qPCR tests and RNAseq analyses (Fig. 28, B1 and B2). While the Tak1 gene, which was greatly increased in the RNAseq data, was not overexpressed in qPCR studies of *M. lignano* (Fig. 33 B2).

3.3.6 JNK and p38 MAP kinase pathway

JNK and p38 MAP kinase pathway are major intracellular signal transduction pathways, which are crucial in many cellular processes such as cell growth, differentiation, development, cell cycle, survival, and cell death (Ravingerová, Barančík, & Strnisková, 2003). These pathways consist of cascades of kinases, consisting of the extracellular signal-related kinase (ERK), p38 kinase (p38), the big MAP kinase 1 (BMK1/ERK5), mitogen-activated protein kinase (MAPK) and the c-Jun N-terminal kinase (JNK) (Xia, Dickens, Raingeaud, Davis, & Greenberg, 1995).

Infected worms are able to allow TNF receptor-associated ASK1 phosphorylation, resulting in the activation of MAPKK3. MAPKK3 could activate MAPKK and then phosphorylating and activating a MAP kinase and activated MAPKs (Pimienta & Pascual, 2007), which could phosphorylate numerous substrate proteins, such as MSK1/2, Cdc25b, and MAFKAFK, resulting in regulation of various cellular activities (Fig. 33 C1 and C2). Actually, two MAP kinases, namely MAPKK3 and MAPKK4, with similarity extracellular or intracellular stimuli, were significantly activated seen in RNA-seq analysis (Fig. 33 C1).

MAPK could interact with JNK activation. In LPV-induced *M. lignano*, protein residue directed serine/threonine kinases JNK were significantly up-regulated (Fig. 33 C2), which indicated the activation of JNK pathway. Interestingly, the growth arrest and DNA damage-inducible 45 proteins (DADD45), which has been implicated in the regulation of many cellular functions including DNA repair, cell cycle control, was apparently up-regulated in both qPCR and RNAseq analysis (Fig. 33 C2).

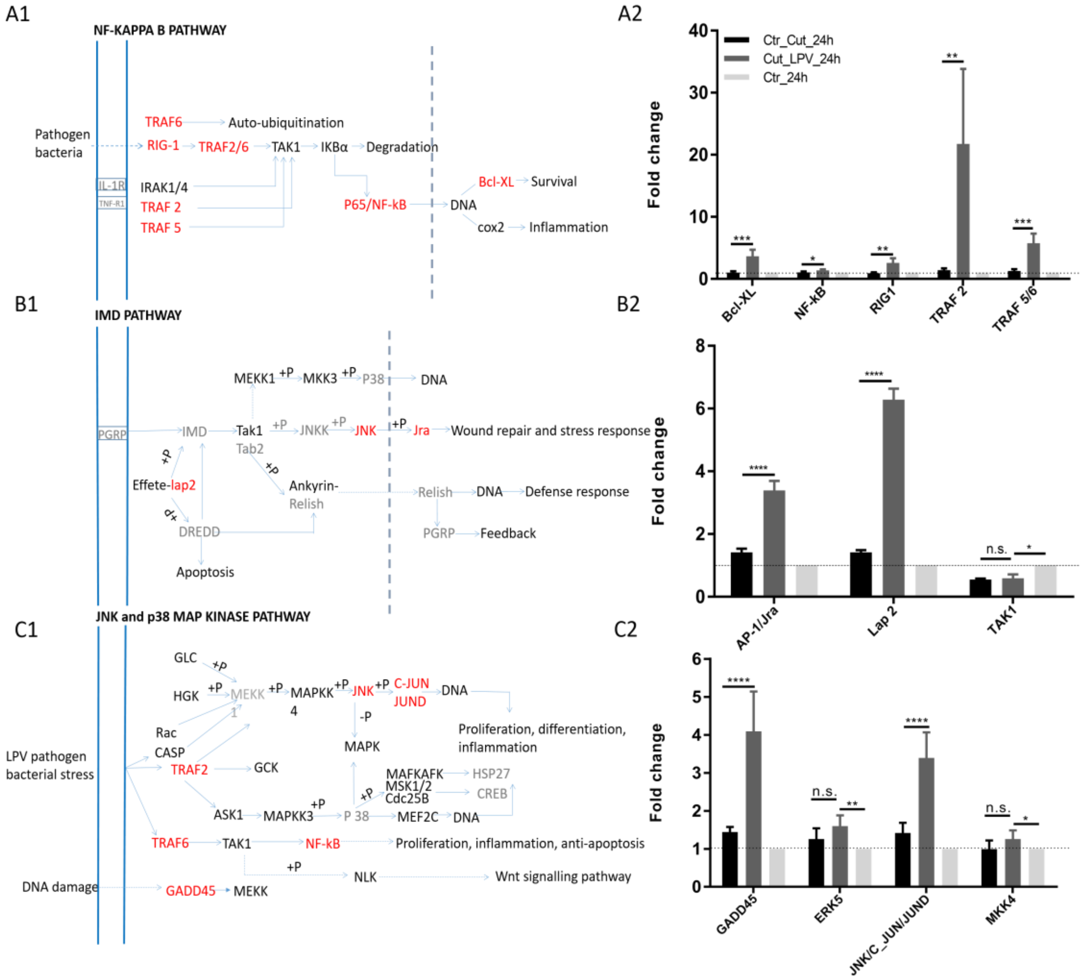

Fig. 33 Putative immune signaling pathways in the wounding response of *M. lignano*.. The putative signaling pathway of *M. lignano* was constructed base on knowledge of NF-kB signaling in invertebrate species. The black fonts shown in the pathways are significant regulated genes base on RNAseq results; the red fonts indicate significant differences also supported by qPCR; the grey fonts show genes that are not significantly regulated.

3.3.7 Other putative immune/stress response genes in *M. lignano*

Compared to wounding control, Serine/threonine kinase (*RSK*2) and *Actin* were greatly up-regulated in the pathogenic bacteria confronted animals (Fig. 34). *RSK*s are downstream of the Ras-extracellular signal-regulated kinases (ERKs)/mitogen-activated protein kinases (MAPKs) signaling cascade. It regulates many substrates involved in cell survival, growth, and proliferation (Anjum & Blenis, 2008). *Actin* is part of a gene family, which encodes a number of structurally related proteins and it also regulates the contractile potential in muscle tissues (Herman, 1993). It is crucially important in the function of controlling the shape and the motility of the cell. The transcriptional induced actin may contribute to repair the damaged structure of the tissue. Ribosomal protein S6 kinase (*S6K*) and *Rho* GTPases (*Rho*) are significantly upregulated in LPV-confronted groups based on RNAseq analysis. While they are not verified by our qPCR result (Ctr_Cut vs. Cut_LPV, RS6, 0.6508; *Rho*, p=0.2508). The protein translated by *S6K* can interact with the actin cytoskeleton and activated the catalytic ability of Rho GTPases (Ip, Cheung, Ngan, & Wong, 2011). The *Rho*-kinase is a downstream effector of *Rho* GTPase signaling that regulates actomyosin dynamics in numerous cell types (Rao, Pattabiraman, & Kopczynski, 2017). Some studies had demonstrated that *Rho* induced a contractile actin-myosin filament network and distinctive effects of *Rho* activation on the organization of the actin cytoskeleton (J. H. Hartwig et al., 1995; Ridley, Comoglio, & Hall, 1995). The *Rho* GTPases are well known for their roles in regulating cell migration and also contributed to a variety of other cellular responses. Interestingly, *Rac1*, another *Rho* GTPase, showed significantly reduced expression in LPV confronted groups. *Rac1* is a central regulator of F-actin organization at the plasma membrane. Activation of *Rac1* could translocate from endosomes to cell borders, which contributes to endothelial barrier formation (Murakami et al., 2019). Marcos-Ramiro et al. reported that high expression of *Rho* inhibits the translocation of *Rac1*, resulting in impaired barrier restoration (Marcos-Ramiro et al., 2016).

In addition to comparing gene expression levels between Cut_LPV and Ctr_Cut, I also compared these two groups with non-wounded animals. Elevated expressions have been recognized for e.g. fibroblast growth factor receptor (FGFR), gram-negative bacteria binding protein3 (GNBP3), Scr-homology 2 domain-containing protein tyrosine phosphatase (SHP2) and on/off switch gene *k-Ras* (Fig. 34).

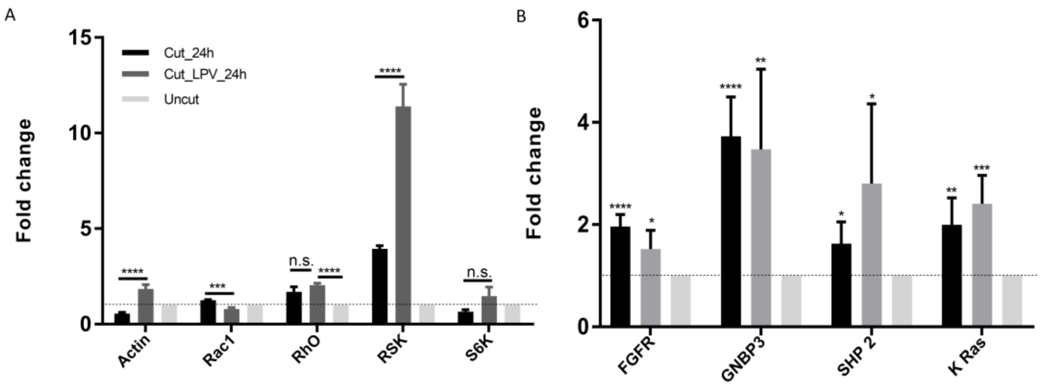

Fig. 34 Transcript levels of genes putatively associated with wound repair. A, Comparison of gene expression between wounded animals with LPV-induced wounded animals. B, Comparison of gene expression between cutting groups (Ctr_Cut) with non-cutting groups (Ctr). Unpaired two-tailed Student's t-test, statistical analysis of significant difference were defined as n. s. (not significant), *, $p < 0.05$, ***, $p < 0.01$, ****, $p < 0.001$ and ****, $p < 0.0001$.

4 Discussion

4.1 Abiotic stressors induced oxidative responses and microbiome dysbiosis of *M. lignano*

Copper frequently exists *in vivo* as a cupric (Cu^{2+}). It is considered as a crucial mineral ion necessary for various biological processes (Divertie, Owen Jr, Barham, & Ludwig, 1982; Su et al., 1982). For instance, Cu^{2+} is necessary for cytochrome c oxidase activity, which can reduce oxygen to water, the inevitable step in mitochondrial respiration. It is also present in copper, zinc-superoxide dismutases (Cu, Zn-SOD), which clear free radical superoxide (Gaetke, Chow-Johnson, & Chow, 2014). Non-specific Cu^{2+} binding to thiol enzymes can regulate the catalytic activities, *e.g.* Cu^{2+} could oxidize and couple with some amino acid residues of P_{450} monooxygenases (M. Letelier et al., 2009). In addition, copper chaperones help to reduce the existence of unbound (free) Cu^{2+} from participating in cellular redox reactions (Burkitt, 2001; Evans & Halliwell, 1994) and guarantee the transport of copper ions to certain target proteins (Boal & Rosenzweig, 2009; Fields, Lewis, & Bureau, 2001; Prohaska, 2008). The quantity of copper absorption is relatively low and animals strictly balance the copper concentrations in the body by either reducing absorption or inducing excretion.

However, Cu^{2+} toxicity is possible and result from over-exposure caused e.g. environmental contaminations. Gray et al. investigated hepatoma cells (HepG2 line) and found that concentrations of 16 µM Cu^{2+} led to a 125-fold increase in the cellular copper content (Gray, Suhali-Amacher, & Ray, 2017). Besides interpreting the direct interaction with essential minerals, several mechanisms, notably free radical-induced oxidative damage, have been proposed to explain Cu^{2+}-induced cellular toxicity. As a transition metal ion, copper is able to participate in redox-cycling reactions and contribute to reactive oxygen species (ROS) formation, which in turn modifies the structure and/or function of important biomolecules (Halliwell & Gutteridge, 1984; Lippard, 1999). As only one electron is needed to transform Cu^{2+} to Cu^{+}, the reduction reaction is easily processed. Cu^{+} is involved in the production of hydroxyl radicals (Huang et al., 1999), which is one of the most powerful oxidizing radicals available in biological systems. The hydroxyl radical is capable of triggering oxidative damage to unsaturated fatty acid and amino-bearing carbon protein (Burkitt, 2001; Chow, 1991; M. E. Letelier, Sánchez-Jofré, Peredo-Silva, Cortés-Troncoso, & Aracena-Parks, 2010; Powell, 2000). These toxicological effects are due to excessive Cu^{2+}. Moreover, Cu potentially increases the risks of oxidation of bases and DNA strand breaks (Buettner, 1993; Hayashi et al., 2000; Kawanishi, Inoue, & Yamamoto, 1989; Liang & Dedon, 2001).

Unlike Cu, Cd is a nonessential metal, with no proven evidence for an association with biological processes. High concentrations of Cd are deleterious to cell proliferation, differentiation and apoptosis (Rahimzadeh, Rahimzadeh, Kazemi, & Moghadamnia, 2017). Hartwig et al. (A. Hartwig et al., 2002) suggested that Cd influences mitogen stimulates cell proliferation, inhibits apoptosis, and DNA repair (Templeton & Liu, 2010). It does this by inducing damage to DNA, cell membranes, and proteins or by inhibiting different types of DNA repair (Yuan, Yang, & Li, 2016). The negative effects of Cd may interfere with the generation of ROS and DNA repair mechanisms. Cd exposure potentially results in chromosomal deletions and mutations, which in turn leads to chromosomal aberrations (Joseph, 2009). Filipic reported that Cd^{2+} does not only enhance the production of $O_2\cdot$, H_2O_2, and $\cdot OH$ but also inhibits the activity of antioxidant enzymes, such as catalase, Mn-SOD, and Cu, Zn-SOD (Filipič, 2012). Moreover, Cd disturbs the cellular calcium homeostasis (Weinsberg, Bickmeyer, & Wiegand, 1995) and the activities of caspases and mitogen-activated protein kinases (MRPKs), therewith indirectly triggering apoptosis in cells (Brama, Politi, Santini, Migliaccio, & Scandurra, 2012).

Both Cu and Cd can induce ROS production and give rise to severe oxidative stress. The direct and indirect effects caused by Cu^{2+} and Cd^{2+} intoxications can lead to the observed reduced lifespan and fitness of these animals. In the present study, metal ion treated animals show a reduced physical activity that comes along with a shorter lifespan. The lower movement might be a result of energy allocated for metal and ROS detoxification. ROS generation affects the function of the electron chain on the mitochondrial membrane, which influences ATP generation. Cadenas (Cadenas, 2018) reported that proton leaks will produce heat instead of ATP and cause substantial energy dissipation. This waste energy accounts for up to 25% of the basic metabolic rate. Since mitochondrial oxidative phosphorylation is incompletely coupled, the protons were returned back to the mitochondrial matrix without ATP synthesis. As a consequence of this malfunctioning, ROS can be produced in higher quantities and these ROS will affect the functioning of the mitochondria. The process is like a snake biting its tail. The less functioning of mitochondria will, in turn, result in less ATP generation. Also, there are some studies that show a direct relationship between superoxide anion production and occurrence of proton leaks, which would aggravate the problem of ATP production and eventually lead to apoptosis (Cadenas, 2018; Cheng et al., 2017; Yang et al., 2017; W. Zhang et al., 2017). My DHE staining results imply an increased production of $O_2\cdot$ after metal treatment. This correlation might explain the attenuated activity due to energy loss. Meanwhile, increased intracellular accumulation of Cd^{2+} may also directly affect neuronal function. Kwakye et al. (Kwakye et al., 2019) demonstrated that Cd^{2+} exposure could cause neurotoxicity and neurodegeneration (Weinsberg et al., 1995). This may explain abnormal behaviors that can be observed in long time metal-induced worms, which lost light sensitivity and kept rotating constantly (results not shown). The results obtained for the programmed cell death showed differences between Cu^{2+} and Cd^{2+} exposure, while we have no obvious explanation for this observation. I can speculate that Cd^{2+} induces neurotoxicity by disturbance of the cellular Ca^{2+} homeostasis, leading to abnormal behaviors (rotating) and loss of sensory function (light sensitivity). Qi et al. suggested that excessive ROS lead to mitochondrial membrane potential dissipation and promote the release of apoptotic factors from mitochondria (Qi, Yao, Tian, & Wang, 2018).

The measurement of regular ROS production in mitochondria give values from 0.25-11% of the total oxygen consumption (Chance, Sies, & Boveris, 1979; Møller, 2001; Møller, Jensen, & Hansson, 2007). These variations are depended on the animal species, tissue, and measurement methods (Aon et al., 2012). Cellular ROS production is initiated in response to metabolic disequilibrium imposed by non-biological and biological stresses and proceeds through similar mechanisms (Mithöfer, Schulze, & Boland, 2004). From the ROS staining experiments, we found increases in ROS production in both Cu^{2+} and Cd^{2+} induced groups. Cd^{2+} can induce ROS through stimulating peroxisome biogenesis and also via altered ROS metabolism of both mitochondria and peroxisomes (Igamberdiev & Lea, 2002; Lopez-Huertas, Charlton, Johnson, Graham, & Baker, 2000). ROS production in Cu^{2+} exposed animals might act through its cellular function or via its effects on antioxidant enzymes (Rout et al., 2013; Song et al., 2014). A high amount of copper-related agents will function as exogenous pro-oxidants that produce ROS, which might lead to the up-modulation of inflammatory markers that further foster pathophysiology (Alsousi & Igwe, 2018).

The harmful effects of excess metals resulting from the formation of ROS in the cell-matrix are, to large extent, prevented by numerous enzymatic antioxidant systems. Superoxide anions are converted to H_2O_2 by a group of metal-enzymes called SODs (Fridovich, 1995). There is a notable evidence that SODs are core components of the biological defense against radical toxicity and keeping the redox balance of the immune system (Marikovsky, Ziv, Nevo, Harris-Cerruti, & Mahler, 2003; Schieber & Chandel, 2014). Among all tested redox enzymes in *M. lignano*, *gstp1* is the only significantly up-regulated gene, which suggests that the corresponding enzyme might be relevant for the physiological reaction towards ROS and metal detoxification. Compared with other redox enzymes, *gstp1* is also the only antioxidant genes showing increased expression in response to other stressors such as hypo/hyper salinity. Rivera-Ingraham et al. (Rivera-Ingraham et al., 2016) speculated that this may relate to bioenergetics costs and it might be less costly to produce glutathione S-transferases (GSTs) compared with other enzymes such as CAT or SOD. Interestingly, another *glutathione-s-transferase* (*mgst1*) is remarkably decreased in all groups, which suggests a complex regulation of the different *glutathione-s-transferases* in *M. lignano* and that disparate functions can be attributed to these diverse genes. *Cox* is another down-regulated gene, which is the last enzyme of the mitochondrial respiratory chain. It is the major oxygen-consuming enzyme in the cell. Regulation of cox assembly involves several reactive oxygen species and redox-regulated steps. Mitochondrial signal increases indicate higher ROS expression. ROS accumulation might affect redox-regulated *cox* biogenesis steps and transcriptional expression of *cox* might later than the ROS expression, which in turn results in a down-regulation of *cox* under transcriptional level.

The membrane transporters, which function in pumping out toxicants, are also generally regulated under stress conditions. The multidrug resistance protein, in humans, belongs to ATP–binding cassette (ABC) transporter that confers resistance to various drugs and mediate hormone secretion, inflammation and redox homeostasis (He et al., 2019; Z. L. Johnson & Chen, 2017; Nagarathinam et al., 2017). Drug transport through transmembrane segments via channel needs ATP expenditure (Hamada & Tsuruo, 1988; Horio, Gottesman, & Pastan, 1988). Tietje et al. confirmed the presence of functional multidrug resistance transporters (*mdr*) in *M. lignano* that have a similar pharmacological profile as those known in mammals (Tietje et al., 2013). Although most tested *mdr* genes showed no transcriptional differences, we still detected a regulated expression of *mdr* genes in some metal-confronted groups. Up-regulated expression was found for *mdr1* and *mdr7* whereas *mdr5* showed a down-regulation. Transcriptional conflicts may come from functional variations. The Multidrug resistance protein1 (MDRP1) transports neutral as well as hydrophobic and amphipathic compounds (Dean, Hamon, & Chimini, 2001). While MDRP7 (ABCC10) is able to transport amphipathic anions (Hopper-Borge, Chen, Shchaveleva, Belinsky, & Kruh, 2004).

The over load of metal ions cause inter- and intra-mitochondrial redox-environment changes leading to ROS production. Apart from O2· other forms of ROS, such as hydrogen peroxide (H_2O_2) and peroxides (HOO-) are also increased, suggesting that metals may also fortify ROS metabolism through changes in peroxisome function. Metals present in the water are crucially important for aquatic organisms to maintain normal cellular physiology. Their accumulation cause pro-oxidant conditions in cells and lead to adverse effects, *e.g.* tissue damage, energy loss, organelle malfunctioning and eventually apoptosis or cell death, which might be responsible for the reduced movement and increased mortality observed in the current experiments. The steady-state concentrations of these oxidants are usually maintained at non-toxic levels by various antioxidant systems. The *gstp1* might be one of the important detoxification enzymes in precisely mediating the balance between antioxidant defenses and ROS production in *M. lignano*. GSTs catalyze the conjugation of reduced glutathione to many xenobiotics and are effective against the toxicities of electrophile compounds and oxidative stress (Markus, Teralı, Dalmizrak, & Ozer, 2018). For instance, it has been shown that the lack of certain GST isozymes in mice made them prone to carcinogen-induced tumorigenesis (Salinas & Wong, 1999), and certain GST isozymes are indicators of sensitivity to specific cancers (Henderson et al., 1998). Besides the detoxification function of GSTs, they also play an important non-catalytic role in glutathionylation of cellular proteins (Townsend et al., 2009), cell survival (Sanchez-Gomez, Díez-Dacal, Pajares, Llorca, & Perez-Sala, 2010; Y. Wu et al., 2006) and stress signalling mechanisms. GSTs are able to form complexes with other proteins and may also bind toxins and function as transport proteins (Leaver & George, 1998). Meanwhile, different types of multidrug resistance (*mdr*) genes are present in *M. lignano* and might be associated with metal ion transports. *M. lignano* might be an ideal model to unravel toxic mechanisms in marine waters and it might be a good bio-indicator for pollutant detection.

M. lignano have their native microbiome in normal lab conditions which is different from that of their living substrates (Fig. 35). This result is coincident with the *C. elegans* microbiome, which is distinct from that of its environment (Dirksen et al., 2016). This phenomenon might be due to the barrier of pH between animals and their environment, with the worms' guts are much more acidic than to culture medium (Fig. 37). In order to identify whether drugs interference with the microbiome composition and distribution, we tested the microbiome not only in the worms but also in their living substrates. After 2 or 5 days incubation with drugs, weighted UniFrac results supported differences from non-treated controls (Fig. 35 A). Primary component analyses with (PC) 1 and 2 separate control group (SMWs_5 d) from metal-confronted groups, Bis and ABD groups; PC 2 and 3 distinguish SMWs from algae and RCM samples. Worm samples and their inoculum clustered closely together in all treatment groups, suggesting the importance of the substrate origin

(Fig. 35 A and B). Drug toxicity tests show a fade away of microbial discrepancy between worms and substrates, indicating that microbial communities may respond to the surrounding environment.

M. lignano possesses a great number of bacterial taxa under lab conditions. The relative abundance and the presence of bacterial taxa vary substantially according to their living substrates (Fig. 36 C). Under normal conditions, worms carry various bacteria and have a stable mutualistic microbiome. After starvation, as most of the bacterial transit through excreta, *Stramenopiles* and *Cytophagales* become the most abundant bacterial groups. Drug treatments changed dominating bacterial groups and decreased in alpha-diversity and Shannon Indexes in general. The relative abundance of *Alteronomadaceae* increased remarkably in $CuSO_4$-, Atr- and Del-confronted groups. *Rhodobacterales* considerably rise in Atr, Del and ABD groups. $CdSO_4$ treatment accumulates *Oceanospirillales* and *Burkholderiales*. Meanwhile, *Kiloniellales* and *Flavobacteriales* increased in Bis-induced animals, altogether indicating that these treatments change the bacterial compositions dramatically.

It is particularly challenging to determine which factors break native microbial communities of *M. lignano*. Worms might shape their microbiome or they passively accept microbiota from the environment. This may involve host-microbe and bacteria-bacteria interactions, including cooperative, competitive and neutral relationships between them. Substrates influence animals' microbial also reported by other groups. Dirksen et al. (Dirksen et al., 2016) found that *C. elegans* enhances *Rhodobacteraceae* population growth under stressful environments such as high temperature, either high or low osmolarity. *Oceanospirillales* were abundant at sites with salt intrusion (Liao et al., 2019). In the corrosion deterioration pipelines of seawater, the dominant bacterial genus includes members of the *Flavobacteriales*, *Rhodobacterales*, *Kiloniellales* (AlAbbas et al., 2013). Some recent findings supported the view that changing the microbiome of animals may have potential benefits for animals' live strategy. Bacosa et al. (Bacosa et al., 2018) reported that *Alteronomadaceae*, *Alcanivoracaceae*, and *Rhodobacteraceae* have oil degradation potential. These bacteria possess a repertoire of genes for hydrocarbon degradation and these genes were highly enriched in response to oil confrontation. Cassidy et al. suggested that the nematode's proteome corresponds to associated microbiome members (Cassidy et al., 2018). Their results showed an increased abundance of proteins potentially regulated via microbiome-host signaling pathways. Based on our observations we found a group of gram-negative bacteria up-regulated according to various drug conditions, including *Alteronomadales*, *Rhodobacterales*, *Oceanospirillales*, *Burkholderiales*, *Kiloniellales*, and *Flavobacteriales*. I hypothesize that the increase in these bacteria may have a positive effect on toxicity degradation and absorption in *M. lignano*. As a small and simple structured invertebrate, *M. lignano* has a limited ability to control its microbiota. Drug mediated worm-specific microbiomes suggested that co-existent microbiomes might act as an assistant sensor for *M. lignano* to react to environmental changes. The microbiome may also reduce the deleterious effects of these stressors and induce positive effects on animals' lifespan through the regulation of cellular responses or gene expression. Environmental toxicity factors, including metal ions and xenobiotics, abundantly found in the estuarine ecosystems influence microbial community composition of the worms. The present results may possibly illustrate how environmental changes influence the microbiome of the animals. The results of this study provide basic insights into the influence of environmental perturbations on microbial community composition in an intertidal system, which may aid in the design of effective remediation and/or restoration strategies in the target watershed and beyond.

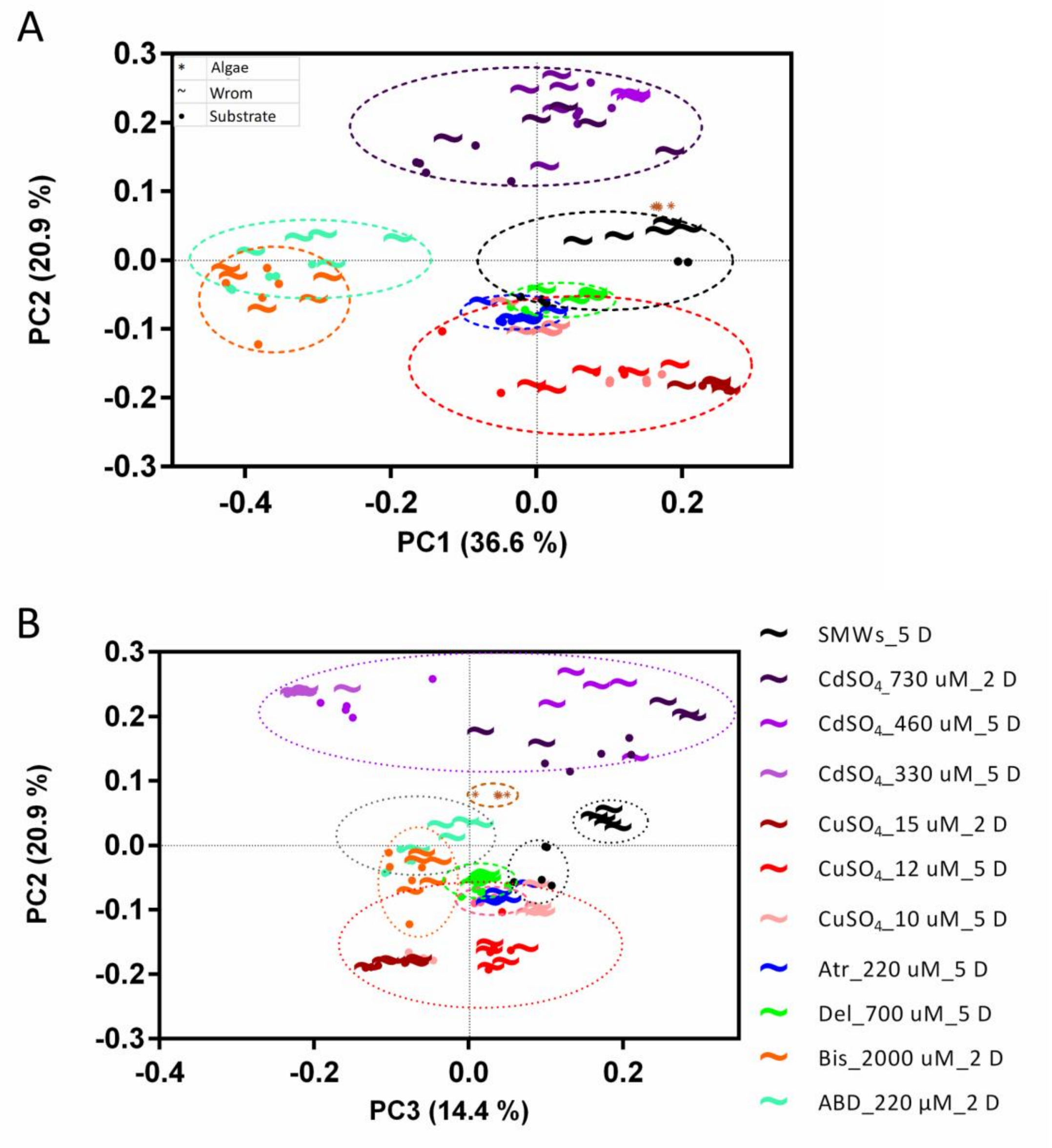

Fig. 35 Principal component (PC) analyses of microbiome distributions of toxicant confronted worms and their corresponding substrates. PC 1 and PC 2 separate control group (SMWs_5 d) from metal-treated groups, Bis and ABD groups; PC 2 and 3 distinguish SMWs from algae and PCM samples (black points). Worm samples and their corresponding substrates clustered closely together in all treatment groups. The color indicates different drug treatments; the wave line indicates worms; the point signs indicate the substrates. SMWs, starved mature worms; Atr, atrazine; Bis, suberoyl bis-hydroxamic acid; Del, deltamethrin; ABD, Atr, Bis and Del mixture under ration 1:1:1.

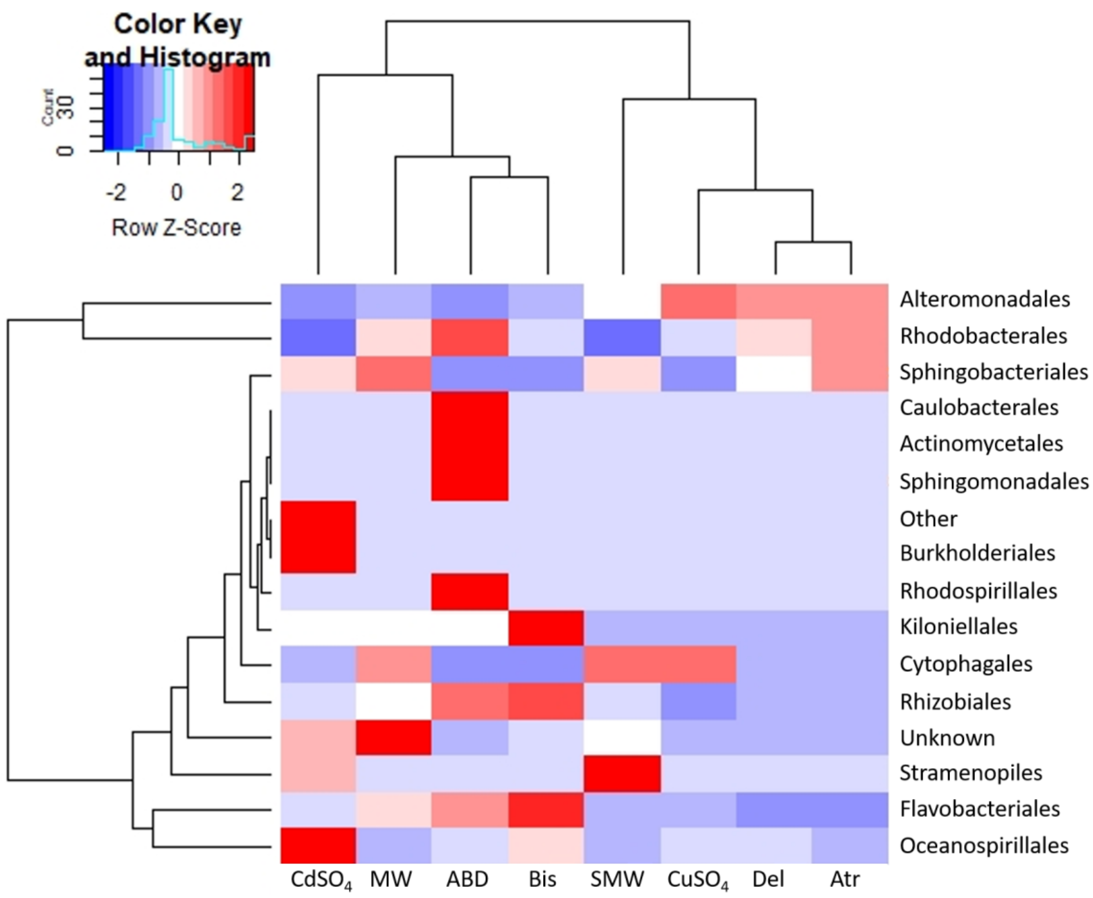

Fig. 36 The major bacterial composition of the microbiota in response to different treatments. The relative abundance and the presence of bacterial taxa vary substantially due to confrontation with different drugs. MWs, mature worms; SMWs, starved mature worms; Atr, atrazine; Bis, suberoyl bis-hydroxamic acid; Del, deltamethrin; ABD, Atr, Bis and Del mixture under ration 1:1:1.

4.2 Biotic stress initiates immune system activity and affects wound repair of worms

M. lignano, as a typical planarian, is well known for its complete regeneration ability. It can regrow nearly any tissue/organ damaged by surgical injury, even forming a new functional head after decapitation. The wounded animals (Ctr_cut) are inevitably exposed to microorganisms from the environment and require defense systems to avoid infectious agents (Elliott & Sánchez Alvarado, 2013). The successfully initiated neoblasts proliferation and wounding signaling reaction guarantees repair. In the present study, the wounding animals' lifespan was extended to 50 days even under starving conditions. While pathogenic bacteria inoculating resulted in a significantly shortened lifespan (<10 days). LPV-induced wounding animals could renew the epithelial cells and repair the damaged surface, but could not completely regenerate.

As evidenced by our findings that listed only genes regulated more than 3-fold with LPV added to wounded animals. Thousands of unigenes, more than 70 % of all genes, were significantly regulated after LPV challenge (Fig. 23). Only 149 genes (4.9 %) were involved in both, wounding (Ctr_Cut) and pathogenic responses (LPV_Cut). It could be demonstrated that the regulated genes with LPV-induced groups were mostly different from those regulated in response to normal wounding and the former trigger stronger regulatory mechanisms than the latter ones. Many of these regulated genes were involved in various biological functions such as immunity, catalytic activities, biogenesis etc., and associated with biosynthesis of secondary metabolites, MAPK signaling pathway, and pathogen interactions. The overall analysis based on transcriptomic data determined that pathogenic exposure affects the biological processes of *M.lignano* at the transcriptional level substantially.

Based on transcriptomic data and analyzing immune-associated signal pathways revealed that NF-κB, IMD, JNK, and p38 MAPK were most suspect in *M. lignano* pathogen infection. 10 genes of the NF-κB pathway; 7 genes of the IMD pathway and 21 genes of the JNK and P38 MAPK pathway were found to be regulated, whereas almost no genes involved in these pathways were regulated after wounding. Pathogen stimulation may activate the above-listed pathways through Toll-like receptors (TRAF2, TRAF5, TRAF6) and RIG-1 like signaling systems. Furthermore, the performed qPCR verified this analysis. We found that the key genes such as Bcl-XL, NF-kB of NF-κB pathway, AP1/Jra, lap 2 of the IMD pathway and JNK/c-JUN/JUND of JNK and P38 MAPK signaling pathway showed a regulation in qPCR experiments.

Other key genes that are not generally involved in these immune-related pathways *e.g. Actin*, *Rac1*, *Rho*, *Rsk* and *S6K* were also re-tested by qPCR. *Actin* was up-regulated in LPV-induced groups (LPV_Cut vs. Ctr_Cut, $p < 0.0001$). Actin provides a cytoskeletal structure and defines cell shape as well as polarity. Its dynamic properties provide a driving force for cell dividing and movement (Hall, 1998). LPV-induced groups exhibited more damages than control groups. Regulating the expression of *Actin* and might be involved in cytoskeletal structure repair. Two p90 ribosomal S6 kinases genes, *RSK* and *S6K*, significantly transcriptional up-regulated. These two genes are physically associated in the cytoplasm. Activated *RSK* and *S6K* will translocate into the nucleus upon phosphorylation by mitogen-activated protein kinases (De Cesare, Jacquot, Hanauer, & Sassone-Corsi, 1998). In addition, *Ras*-dependent signaling cascade reactions regulate cell growth, cell motility, cell survival and cell proliferation (Anjum & Blenis, 2008). While comparing with wounded animals, *Rac* was significantly down-regulated in LPV-induced groups. *Rho* and *Rac* are members of the Rho family of *Ras*-related proteins. Westwick et al. (Westwick et al., 1997) suggested that *Rac* regulates effector-mediated functions and contributes to cellular transformation. *Rho* family members of the small guanosine triphosphatases are key regulators of the actin cytoskeleton (Hall, 1998). However, the interrelationship between *Rac* and *Rho* is still poorly understood.

Some genes associated with developmental processes were up-regulated in all wounding animals (LPV_cut and Ctr_cut), including *FGFR*, *GNBP3*, *k-Ras*, and *Shp2*. *FGFR* transduces the signal by activating different pathways including *Ras*/MAP kinase pathways (Thisse & Thisse, 2005). *GNBP3* senses microorganism infections and activates the Toll-signalling pathway in *Drosophila* (Matskevich, Quintin, & Ferrandon, 2010). *Ras* genes are thought to be crucially important in the regulation of cellular proliferation and differentiation and are mutated in about 30% of all human tumors (Bos, 1989; Khosravi-Far & Der, 1994). Johnson et al. found most animals lacking *Ras* functions exhibit abnormal hematopoietic development and lethal to embryogenesis (L. Johnson et al., 1997). The *Shp2* acts upstream of *Ras* in many pathways and is required for normal developmental. *Shp2* can be initiated by growth factors, cytokines, and extracellular matrix (Bentires-Alj et al., 2004).

Numerous interesting questions still remain unanswered. Why do wounded animals (Ctr_Cut), which are also exposed to diverse microbes, not strongly trigger the innate immune system? The injury exposes the animal's internal tissues to the external media and should lead to extensive confrontation with bacteria. What plays a major role in protecting worm from infections during regeneration? One possible way is based on neoblasts, which are pluripotent adult stem cells in planarians. Petersen (Petersen, 2014) found that planarian gut cells constantly replace the exhausted gut cells and have a robust phagocytic capability. So perhaps the animal's powerful regenerative capability enables fast replacement of infectious cells, leading the less damage from infection. The initiation of neoblast activity instead of starting the complex immune-related system may be an energy-saving strategy in extreme conditions, such as food restriction, warm/cold temperature, high/low salinity etc. I observed that "wound response" can initially be detected in the anterior region (<2 h) (a region before "eyes"), even though the injuring was at the posterior part (tail plate). Thus, the "wound response" was initially in the anterior region and the posterior region exhibited a "regenerative response" afterward (24~72h). During 48~96 h regeneration, more large and clustered cells ("type I") present in the anterior regions of LPV-induced animals. While Ctr_cut has more middle-sized ("type II") cells in their posterior regions. Since LPV-induced animals were finally present with an uncompleted wounding repair, I guess the type I cells might mainly be associated with signal responses and collection, the type II cells modulate cell diving and differentiation. Apparently, *M. lignano* has evolved strong responses during wounding and infection and thus, it could develop into a highly versatile model for the understanding of human immunity.

References

Abnave, P., Mottola, G., Gimenez, G., Boucherit, N., Trouplin, V., Torre, C., . . . Djian, B. (2014). Screening in planarians identifies MORN2 as a key component in LC3-associated phagocytosis and resistance to bacterial infection. *Cell host & microbe, 16*(3), 338-350.

Aboobaker, A. A. (2011). Planarian stem cells: a simple paradigm for regeneration. *Trends in cell biology, 21*(5), 304-311.

AlAbbas, F. M., Kakpovbia, A., Mishra, B., Williamson, C., Spear, J. R., & Olson, D. L. (2013). *Microbial Community Associated With Corrosion Products Collected From Sour Oil Crude and Seawater Injection Pipelines.* Paper presented at the CORROSION 2013.

Alsousi, A. A., & Igwe, O. J. (2018). Redox-active trace metal-induced release of high mobility group box 1 (HMGB1) and inflammatory cytokines in fibroblast-like synovial cells is Toll-like receptor 4 (TLR4) dependent. *Biochimica et Biophysica Acta (BBA)-Molecular Basis of Disease, 1864*(11), 3847-3858.

Anderson, M. J. (2001). A new method for non-parametric multivariate analysis of variance. *Austral ecology, 26*(1), 32-46.

Anjum, R., & Blenis, J. (2008). The RSK family of kinases: emerging roles in cellular signalling. *Nature reviews Molecular cell biology, 9*(10), 747.

Ansari, M., & Razdan, R. (2001). Concurrent control of mosquitoes and domestic pests by use of deltamethrin-treated curtains in the New Delhi Municipal Committee, India. *Journal of the American Mosquito Control Association-Mosquito News, 17*(2), 131-136.

Aon, M. A., Stanley, B. A., Sivakumaran, V., Kembro, J. M., O'Rourke, B., Paolocci, N., & Cortassa, S. (2012). Glutathione/thioredoxin systems modulate mitochondrial H2O2 emission: an experimental-computational study. *The Journal of general physiology, 139*(6), 479-491.

Apprill, A. (2017). Marine animal microbiomes: toward understanding host–microbiome interactions in a changing ocean. *Frontiers in Marine Science, 4*, 222.

Ashburner, M., Ball, C. A., Blake, J. A., Botstein, D., Butler, H., Cherry, J. M., . . . Eppig, J. T. (2000). Gene ontology: tool for the unification of biology. *Nature genetics, 25*(1), 25.

Ashton, F. M., & Crafts, A. S. (1973). Mode of action of herbicides. *Mode of action of herbicides.*

Bacosa, H. P., Erdner, D. L., Rosenheim, B. E., Shetty, P., Seitz, K. W., Baker, B. J., & Liu, Z. (2018). Hydrocarbon degradation and response of seafloor sediment bacterial community in the northern Gulf of Mexico to light Louisiana sweet crude oil. *The ISME journal, 12*(10), 2532.

Bely, A. E., & Nyberg, K. G. (2010). Evolution of animal regeneration: re-emergence of a field. *Trends in ecology & evolution, 25*(3), 161-170.

Bentires-Alj, M., Paez, J. G., David, F. S., Keilhack, H., Halmos, B., Naoki, K., . . . Sugarbaker, D. J. (2004). Activating mutations of the noonan syndrome-associated SHP2/PTPN11 gene in human solid tumors and adult acute myelogenous leukemia. *Cancer research, 64*(24), 8816-8820.

Boal, A. K., & Rosenzweig, A. C. (2009). Structural biology of copper trafficking. *Chemical reviews, 109*(10), 4760-4779.

Bolger, A. M., Lohse, M., & Usadel, B. (2014). Trimmomatic: a flexible trimmer for Illumina sequence data. *Bioinformatics, 30*(15), 2114-2120.

Bos, J. L. (1989). Ras oncogenes in human cancer: a review. *Cancer research, 49*(17), 4682-4689.

Bosch, T. C. (2013). Cnidarian-microbe interactions and the origin of innate immunity in metazoans. *Annual review of microbiology, 67*, 499-518.

Bosch, T. C., Augustin, R., Anton-Erxleben, F., Fraune, S., Hemmrich, G., Zill, H., . . . Leippe, M. (2009). Uncovering the evolutionary history of innate immunity: the simple metazoan Hydra uses epithelial cells for host defence. *Developmental & Comparative Immunology, 33*(4), 559-569.

Brama, M., Politi, L., Santini, P., Migliaccio, S., & Scandurra, R. (2012). Cadmium-induced apoptosis and necrosis in human osteoblasts: role of caspases and mitogen-activated protein kinases pathways. *Journal of endocrinological investigation, 35*(2), 198-208.

Bremner, I. (1998). Manifestations of copper excess. *The American journal of clinical nutrition, 67*(5), 1069S-1073S.

Buettner, G. R. (1993). The pecking order of free radicals and antioxidants: lipid peroxidation, α-tocopherol, and ascorbate. *Archives of biochemistry and biophysics, 300*(2), 535-543.

Burkitt, M. J. (2001). A critical overview of the chemistry of copper-dependent low density lipoprotein oxidation: roles of lipid hydroperoxides, α-tocopherol, thiols, and ceruloplasmin. *Archives of biochemistry and biophysics, 394*(1), 117-135.

Cadenas, S. (2018). Mitochondrial uncoupling, ROS generation and cardioprotection. *Biochimica et Biophysica Acta (BBA)-Bioenergetics, 1859*(9), 940-950.

Caporaso, J. G., Kuczynski, J., Stombaugh, J., Bittinger, K., Bushman, F. D., Costello, E. K., . . . Gordon, J. I. (2010). QIIME allows analysis of high-throughput community sequencing data. *Nature methods, 7*(5), 335.

Cassidy, L., Petersen, C., Treitz, C., Dierking, K., Schulenburg, H., Leippe, M., & Tholey, A. (2018). The Caenorhabditis elegans proteome response to naturally associated microbiome members of the genus Ochrobactrum. *Proteomics, 18*(8), 1700426.

Chance, B., Sies, H., & Boveris, A. (1979). Hydroperoxide metabolism in mammalian organs. *Physiological reviews, 59*(3), 527-605.

Cheng, J., Nanayakkara, G., Shao, Y., Cueto, R., Wang, L., Yang, W. Y., . . . Yang, X. (2017). Mitochondrial proton leak plays a critical role in pathogenesis of cardiovascular diseases. In *Mitochondrial Dynamics in Cardiovascular Medicine* (pp. 359-370): Springer.

Cho, I., & Blaser, M. J. (2012). The human microbiome: at the interface of health and disease. *Nature Reviews Genetics, 13*(4), 260.

Chow, C. K. (1991). Vitamin E and oxidative stress. *Free Radical Biology and Medicine, 11*(2), 215-232.

Christopher, M. (1992). *Logistics and supply chain management*: Irwin Professional Publishing.

Claudianos, C., Ranson, H., Johnson, R., Biswas, S., Schuler, M. A., Berenbaum, M. R., . . . Oakeshott, J. G. (2006). A deficit of detoxification enzymes: pesticide sensitivity and environmental response in the honeybee. *Insect molecular biology, 15*(5), 615-636.

Collins, S. M., Surette, M., & Bercik, P. (2012). The interplay between the intestinal microbiota and the brain. *Nature Reviews Microbiology, 10*(11), 735.

D'Autréaux, B., & Toledano, M. B. (2007). ROS as signalling molecules: mechanisms that generate specificity in ROS homeostasis. *Nature reviews Molecular cell biology, 8*(10), 813.

Davies, P., Cook, L., & Barton, J. (1994). Triazine herbicide contamination of Tasmanian streams: sources, concentrations and effects on biota. *Marine and Freshwater Research, 45*(2), 209-226.

De Cesare, D., Jacquot, S., Hanauer, A., & Sassone-Corsi, P. (1998). Rsk-2 activity is necessary for epidermal growth factor-induced phosphorylation of CREB protein and transcription of c-fos gene. *Proceedings of the National Academy of Sciences, 95*(21), 12202-12207.

Dean, M., Hamon, Y., & Chimini, G. (2001). The human ATP-binding cassette (ABC) transporter superfamily. *Journal of lipid research, 42*(7), 1007-1017.

Delaney, J. R., Stöven, S., Uvell, H., Anderson, K. V., Engström, Y., & Mlodzik, M. (2006). Cooperative control of Drosophila immune responses by the JNK and NF-κB signaling pathways. *The EMBO journal, 25*(13), 3068-3077.

DeNoyelles, F., Kettle, W. D., & Sinn, D. E. (1982). The responses of plankton communities in experimental ponds to atrazine, the most heavily used pesticide in the United States. *Ecology, 63*(5), 1285-1293.

DeSantis, T. Z., Hugenholtz, P., Larsen, N., Rojas, M., Brodie, E. L., Keller, K., . . . Andersen, G. L. (2006). Greengenes, a chimera-checked 16S rRNA gene database and workbench compatible with ARB. *Appl. Environ. Microbiol., 72*(7), 5069-5072.

Dirksen, P., Marsh, S. A., Braker, I., Heitland, N., Wagner, S., Nakad, R., . . . Rosenstiel, P. (2016). The native microbiome of the nematode Caenorhabditis elegans: gateway to a new host-microbiome model. *BMC biology, 14*(1), 38.

Divertie, M. B., Owen Jr, C. A., Barham, S. S., & Ludwig, J. (1982). Accumulation of radionuclide-labeled platelets and fibrinogen in paraquat-damaged rat lungs. *American Review of Respiratory Disease, 125*(5), 574-578.

Domin, H., Zurita-Gutiérrez, Y. H., Scotti, M., Buttlar, J., Hentschel Humeida, U., & Fraune, S. (2018). Predicted bacterial interactions affect in vivo microbial colonization dynamics in Nematostella. *Frontiers in microbiology, 9*, 728.

Douglas, A. E. (2010). *The symbiotic habit*: Princeton University Press.

Elliott, S. A., & Sánchez Alvarado, A. (2013). The history and enduring contributions of planarians to the study of animal regeneration. *Wiley Interdisciplinary Reviews: Developmental Biology, 2*(3), 301-326.

Eming, S. A., Hammerschmidt, M., Krieg, T., & Roers, A. (2009). *Interrelation of immunity and tissue repair or regeneration.* Paper presented at the Seminars in cell & developmental biology.

Evans, P., & Halliwell, B. (1994). [7] Measurement of iron and copper in biological systems: Bleomycin and copper-phenanthroline assays. In *Methods in enzymology* (Vol. 233, pp. 82-92): Elsevier.

Faith, J. J., Guruge, J. L., Charbonneau, M., Subramanian, S., Seedorf, H., Goodman, A. L., . . . Leibel, R. L. (2013). The long-term stability of the human gut microbiota. *Science, 341*(6141), 1237439.

Fan, X.-Y., Yuan, L., Wu, C., Liu, Y.-J., Jiang, F.-L., Hu, Y.-J., & Liu, Y. (2018). Mitochondrial toxicity of organic arsenicals: membrane permeability transition pore opening and respiratory dysfunction. *Toxicology research, 7*(2), 191-200.

Fattouch, S., Raboudi-Fattouch, F., Ponce, J. V. G., Forment, J. V., Lukovic, D., Marzouki, N., & Vidal, D. R. (2010). Concentration dependent effects of commonly used pesticides on activation versus inhibition of the quince (Cydonia Oblonga) polyphenol oxidase. *Food and Chemical Toxicology, 48*(3), 957-963.

Faust, S. D., & Aly, O. M. (1964). Water pollution by organic pesticides. *Journal-American Water Works Association, 56*(3), 267-279.

Fernando, M. D. A., Kounatidis, I., & Ligoxygakis, P. (2014). Loss of Trabid, a new negative regulator of the Drosophila immune-deficiency pathway at the level of TAK1, reduces life span. *PLoS genetics, 10*(2), e1004117.

Fields, M., Lewis, C. G., & Bureau, I. (2001). Aspirin reduces blood cholesterol in copper-deficient rats: a potential antioxidant agent? *Metabolism-Clinical and Experimental, 50*(5), 558-561.

Filipič, M. (2012). Mechanisms of cadmium induced genomic instability. *mutation research/fundamental and molecular mechanisms of mutagenesis, 733*(1-2), 69-77.

Fridovich, I. (1995). Superoxide radical and superoxide dismutases. *Annual review of biochemistry, 64*(1), 97-112.

Gaetke, L. M., Chow-Johnson, H. S., & Chow, C. K. (2014). Copper: toxicological relevance and mechanisms. *Archives of toxicology, 88*(11), 1929-1938.

Galliot, B. (2012). Hydra, a fruitful model system for 270 years. *International Journal of Developmental Biology, 56*(6-7-8), 411-423.

Gentile, L., Cebrià, F., & Bartscherer, K. (2011). The planarian flatworm: an in vivo model for stem cell biology and nervous system regeneration. *Disease models & mechanisms, 4*(1), 12-19.

Godwin, J. W., & Brockes, J. P. (2006). Regeneration, tissue injury and the immune response. *Journal of anatomy, 209*(4), 423-432.

Godwin, J. W., Pinto, A. R., & Rosenthal, N. A. (2013). Macrophages are required for adult salamander limb regeneration. *Proceedings of the National Academy of Sciences, 110*(23), 9415-9420.

Godwin, J. W., & Rosenthal, N. (2014). Scar-free wound healing and regeneration in amphibians: immunological influences on regenerative success. *Differentiation, 87*(1-2), 66-75.

Goldman, L. (1994). Atrazine, simazine and cyanazine: notice of initiation of special review. *Fed Reg, 59*, 60412-60443.

Goldscheider, N. (2010). Delineation of spring protection zones. In *Groundwater hydrology of springs* (pp. 305-338): Elsevier.

Gray, J. P., Suhali-Amacher, N., & Ray, S. D. (2017). Metals and Metal Antagonists. In *Side Effects of Drugs Annual* (Vol. 39, pp. 197-208): Elsevier.

Gutiérrez-Gutiérrez, Ó., Felix, D. A., & González-Estévez, C. (2017). Planarian finds time (less) to fight infection. *Virulence, 8*(7), 1043-1048.

Haas, B. J., Gevers, D., Earl, A. M., Feldgarden, M., Ward, D. V., Giannoukos, G., . . . Sodergren, E. (2011). Chimeric 16S rRNA sequence formation and detection in Sanger and 454-pyrosequenced PCR amplicons. *Genome research, 21*(3), 494-504.

Hall, A. (1998). Rho GTPases and the actin cytoskeleton. *Science, 279*(5350), 509-514.

Halliwell, B., & Gutteridge, J. (1984). Oxygen toxicity, oxygen radicals, transition metals and disease. *Biochemical journal, 219*(1), 1.

Hamada, H., & Tsuruo, T. (1988). Characterization of the ATPase activity of the Mr 170,000 to 180,000 membrane glycoprotein (P-glycoprotein) associated with multidrug resistance in K562/ADM cells. *Cancer research, 48*(17), 4926-4932.

Hartwig, A., Asmuss, M., Blessing, H., Hoffmann, S., Jahnke, G., Khandelwal, S., . . . Bürkle, A. (2002). Interference by toxic metal ions with zinc-dependent proteins involved in maintaining genomic stability. *Food and Chemical Toxicology, 40*(8), 1179-1184.

Hartwig, J. H., Bokoch, G. M., Carpenter, C. L., Janmey, P. A., Taylor, L. A., Toker, A., & Stossel, T. P. (1995). Thrombin receptor ligation and activated Rac uncap actin filament barbed ends through phosphoinositide synthesis in permeabilized human platelets. *Cell, 82*(4), 643-653.

Hayashi, M., Kuge, T., Endoh, D., Nakayama, K., Arikawa, J., Takazawa, A., & Okui, T. (2000). Hepatic copper accumulation induces DNA strand breaks in the liver cells of Long-Evans Cinnamon strain rats. *Biochemical and biophysical research communications, 276*(1), 174-178.

He, Q., Vossbrinck, C. R., Yang, Q., Meng, X.-Z., Luo, J., Pan, G.-Q., . . . Li, T. (2019). Evolutionary and functional studies on microsporidian ATP-binding cassettes: Insights into the adaptation of microsporidia to obligated intracellular parasitism. *Infection, Genetics and Evolution, 68*, 136-144.

Henderson, C. J., Smith, A. G., Ure, J., Brown, K., Bacon, E. J., & Wolf, C. R. (1998). Increased skin tumorigenesis in mice lacking pi class glutathione S-transferases. *Proceedings of the National Academy of Sciences, 95*(9), 5275-5280.

Herman, I. M. (1993). Actin isoforms. *Current opinion in cell biology, 5*(1), 48-55.

Holmes, E., Li, J. V., Athanasiou, T., Ashrafian, H., & Nicholson, J. K. (2011). Understanding the role of gut microbiome–host metabolic signal disruption in health and disease. *Trends in microbiology, 19*(7), 349-359.

Hopper-Borge, E., Chen, Z.-S., Shchaveleva, I., Belinsky, M. G., & Kruh, G. D. (2004). Analysis of the drug resistance profile of multidrug resistance protein 7 (ABCC10): resistance to docetaxel. *Cancer research, 64*(14), 4927-4930.

Horio, M., Gottesman, M. M., & Pastan, I. (1988). ATP-dependent transport of vinblastine in vesicles from human multidrug-resistant cells. *Proceedings of the National Academy of Sciences, 85*(10), 3580-3584.

Hu, Y. (2016). Early generation of nitric oxide contributes to copper tolerance through reducing oxidative stress and cell death in hulless barley roots. *Journal of plant research, 129*(5), 963-978.

Huang, X., Atwood, C. S., Hartshorn, M. A., Multhaup, G., Goldstein, L. E., Scarpa, R. C., . . . Moir, R. D. (1999). The Aβ peptide of Alzheimer's disease directly produces hydrogen peroxide through metal ion reduction. *Biochemistry, 38*(24), 7609-7616.

Igamberdiev, A. U., & Lea, P. J. (2002). The role of peroxisomes in the integration of metabolism and evolutionary diversity of photosynthetic organisms. *Phytochemistry, 60*(7), 651-674.

Ip, C., Cheung, A., Ngan, H., & Wong, A. (2011). p70 S6 kinase in the control of actin cytoskeleton dynamics and directed migration of ovarian cancer cells. *Oncogene, 30*(21), 2420.

Jana-Kara, B., Jihullah, W., Shahi, B., Dev, V., Curtis, C., & Sharma, V. (1995). Deltamethrin impregnated bednets against Anopheles minimus transmitted malaria in Assam, India. *The Journal of tropical medicine and hygiene, 98*(2), 73-83.

Johnson, L., Greenbaum, D., Cichowski, K., Mercer, K., Murphy, E., Schmitt, E., . . . Kucherlapati, R. (1997). K-ras is an essential gene in the mouse with partial functional overlap with N-ras. *Genes & development, 11*(19), 2468-2481.

Johnson, Z. L., & Chen, J. (2017). Structural basis of substrate recognition by the multidrug resistance protein MRP1. *Cell, 168*(6), 1075-1085. e1079.

Joseph, P. (2009). Mechanisms of cadmium carcinogenesis. *Toxicology and applied pharmacology, 238*(3), 272-279.

Ju, E., Dong, K., Chen, Z., Liu, Z., Liu, C., Huang, Y., . . . Qu, X. (2016). Copper (II)–graphitic carbon nitride triggered synergy: Improved ROS generation and reduced glutathione levels for enhanced photodynamic therapy. *Angewandte Chemie, 128*(38), 11639-11643.

Kanehisa, M., & Goto, S. (2000). KEGG: kyoto encyclopedia of genes and genomes. *Nucleic acids research, 28*(1), 27-30.

Kawanishi, S., Inoue, S., & Yamamoto, K. (1989). Hydroxyl radical and singlet oxygen production and DNA damage induced by carcinogenic metal compounds and hydrogen peroxide. *Biological trace element research, 21*(1), 367-372.

Kennedy, C. J. (2011). *The toxicology of metals in fishes, in Encyclopedia of Fish Physiology: From Genome to Environment.* (A. P. Farrell Ed.). San Diego, Calif, USA Academic Press.

Khosravi-Far, R., & Der, C. J. (1994). The Ras signal transduction pathway. *Cancer and Metastasis Reviews, 13*(1), 67-89.

King, R. S., & Newmark, P. A. (2012). The cell biology of regeneration. *J Cell Biol, 196*(5), 553-562.

Krishna, I. M., Manickam, V., Shah, A., & Davergave, N. (2017). *Environmental management: science and engineering for industry*. Butterworth-Heinemann.

Kwakye, G. F., Jiménez, J. A., Thomas, M. G., Kingsley, B. A., McIlvin, M., Saito, M. A., & Korley, E. M. (2019). Heterozygous huntingtin promotes cadmium neurotoxicity and neurodegeneration in striatal cells via altered metal transport and protein kinase C delta dependent oxidative stress and apoptosis signaling mechanisms. *Neurotoxicology, 70*, 48-61.

Ladurner, P., Schärer, L., Salvenmoser, W., & Rieger, R. M. (2005). A new model organism among the lower Bilateria and the use of digital microscopy in taxonomy of meiobenthic Platyhelminthes: Macrostomum lignano, n. sp.(Rhabditophora, Macrostomorpha). *Journal of Zoological Systematics and Evolutionary Research, 43*(2), 114-126.

Lamothe, B., Besse, A., Campos, A. D., Webster, W. K., Wu, H., & Darnay, B. G. (2007). Site-specific Lys-63-linked tumor necrosis factor receptor-associated factor 6 auto-ubiquitination is a critical determinant of IκB kinase activation. *Journal of biological chemistry, 282*(6), 4102-4112.

Leaver, M., & George, S. (1998). A piscine glutathione S-transferase which efficiently conjugates the end-products of lipid peroxidation. *Marine Environmental Research, 46*(1-5), 71-74.

Lengerer, B., Pjeta, R., Wunderer, J., Rodrigues, M., Arbore, R., Schärer, L., . . . Egger, B. (2014). Biological adhesion of the flatworm Macrostomum lignano relies on a duo-gland system and is mediated by a cell type-specific intermediate filament protein. *Frontiers in zoology, 11*(1), 12.

Letelier, M., Faúndez, M., Jara-Sandoval, J., Molina-Berríos, A., Cortés-Troncoso, J., Aracena-Parks, P., & Marín-Catalán, R. (2009). Mechanisms underlying the inhibition of the cytochrome P450 system by copper ions. *Journal of Applied Toxicology: An International Journal, 29*(8), 695-702.

Letelier, M. E., Sánchez-Jofré, S., Peredo-Silva, L., Cortés-Troncoso, J., & Aracena-Parks, P. (2010). Mechanisms underlying iron and copper ions toxicity in biological systems: Pro-oxidant activity and protein-binding effects. *Chemico-biological interactions, 188*(1), 220-227.

Levin, M. (2007). Large-scale biophysics: ion flows and regeneration. *Trends in cell biology, 17*(6), 261-270.

Ley, R. E. (2010). Obesity and the human microbiome. *Current opinion in gastroenterology, 26*(1), 5-11.

Liang, Q., & Dedon, P. C. (2001). Cu (II)/H2O2-induced DNA damage is enhanced by packaging of DNA as a nucleosome. *Chemical research in toxicology, 14*(4), 416-422.

Liao, H., Yu, K., Duan, Y., Ning, Z., Li, B., He, L., & Liu, C. (2019). Profiling microbial communities in a watershed undergoing intensive anthropogenic activities. *Science of The Total Environment, 647*, 1137-1147.

Lippard, S. J. (1999). Free copper ions in the cell? *Science, 284*(5415), 748-749.

Lopez-Huertas, E., Charlton, W. L., Johnson, B., Graham, I. A., & Baker, A. (2000). Stress induces peroxisome biogenesis genes. *The EMBO journal, 19*(24), 6770-6777.

Maguire, R., Germain, A., Tkacz, R., & Forrest, S. (1989). PCBs and pesticides in water at the mouths of the Yamaska and Saint Francois Rivers, Quebec in 1987. *National Water Research Institute Contribution*, 89-150.

Marcos-Ramiro, B., García-Weber, D., Barroso, S., Feito, J., Ortega, M. C., Cernuda-Morollón, E., . . . Alonso, M. A. (2016). RhoB controls endothelial barrier recovery by inhibiting Rac1 trafficking to the cell border. *J Cell Biol, 213*(3), 385-402.

Marikovsky, M., Ziv, V., Nevo, N., Harris-Cerruti, C., & Mahler, O. (2003). Cu/Zn superoxide dismutase plays important role in immune response. *The Journal of Immunology, 170*(6), 2993-3001.

Markus, V., Teralı, K., Dalmizrak, O., & Ozer, N. (2018). Assessment of the inhibitory activity of the pyrethroid pesticide deltamethrin against human placental glutathione transferase P1-1: A combined kinetic and docking study. *Environmental toxicology and pharmacology, 61*, 18-23.

Martin, M. U., & Wesche, H. (2002). Summary and comparison of the signaling mechanisms of the Toll/interleukin-1 receptor family. *Biochimica et Biophysica Acta (BBA)-Molecular Cell Research, 1592*(3), 265-280.

Matskevich, A. A., Quintin, J., & Ferrandon, D. (2010). The Drosophila PRR GNBP3 assembles effector complexes involved in antifungal defenses independently of its Toll-pathway activation function. *European journal of immunology, 40*(5), 1244-1254.

McFall-Ngai, M., Hadfield, M. G., Bosch, T. C., Carey, H. V., Domazet-Lošo, T., Douglas, A. E., . . . Gilbert, S. F. (2013). Animals in a bacterial world, a new imperative for the life sciences. *Proceedings of the National Academy of Sciences, 110*(9), 3229-3236.

Mease, K., Sane, R., Podila, L., & Taub, M. E. (2012). Differential selectivity of efflux transporter inhibitors in Caco-2 and MDCK–MDR1 monolayers: A strategy to assess the interaction of a new chemical entity with P-gp, BCRP, and MRP2. *Journal of pharmaceutical sciences, 101*(5), 1888-1897.

Meinander, A., Runchel, C., Tenev, T., Chen, L., Kim, C. H., Ribeiro, P. S., . . . Silverman, N. (2012). Ubiquitylation of the initiator caspase DREDD is required for innate immune signalling. *The EMBO journal, 31*(12), 2770-2783.

Mishra, S., Bharagava, R. N., More, N., Yadav, A., Zainith, S., Mani, S., & Chowdhary, P. (2019). Heavy Metal Contamination: An Alarming Threat to Environment and Human Health. In *Environmental Biotechnology: For Sustainable Future* (pp. 103-125): Springer.

Mithöfer, A., Schulze, B., & Boland, W. (2004). Biotic and heavy metal stress response in plants: evidence for common signals. *FEBS letters, 566*(1-3), 1-5.

Møller, I. M. (2001). Plant mitochondria and oxidative stress: electron transport, NADPH turnover, and metabolism of reactive oxygen species. *Annual review of plant biology, 52*(1), 561-591.

Møller, I. M., Jensen, P. E., & Hansson, A. (2007). Oxidative modifications to cellular components in plants. *Annu. Rev. Plant Biol., 58*, 459-481.

Morita, M. (1991). Phagocytic response of planarian reticular cells to heat-killed bacteria. *Hydrobiologia, 227*(1), 193-199.

Morita, M., & Best, J. B. (1974). Electron microscopic studies of planarian regeneration. II. Changes in epidermis during regeneration. *Journal of Experimental Zoology, 187*(3), 345-373.

Mouton, S., Willems, M., Braeckman, B. P., Egger, B., Ladurner, P., Schärer, L., & Borgonie, G. (2009). The free-living flatworm Macrostomum lignano: a new model organism for ageing research. *Experimental gerontology, 44*(4), 243-249.

Mouton, S., Wudarski, J., Grudniewska, M., & Berezikov, E. (2018). The regenerative flatworm Macrostomum lignano, a model organism with high experimental potential. *The International journal of developmental biology, 62*(6-7-8), 551.

Murakami, A., Maekawa, M., Kawai, K., Nakayama, J., Araki, N., Semba, K., . . . Higashiyama, S. (2019). Cullin-3/KCTD10 E3 complex is essential for Rac1 activation through RhoB degradation in human epidermal growth factor receptor 2-positive breast cancer cells. *Cancer science, 110*(2), 650.

Murawala, P., Tanaka, E. M., & Currie, J. D. (2012). *Regeneration: the ultimate example of wound healing.* Paper presented at the Seminars in cell & developmental biology.

Myers, B. M., Prendergast, F. G., Holman, R., Kuntz, S. M., & Larusso, N. F. (1993). Alterations in hepatocyte lysosomes in experimental hepatic copper overload in rats. *Gastroenterology, 105*(6), 1814-1823.

Nagarathinam, K., Jaenecke, F., Nakada-Nakura, Y., Hotta, Y., Liu, K., Iwata, S., . . . Tanabe, M. (2017). The multidrug-resistance transporter MdfA from Escherichia coli: crystallization and X-ray diffraction analysis. *Acta Crystallographica Section F: Structural Biology Communications, 73*(7), 423-430.

Nemcsók, J., Bálint, T., Fazakas, J., Kátai, F., Kiss, I., Hieu, L. H., . . . Szabo, I. (1999). The contribution of a pyrethroid insecticide to the massive eel (Anguilla anguilla) devastation, in Lake Balaton, in 1995. *Acta Biologica Hungarica, 50*(1-3), 161-173.

Nonaka, M., & Kimura, A. (2006). Genomic view of the evolution of the complement system. *Immunogenetics, 58*(9), 701-713.

Nwani, C. D., Lakra, W. S., Nagpure, N. S., Kumar, R., Kushwaha, B., & Srivastava, S. K. (2010). Toxicity of the herbicide atrazine: effects on lipid peroxidation and activities of antioxidant enzymes in the freshwater fish Channa punctatus (Bloch). *International journal of environmental research and public health, 7*(8), 3298-3312.

Ohhira, M., Ono, M., Ohhira, M., Sekiya, C., Namiki, M., Fujimoto, Y., . . . Mori, M. (1995). Changes in free radical-metabolizing enzymes and lipid peroxides in the liver of Long-Evans with cinnamon-like coat color rats. *Journal of gastroenterology, 30*(5), 619-623.

Oksanen, J., Blanchet, F. G., Kindt, R., Legendre, P., Minchin, P. R., O'Hara, R., . . . Stevens, H. (2014). Package 'vegan'. *Community Ecology Package, R Package Version, 2*(2).

Paquette, N., Broemer, M., Aggarwal, K., Chen, L., Husson, M., Ertürk-Hasdemir, D., . . . Silverman, N. (2010). Caspase-mediated cleavage, IAP binding, and ubiquitination: linking three mechanisms crucial for Drosophila NF-κB signaling. *Molecular cell, 37*(2), 172-182.

Pedersen, K. J. (1959). Some features of the fine structure and histochemistry of planarian subepidermal gland cells. *Zeitschrift für Zellforschung und Mikroskopische Anatomie, 50*(2), 121-142.

Pedersen, K. J. (1963). SLIIME-SECRETING CELLS OF PLANARIANS. *Annals of the New York Academy of Sciences, 106*(2), 424-443.

Peiris, T. H., Hoyer, K. K., & Oviedo, N. J. (2014). *Innate immune system and tissue regeneration in planarians: an area ripe for exploration.* Paper presented at the Seminars in immunology.

Petersen, C. P. (2014). Planarian resistance to blades and bugs. *Cell host & microbe, 16*(3), 271-272.

Pfaffl, M. W. (2001). A new mathematical model for relative quantification in real-time RT–PCR. *Nucleic acids research, 29*(9), e45-e45.

Pfister, D., De Mulder, K., Philipp, I., Kuales, G., Hrouda, M., Eichberger, P., . . . Ladurner, P. (2007). The exceptional stem cell system of Macrostomum lignano: screening for gene expression and studying cell proliferation by hydroxyurea treatment and irradiation. *Frontiers in zoology, 4*(1), 9.

Pimienta, G., & Pascual, J. (2007). Canonical and alternative MAPK signaling. *Cell cycle, 6*(21), 2628-2632.

Piper, J. T., Singhal, S. S., Salameh, M. S., Torman, R. T., Awasthi, Y. C., & Awasthi, S. (1998). Mechanisms of anticarcinogenic properties of curcumin: the effect of curcumin on glutathione linked detoxification enzymes in rat liver. *The international journal of biochemistry & cell biology, 30*(4), 445-456.

Polak-Juszczak, L. (2013). Trace metals in flounder, Platichthys flesus (Linnaeus, 1758), and sediments from the Baltic Sea and the Portuguese Atlantic coast. *Environmental Science and Pollution Research, 20*(10), 7424-7432.

Poss, K. D. (2010). Advances in understanding tissue regenerative capacity and mechanisms in animals. *Nature Reviews Genetics, 11*(10), 710.

Powell, S. R. (2000). The antioxidant properties of zinc. *The Journal of nutrition, 130*(5), 1447S-1454S.

Prego, R., & Cobelo-Garcıa, A. (2004). Cadmium, copper and lead contamination of the seawater column on the Prestige shipwreck (NE Atlantic Ocean). *Analytica Chimica Acta, 524*(1-2), 23-26.

Prohaska, J. R. (2008). Role of copper transporters in copper homeostasis. *The American journal of clinical nutrition, 88*(3), 826S-829S.

Qi, J., Yao, Q., Tian, L., & Wang, Y. (2018). Piperidylthiosemicarbazones Cu (II) complexes with a high anticancer activity by catalyzing hydrogen peroxide to degrade DNA and promote apoptosis. *European journal of medicinal chemistry, 158*, 853-862.

Rahimzadeh, M. R., Rahimzadeh, M. R., Kazemi, S., & Moghadamnia, A.-a. (2017). Cadmium toxicity and treatment: An update. *Caspian journal of internal medicine, 8*(3), 135.

Rao, P. V., Pattabiraman, P. P., & Kopczynski, C. (2017). Role of the Rho GTPase/Rho kinase signaling pathway in pathogenesis and treatment of glaucoma: Bench to bedside research. *Experimental eye research, 158*, 23-32.

Ravingerová, T., Barančík, M., & Strnisková, M. (2003). Mitogen-activated protein kinases: a new therapeutic target in cardiac pathology. *Molecular and cellular biochemistry, 247*(1-2), 127-138.

Ridley, A. J., Comoglio, P. M., & Hall, A. (1995). Regulation of scatter factor/hepatocyte growth factor responses by Ras, Rac, and Rho in MDCK cells. *Molecular and cellular biology, 15*(2), 1110-1122.

Rieger, R. (2001). Phylogenetic systematics of the Macrostomorpha. *Interrelationships of the Platyhelminthes*, 28-38.

Ritter, L., Solomon, K., Forget, J., Stemeroff, M., & O'Leary, C. (1995). Persistent organic pollutants: an assessment report on: DDT, aldrin, dieldrin, endrin, chlordane, heptachlor, hexachlorobenzene, mirex, toxaphene, polychlorinated biphenyls, dioxins and furans. *International Programme on Chemical Safety (IPCS)*.

Rivera-Ingraham, G. A., Bickmeyer, U., & Abele, D. (2013). The physiological response of the marine platyhelminth Macrostomum lignano to different environmental oxygen concentrations. *Journal of Experimental Biology, 216*(14), 2741-2751.

Rivera-Ingraham, G. A., Nommick, A., Blondeau-Bidet, E., Ladurner, P., & Lignot, J.-H. (2016). Salinity stress from the perspective of the energy-redox axis: Lessons from a marine intertidal flatworm. *Redox biology, 10*, 53-64.

Rout, J. R., Ram, S. S., Das, R., Chakraborty, A., Sudarshan, M., & Sahoo, S. L. (2013). Copper-stress induced alterations in protein profile and antioxidant enzymes activities in the in vitro grown Withania somnifera L. *Physiology and molecular biology of plants, 19*(3), 353-361.

Salinas, A. E., & Wong, M. G. (1999). Glutathione S-transferases-a review. *Current medicinal chemistry, 6*(4), 279-310.

Sanchez-Gomez, F. J., Díez-Dacal, B., Pajares, M. A., Llorca, O., & Perez-Sala, D. (2010). Cyclopentenone prostaglandins with dienone structure promote cross-linking of the chemoresistance-inducing enzyme glutathione transferase P1-1. *Molecular pharmacology, 78*(4), 723-733.

Sansinanea, A., Cerone, S., Streitenberger, S., Garcia, C., & Auza, N. (1998). Oxidative effect of hepatic copper overload. *Acta physiologica, pharmacologica et therapeutica latinoamericana: organo de la Asociacion Latinoamericana de Ciencias Fisiologicas y [de] la Asociacion Latinoamericana de Farmacologia, 48*(1), 25-31.

Santini, C., Pellei, M., Gandin, V., Porchia, M., Tisato, F., & Marzano, C. (2013). Advances in copper complexes as anticancer agents. *Chemical reviews, 114*(1), 815-862.

Schärer, L., Sandner, P., & Michiels, N. K. (2005). Trade-off between male and female allocation in the simultaneously hermaphroditic flatworm Macrostomum sp. *Journal of evolutionary biology, 18*(2), 396-404.

Schieber, M., & Chandel, N. S. (2014). ROS function in redox signaling and oxidative stress. *Current biology, 24*(10), R453-R462.

Scimone, M. L., Cote, L. E., & Reddien, P. W. (2017). Orthogonal muscle fibres have different instructive roles in planarian regeneration. *Nature, 551*(7682), 623.

Sfakianakis, D., Renieri, E., Kentouri, M., & Tsatsakis, A. (2015). Effect of heavy metals on fish larvae deformities: a review. *Environmental research, 137*, 246-255.

Silverman, N., Zhou, R., Stöven, S., Pandey, N., Hultmark, D., & Maniatis, T. (2000). A Drosophila IκB kinase complex required for Relish cleavage and antibacterial immunity. *Genes & development, 14*(19), 2461-2471.

Sokol, R. J., Deverbaux, M., Mierau, G. W., Hambidge, K. M., & Shikes, R. H. (1990). Oxidant injury to hepatic mitochondrial lipids in rats with dietary copper overload: modification by vitamin E deficiency. *Gastroenterology, 99*(4), 1061-1071.

Sommer, F., & Bäckhed, F. (2013). The gut microbiota—masters of host development and physiology. *Nature Reviews Microbiology, 11*(4), 227.

Song, S., Zhang, X., Wu, H., Han, Y., Zhang, J., Ma, E., & Guo, Y. (2014). Molecular basis for antioxidant enzymes in mediating copper detoxification in the nematode Caenorhabditis elegans. *PLoS One, 9*(9), e107685.

Steinberg, C. E., Lorenz, R., & Spieser, O. H. (1995). Effects of atrazine on swimming behavior of zebrafish, Brachydanio rerio. *Water Research, 29*(3), 981-985.

Storelli, G., Strigini, M., Grenier, T., Bozonnet, L., Schwarzer, M., Daniel, C., . . . Leulier, F. (2018). Drosophila perpetuates nutritional mutualism by promoting the fitness of its intestinal symbiont Lactobacillus plantarum. *Cell metabolism, 27*(2), 362-377. e368.

Su, L., Ravanshad, S., Owen Jr, C. A., McCall, J. T., Zollman, P. E., & Hardy, R. M. (1982). A comparison of copper-loading disease in Bedlington terriers and Wilson's disease in humans. *American Journal of Physiology-Gastrointestinal and Liver Physiology, 243*(3), G226-G230.

Tang, H., Kambris, Z., Lemaitre, B., & Hashimoto, C. (2008). A serpin that regulates immune melanization in the respiratory system of Drosophila. *Developmental cell, 15*(4), 617-626.

Templeton, D. M., & Liu, Y. (2010). Multiple roles of cadmium in cell death and survival. *Chemico-biological interactions, 188*(2), 267-275.

Thisse, B., & Thisse, C. (2005). Functions and regulations of fibroblast growth factor signaling during embryonic development. *Developmental biology, 287*(2), 390-402.

Tietje, K., Rivera-Ingraham, G., Petters, C., Abele, D., Dringen, R., & Bickmeyer, U. (2013). Reporter dyes demonstrate functional expression of multidrug resistance proteins in the marine flatworm Macrostomum lignano: The sponge-derived dye Ageladine A is not a substrate of these transporters. *Marine drugs, 11*(10), 3951-3969.

Townsend, D. M., Manevich, Y., He, L., Hutchens, S., Pazoles, C. J., & Tew, K. D. (2009). Novel role for glutathione S-transferase π regulator of protein S-glutathionylation following oxidative and nitrosative stress. *Journal of biological chemistry, 284*(1), 436-445.

Uhr, M., Tontsch, A., Namendorf, C., Ripke, S., Lucae, S., Ising, M., . . . Kohli, M. (2008). Polymorphisms in the drug transporter gene ABCB1 predict antidepressant treatment response in depression. *Neuron, 57*(2), 203-209.

Viran, R., Erkoç, F. Ü., Polat, H., & Koçak, O. (2003). Investigation of acute toxicity of deltamethrin on guppies (Poecilia reticulata). *Ecotoxicology and environmental safety, 55*(1), 82-85.

Wagner, D. E., Wang, I. E., & Reddien, P. W. (2011). Clonogenic neoblasts are pluripotent adult stem cells that underlie planarian regeneration. *Science, 332*(6031), 811-816.

Wang, J., Luo, C., Shan, C., You, Q., Lu, J., Elf, S., . . . Fan, J. (2015). Inhibition of human copper trafficking by a small molecule significantly attenuates cancer cell proliferation. *Nature chemistry, 7*(12), 968.

Weinsberg, F., Bickmeyer, U., & Wiegand, H. (1995). Effects of inorganic mercury (Hg 2+) on calcium channel currents and catecholamine release from bovine chromaffin cells. *Archives of toxicology, 69*(3), 191.

Westwick, J. K., Lambert, Q. T., Clark, G. J., Symons, M., Van Aelst, L., Pestell, R. G., & Der, C. J. (1997). Rac regulation of transformation, gene expression, and actin organization by multiple, PAK-independent pathways. *Molecular and cellular biology, 17*(3), 1324-1335.

Wiegand, C., Pflugmacher, S., Giese, M., Frank, H., & Steinberg, C. (2000). Uptake, toxicity, and effects on detoxication enzymes of atrazine and trifluoroacetate in embryos of zebrafish. *Ecotoxicology and environmental safety, 45*(2), 122-131.

Wilson, A. C., Ashton, P. D., Calevro, F., Charles, H., Colella, S., Febvay, G., . . . Schwartz, J. F. (2010). Genomic insight into the amino acid relations of the pea aphid, Acyrthosiphon pisum, with its symbiotic bacterium Buchnera aphidicola. *Insect molecular biology, 19*, 249-258.

Wu, X., Cobbina, S. J., Mao, G., Xu, H., Zhang, Z., & Yang, L. (2016). A review of toxicity and mechanisms of individual and mixtures of heavy metals in the environment. *Environmental Science and Pollution Research, 23*(9), 8244-8259.

Wu, Y., Fan, Y., Xue, B., Luo, L., Shen, J., Zhang, S., . . . Yin, Z. (2006). Human glutathione S-transferase P1-1 interacts with TRAF2 and regulates TRAF2–ASK1 signals. *Oncogene, 25*(42), 5787.

Wudarski, J., Ustyantsev, K., Glazenburg, L., & Berezikov, E. (2019). Influence of temperature on development, reproduction and regeneration in the flatworm model organism, Macrostomum lignano. *Zoological letters, 5*(1), 7.

Wyse, E., Azemard, S., & De Mora, S. (2004). *World-wide intercomparison exercise for the determination of trace elements and methylmercury in marine sediment IAEA-433*: Citeseer.

Xia, Z., Dickens, M., Raingeaud, J., Davis, R. J., & Greenberg, M. E. (1995). Opposing effects of ERK and JNK-p38 MAP kinases on apoptosis. *Science, 270*(5240), 1326-1331.

Yang, L., Chen, Y., Yu, Z., Pan, W., Wang, H., Li, N., & Tang, B. (2017). Dual-ratiometric fluorescent nanoprobe for visualizing the dynamic process of pH and superoxide anion changes in autophagy and apoptosis. *ACS applied materials & interfaces, 9*(33), 27512-27521.

Yousef, M. I., Awad, T. I., & Mohamed, E. H. (2006). Deltamethrin-induced oxidative damage and biochemical alterations in rat and its attenuation by Vitamin E. *Toxicology, 227*(3), 240-247.

Yuan, W., Yang, N., & Li, X. (2016). Advances in understanding how heavy metal pollution triggers gastric cancer. *BioMed research international, 2016*.

Zandi, E., Rothwarf, D. M., Delhase, M., Hayakawa, M., & Karin, M. (1997). The IkB kinase complex (IKK) contains two kinase subunits, IKKa and IKKb, necessary for IkB phosphorylation and NF-kB activation. *Cell, 91*(2), 243-252.

Zhang, S., Noordin, M., Rahman, S., & Haron, J. (2000). Effects of copper overload on hepatic lipid peroxidation and antioxidant defense in rats. *Veterinary and human toxicology, 42*(5), 261-264.

Zhang, W., Wang, X., Li, P., Xiao, H., Zhang, W., Wang, H., & Tang, B. (2017). Illuminating superoxide anion and pH enhancements in apoptosis of breast cancer cells induced by mitochondrial hyperfusion using a new two-photon fluorescence probe. *Analytical chemistry, 89*(12), 6840-6845.

Zhou, L., Wu, S., Liu, D., Xu, B., Zhang, X., & Zhao, B. (2012). Characterization and expression analysis of a trypsin-like serine protease from planarian Dugesia japonica. *Molecular biology reports, 39*(6), 7041-7047.

Zhou, R., Silverman, N., Hong, M., Liao, D. S., Chung, Y., Chen, Z. J., & Maniatis, T. (2005). The role of ubiquitination in Drosophila innate immunity. *Journal of biological chemistry, 280*(40), 34048-34055.

Acknowledgements

I sincerely thank my supervisor Prof. Dr. Thomas Roeder for providing constant support and guidance through all projects. He helps me a lot in choosing an interesting topic, designing details of each experiment, optimizing the writing of the thesis etc. He's conscientious and diligent working attitude deeply impressed me. I benefit a lot from his daily behavior in terms of learning and being a nice person. Thanks again for providing me constructive suggestions and ideas during the past 4 years.

I am deeply thanks to Christiane Sandberg, Britta Laubenstein and Heidrum Wegner for their outstanding technical help. I am greatly appreciated to Dr. Christine Fink, Dr. Judith Bossen, Dr. Roxana Pfefferkorn, Jakob von Frieling, Ruben Prange, Xiao Niu and Mirjam Knop for their critical experimental support. I am especially thanks to Dr, Christine Fink and Dr. Judith Bossen for their living issue organizing and chemical ordering. I am also thanks to Dr. Gu Tian, Dr. Yang Li, Xiaoying Zhang, XiaoNiu, XiaoFu Wang, Vaibhvi, Navid Tahanzadeh who's nicely around me and offers a nice atmosphere in the office. I am also thanks to all the other friendly members of our Zoological Institute for their kindness help.

Then I am great thanks to my lovely family members, father Gongshi Ma, mother Xiuyun Yang, brother Chuangxin Ma and also my boyfriend Dr. Peng Xue. These years they continuously support and encouragement makes my life much more interesting, meaningful and enjoyable.

Finally, I am especially appreciated to the China Scholarship Council and Deutscher Akademischer Austauschdienst (DAAD) for my financial support.

Appendix

Fig. 37 Gut PH of drug treated animals. MW, mature worms; IMW, immature worms; Atr, atrazine; Del, deltamethrin; ABD, Atrazine deltamethrin and suberoyl bis-hydroxamic acid.

Table7 Bacteria composition in the *M.lignano* and their living substrates

# Constructed from biom file	Algae				
#OTU ID	H06512-L1	H06513-L1	H06514-L1	H06515-L1	H06516-L1
Kineosporiaceae	0	0	0	0	0
Microbacteriaceae	0	0	0	0	0
o__Bacteroidales;	2.83E-05	3.28E-05	0	0	3.72E-05
Cyclobacteriaceae	0.00716	0.010251	0.005242	0.007292	0.006805
Cytophagaceae	0	0	0	0	0
Flammeovirgaceae	0.14105	0.11155	0.131556	0.148829	0.148563
Weeksellaceae	0	0	0	0	0
Cryomorphaceae	0	0	0	0	0
Flavobacteriaceae	0.052696	0.065953	0.071928	0.052432	0.04879
o__Sphingobacteriales;f	0.011207	0.018009	0.012511	0.010937	0.01071
Sphingobacteriaceae	0	0	7.42E-05	9.27E-05	0.000186
o__SBR1031;f__A4b	0	0	0	0	0
Chlamydomonadaceae	0	0	0	0	0
o__Stramenopiles;f__	0.107259	0.17022	0.151485	0.110239	0.140419
Staphylococcaceae	0	0	0	3.09E-05	0
o__Bacillales;Other	0	0	0	0	0
Lactobacillales;f__	0	0	0	0	0
Aerococcaceae	0	0	0	0	0
Enterococcaceae	0	0	0	0	0.000112
Lactobacillaceae	8.49E-05	1.64E-05	0	3.09E-05	3.72E-05
Turicibacteraceae	0	0	0	0	0
Clostridiales;f__	0.000113	0.00023	0.000346	0.00105	0.000483
Clostridiaceae	0	0	0	0	0
Lachnospiraceae	2.83E-05	8.20E-05	2.47E-05	0.000216	7.44E-05
Peptococcaceae	0	0	0	0	0
Ruminococcaceae	5.66E-05	3.28E-05	3.71E-05	0.000154	0.000149
Clostridiales;Other	0	0	0	0	0
Erysipelotrichaceae	0	0	0	0	0
Fusobacteriaceae	0	0	0	0	0
Gemmatimonadaceae	0	0	0	0	0
Gemmatimonadetes;Other	0	0	0	0	0
c__3BR-5F;o__;f__	0.184548	0.184999	0.157988	0.124266	0.136068
c__GKS2-174;o__;f__	0	0	0	0	0

c__ZB2;o__;f__	0	0	0	0	0
Kiloniellales;f__	0.021961	0.020798	0.011757	0.026139	0.023205
Rhizobiales;f__	0.000481	0.000738	0.000878	0.000463	0.000669
Hyphomicrobiaceae	0.004047	0.004051	0.003202	0.004295	0.004016
Phyllobacteriaceae	0.007613	0.006479	0.007121	0.010072	0.007586
Rhizobiaceae	0.002858	0.002559	0.002794	0.003028	0.002082
Rhizobiales;Other	0.105476	0.094771	0.11536	0.106995	0.112305
Hyphomonadaceae	0.10825	0.104875	0.100611	0.103936	0.113123
Rhodobacteraceae	0.038857	0.046041	0.045385	0.045171	0.055669
Rhodobacterales;Other	0.000736	0.000705	0.000618	0.000618	0.000632
Acetobacteraceae	2.83E-05	0	0	0	0
Rickettsiaceae	2.83E-05	1.64E-05	3.71E-05	0	7.44E-05
Sphingomonadales;f__	0	0	0	0	0
Sphingomonadaceae	0	0	0	0	0
Alphaproteobacteria;Other	0.000623	0.001017	0.000828	0.000618	0.000818
Comamonadaceae	2.83E-05	6.56E-05	2.47E-05	0	0
o__GMD14H09;f__	0.009877	0.006462	0.005094	0.010628	0.009743
Spirobacillales;f__	0	0	0	0	0
Helicobacteraceae	0.000736	0.000377	6.18E-05	0.000649	0.00093
Chromatiaceae	0	1.64E-05	0	0	0
Alteromonadaceae	0.175294	0.129904	0.156999	0.212661	0.15957
Colwelliaceae	2.83E-05	0	0	0	0
Alteromonadales; HTCC2188	0	0	0	0	3.72E-05
Alteromonadales;Other	5.66E-05	1.64E-05	1.24E-05	0	0
Alcanivoracaceae	2.83E-05	0	4.95E-05	3.09E-05	7.44E-05
Halomonadaceae	0.000538	0.000968	0.000519	0.000525	0.000446
Pseudomonadaceae	5.66E-05	1.64E-05	0.000136	6.18E-05	0.000149
Unassigned;Other;Other	0.017914	0.018419	0.01716	0.018198	0.016102

# Constructed from biom file	Pre-colonization Medium				
#OTU ID	H20481-L1	H20482-L1	H20483-L1	H20484-L1	H20485-L1
Kineosporiaceae	0	0	0	0	0
Microbacteriaceae	0	0	0	0	0
o__Bacteroidales;f__S24-7	0	0	0	0	0
Cyclobacteriaceae	0.025872	0.001978	0.02348	0.004978	0.01478

Cytophagaceae	2.12E-05	0	0	0	0
Flammeovirgaceae	0.08031	0.003796	0.060959	0.012133	0.0164
Weeksellaceae	0	0	0	0	0
Cryomorphaceae	0	0	0	2.16E-05	0
Flavobacteriaceae	0.015205	0.073869	0.012916	0.065234	0.083935
o__Sphingobacteriales;f__	0.062008	0.001515	0.044516	0.007263	0.019235
Sphingobacteriaceae	0	0	0	0	0
o__SBR1031;f__A4b	0	0	0	0	0
Chlamydomonadaceae	0	0	0	0	0
o__Stramenopiles;f__	0.000636	0.000107	0.002682	0.000259	0.00081
Staphylococcaceae	0	0	0	4.31E-05	0
o__Bacillales;Other	0.00E+00	0	0	0	0
Lactobacillales;f__	0	0	0	0	4.50E-05
Aerococcaceae	0	0	0	0	0.00E+00
Enterococcaceae	0	0	0	0	0
Lactobacillaceae	0	1.78E-05	0	0	0.00E+00
Turicibacteraceae	0	0	0	8.62E-05	0
Clostridiales;f__	0	0	1.84E-05	0.00E+00	0
Clostridiaceae	0	0	0	0	0
Lachnospiraceae	0	0.00E+00	0	0	0
Peptococcaceae	0	0	1.84E-05	0	0
Ruminococcaceae	0	0.00E+00	0.00E+00	0.00E+00	0.00E+00
Clostridiales;Other	0	0	1.84E-05	0	0
Erysipelotrichaceae	0	0	0	0	0
Fusobacteriaceae	0	0	0.00011	2.16E-05	0
Gemmatimonadaceae	0	0	0	0	0
Gemmatimonadetes;Other	0	0	0	0	0
c__3BR-5F;o__;f__	0.018301	0.011192	0.03454	0.007133	0.010798
c__GKS2-174;o__;f__	0	0	0	0	2.25E-05
c__ZB2;o__;f__	0	1.78E-05	1.84E-05	4.31E-05	2.25E-05
Kiloniellales;f__	0	0.000588	0	0.003362	0.003824
Rhizobiales;f__	0	1.78E-05	0	0	0
Hyphomicrobiaceae	0.002608	0.002049	0.003987	0.002047	0.002205
Phyllobacteriaceae	0.000254	0.00016	0.000147	0.00028	0.000315
Rhizobiaceae	2.12E-05	0	0	0	0
Rhizobiales;Other	0.001654	0.000624	0.002315	0.002155	0.001147
Hyphomonadaceae	0.008695	0.011673	0.012971	0.058295	0.032935

Rhodobacteraceae	0.023433	0.191524	0.02686	0.213051	0.188072
Rhodobacterales;Other	0.000106	0.000624	0.000202	0.000302	0.00036
Acetobacteraceae	6.36E-05	0	3.67E-05	0	0
Rickettsiaceae	2.12E-05	0	0	0.00E+00	2.25E-05
Sphingomonadales;f__	6.36E-05	0	0	0	0
Sphingomonadaceae	0	1.78E-05	0	0	0
Alphaproteobacteria;Other	0.000106	0.001408	7.35E-05	0.003987	0.004589
Comamonadaceae	6.36E-05	0	1.84E-05	8.62E-05	2.25E-05
o__GMD14H09;f__	0.000191	0.008839	0.000459	0.002134	0.00261
Spirobacillales;f__	0	0	0	0	0
Helicobacteraceae	0	0	0	0	0
Chromatiaceae	0	0	0	0	0
Alteromonadaceae	0.626996	0.5436	6.71E-01	0.527413	0.532519
Colwelliaceae	0.002121	0.001729	0.001984	0.001789	0.001822
Alteromonadales; HTCC2188	0	0	0	0	0
Alteromonadales;Other	2.12E-05	7.13E-05	1.84E-05	4.31E-05	0
Alcanivoracaceae	0	0.005239	0	0.027413	0.018672
Halomonadaceae	0	8.91E-05	3.67E-05	0.000259	0.00045
Pseudomonadaceae	0	1.78E-05	0	0	0
Unassigned;Other;Other	0.131036	0.139237	0.100827	0.060127	0.064363

# Constructed from biom file			Immature worms		
#OTU ID	H06502-L1	H06503-L1	H06504-L1	H06505-L1	H06506-L1
Kineosporiaceae	0	0	0	0	0
Microbacteriaceae	0	0	0	0	0
o__Bacteroidales;f__S24-7	1.43E-05	7.94E-05	0	8.11E-05	6.67E-05
Cyclobacteriaceae	0.000242	0.000159	0.000723	0.000486	0.0008
Cytophagaceae	1.43E-05	2.65E-05	0	0	0
Flammeovirgaceae	0.077306	0.078568	0.042348	0.043794	0.039195
Weeksellaceae	1.43E-05	2.65E-05	0	0	0
Cryomorphaceae	0	0	0	0	0
Flavobacteriaceae	0.106132	0.118779	0.166957	0.169152	0.172144
o__Sphingobacteriales;f__	0.059392	0.059615	0.039684	0.042092	0.039528
Sphingobacteriaceae	1.43E-05	0	3.29E-05	0	0
o__SBR1031;f__A4b	0	0	0	0	0

Chlamydomonadaceae	0	0	0	0	0
o__Stramenopiles;f__	0.000342	0.000291	0.000789	2.70E-05	6.67E-05
Staphylococcaceae	0	0	0	0	0
o__Bacillales;Other	0	0	0	0	0
Lactobacillales;f__	0	0	0	0	0
Aerococcaceae	0	0	0	0	0
Enterococcaceae	0	0	0	2.70E-05	0
Lactobacillaceae	5.71E-05	0.000106	0	5.40E-05	6.67E-05
Turicibacteraceae	0	0	0	0	0
Clostridiales;f__	0.0003	0.000318	0.000132	0.000459	0.000367
Clostridiaceae	0	0	0	0	0
Lachnospiraceae	0.000185	7.94E-05	0.000263	2.70E-05	0.000267
Peptococcaceae	0	0	0	0	0
Ruminococcaceae	1.43E-05	5.29E-05	0.000526	5.40E-05	6.67E-05
Clostridiales;Other	0	0	0	0	0
Erysipelotrichaceae	0	0	0	0	0
Fusobacteriaceae	0	0	0	0	0
Gemmatimonadaceae	0	0	0	0	0
Gemmatimonadetes	0	0	0	0	0
c__3BR-5F;o__;f__	0.269145	0.273401	0.308466	0.286432	0.319291
c__GKS2-174;o__;f__	0	0	0	0	0
c__ZB2;o__;f__	0	0	0	0	0
Kiloniellales;f__	0.015818	0.014851	0.005063	0.006835	0.004566
Rhizobiales;f__	0.000599	0.00045	0.000953	0.001027	0.0006
Hyphomicrobiaceae	0.003494	0.003627	0.003025	0.003863	0.004033
Phyllobacteriaceae	0.001583	0.001747	0.002137	0.001945	0.001167
Rhizobiaceae	0.001084	0.001324	0.000756	0.000756	0.000833
Rhizobiales;Other	0.019426	0.02769	0.029262	0.031799	0.029063
Hyphomonadaceae	0.292465	0.253812	0.231366	0.225374	0.215138
Rhodobacteraceae	0.039423	0.045796	0.049647	0.057222	0.05366
Rhodobacterales;Other	0.001326	0.001271	0.001052	0.001324	0.0009
Acetobacteraceae	1.43E-05	7.94E-05	0	2.70E-05	0
Rickettsiaceae	1.43E-05	2.65E-05	0	2.70E-05	3.33E-05
Sphingomonadales;f__	0	0	0	0	0
Sphingomonadaceae	0	0	0	0	0
Alphaproteobacteria;Other	0.000913	0.000741	0.000658	0.001054	0.001067
Comamonadaceae	7.13E-05	0.000106	0.000132	5.40E-05	1.00E-04

o__GMD14H09;f__	0.000628	0.000847	0.000526	0.000351	0.0004
Spirobacillales;f__	0	0	0	0	0
Helicobacteraceae	0.000328	0.000874	0.001545	0.000811	0.0007
Chromatiaceae	1.43E-05	2.65E-05	0	0	0
Alteromonadaceae	0.086791	0.092228	0.09492	0.106122	0.097854
Colwelliaceae	1.43E-05	0	0	0	0
Alteromonadales; HTCC2188	0	0	3.29E-05	0	0
Alteromonadales;Other	4.28E-05	2.65E-05	6.58E-05	2.70E-05	0
Alcanivoracaceae	2.85E-05	7.94E-05	3.29E-05	5.40E-05	0.000167
Halomonadaceae	0.000556	0.000582	0.001414	0.001459	0.001666
Pseudomonadaceae	0.000128	0.000106	0	8.11E-05	1.00E-04
Unassigned;Other;Other	0.021765	0.022051	0.0169	0.016886	0.015765

# Constructed from biom file	Starvation Mature worms_5 D				
#OTU ID	H20476-L1	H20477-L1	H20478-L1	H20479-L1	H20480-L1
Kineosporiaceae	0.000374	0.000593	0.000496	0	0
Microbacteriaceae	0	0.000132	0	0	0
o__Bacteroidales;f__S24-7	0	0	0	0	0
Cyclobacteriaceae	0.014312	0.010905	0.009731	0.0127	0.008578
Cytophagaceae	9.35E-05	0	0.000307	5.41E-05	0
Flammeovirgaceae	0.027384	0.022733	0.039845	0.040013	0.050016
Weeksellaceae	0	8.24E-05	7.09E-05	0	0
Cryomorphaceae	7.02E-05	0.000181	9.45E-05	0	1.36E-05
Flavobacteriaceae	0.055213	4.66E-02	0.028366	0.001227	0.001574
o__Sphingobacteriales;f__	0.076236	0.070127	0.063629	0.069617	0.061593
Sphingobacteriaceae	0	0	0	0	0
o__SBR1031;f__A4b	0	0	9.45E-05	0	0
Chlamydomonadaceae	0	0	0.000165	0	0
o__Stramenopiles;f__	7.02E-05	1.24E-03	9.45E-05	0.00101	0.00965
Staphylococcaceae	0.00E+00	0.000132	0.000331	0	1.36E-05
o__Bacillales;Other	0.00E+00	4.94E-05	0	0.00E+00	0
Lactobacillales;f__	0	0	0	0	0
Aerococcaceae	0	1.65E-05	0	0	0.00E+00
Enterococcaceae	0	1.65E-05	0	0	0
Lactobacillaceae	0.00E+00	1.65E-05	0.00E+00	0.00E+00	0.00E+00
Turicibacteraceae	0	0.00E+00	0.00E+00	0	0

Clostridiales;f__	0	0	0.00E+00	0	0
Clostridiaceae	0.00E+00	0	4.72E-05	0	4.48E-04
Lachnospiraceae	0.00E+00	0	0	0	0
Peptococcaceae	0	0	0	0	0
Ruminococcaceae	0	0	0	0	0
Clostridiales;Other	0	0	0	0	0.000149
Erysipelotrichaceae	0	0	0	0	0
Fusobacteriaceae	0	0	0	0	0
Gemmatimonadaceae	2.34E-05	0	0	0	0
Gemmatimonadetes	0	0	0.00E+00	0	0
c__3BR-5F;o__;f__	0.149783	0.134901	0.120527	0.14737	0.174668
c__GKS2-174;o__;f__	9.35E-05	0.000313	0.000213	0.000613	0.000176
c__ZB2;o__;f__	0.000421	0.000445	0.00052	0.000144	6.79E-05
Kiloniellales;f__	0.003531	0.005074	0.000165	0	0
Rhizobiales;f__	0.000117	0	0	0	4.07E-05
Hyphomicrobiaceae	0.006548	0.00822	0.007534	0.004528	0.008809
Phyllobacteriaceae	0.001216	0.000379	0.00085	0.000631	0.001127
Rhizobiaceae	2.34E-05	0	2.36E-05	1.80E-05	8.14E-05
Rhizobiales;Other	0.017118	0.009143	0.010085	0.008371	0.015161
Hyphomonadaceae	0.07226	0.017281	0.007298	0.006621	0.004655
Rhodobacteraceae	0.081708	0.065235	0.029665	0.015136	0.025788
Rhodobacterales;Other	0.000959	4.94E-05	0	0	1.36E-05
Acetobacteraceae	7.02E-05	9.88E-05	7.09E-05	0	2.71E-05
Rickettsiaceae	0	0.000132	9.45E-05	0	0.00E+00
Sphingomonadales;f__	2.34E-05	2.31E-04	0.000189	0	9.50E-05
Sphingomonadaceae	7.02E-05	0.000132	0.000449	0	9.50E-05
Alphaproteobacteria	0.002081	0.000544	9.45E-05	0	4.07E-05
Comamonadaceae	0.000281	1.09E-03	0.000756	0.000271	0.000244
o__GMD14H09;f__	0.000234	0.000428	0.001016	0.000162	0.001032
Spirobacillales;f__	4.68E-05	3.29E-05	0	0.000216	0
Helicobacteraceae	0	0	0	0	0
Chromatiaceae	0	0	0	0	0
Alteromonadaceae	0.417333	0.530459	0.547131	0.559208	0.510309
Colwelliaceae	0.001333	0.001516	0.001819	0.001551	0.001642
Alteromonadales; HTCC2188	0	0	0	0	0
Alteromonadales;Other	2.34E-05	0	0	0	2.71E-05
Alcanivoracaceae	0.000117	0.000313	0	0	0

Halomonadaceae	0.00021	0.000511	0.000118	0	0
Pseudomonadaceae	0	1.65E-05	0	0	0
Unassigned;Other	0.070109	0.069056	0.126786	0.130051	0.123621

# Constructed from biom file			Mature worms		
#OTU ID	H06507-L1	H06508-L1	H06509-L1	H06510-L1	H06511-L1
Kineosporiaceae	0	0	0	0	0
Microbacteriaceae	0	0	0	0	0
o__Bacteroidales;f__S24-7	0	4.76E-05	8.83E-05	1.88E-05	0.000122
Cyclobacteriaceae	0.001248	0.001951	0.000883	0.001184	0.000974
Cytophagaceae	0	0	0	0	0
Flammeovirgaceae	0.058606	0.05706	0.049656	0.063699	0.05766
Weeksellaceae	0	0	0	0	0
Cryomorphaceae	0	0	0	0	0
Flavobacteriaceae	0.153369	0.151977	0.138665	0.143394	0.135198
o__Sphingobacteriales;f__	0.03999	0.042973	0.035851	0.04214	0.041951
Sphingobacteriaceae	0	0	0	1.88E-05	0
o__SBR1031;f__A4b	0	0	0	0	0
Chlamydomonadaceae	0	0	0	0	0
o__Stramenopiles;f__	0.022295	0.004402	0.003915	0.005131	0.000944
Staphylococcaceae	0	0	0	0	0
o__Bacillales;Other	0	0	0	0	0
Lactobacillales;f__	0	0	0	0	0
Aerococcaceae	0	0	0	0	0
Enterococcaceae	0	2.38E-05	2.94E-05	0	0
Lactobacillaceae	0.00011	0.000143	8.83E-05	1.88E-05	9.13E-05
Turicibacteraceae	0	0	0	0	0
Clostridiales;f__	0.000679	0.000452	0.000294	0.000376	0.000244
Clostridiaceae	0	0	0	0	0
Lachnospiraceae	2.19E-05	0.000143	0.000412	9.40E-05	6.09E-05
Peptococcaceae	0	0	0	0	0
Ruminococcaceae	2.19E-05	2.38E-05	2.94E-05	5.64E-05	3.04E-05
Clostridiales;Other	0	0	0	0	0
Erysipelotrichaceae	0	0	5.89E-05	0	0
Fusobacteriaceae	0	0	0	0	0
Gemmatimonadaceae	0	0	0	0	0

Gemmatimonadetes;	0	0	0	0	0
c__3BR-5F;o__;f__	0.262215	0.254057	0.294843	0.279195	0.290672
c__GKS2-174;o__;f__	0	0	0	0	0
c__ZB2;o__;f__	0	0	0	0	0
Kiloniellales;f__	0.005453	0.006472	0.005416	0.006654	0.00618
Rhizobiales;f__	0.000832	0.000904	0.001266	0.001071	0.001309
Hyphomicrobiaceae	0.003811	0.004069	0.003974	0.003477	0.003866
Phyllobacteriaceae	0.002059	0.002498	0.001943	0.002068	0.002192
Rhizobiaceae	0.001007	0.00119	0.001001	0.001278	0.001553
Rhizobiales;Other	0.030814	0.037691	0.029258	0.031352	0.03023
Hyphomonadaceae	0.229014	0.239709	0.225879	0.21854	0.227533
Rhodobacteraceae	0.082718	0.082092	0.094043	0.078153	0.080553
Rhodobacterales;Other	0.000854	0.000785	0.00103	0.001353	0.001005
Acetobacteraceae	0	0	5.89E-05	3.76E-05	6.09E-05
Rickettsiaceae	0	2.38E-05	0	0	0
Sphingomonadales;f__	0	0	0	0	0
Sphingomonadaceae	0	0	0	0	0
Alphaproteobacteria;Other	0.00092	0.000999	0.001119	0.001428	0.001492
Comamonadaceae	8.76E-05	4.76E-05	2.94E-05	3.76E-05	0.000122
o__GMD14H09;f__	0.000241	0.000999	0.000383	0.000601	0.000244
Spirobacillales;f__	0	0	0	0	0
Helicobacteraceae	4.38E-05	0.000214	0.0005	0.000113	0.000822
Chromatiaceae	2.19E-05	2.38E-05	2.94E-05	0	3.04E-05
Alteromonadaceae	0.086091	0.090872	0.091305	0.100746	0.095927
Colwelliaceae	0	0	0	0	0
Alteromonadales; HTCC2188	0	0	0	0	0
Alteromonadales;Other	0	0	0	0	6.09E-05
Alcanivoracaceae	2.19E-05	7.14E-05	2.94E-05	1.88E-05	0
Halomonadaceae	0.00173	0.001095	0.001707	0.001616	0.001431
Pseudomonadaceae	4.38E-05	9.52E-05	5.89E-05	7.52E-05	9.13E-05
Unassigned;Other	0.015462	0.016656	0.016012	0.01592	0.016896

Table 6 Alpha diversity and Simpson's index of worms, algae and pre-colonized medium

Sample name	#OTU ID	Alpha diversity	Simpson's index
	H06512-L1	0.9231298	0.9231298
	H06513-L1	0.9184796	0.9184796
Algae	H06514-L1	0.7813383	0.7813383
	H06515-L1	1.00765	1.00765
	H06516-L1	0.8454561	0.8454561
	H20481-L1	2.76418103	2.76418103
	H20482-L1	2.84272665	2.84272665
PCM	H20483-L1	2.78606489	2.78606489
	H20484-L1	2.85364979	2.85364979
	H20485-L1	2.82028631	2.82028631
	H20476-L1	2.258818	2.258818
	H20477-L1	1.95099	1.95099
SWMs	H20478-L1	1.784506	1.784506
	H20479-L1	1.556563	1.556563
	H20480-L1	1.756543	1.756543
	H06507-L1	2.51758824	2.51758824
	H06508-L1	2.4968379	2.4968379
MWs	H06509-L1	2.47453583	2.47453583
	H06510-L1	2.51675349	2.51675349
	H06511-L1	2.47132045	2.47132045
	H06502-L1	2.39329594	2.39329594
	H06503-L1	2.43385199	2.43385199
IMWs	H06504-L1	2.31616895	2.31616895
	H06505-L1	2.398357	2.398357
	H06506-L1	2.29676438	2.29676438

Table 7: Weighted UniFrac analysis of worms, algae and pre-colonized medium.

Sample name	Seq_ID	PC1 (0.515)	PC2 (0.305)	PC3 (0.114)
PCM_1	H20481-L1	0.2191242	0.01584555	-0.06658901
PCM_2	H20482-L1	0.22682906	0.03579017	-0.07805446
PCM_3	H20483-L1	0.22086986	0.03290055	-0.06149929
PCM_4	H20484-L1	0.20837478	0.00146864	-0.04468497
PCM_5	H20485-L1	0.21912767	0.0252527	-0.05686066

MWs_1	H06507-L1	0.25257372	0.0827491	-0.08409545
MWs_2	H06508-L1	0.25567463	0.08380845	-0.07849644
MWs_3	H06509-L1	0.25616733	0.08495927	-0.08702439
MWs_4	H06510-L1	0.25246898	0.07027544	-0.08493741
MWs_5	H06511-L1	0.25336549	0.06363319	-0.08566256
SMWs_1	H20476-L1	0.05808223	0.02753649	0.1942579
SMWs_2	H20477-L1	0.11470612	0.03496089	0.1809343
SMWs_3	H20478-L1	0.17020143	0.04224452	0.17348387
SMWs_4	H20479-L1	0.20808758	0.04599121	0.16367524
SMWs_5	H20480-L1	0.18089229	0.05559114	0.18291134
Algae_1	H20486-L1	0.16471952	0.07928484	0.03708793
Algae_2	H20487-L1	0.16127711	0.0779301	0.04054245
Algae_3	H20488-L1	0.18512504	0.07909034	0.00886193
Algae_4	H20489-L1	0.16792933	0.0789564	0.05008936
Algae_5	H20490-L1	0.16803943	0.0761747	0.0377605

Table 8: Unweighted UniFrac analysis of worms, algae and pre-colonized medium.

Sample name	Seq_ID	PC1 (0.285)	PC2 (0.094)	PC3 (0.079)
PCM_1	H20481-L1	0.36045099	0.09817498	0.08451792
PCM_2	H20482-L1	0.36471381	0.07024344	0.08476858
PCM_3	H20483-L1	0.38020819	0.04793535	0.06963659
PCM_4	H20484-L1	0.31339414	0.07087817	0.05872854
PCM_5	H20485-L1	0.35133107	0.06522382	0.00353451
MWs_1	H06507-L1	0.35497729	0.12015253	0.05975333
MWs_2	H06508-L1	0.36193615	0.12460402	0.06605892
MWs_3	H06509-L1	0.37871479	0.07784069	0.02916755
MWs_4	H06510-L1	0.39100144	0.11353002	0.04102789
MWs_5	H06511-L1	0.4030131	0.05499979	0.05775541
SMWs_1	H20476-L1	0.03087684	0.22598193	0.04653367
SMWs_2	H20477-L1	0.14660433	0.05211133	-0.05434322
SMWs_3	H20478-L1	0.10345626	0.19137503	-0.02510707
SMWs_4	H20479-L1	0.0434085	0.17397409	-0.20442619
SMWs_5	H20480-L1	-0.0726343	0.19985952	-0.06616122
Algae_1	H20486-L1	-0.10986407	-0.00614803	-0.10372267
Algae_2	H20487-L1	-0.16235702	0.01146242	0.00196643
Algae_3	H20488-L1	-0.1550021	-0.04327803	-0.16867213

Algae_4	H20489-L1	-0.15231852	0.0038825	-0.08075729
Algae_5	H20490-L1	-0.12043471	0.03063084	-0.10159129

Table 9 Tukey's multiple comparisons test of OTU (Chao)

Sample name	Mean Diff,	95% CI of diff,	Significant?	Summary
MWs vs. SMWs	90.56	51,51 to 129,6	Yes	****
MWs vs. Del_ 700 µM_2 D	25.06	-13,99 to 64,11	No	ns
MWs vs. Amp_60 µg/ml_2 D	126.8	87,79 to 165,9	Yes	****
MWs vs. $CuSO_4$_14 µM_2 D	148.7	109,7 to 187,8	Yes	****
MWs vs. $CuSO_4$_12 µM_2 D	125.7	86,64 to 164,7	Yes	****
MWs vs. $CuSO_4$_10 µM_ 2 D	116	76,91 to 155,0	Yes	****
MWs vs. $CdSO_4$_730 µM_2 D	95.09	56,04 to 134,1	Yes	****
MWs vs. $CdSO_4$_460 µM_2 D	79.75	40,70 to 118,8	Yes	****
MWs vs. $CdSO_4$_330 µM_2 D	134.8	95,79 to 173,9	Yes	****
SMWs vs. Del_ 700 µM_2 D	-65.5	-104,6 to -26,45	Yes	****
SMWs vs. Amp_60 µg/ml_2 D	36.28	-2,768 to 75,33	No	ns
SMWs vs. $CuSO_4$_14 µM_2 D	58.17	19,12 to 97,22	Yes	***
SMWs vs. $CuSO_4$_12 µM_2 D	35.14	-3,916 to 74,19	No	ns
SMWs vs. $CuSO_4$_10 µM_ 2 D	25.4	-13,65 to 64,46	No	ns
SMWs vs. $CdSO_4$_730 µM_2 D	4.533	-34,52 to 43,58	No	ns
SMWs vs. $CdSO_4$_460 µM_2 D	-10.81	-49,86 to 28,24	No	ns
SMWs vs. $CdSO_4$_330 µM_2 D	44.28	5,232 to 83,33	Yes	*
Del_ 700 µM_2 D vs. Amp_60 µg/ml_2 D	101.8	62,73 to 140,8	Yes	****
Del_ 700 µM_2 D vs. $CuSO_4$_14 µM_2 D	123.7	84,62 to 162,7	Yes	****
Del_ 700 µM_2 D vs. $CuSO_4$_12 µM_2 D	100.6	61,58 to 139,7	Yes	****
Del_ 700 µM_2 D vs. $CuSO_4$_10 µM_ 2 D	90.9	51,85 to 130,0	Yes	****
Del_ 700 µM_2 D vs. $CdSO_4$_730 µM_2 D	70.03	30,98 to 109,1	Yes	****
Del_ 700 µM_2 D vs. $CdSO_4$_460 µM_2 D	54.69	15,64 to 93,74	Yes	**
Del_ 700 µM_2 D vs. $CdSO_4$_330 µM_2 D	109.8	70,73 to 148,8	Yes	****
Amp_60 µg/ml_2 D vs. $CuSO_4$_14 µM_2 D	21.89	-17,16 to 60,94	No	ns
Amp_60 µg/ml_2 D vs. $CuSO_4$_12 µM_2 D	-1.148	-40,20 to 37,90	No	ns
Amp_60 µg/ml_2 D vs. $CuSO_4$_10 µM_ 2 D	-10.88	-49,93 to 28,17	No	ns
Amp_60 µg/ml_2 D vs. $CdSO_4$_730 µM_2 D	-31.75	-70,80 to 7,301	No	ns
Amp_60 µg/ml_2 D vs. $CdSO_4$_460 µM_2 D	-47.09	-86,14 to -8,040	Yes	**
Amp_60 µg/ml_2 D vs. $CdSO_4$_330 µM_2 D	8	-31,05 to 47,05	No	ns

$CuSO_4$_14 µM_2 D vs. $CuSO_4$_12 µM_2 D	-23.04	-62,09 to 16,01	No	ns
$CuSO_4$_14 µM_2 D vs. $CuSO_4$_10 µM_ 2 D	-32.77	-71,82 to 6,284	No	ns
$CuSO_4$_14 µM_2 D vs. $CdSO_4$_730 µM_2 D	-53.64	-92,69 to -14,59	Yes	**
$CuSO_4$_14 µM_2 D vs. $CdSO_4$_460 µM_2 D	-68.98	-108,0 to -29,93	Yes	****
$CuSO_4$_14 µM_2 D vs. $CdSO_4$_330 µM_2 D	-13.89	-52,94 to 25,16	No	ns
$CuSO_4$_12 µM_2 D vs. $CuSO_4$_10 µM_ 2 D	-9.731	-48,78 to 29,32	No	ns
$CuSO_4$_12 µM_2 D vs. $CdSO_4$_730 µM_2 D	-30.6	-69,65 to 8,449	No	ns
$CuSO_4$_12 µM_2 D vs. $CdSO_4$_460 µM_2 D	-45.94	-84,99 to -6,892	Yes	*
$CuSO_4$_12 µM_2 D vs. $CdSO_4$_330 µM_2 D	9.148	-29,90 to 48,20	No	ns
$CuSO_4$_10 µM_ 2 D vs. $CdSO_4$_730 µM_2 D	-20.87	-59,92 to 18,18	No	ns
$CuSO_4$_10 µM_ 2 D vs. $CdSO_4$_460 µM_2 D	-36.21	-75,26 to 2,839	No	ns
$CuSO_4$_10 µM_ 2 D vs. $CdSO_4$_330 µM_2 D	18.88	-20,17 to 57,93	No	ns
$CdSO_4$_730 µM_2 D vs. $CdSO_4$_460 µM_2 D	-15.34	-54,39 to 23,71	No	ns
$CdSO_4$_730 µM_2 D vs. $CdSO_4$_330 µM_2 D	39.75	0,6989 to 78,80	Yes	*
$CdSO_4$_460 µM_2 D vs. $CdSO_4$_330 µM_2 D	55.09	16,04 to 94,14	Yes	**

Table 10 Tukey's multiple comparisons test of Shannon-Index

Tukey's multiple comparisons test	Mean Diff,	95% CI of diff,	Significant?	Summary
MWs vs. SMW_5 D	0.6339	0,3095 to 0,9583	Yes	****
MWs vs. Del_700 µM_2 D	0.04719	-0,2772 to 0,3716	No	ns
MWs vs. Amp_60 µg/ml_2 D	1.596	1,272 to 1,920	Yes	****
MWs vs. $CuSO_4$_14 µM_2 D	1.11	0,7859 to 1,435	Yes	****
MWs vs. $CuSO_4$_12 µM_2 D	0.8677	0,5433 to 1,192	Yes	****
MWs vs. $CuSO_4$_10 µM_2 D	0.806	0,4816 to 1,130	Yes	****
MWs vs. $CdSO_4$_730 µM_2 D	2.121	1,796 to 2,445	Yes	****
MWs vs. $CdSO_4$_460 µM_2 D	2.308	1,983 to 2,632	Yes	****
MWs vs. $CdSO_4$_330 µM_2 D	2.313	1,989 to 2,637	Yes	****
SMW_5 D vs. Del_700 µM_2 D	-0.5867	-0,9111 to -0,2623	Yes	****
SMW_5 D vs. Amp_60 µg/ml_2 D	0.9622	0,6378 to 1,287	Yes	****
SMW_5 D vs. $CuSO_4$_14 µM_2 D	0.4764	0,1520 to 0,8008	Yes	***
SMW_5 D vs. $CuSO_4$_12 µM_2 D	0.2337	-0,09066 to 0,5581	No	ns
SMW_5 D vs. $CuSO_4$_10 µM_2 D	0.1721	-0,1523 to 0,4965	No	ns
SMW_5 D vs. $CdSO_4$_730 µM_2 D	1.487	1,162 to 1,811	Yes	****
SMW_5 D vs. $CdSO_4$_460 µM_2 D	1.674	1,349 to 1,998	Yes	****
SMW_5 D vs. $CdSO_4$_330 µM_2 D	1.679	1,355 to 2,004	Yes	****
Del_700 µM_2 D vs. Amp_60 µg/ml_2 D	1.549	1,225 to 1,873	Yes	****

Del_700 µM_2 D vs. $CuSO_4$_14 µM_2 D	1.063	0,7387 to 1,387	Yes	****
Del_700 µM_2 D vs. $CuSO_4$_12 µM_2 D	0.8205	0,4961 to 1,145	Yes	****
Del_700 µM_2 D vs. $CuSO_4$_10 µM_2 D	0.7588	0,4344 to 1,083	Yes	****
Del_700 µM_2 D vs. $CdSO_4$_730 µM_2 D	2.073	1,749 to 2,398	Yes	****
Del_700 µM_2 D vs. $CdSO_4$_460 µM_2 D	2.26	1,936 to 2,585	Yes	****
Del_700 µM_2 D vs. $CdSO_4$_330 µM_2 D	2.266	1,941 to 2,590	Yes	****
Amp_60 µg/ml_2 D vs. $CuSO_4$_14 µM_2 D	-0.4858	-0,8102 to -0,1614	Yes	***
Amp_60 µg/ml_2 D vs. $CuSO_4$_12 µM_2 D	-0.7285	-1,053 to -0,4041	Yes	****
Amp_60 µg/ml_2 D vs. $CuSO_4$_10 µM_2 D	-0.7901	-1,115 to -0,4657	Yes	****
Amp_60 µg/ml_2 D vs. $CdSO_4$_730 µM_2 D	0.5245	0,2001 to 0,8489	Yes	***
Amp_60 µg/ml_2 D vs. $CdSO_4$_460 µM_2 D	0.7115	0,3871 to 1,036	Yes	****
Amp_60 µg/ml_2 D vs. $CdSO_4$_330 µM_2 D	0.7169	0,3925 to 1,041	Yes	****
$CuSO_4$_14 µM_2 D vs. $CuSO_4$_12 µM_2 D	-0.2426	-0,5670 to 0,08175	No	ns
$CuSO_4$_14 µM_2 D vs. $CuSO_4$_10 µM_2 D	-0.3043	-0,6287 to 0,02008	No	ns
$CuSO_4$_14 µM_2 D vs. $CdSO_4$_730 µM_2 D	1.01	0,6859 to 1,335	Yes	****
$CuSO_4$_14 µM_2 D vs. $CdSO_4$_460 µM_2 D	1.197	0,8729 to 1,522	Yes	****
$CuSO_4$_14 µM_2 D vs. $CdSO_4$_330 µM_2 D	1.203	0,8784 to 1,527	Yes	****
$CuSO_4$_12 µM_2 D vs. $CuSO_4$_10 µM_2 D	-0.06166	-0,3860 to 0,2627	No	ns
$CuSO_4$_12 µM_2 D vs. $CdSO_4$_730 µM_2 D	1.253	0,9286 to 1,577	Yes	****
$CuSO_4$_12 µM_2 D vs. $CdSO_4$_460 µM_2 D	1.44	1,116 to 1,764	Yes	****
$CuSO_4$_12 µM_2 D vs. $CdSO_4$_330 µM_2 D	1.445	1,121 to 1,770	Yes	****
$CuSO_4$_10 µM_2 D vs. $CdSO_4$_730 µM_2 D	1.315	0,9902 to 1,639	Yes	****
$CuSO_4$_10 µM_2 D vs. $CdSO_4$_460 µM_2 D	1.502	1,177 to 1,826	Yes	****
$CuSO_4$_10 µM_2 D vs. $CdSO_4$_330 µM_2 D	1.507	1,183 to 1,831	Yes	****
$CdSO_4$_730 µM_2 D vs. $CdSO_4$_460 µM_2 D	0.187	-0,1374 to 0,5114	No	ns
$CdSO_4$_730 µM_2 D vs. $CdSO_4$_330 µM_2 D	0.1924	-0,1320 to 0,5168	No	ns
$CdSO_4$_460 µM_2 D vs. $CdSO_4$_330 µM_2 D	0.005433	-0,3190 to 0,3298	No	ns

Table 11 Weighted UniFrac analysis of drug-treated worms

Sample name	Seq_ID	PC1 (0.515)	PC2 (0.305)	PC3 (0.114)
MWs_2D_1	H06507-L1	0.25257372	0.0827491	-0.08409545
MWs_2D_2	H06508-L1	0.25567463	0.08380845	-0.07849644
MWs_2D_3	H06509-L1	0.25616733	0.08495927	-0.08702439
MWs_2D_4	H06510-L1	0.25246898	0.07027544	-0.08493741
MWs_2D_5	H06511-L1	0.25336549	0.06363319	-0.08566256
Amp_60 µg/ml_2D_1	H06517-L1	0.02908428	-0.24170176	-0.00321347

Amp_60 µg/ml_2D_2	H06518-L1	0.00797704	-0.25042851	-0.00327732
Amp_60 µg/ml_2D_3	H06519-L1	0.01835212	-0.24871147	-0.01497974
Amp_60 µg/ml_2D_4	H06520-L1	0.04192772	-0.23217368	-0.01349857
Amp_60 µg/ml_2D_5	H06521-L1	0.02620678	-0.24339609	0.00667085
CuSO4_15µM_2D_1	H06522-L1	-0.05439585	-0.19922614	0.02969606
CuSO4_15µM_2D_2	H06523-L1	-0.04375643	-0.19570129	0.02922245
CuSO4_15µM_2D_3	H06524-L1	-0.05088309	-0.20165465	0.02410586
CuSO4_15µM_2D_4	H06525-L1	-0.04823841	-0.20051098	0.02497064
CuSO4_15µM_2D_5	H06526-L1	-0.02101984	-0.18189357	0.03503112
CuSO4_12µM_2D_1	H06527-L1	-0.06374837	-0.16047394	0.01973892
CuSO4_12µM_2D_2	H06528-L1	-0.09420567	-0.1534707	0.01838281
CuSO4_12µM_2D_3	H06529-L1	-0.11319845	-0.13644703	0.01438202
CuSO4_12µM_2D_4	H06530-L1	-0.10685728	-0.14719455	0.0173264
CuSO4_12µM_2D_5	H06531-L1	-0.11275815	-0.13563702	0.01247934
CuSO4_10µM_2D_1	H06532-L1	-0.08706639	-0.13919954	0.01072599
CuSO4_10µM_2D_2	H06533-L1	-0.07059562	-0.136214	0.00229517
CuSO4_10µM_2D_3	H06534-L1	-0.08808308	-0.15490306	0.02129354
CuSO4_10µM_2D_4	H06535-L1	-0.09425737	-0.15433013	0.02288849
CuSO4_10µM_2D_5	H06536-L1	-0.12463912	-0.11905847	0.00840732
CdSO4_730µM_2D_1	H06537-L1	-0.20456687	0.12864392	-0.05142138
CdSO4_730µM_2D_2	H06538-L1	-0.23569846	0.14155819	-0.02119009
CdSO4_730µM_2D_3	H06539-L1	-0.23366514	0.14115532	-0.02194542
CdSO4_730µM_2D_4	H06540-L1	-0.20528973	0.14578471	-0.03206373
CdSO4_730µM_2D_5	H06541-L1	-0.22304981	0.14324455	-0.02321412
CdSO4_460µM_2D_1	H06542-L1	-0.23530305	0.14217056	-0.02021549
CdSO4_460µM_2D_2	H06543-L1	-0.21699571	0.11939983	-0.04283651
CdSO4_460µM_2D_3	H06544-L1	-0.2348994	0.14233631	-0.02062586
CdSO4_460µM_2D_4	H06545-L1	-0.23517223	0.14183623	-0.02090084
CdSO4_460µM_2D_5	H06546-L1	-0.23645202	0.14263321	-0.01955457
CdSO4_330µM_2D_1	H06547-L1	-0.22467137	0.14119691	-0.02354475
CdSO4_330µM_2D_2	H06548-L1	-0.23752838	0.14253206	-0.02012464
CdSO4_330µM_2D_3	H06549-L1	-0.23838112	0.14242409	-0.01903588
CdSO4_330µM_2D_4	H06550-L1	-0.23356115	0.14155207	-0.02053031
CdSO4_330µM_2D_5	H06551-L1	-0.23480266	0.14111158	-0.0211794
Del_700µM_2D_1	H06552-L1	0.18961979	0.13212454	0.24507731
Del_700µM_2D_2	H06553-L1	0.17108586	0.13231658	0.24087002
Del_700µM_2D_3	H06554-L1	0.1715007	0.13138073	0.25158602

Del_700µM_2D_4	H06555-L1	0.16823968	0.13098638	0.25358737
Del_700µM_2D_5	H06556-L1	0.15395452	0.13291693	0.26610741

Table 12 Unweighted UniFrac analysis of drug-treated worms

Sample name	Seq_ID	PC1 (0.285)	PC2 (0.094)	PC3 (0.079)
MWs_2D_1	H06507-L1	0.35497729	0.12015253	0.05975333
MWs_2D_2	H06508-L1	0.36193615	0.12460402	0.06605892
MWs_2D_3	H06509-L1	0.37871479	0.07784069	0.02916755
MWs_2D_4	H06510-L1	0.39100144	0.11353002	0.04102789
MWs_2D_5	H06511-L1	0.4030131	0.05499979	0.05775541
Amp_60 µg/ml_2D_1	H06517-L1	0.05141511	0.09015956	-0.08227548
Amp_60 µg/ml_2D_2	H06518-L1	0.02824512	0.1246271	-0.12178529
Amp_60 µg/ml_2D_3	H06519-L1	0.01822401	0.11369774	0.03164441
Amp_60 µg/ml_2D_4	H06520-L1	0.00784282	0.11572918	-0.11575266
Amp_60 µg/ml_2D_5	H06521-L1	0.05117016	0.03740921	-0.13326246
CuSO4_15µM_2D_1	H06522-L1	-0.21806487	-0.00892148	-0.01059091
CuSO4_15µM_2D_2	H06523-L1	-0.23504936	0.04113393	0.04786548
CuSO4_15µM_2D_3	H06524-L1	-0.2760606	0.08093785	-0.14612845
CuSO4_15µM_2D_4	H06525-L1	-0.25912218	0.05142461	0.0184081
CuSO4_15µM_2D_5	H06526-L1	-0.16215576	-0.05702932	-5.40E-05
CuSO4_12µM_2D_1	H06527-L1	-0.20905712	0.09498778	-0.07002006
CuSO4_12µM_2D_2	H06528-L1	-0.32065903	0.08481191	-0.07869904
CuSO4_12µM_2D_3	H06529-L1	-0.27619449	0.0223589	-0.10538313
CuSO4_12µM_2D_4	H06530-L1	-0.23951921	0.14792919	-0.13042826
CuSO4_12µM_2D_5	H06531-L1	-0.27287921	0.13148067	-0.11176069
CuSO4_10µM_2D_1	H06532-L1	-0.24333762	0.01616349	-0.00871597
CuSO4_10µM_2D_2	H06533-L1	-0.28731279	0.07410073	-0.09498396
CuSO4_10µM_2D_3	H06534-L1	-0.22999208	0.12142426	-0.19453328
CuSO4_10µM_2D_4	H06535-L1	-0.28664709	0.10265031	-0.14032263
CuSO4_10µM_2D_5	H06536-L1	-0.22404126	0.10391483	-0.22027791
CdSO4_730µM_2D_1	H06537-L1	-0.15627045	-0.15588719	0.18772973
CdSO4_730µM_2D_2	H06538-L1	-0.16183701	-0.00981195	-0.13784723
CdSO4_730µM_2D_3	H06539-L1	-0.08266361	-0.15013378	0.26041852
CdSO4_730µM_2D_4	H06540-L1	-0.04258497	-0.07587608	0.17263116

CdSO4_730µM_2D_5	H06541-L1	-0.13170896	-0.15552582	0.28355406
CdSO4_460µM_2D_1	H06542-L1	-0.19417042	-0.08428465	0.19545381
CdSO4_460µM_2D_2	H06543-L1	-0.27335546	0.0527461	-0.00961366
CdSO4_460µM_2D_3	H06544-L1	-0.23226209	-0.10456916	0.19502131
CdSO4_460µM_2D_4	H06545-L1	-0.24654128	0.00997053	0.13721317
CdSO4_460µM_2D_5	H06546-L1	-0.21054058	-0.13823603	0.2523474
CdSO4_330µM_2D_1	H06547-L1	-0.11311924	-0.03875012	0.21839163
CdSO4_330µM_2D_2	H06548-L1	-0.19545639	0.01074083	0.12705143
CdSO4_330µM_2D_3	H06549-L1	-0.21800193	0.01701423	-0.17214828
CdSO4_330µM_2D_4	H06550-L1	-0.23213284	-0.03307422	0.15817516
CdSO4_330µM_2D_5	H06551-L1	-0.24182874	-0.06303444	0.16722963
Del_700µM_2D_1	H06552-L1	0.17766954	-0.4153594	-0.22147966
Del_700µM_2D_2	H06553-L1	0.2542905	-0.33333514	-0.06528731
Del_700µM_2D_3	H06554-L1	0.18432059	-0.40678809	-0.18557169
Del_700µM_2D_4	H06555-L1	0.18588798	-0.41475071	-0.14501807
Del_700µM_2D_5	H06556-L1	0.16951758	-0.37901473	-0.25099441

Table 13 Bray-Curtis index of drug-treated animals

	H06507	H06508	H06509	H06510	H06511	H06517	H06518	H06519	H06520
H06507	0	0.031	0.052	0.043	0.046	0.752	0.782	0.785	0.695
H06508	0.031	0	0.055	0.044	0.046	0.748	0.776	0.779	0.691
H06509	0.052	0.055	0	0.041	0.025	0.738	0.776	0.779	0.696
H06510	0.043	0.044	0.041	0	0.026	0.743	0.767	0.77	0.68
H06511	0.046	0.046	0.025	0.026	0	0.745	0.772	0.774	0.688
H06517	0.752	0.748	0.738	0.743	0.745	0	0.057	0.047	0.08
H06518	0.782	0.776	0.776	0.767	0.772	0.057	0	0.027	0.111
H06519	0.785	0.779	0.779	0.77	0.774	0.047	0.027	0	0.114
H06520	0.695	0.691	0.696	0.68	0.688	0.08	0.111	0.114	0
H06521	0.757	0.751	0.751	0.742	0.747	0.054	0.076	0.076	0.087
H06522	0.903	0.898	0.898	0.889	0.894	0.165	0.124	0.122	0.232
H06523	0.867	0.862	0.862	0.853	0.858	0.131	0.089	0.092	0.197
H06524	0.894	0.89	0.889	0.88	0.885	0.156	0.116	0.112	0.223
H06525	0.888	0.883	0.883	0.873	0.879	0.151	0.11	0.107	0.218
H06526	0.809	0.815	0.815	0.805	0.813	0.135	0.097	0.094	0.197
H06527	0.852	0.847	0.847	0.838	0.842	0.155	0.158	0.156	0.182
H06528	0.893	0.888	0.887	0.878	0.883	0.178	0.179	0.178	0.221

H06529	0.901	0.896	0.896	0.886	0.891	0.237	0.238	0.237	0.237
H06530	0.904	0.899	0.898	0.889	0.893	0.195	0.196	0.194	0.232
H06531	0.896	0.891	0.891	0.881	0.886	0.208	0.208	0.207	0.225
H06532	0.859	0.854	0.853	0.844	0.849	0.203	0.205	0.204	0.198
H06533	0.805	0.8	0.799	0.79	0.795	0.227	0.225	0.233	0.198
H06534	0.887	0.882	0.881	0.872	0.876	0.171	0.171	0.17	0.215
H06535	0.888	0.883	0.882	0.873	0.878	0.18	0.18	0.18	0.216
H06536	0.9	0.895	0.895	0.886	0.89	0.271	0.272	0.27	0.271
H06537	0.949	0.967	0.967	0.966	0.97	0.972	0.974	0.97	0.971
H06538	0.988	0.988	0.988	0.988	0.988	0.986	0.987	0.986	0.986
H06539	0.983	0.982	0.982	0.983	0.983	0.983	0.984	0.982	0.982
H06540	0.931	0.948	0.949	0.948	0.952	0.966	0.968	0.964	0.965
H06541	0.957	0.971	0.971	0.97	0.974	0.982	0.983	0.979	0.98
H06542	0.985	0.984	0.984	0.984	0.986	0.987	0.987	0.985	0.986
H06543	0.927	0.926	0.926	0.927	0.926	0.926	0.926	0.924	0.924
H06544	0.987	0.987	0.987	0.987	0.989	0.989	0.99	0.988	0.988
H06545	0.99	0.989	0.989	0.99	0.99	0.989	0.99	0.988	0.988
H06546	0.99	0.99	0.99	0.99	0.991	0.992	0.992	0.991	0.991
H06547	0.965	0.968	0.968	0.968	0.971	0.972	0.975	0.973	0.969
H06548	0.992	0.992	0.991	0.992	0.992	0.992	0.992	0.991	0.991
H06549	0.993	0.993	0.993	0.993	0.993	0.991	0.992	0.991	0.991
H06550	0.978	0.977	0.977	0.978	0.978	0.976	0.979	0.977	0.975
H06551	0.978	0.978	0.978	0.979	0.98	0.98	0.981	0.98	0.979
H06552	0.664	0.66	0.672	0.665	0.667	0.959	0.961	0.967	0.951
H06553	0.734	0.721	0.739	0.73	0.73	0.942	0.945	0.95	0.933
H06554	0.785	0.78	0.789	0.783	0.784	0.959	0.961	0.967	0.951
H06555	0.742	0.75	0.759	0.752	0.755	0.958	0.959	0.965	0.95
H06556	0.796	0.791	0.8	0.794	0.792	0.962	0.963	0.969	0.953

	H06521	H06522	H06523	H06524	H06525	H06526	H06527	H06528	H06529
H06507	0.757	0.903	0.867	0.894	0.888	0.809	0.852	0.893	0.901
H06508	0.751	0.898	0.862	0.89	0.883	0.815	0.847	0.888	0.896
H06509	0.751	0.898	0.862	0.889	0.883	0.815	0.847	0.887	0.896
H06510	0.742	0.889	0.853	0.88	0.873	0.805	0.838	0.878	0.886
H06511	0.747	0.894	0.858	0.885	0.879	0.813	0.842	0.883	0.891
H06517	0.054	0.165	0.131	0.156	0.151	0.135	0.155	0.178	0.237

H06518	0.076	0.124	0.089	0.116	0.11	0.097	0.158	0.179	0.238
H06519	0.076	0.122	0.092	0.112	0.107	0.094	0.156	0.178	0.237
H06520	0.087	0.232	0.197	0.223	0.218	0.197	0.182	0.221	0.237
H06521	0	0.181	0.148	0.174	0.168	0.155	0.166	0.189	0.238
H06522	0.181	0	0.037	0.01	0.016	0.104	0.187	0.184	0.234
H06523	0.148	0.037	0	0.034	0.027	0.089	0.167	0.188	0.237
H06524	0.174	0.01	0.034	0	0.011	0.103	0.189	0.192	0.241
H06525	0.168	0.016	0.027	0.011	0	0.096	0.184	0.193	0.243
H06526	0.155	0.104	0.089	0.103	0.096	0	0.161	0.175	0.225
H06527	0.166	0.187	0.167	0.189	0.184	0.161	0	0.043	0.096
H06528	0.189	0.184	0.188	0.192	0.193	0.175	0.043	0	0.065
H06529	0.238	0.234	0.237	0.241	0.243	0.225	0.096	0.065	0
H06530	0.196	0.191	0.194	0.198	0.2	0.182	0.054	0.02	0.049
H06531	0.214	0.21	0.213	0.216	0.219	0.2	0.067	0.035	0.032
H06532	0.214	0.236	0.216	0.238	0.233	0.21	0.058	0.056	0.043
H06533	0.235	0.267	0.239	0.269	0.264	0.242	0.086	0.089	0.097
H06534	0.175	0.181	0.173	0.184	0.18	0.161	0.037	0.016	0.069
H06535	0.181	0.189	0.176	0.193	0.187	0.166	0.039	0.024	0.063
H06536	0.272	0.269	0.267	0.272	0.272	0.254	0.131	0.104	0.042
H06537	0.976	0.982	0.984	0.988	0.989	0.95	0.837	0.809	0.751
H06538	0.987	0.985	0.987	0.991	0.994	0.974	0.847	0.814	0.752
H06539	0.984	0.983	0.984	0.988	0.99	0.969	0.843	0.814	0.751
H06540	0.974	0.982	0.983	0.987	0.989	0.95	0.833	0.805	0.752
H06541	0.981	0.983	0.985	0.989	0.991	0.952	0.844	0.815	0.753
H06542	0.986	0.985	0.986	0.991	0.992	0.97	0.846	0.814	0.753
H06543	0.926	0.92	0.922	0.927	0.928	0.91	0.785	0.751	0.691
H06544	0.989	0.986	0.987	0.992	0.993	0.972	0.849	0.817	0.755
H06545	0.99	0.986	0.988	0.992	0.994	0.974	0.85	0.817	0.756
H06546	0.991	0.986	0.987	0.992	0.993	0.972	0.851	0.818	0.757
H06547	0.973	0.982	0.984	0.988	0.989	0.959	0.838	0.807	0.75
H06548	0.991	0.984	0.986	0.991	0.992	0.973	0.85	0.818	0.757
H06549	0.991	0.985	0.987	0.991	0.993	0.974	0.852	0.818	0.757
H06550	0.98	0.985	0.987	0.99	0.993	0.97	0.841	0.81	0.752
H06551	0.98	0.982	0.983	0.987	0.989	0.968	0.842	0.811	0.75
H06552	0.958	0.981	0.978	0.983	0.985	0.9	0.955	0.962	0.959
H06553	0.952	0.981	0.979	0.984	0.985	0.906	0.937	0.944	0.953
H06554	0.96	0.981	0.979	0.984	0.985	0.903	0.948	0.956	0.953

H06555	0.961	0.981	0.979	0.984	0.985	0.892	0.949	0.956	0.954
H06556	0.962	0.981	0.98	0.983	0.986	0.908	0.936	0.943	0.94

	H06530	H06531	H06532	H06533	H06534	H06535	H06536	H06537	H06538
H06507	0.904	0.896	0.859	0.805	0.887	0.888	0.9	0.949	0.988
H06508	0.899	0.891	0.854	0.8	0.882	0.883	0.895	0.967	0.988
H06509	0.898	0.891	0.853	0.799	0.881	0.882	0.895	0.967	0.988
H06510	0.889	0.881	0.844	0.79	0.872	0.873	0.886	0.966	0.988
H06511	0.893	0.886	0.849	0.795	0.876	0.878	0.89	0.97	0.988
H06517	0.195	0.208	0.203	0.227	0.171	0.18	0.271	0.972	0.986
H06518	0.196	0.208	0.205	0.225	0.171	0.18	0.272	0.974	0.987
H06519	0.194	0.207	0.204	0.233	0.17	0.18	0.27	0.97	0.986
H06520	0.232	0.225	0.198	0.198	0.215	0.216	0.271	0.971	0.986
H06521	0.196	0.214	0.214	0.235	0.175	0.181	0.272	0.976	0.987
H06522	0.191	0.21	0.236	0.267	0.181	0.189	0.269	0.982	0.985
H06523	0.194	0.213	0.216	0.239	0.173	0.176	0.267	0.984	0.987
H06524	0.198	0.216	0.238	0.269	0.184	0.193	0.272	0.988	0.991
H06525	0.2	0.219	0.233	0.264	0.18	0.187	0.272	0.989	0.994
H06526	0.182	0.2	0.21	0.242	0.161	0.166	0.254	0.95	0.974
H06527	0.054	0.067	0.058	0.086	0.037	0.039	0.131	0.837	0.847
H06528	0.02	0.035	0.056	0.089	0.016	0.024	0.104	0.809	0.814
H06529	0.049	0.032	0.043	0.097	0.069	0.063	0.042	0.751	0.752
H06530	0	0.024	0.051	0.1	0.026	0.02	0.088	0.798	0.799
H06531	0.024	0	0.039	0.092	0.042	0.039	0.072	0.776	0.781
H06532	0.051	0.039	0	0.057	0.057	0.048	0.075	0.781	0.79
H06533	0.1	0.092	0.057	0	0.09	0.084	0.097	0.802	0.811
H06534	0.026	0.042	0.057	0.09	0	0.018	0.103	0.815	0.818
H06535	0.02	0.039	0.048	0.084	0.018	0	0.093	0.812	0.814
H06536	0.088	0.072	0.075	0.097	0.103	0.093	0	0.722	0.723
H06537	0.798	0.776	0.781	0.802	0.815	0.812	0.722	0	0.191
H06538	0.799	0.781	0.79	0.811	0.818	0.814	0.723	0.191	0
H06539	0.798	0.781	0.787	0.809	0.817	0.812	0.722	0.186	0.008
H06540	0.798	0.776	0.776	0.798	0.814	0.812	0.722	0.134	0.078
H06541	0.798	0.783	0.787	0.81	0.819	0.812	0.722	0.167	0.034
H06542	0.798	0.782	0.79	0.811	0.82	0.813	0.723	0.187	0.007
H06543	0.735	0.72	0.729	0.75	0.758	0.748	0.658	0.195	0.069

H06544	0.801	0.784	0.793	0.814	0.823	0.815	0.724	0.19	0.009
H06545	0.801	0.785	0.793	0.814	0.823	0.815	0.724	0.192	0.009
H06546	0.802	0.786	0.794	0.816	0.824	0.814	0.724	0.193	0.009
H06547	0.795	0.775	0.781	0.804	0.814	0.811	0.721	0.173	0.029
H06548	0.802	0.786	0.794	0.816	0.824	0.814	0.723	0.196	0.012
H06549	0.802	0.786	0.795	0.816	0.825	0.815	0.724	0.196	0.01
H06550	0.798	0.778	0.785	0.807	0.816	0.813	0.723	0.183	0.014
H06551	0.796	0.778	0.786	0.808	0.817	0.811	0.721	0.186	0.013
H06552	0.961	0.96	0.954	0.953	0.958	0.96	0.961	0.942	0.959
H06553	0.955	0.948	0.937	0.936	0.948	0.956	0.957	0.935	0.952
H06554	0.954	0.954	0.948	0.947	0.952	0.953	0.953	0.938	0.953
H06555	0.955	0.954	0.949	0.947	0.952	0.953	0.954	0.926	0.954
H06556	0.941	0.94	0.936	0.934	0.939	0.939	0.94	0.929	0.94

	H06539	H06540	H06541	H06542	H06543	H06544	H06545	H06546	H06547
H06507	0.983	0.931	0.957	0.985	0.927	0.987	0.99	0.99	0.965
H06508	0.982	0.948	0.971	0.984	0.926	0.987	0.989	0.99	0.968
H06509	0.982	0.949	0.971	0.984	0.926	0.987	0.989	0.99	0.968
H06510	0.983	0.948	0.97	0.984	0.927	0.987	0.99	0.99	0.968
H06511	0.983	0.952	0.974	0.986	0.926	0.989	0.99	0.991	0.971
H06517	0.983	0.966	0.982	0.987	0.926	0.989	0.989	0.992	0.972
H06518	0.984	0.968	0.983	0.987	0.926	0.99	0.99	0.992	0.975
H06519	0.982	0.964	0.979	0.985	0.924	0.988	0.988	0.991	0.973
H06520	0.982	0.965	0.98	0.986	0.924	0.988	0.988	0.991	0.969
H06521	0.984	0.974	0.981	0.986	0.926	0.989	0.99	0.991	0.973
H06522	0.983	0.982	0.983	0.985	0.92	0.986	0.986	0.986	0.982
H06523	0.984	0.983	0.985	0.986	0.922	0.987	0.988	0.987	0.984
H06524	0.988	0.987	0.989	0.991	0.927	0.992	0.992	0.992	0.988
H06525	0.99	0.989	0.991	0.992	0.928	0.993	0.994	0.993	0.989
H06526	0.969	0.95	0.952	0.97	0.91	0.972	0.974	0.972	0.959
H06527	0.843	0.833	0.844	0.846	0.785	0.849	0.85	0.851	0.838
H06528	0.814	0.805	0.815	0.814	0.751	0.817	0.817	0.818	0.807
H06529	0.751	0.752	0.753	0.753	0.691	0.755	0.756	0.757	0.75
H06530	0.798	0.798	0.798	0.798	0.735	0.801	0.801	0.802	0.795
H06531	0.781	0.776	0.783	0.782	0.72	0.784	0.785	0.786	0.775
H06532	0.787	0.776	0.787	0.79	0.729	0.793	0.793	0.794	0.781

H06533	0.809	0.798	0.81	0.811	0.75	0.814	0.814	0.816	0.804
H06534	0.817	0.814	0.819	0.82	0.758	0.823	0.823	0.824	0.814
H06535	0.812	0.812	0.812	0.813	0.748	0.815	0.815	0.814	0.811
H06536	0.722	0.722	0.722	0.723	0.658	0.724	0.724	0.724	0.721
H06537	0.186	0.134	0.167	0.187	0.195	0.19	0.192	0.193	0.173
H06538	0.008	0.078	0.034	0.007	0.069	0.009	0.009	0.009	0.029
H06539	0	0.073	0.028	0.007	0.068	0.009	0.01	0.011	0.026
H06540	0.073	0	0.047	0.075	0.083	0.078	0.08	0.081	0.059
H06541	0.028	0.047	0	0.03	0.068	0.033	0.035	0.035	0.02
H06542	0.007	0.075	0.03	0	0.067	0.005	0.007	0.007	0.025
H06543	0.068	0.083	0.068	0.067	0	0.068	0.068	0.068	0.064
H06544	0.009	0.078	0.033	0.005	0.068	0	0.004	0.004	0.027
H06545	0.01	0.08	0.035	0.007	0.068	0.004	0	0.004	0.03
H06546	0.011	0.081	0.035	0.007	0.068	0.004	0.004	0	0.03
H06547	0.026	0.059	0.02	0.025	0.064	0.027	0.03	0.03	0
H06548	0.013	0.084	0.038	0.01	0.068	0.007	0.006	0.004	0.032
H06549	0.012	0.084	0.038	0.01	0.069	0.009	0.008	0.009	0.034
H06550	0.012	0.071	0.031	0.012	0.067	0.014	0.014	0.017	0.016
H06551	0.009	0.074	0.03	0.009	0.064	0.01	0.013	0.013	0.019
H06552	0.954	0.927	0.939	0.955	0.96	0.956	0.958	0.958	0.94
H06553	0.948	0.917	0.939	0.951	0.957	0.954	0.954	0.956	0.935
H06554	0.948	0.923	0.935	0.949	0.954	0.95	0.951	0.951	0.936
H06555	0.949	0.911	0.923	0.949	0.954	0.95	0.952	0.952	0.934
H06556	0.936	0.915	0.927	0.939	0.941	0.939	0.939	0.941	0.928

	H06548	H06549	H06550	H06551	H06552	H06553	H06554	H06555	H06556
H06507	0.992	0.993	0.978	0.978	0.664	0.734	0.785	0.742	0.796
H06508	0.992	0.993	0.977	0.978	0.66	0.721	0.78	0.75	0.791
H06509	0.991	0.993	0.977	0.978	0.672	0.739	0.789	0.759	0.8
H06510	0.992	0.993	0.978	0.979	0.665	0.73	0.783	0.752	0.794
H06511	0.992	0.993	0.978	0.98	0.667	0.73	0.784	0.755	0.792
H06517	0.992	0.991	0.976	0.98	0.959	0.942	0.959	0.958	0.962
H06518	0.992	0.992	0.979	0.981	0.961	0.945	0.961	0.959	0.963
H06519	0.991	0.991	0.977	0.98	0.967	0.95	0.967	0.965	0.969
H06520	0.991	0.991	0.975	0.979	0.951	0.933	0.951	0.95	0.953
H06521	0.991	0.991	0.98	0.98	0.958	0.952	0.96	0.961	0.962

H06522	0.984	0.985	0.985	0.982	0.981	0.981	0.981	0.981	0.981
H06523	0.986	0.987	0.987	0.983	0.978	0.979	0.979	0.979	0.98
H06524	0.991	0.991	0.99	0.987	0.983	0.984	0.984	0.984	0.983
H06525	0.992	0.993	0.993	0.989	0.985	0.985	0.985	0.985	0.986
H06526	0.973	0.974	0.97	0.968	0.9	0.906	0.903	0.892	0.908
H06527	0.85	0.852	0.841	0.842	0.955	0.937	0.948	0.949	0.936
H06528	0.818	0.818	0.81	0.811	0.962	0.944	0.956	0.956	0.943
H06529	0.757	0.757	0.752	0.75	0.959	0.953	0.953	0.954	0.94
H06530	0.802	0.802	0.798	0.796	0.961	0.955	0.954	0.955	0.941
H06531	0.786	0.786	0.778	0.778	0.96	0.948	0.954	0.954	0.94
H06532	0.794	0.795	0.785	0.786	0.954	0.937	0.948	0.949	0.936
H06533	0.816	0.816	0.807	0.808	0.953	0.936	0.947	0.947	0.934
H06534	0.824	0.825	0.816	0.817	0.958	0.948	0.952	0.952	0.939
H06535	0.814	0.815	0.813	0.811	0.96	0.956	0.953	0.953	0.939
H06536	0.723	0.724	0.723	0.721	0.961	0.957	0.953	0.954	0.94
H06537	0.196	0.196	0.183	0.186	0.942	0.935	0.938	0.926	0.929
H06538	0.012	0.01	0.014	0.013	0.959	0.952	0.953	0.954	0.94
H06539	0.013	0.012	0.012	0.009	0.954	0.948	0.948	0.949	0.936
H06540	0.084	0.084	0.071	0.074	0.927	0.917	0.923	0.911	0.915
H06541	0.038	0.038	0.031	0.03	0.939	0.939	0.935	0.923	0.927
H06542	0.01	0.01	0.012	0.009	0.955	0.951	0.949	0.949	0.939
H06543	0.068	0.069	0.067	0.064	0.96	0.957	0.954	0.954	0.941
H06544	0.007	0.009	0.014	0.01	0.956	0.954	0.95	0.95	0.939
H06545	0.006	0.008	0.014	0.013	0.958	0.954	0.951	0.952	0.939
H06546	0.004	0.009	0.017	0.013	0.958	0.956	0.951	0.952	0.941
H06547	0.032	0.034	0.016	0.019	0.94	0.935	0.936	0.934	0.928
H06548	0	0.009	0.018	0.015	0.961	0.958	0.953	0.954	0.941
H06549	0.009	0	0.019	0.017	0.96	0.957	0.952	0.954	0.939
H06550	0.018	0.019	0	0.008	0.952	0.941	0.945	0.946	0.932
H06551	0.015	0.017	0.008	0	0.952	0.948	0.946	0.947	0.936
H06552	0.961	0.96	0.952	0.952	0	0.208	0.205	0.123	0.166
H06553	0.958	0.957	0.941	0.948	0.208	0	0.172	0.18	0.161
H06554	0.953	0.952	0.945	0.946	0.205	0.172	0	0.108	0.105
H06555	0.954	0.954	0.946	0.947	0.123	0.18	0.108	0	0.113
H06556	0.941	0.939	0.932	0.936	0.166	0.161	0.105	0.113	0

Table 14 Dunnett's multiple comparisons test of OTU (Chao)

Sample name	Mean Diff,	95% CI of diff,	Significant?	Summary
SMWs_ 5 D vs. MWs	-90.56	-121,8 to -59,33	Yes	****
SMWs_ 5 D vs. Atr_220 uM_5 D	4.4	-26,83 to 35,63	No	ns
SMWs_ 5 D vs. Bis_ 2000 uM_2 D	-5.161	-36,39 to 26,07	No	ns
SMWs_ 5 D vs. Del_700 uM_5 D	26.3	-4,929 to 57,53	No	ns
SMWs_ 5 D vs. ABD_220 µM_5 D	-6.388	-37,62 to 24,84	No	ns

Table 15 Turkey's multiple comparisons test of Shannon-Index

	Mean Diff,	95% CI of diff,	Significant ?	Summary
MWs vs. SMWs_5 D	0.6339	0,04342 to 1,224	Yes	*
MWs vs. Atr_220 uM_5 D	0.3584	-0,2321 to 0,9489	No	ns
MWs vs. Bis_2000 uM_2D	0.7539	0,1634 to 1,344	Yes	**
MWs vs. Del _700 uM_5 D	-0.1477	-0,7382 to 0,4428	No	ns
MWs vs. ABD_220 µM_5 D	0.04001	-0,5505 to 0,6305	No	ns
SMWs_5 D vs. Atr_220 uM_5 D	-0.2755	-0,8660 to 0,3150	No	ns
SMWs_5 D vs. Bis_2000 uM_2D	0.12	-0,4705 to 0,7105	No	ns
SMWs_5 D vs. Del _700 uM_5 D	-0.7816	-1,372 to -0,1911	Yes	**
SMWs_5 D vs. ABD_220 µM_5 D	-0.5939	-1,184 to -0,003408	Yes	*
Atr_220 uM_5 D vs. Bis_2000 uM_2D	0.3955	-0,1950 to 0,9860	No	ns
Atr_220 uM_5 D vs. Del _700 uM_5 D	-0.5061	-1,097 to 0,08441	No	ns
Atr_220 uM_5 D vs. ABD_220 µM_5 D	-0.3184	-0,9089 to 0,2721	No	ns
Bis_2000 uM_2D vs. Del _700 uM_5 D	-0.9016	-1,492 to -0,3111	Yes	**
Bis_2000 uM_2D vs. ABD_220 µM_5 D	-0.7139	-1,304 to -0,1234	Yes	*
Del _700 uM_5 D vs. ABD_220 µM_5 D	0.1877	-0,4028 to 0,7782	No	ns

Table 16 Weighted Unifrac analysis of drug treated animals

Sample name	Seq_ID	PC1 (0.366)	PC2 (0.209)	PC3 (0.143)
SMWs_5D_1	H20476-L1	0.05808223	0.02753649	0.1942579
SMWs_5D_2	H20477-L1	0.11470612	0.03496089	0.1809343
SMWs_5D_3	H20478-L1	0.17020143	0.04224452	0.17348387
SMWs_5D_4	H20479-L1	0.20808758	0.04599121	0.16367524
SMWs_5D_5	H20480-L1	0.18089229	0.05559114	0.18291134
Algae_20D_1	H20481-L1	0.20826176	-0.00281653	0.10160395

Algae_20D_2	H20482-L1	0.01354913	-0.06215594	0.10754631
Algae_20D_3	H20483-L1	0.194315	-0.00168677	0.09931517
Algae_20D_4	H20484-L1	0.00696824	-0.05678026	0.05909898
Algae_20D_5	H20485-L1	-0.02168247	-0.05300522	0.09499796
$CdSO_4$_730 uM_2D_1	H20486-L1	0.16471952	0.07928484	0.03708793
$CdSO_4$_730 uM_2D_2	H20487-L1	0.16127711	0.0779301	0.04054245
$CdSO_4$_730 uM_2D_3	H20488-L1	0.18512504	0.07909034	0.00886193
$CdSO_4$_730 uM_2D_4	H20489-L1	0.16792933	0.0789564	0.05008936
$CdSO_4$_460 uM_2D_1	H20501-L1	0.01204797	0.13647737	0.2168453
$CdSO_4$_460 uM_2D_2	H20502-L1	0.02842951	0.21942524	0.10906178
$CdSO_4$_460 uM_2D_3	H20503-L1	0.03849776	0.25161575	0.20164194
$CdSO_4$_460 uM_2D_4	H20504-L1	-0.01539578	0.24770557	0.16662593
$CdSO_4$_460 uM_2D_5	H20505-L1	0.0286643	0.26880929	0.13365745
$CdSO_4$_330 uM_2D_1	H20511-L1	0.12245279	0.24270934	-0.1560742
$CdSO_4$_330 uM_2D_2	H20512-L1	0.13676979	0.24235641	-0.21110953
$CdSO_4$_330 uM_2D_3	H20513-L1	0.13752116	0.23819238	-0.22550725
$CdSO_4$_330 uM_2D_4	H20514-L1	0.13083786	0.23674595	-0.21276717
$CdSO_4$_330 uM_2D_5	H20515-L1	0.13671655	0.23779785	-0.22159203
$CuSO_4$_15 uM_5D_1	H20521-L1	0.26164333	-0.18816581	-0.12960918
$CuSO_4$_15 uM_5D_2	H20522-L1	0.20004	-0.18236042	-0.0678046
$CuSO_4$_15 uM_5D_3	H20523-L1	0.24790798	-0.17984666	-0.10698331
$CuSO_4$_15 uM_5D_4	H20524-L1	0.24846274	-0.1757811	-0.0641283
$CuSO_4$_15 uM_5D_5	H20525-L1	0.24715877	-0.17778241	-0.09849192
$CuSO_4$_12 uM_5D_1	H20531-L1	0.02188172	-0.18846661	0.02995447
$CuSO_4$_12 uM_5D_2	H20532-L1	-0.00576361	-0.18046733	0.04910299
$CuSO_4$_12 uM_5D_3	H20533-L1	0.19107712	-0.15187699	0.0283769
$CuSO_4$_12 uM_5D_4	H20534-L1	0.135744	-0.16273015	0.02785586
$CuSO_4$_12 uM_5D_5	H20535-L1	0.06969337	-0.15950847	0.07402439
$CuSO_4$_10 uM_5D_1	H20541-L1	-0.02063214	-0.10288997	0.09555816
$CuSO_4$_10 uM_5D_2	H20542-L1	0.02721484	-0.09463074	0.09056919
$CuSO_4$_10 uM_5D_3	H20543-L1	0.01685729	-0.10381355	0.07932101
$CuSO_4$_10 uM_5D_4	H20544-L1	0.01456292	-0.1048942	0.09220193
$CuSO_4$_10 uM_5D_5	H20545-L1	-0.04276181	-0.06005838	0.08750993
Atr_220 uM_5D_1	H20551-L1	-0.01222676	-0.0879752	0.0276487
Atr_220 uM_5D_2	H20552-L1	-0.03162955	-0.08432003	0.0326857
Atr_220 uM_5D_3	H20553-L1	-0.07193556	-0.0600494	0.07875317
Atr_220 uM_5D_4	H20554-L1	0.02498122	-0.07275522	0.03967218
Atr_220 uM_5D_5	H20555-L1	-0.00962334	-0.08382747	0.05206344

Del_700 uM_5D_1	H20561-L1	0.00782238	-0.04340103	0.02379155
Del_700 uM_5D_2	H20562-L1	0.07650545	-0.05326889	0.01458349
Del_700 uM_5D_3	H20563-L1	0.07916171	-0.05137697	0.0257839
Del_700 uM_5D_4	H20564-L1	0.07820417	-0.04638818	0.01980959
Del_700 uM_5D_5	H20565-L1	0.05395245	-0.05829166	0.00788347
Bis_2000 uM_2D_1	H20571-L1	-0.42593628	-0.011591	-0.05976495
Bis_2000 uM_2D_2	H20572-L1	-0.41564965	-0.02277756	-0.0646636
Bis_2000 uM_2D_3	H20573-L1	-0.37626544	-0.07068965	-0.07491456
Bis_2000 uM_2D_4	H20574-L1	-0.28598525	-0.02450167	-0.038334
Bis_2000 uM_2D_5	H20575-L1	-0.30514124	-0.05651851	-0.0453473
ABD_2D_w_1	H20581-L1	-0.18950454	0.03198144	-0.03526749
ABD_2D_w_2	H20582-L1	-0.29303717	0.03796893	-0.00330831
ABD_2D_w_3	H20583-L1	-0.32506248	0.03290006	0.01613797
ABD_2D_w_4	H20584-L1	-0.39150372	0.01209589	-0.02071003
ABD_2D_w_5	H20585-L1	-0.28108338	-0.00594983	-0.06649815
$CdSO_4$_730 uM_2D_5	H22835-L1	-0.12046576	0.17698734	0.01650272

Table 17 Unweighted UniFrac analysis of drug treated animals

Sample name	Seq_ID	PC1 (0.185)	PC2 (0.108)	PC3 (0.06)
SMWs_5D_1	H20476-L1	0.03087684	0.22598193	0.04653367
SMWs_5D_2	H20477-L1	0.14660433	0.05211133	-0.05434322
SMWs_5D_3	H20478-L1	0.10345626	0.19137503	-0.02510707
SMWs_5D_4	H20479-L1	0.0434085	0.17397409	-0.20442619
SMWs_5D_5	H20480-L1	-0.0726343	0.19985952	-0.06616122
Algae_20D_1	H20481-L1	-0.07725028	0.23245836	-0.06853386
Algae_20D_2	H20482-L1	-0.18091991	0.17994643	0.13371703
Algae_20D_3	H20483-L1	-0.09744847	0.19330108	0.01526673
Algae_20D_4	H20484-L1	-0.14739106	0.23192564	0.05692364
Algae_20D_5	H20485-L1	-0.13381114	0.23896039	0.05965753
$CdSO_4$_730 uM_2D_1	H20486-L1	-0.10986407	-0.00614803	-0.10372267
$CdSO_4$_730 uM_2D_2	H20487-L1	-0.16235702	0.01146242	0.00196643
$CdSO_4$_730 uM_2D_3	H20488-L1	-0.1550021	-0.04327803	-0.16867213
$CdSO_4$_730 uM_2D_4	H20489-L1	-0.15231852	0.0038825	-0.08075729
$CdSO_4$_460 uM_2D_1	H20501-L1	0.36570622	-0.08182365	0.02300969
$CdSO_4$_460 uM_2D_2	H20502-L1	0.38341546	-0.08185385	0.08171084
$CdSO_4$_460 uM_2D_3	H20503-L1	0.37940229	-0.093442	0.10783956
$CdSO_4$_460 uM_2D_4	H20504-L1	0.35443115	-0.10623185	0.08624284

$CdSO_4$_460 uM_2D_5	H20505-L1	0.35601998	-0.17256867	0.06751152
$CdSO_4$_330 uM_2D_1	H20511-L1	0.05188111	0.02260786	-0.17029791
$CdSO_4$_330 uM_2D_2	H20512-L1	0.12157054	-0.11173948	-0.13652027
$CdSO_4$_330 uM_2D_3	H20513-L1	0.1240271	-0.11124599	-0.22292328
$CdSO_4$_330 uM_2D_4	H20514-L1	0.20118534	-0.12551208	-0.10224646
$CdSO_4$_330 uM_2D_5	H20515-L1	0.16835114	-0.12689362	-0.23474005
$CuSO_4$_15 uM_5D_1	H20521-L1	-0.19555671	-0.30362118	-0.08869452
$CuSO_4$_15 uM_5D_2	H20522-L1	-0.17433013	-0.28545792	-0.10727197
$CuSO_4$_15 uM_5D_3	H20523-L1	-0.00951181	-0.31823538	-0.06132498
$CuSO_4$_15 uM_5D_4	H20524-L1	-0.10367464	-0.28031804	-0.10834626
$CuSO_4$_15 uM_5D_5	H20525-L1	-0.11408483	-0.31158916	-0.13187342
$CuSO_4$_12 uM_5D_1	H20531-L1	-0.0597745	-0.14387602	0.20699508
$CuSO_4$_12 uM_5D_2	H20532-L1	-0.12837304	-0.13244537	0.14080672
$CuSO_4$_12 uM_5D_3	H20533-L1	-0.22116126	-0.02645718	0.09279642
$CuSO_4$_12 uM_5D_4	H20534-L1	-0.13100982	-0.07876528	0.09586222
$CuSO_4$_12 uM_5D_5	H20535-L1	-0.11954537	-0.21280071	0.14525488
$CuSO_4$_10 uM_5D_1	H20541-L1	-0.28017258	-0.09161386	0.1673903
$CuSO_4$_10 uM_5D_2	H20542-L1	-0.2010722	-0.15214911	0.14002829
$CuSO_4$_10 uM_5D_3	H20543-L1	-0.21077171	-0.19307596	0.1225953
$CuSO_4$_10 uM_5D_4	H20544-L1	-0.20777502	-0.1210326	0.13175121
$CuSO_4$_10 uM_5D_5	H20545-L1	-0.28288441	-0.10937406	0.2010067
Atr_220 uM_5D_1	H20551-L1	-0.03471128	0.23056474	0.10597057
Atr_220 uM_5D_2	H20552-L1	-0.03172247	0.15792816	0.07340143
Atr_220 uM_5D_3	H20553-L1	0.09995374	0.16286942	0.06367734
Atr_220 uM_5D_4	H20554-L1	-0.06252726	0.2701981	-0.03185407
Atr_220 uM_5D_5	H20555-L1	-0.06105001	0.22406315	-0.02874597
Del_700 uM_5D_1	H20561-L1	0.01157066	0.16947711	0.06196215
Del_700 uM_5D_2	H20562-L1	-0.07912897	0.19039105	0.00920325
Del_700 uM_5D_3	H20563-L1	-0.12666484	0.19939127	0.0612196
Del_700 uM_5D_4	H20564-L1	-0.0836988	0.16210106	-0.03446942
Del_700 uM_5D_5	H20565-L1	0.06942975	0.15128085	-0.05623775
Bis_2000 uM_2D_1	H20571-L1	0.27337397	-0.0284801	0.11436588
Bis_2000 uM_2D_2	H20572-L1	0.20470173	0.01367518	0.13734087
Bis_2000 uM_2D_3	H20573-L1	0.06993624	0.1241582	0.03573734
Bis_2000 uM_2D_4	H20574-L1	0.07705127	0.1469384	0.06018352
Bis_2000 uM_2D_5	H20575-L1	0.12199328	-0.03031139	0.09614668
ABD_2D_w_1	H20581-L1	0.30888957	-0.09265695	0.06041789
ABD_2D_w_2	H20582-L1	0.38904238	-0.10357899	0.09548804

ABD_2D_w_3	H20583-L1	0.38826178	-0.10104604	0.10070539
ABD_2D_w_4	H20584-L1	0.3608779	-0.09514831	0.14314264
ABD_2D_w_5	H20585-L1	0.27464306	-0.15319052	0.04693717
$CdSO_4$_730 uM_2D_5	H22835-L1	0.35313826	-0.10832706	0.08654541

Table 18 Differential expressed genes of wounding animals (Ctr vs. Ctr_Cut)

GeneID	Length	Ctr-Expression	Ctr_cut-Expression	log2FoldChange(Ctr_cut/Ctr)	Padj	Up/Down-Regulation	P-value
BOX15_Mlig029642g1	2455	40.32677	4.358759	-3.20975	6.96E-15	Down	3.84E-17
BOX15_Mlig025900g2	3200	95.34322	10.6918	-3.15663	1.09E-32	Down	9.36E-36
BOX15_Mlig012673g1	1792	133.8678	24.50824	-2.44947	4.49E-14	Down	3.00E-16
BOX15_Mlig008200g3	1934	33.22738	6.433108	-2.36878	5.72E-08	Down	1.14E-09
BOX15_Mlig018545g3	1693	20.64856	4.197983	-2.29827	9.52E-08	Down	1.98E-09
BOX15_Mlig020368g1	16186	7729.231	1625.59	-2.24936	5.32E-78	Down	4.47E-82
BOX15_Mlig005876g1	15645	3276.446	694.3052	-2.23849	2.04E-127	Down	4.29E-132
BOX15_Mlig000334g7	669	88.13621	18.75519	-2.23245	1.29E-11	Down	1.33E-13
BOX15_Mlig003980g1	3484	79.6029	17.74581	-2.16534	4.23E-15	Down	2.25E-17
BOX15_Mlig024285g2	1379	1296.894	289.711	-2.16237	2.62E-69	Down	3.85E-73
BOX15_Mlig023775g1	3664	534.8521	120.0777	-2.15517	7.95E-22	Down	1.70E-24
BOX15_Mlig021499g1	1797	579.2493	131.8797	-2.13496	9.87E-38	Down	5.18E-41
BOX15_Mlig019159g3	527	105.9529	24.93122	-2.0874	4.25E-14	Down	2.82E-16
BOX15_Mlig019159g2	486	448.1216	106.3692	-2.07481	1.60E-18	Down	5.17E-21
BOX15_Mlig016452g5	4631	13.79795	3.287134	-2.06955	3.71E-06	Down	1.06E-07
BOX15_Mlig006891g1	1012	45.17807	11.2837	-2.00138	1.88E-08	Down	3.45E-10
BOX15_Mlig000334g3	1521	184.4495	46.35131	-1.99254	3.51E-14	Down	2.29E-16
BOX15_Mlig024555g2	866	553.1881	140.6129	-1.97604	4.30E-46	Down	1.27E-49
BOX15_Mlig027532g1	758	147.5155	37.57655	-1.97296	9.11E-20	Down	2.41E-22

BOX15_Mlig021174g1	6958	952.0849	245.0413	-1.95807	7.52E-22	Down	1.59E-24
BOX15_Mlig025175g3	1442	1228.467	316.6763	-1.95578	1.56E-38	Down	7.52E-42
BOX15_Mlig024285g1	1378	1091.961	283.8528	-1.94371	1.90E-40	Down	8.38E-44
BOX15_Mlig014767g1	2028	259.5702	67.52129	-1.94271	3.29E-09	Down	5.08E-11
BOX15_Mlig005977g1	994	67.40858	17.54537	-1.94184	9.41E-14	Down	6.60E-16
BOX15_Mlig005977g3	994	67.40858	17.54537	-1.94184	9.41E-14	Down	6.60E-16
BOX15_Mlig014470g1	4126	277.2984	73.19522	-1.92162	8.30E-11	Down	1.00E-12
BOX15_Mlig022476g2	905	36.97801	9.935894	-1.89595	5.47E-07	Down	1.31E-08
BOX15_Mlig005822g1	3157	1415.956	381.4642	-1.89216	3.43E-14	Down	2.23E-16
BOX15_Mlig025175g2	1437	1159.297	312.4632	-1.89149	1.54E-56	Down	3.23E-60
BOX15_Mlig026074g1	1260	78.73355	21.22966	-1.8909	1.31E-12	Down	1.10E-14
BOX15_Mlig025084g1	1060	23.73128	6.458852	-1.87744	1.18E-05	Down	3.79E-07
BOX15_Mlig003244g1	2303	918.6808	250.9157	-1.87236	2.34E-69	Down	2.95E-73
BOX15_Mlig000334g1	1522	109.3905	29.97298	-1.86775	8.72E-12	Down	8.69E-14
BOX15_Mlig023885g1	940	88.29657	24.4928	-1.85	9.97E-08	Down	2.08E-09
BOX15_Mlig020547g1	1115	1056.396	293.4849	-1.84779	1.80E-49	Down	4.55E-53
BOX15_Mlig014767g3	1398	194.4318	54.09281	-1.84576	3.95E-09	Down	6.20E-11
BOX15_Mlig011622g1	2141	1594.684	447.6936	-1.83269	1.41E-66	Down	2.37E-70
BOX15_Mlig012476g1	1939	451.0049	127.0797	-1.82741	2.92E-26	Down	4.23E-29
BOX15_Mlig018513g1	3695	50.05742	14.14788	-1.823	2.94E-09	Down	4.49E-11
BOX15_Mlig031887g1	1713	539.2543	152.671	-1.82054	2.91E-41	Down	1.22E-44
BOX15_Mlig005059g1	850	383.8533	111.0691	-1.7891	9.93E-40	Down	4.59E-43

BOX15_Mlig016455g3	929	1097.983	319.902	-1.77915	6.55E-42	Down	2.48E-45
BOX15_Mlig001594g1	1058	1294.189	379.2162	-1.77096	1.01E-45	Down	3.18E-49
BOX15_Mlig028568g1	738	1727.953	510.8839	-1.758	2.51E-07	Down	5.62E-09
BOX15_Mlig011944g2	1640	141.5934	41.92378	-1.75591	2.65E-13	Down	2.00E-15
BOX15_Mlig005879g1	561	622.5596	184.9628	-1.75098	2.37E-06	Down	6.41E-08
BOX15_Mlig019353g2	1843	1740.52	518.2901	-1.74769	3.90E-59	Down	7.37E-63
BOX15_Mlig005727g1	1257	1071.775	319.2376	-1.7473	1.10E-16	Down	4.35E-19
BOX15_Mlig001594g5	1277	1682.166	503.4561	-1.74038	3.02E-73	Down	3.18E-77
BOX15_Mlig000897g2	764	44.09655	13.2181	-1.73815	3.55E-06	Down	1.00E-07
BOX15_Mlig028498g1	6119	65.27451	19.93826	-1.71098	0.0001319	Down	5.35E-06
BOX15_Mlig017934g1	691	690.822	211.667	-1.70652	1.79E-37	Down	9.78E-41
BOX15_Mlig011944g3	1466	179.6727	55.16991	-1.70342	1.10E-19	Down	2.98E-22
BOX15_Mlig009561g1	638	17.23459	5.324469	-1.6946	0.0002197	Down	9.58E-06
BOX15_Mlig003757g1	2934	15.74906	4.868194	-1.69381	0.0002934	Down	1.32E-05
BOX15_Mlig006775g1	1206	823.4123	254.9765	-1.69125	1.80E-34	Down	1.28E-37
BOX15_Mlig009561g2	2938	53.43513	16.58794	-1.68765	1.13E-07	Down	2.37E-09
BOX15_Mlig019538g2	1351	458.2312	142.3226	-1.68691	1.34E-19	Down	3.71E-22
BOX15_Mlig019538g1	1351	458.2312	142.3226	-1.68691	1.34E-19	Down	3.71E-22
BOX15_Mlig001137g2	754	970.4489	301.8848	-1.68465	4.04E-55	Down	9.34E-59
BOX15_Mlig003972g1	941	651.0091	202.8921	-1.68196	2.86E-43	Down	9.61E-47
BOX15_Mlig031339g2	971	1243.742	389.472	-1.6751	7.44E-28	Down	9.06E-31
BOX15_Mlig000890g2	2695	2448.651	768.6891	-1.67152	5.90E-34	Down	4.63E-37

BOX15_Mlig030948g3	1300	72.80483	22.93543	-1.66646	2.32E-07	Down	5.19E-09
BOX15_Mlig025960g1	1222	75.6037	23.81735	-1.66644	1.16E-08	Down	2.02E-10
BOX15_Mlig033514g1	558	69.40247	22.05999	-1.65356	5.08E-08	Down	1.00E-09
BOX15_Mlig000897g8	886	56.26528	17.9093	-1.65154	7.34E-06	Down	2.25E-07
BOX15_Mlig000334g4	11605	823.5444	262.9104	-1.64727	7.57E-42	Down	3.02E-45
BOX15_Mlig003555g1	478	347.1651	110.9472	-1.64575	2.06E-35	Down	1.34E-38
BOX15_Mlig001203g1	1734	342.3922	109.445	-1.64544	4.45E-30	Down	4.49E-33
BOX15_Mlig014133g2	1316	2218.067	709.4823	-1.64446	8.48E-38	Down	4.28E-41
BOX15_Mlig019024g1	878	50.59981	16.18902	-1.64412	5.43E-06	Down	1.61E-07
BOX15_Mlig022002g1	725	14881.61	4768.999	-1.64177	4.66E-27	Down	6.37E-30
BOX15_Mlig017472g1	2855	900.1317	288.6429	-1.64085	4.14E-46	Down	1.13E-49
BOX15_Mlig001137g6	577	927.3632	297.5656	-1.63993	5.90E-34	Down	4.71E-37
BOX15_Mlig011934g1	862	11728.06	3793.891	-1.62821	4.36E-29	Down	4.67E-32
BOX15_Mlig031901g1	4993	1751.067	567.6275	-1.62522	1.07E-34	Down	7.40E-38
BOX15_Mlig029702g1	4980	5412.5	1755.276	-1.6246	5.99E-12	Down	5.78E-14
BOX15_Mlig019538g3	1230	609.8396	198.3529	-1.62036	1.11E-33	Down	9.06E-37
BOX15_Mlig030891g1	791	442.0041	144.0532	-1.61746	1.64E-25	Down	2.51E-28
BOX15_Mlig030891g4	791	442.0041	144.0532	-1.61746	1.64E-25	Down	2.51E-28
BOX15_Mlig002592g2	3072	326.7539	107.4833	-1.60409	1.53E-12	Down	1.30E-14
BOX15_Mlig027369g1	11401	411.3861	136.2032	-1.59473	6.57E-10	Down	9.04E-12
BOX15_Mlig020751g2	1041	1267.9	420.0371	-1.59385	3.26E-26	Down	4.79E-29
BOX15_Mlig008010g3	805	18.23786	6.044407	-1.59326	0.0002076	Down	8.99E-06

BOX15_Mlig008010g4	805	18.23786	6.044407	-1.59326	0.0002076	Down	8.99E-06
BOX15_Mlig028433g1	826	219.8357	72.94345	-1.59158	1.87E-08	Down	3.41E-10
BOX15_Mlig027242g1	1127	1541.181	512.6489	-1.58799	6.02E-31	Down	5.69E-34
BOX15_Mlig001328g3	1911	44.71133	14.87458	-1.58779	2.60E-05	Down	9.01E-07
BOX15_Mlig020751g3	1039	1653.435	553.2886	-1.57936	3.87E-25	Down	6.18E-28
BOX15_Mlig005381g2	952	11864.62	3971.858	-1.57878	2.78E-20	Down	7.06E-23
BOX15_Mlig010841g2	1109	43.21645	14.46934	-1.57858	0.000297	Down	1.34E-05
BOX15_Mlig024285g3	1380	678.3991	227.1722	-1.57835	0.0003526	Down	1.63E-05
BOX15_Mlig019353g1	1196	1395.326	467.9734	-1.5761	2.60E-35	Down	1.75E-38
BOX15_Mlig031339g3	971	1045.796	352.3727	-1.56943	5.65E-24	Down	9.62E-27
BOX15_Mlig024117g1	1764	1243.071	418.9317	-1.56912	2.87E-37	Down	1.63E-40
BOX15_Mlig018545g1	2510	83.85967	28.38278	-1.56296	4.06E-09	Down	6.40E-11
BOX15_Mlig026251g1	2075	15.46519	5.265943	-1.55426	0.0010088	Down	5.38E-05
BOX15_Mlig001771g1	952	5418.809	1845.128	-1.55426	8.01E-37	Down	4.88E-40
BOX15_Mlig009405g2	687	34.87447	11.88545	-1.55297	0.0004144	Down	1.95E-05
BOX15_Mlig005059g3	823	359.1438	122.7892	-1.54838	4.46E-19	Down	1.32E-21
BOX15_Mlig029370g1	1722	1583.135	541.4964	-1.54776	7.77E-33	Down	6.53E-36
BOX15_Mlig017920g1	1055	481.0584	164.7113	-1.54627	2.93E-16	Down	1.22E-18
BOX15_Mlig028381g1	1664	27.82132	9.541995	-1.54383	0.0013136	Down	7.30E-05
BOX15_Mlig011944g1	1648	52.21534	17.96532	-1.53926	1.81E-07	Down	3.96E-09
BOX15_Mlig016501g1	965	1023.288	352.5519	-1.5373	5.12E-24	Down	8.60E-27
BOX15_Mlig000890g4	3178	2884.358	994.4115	-1.53634	4.42E-19	Down	1.30E-21

BOX15_Mlig009561g4	585	28.06184	9.689551	-1.53411	8.37E-05	Down	3.24E-06
BOX15_Mlig009561g5	585	28.06184	9.689551	-1.53411	8.37E-05	Down	3.24E-06
BOX15_Mlig023297g1	666	226.6975	78.38217	-1.53217	3.72E-22	Down	7.59E-25
BOX15_Mlig014603g1	1852	663.803	229.7114	-1.53093	6.96E-21	Down	1.64E-23
BOX15_Mlig027242g2	1193	1066.843	371.3444	-1.52252	4.04E-15	Down	2.14E-17
BOX15_Mlig007942g1	1702	175.7163	61.2973	-1.51935	4.54E-10	Down	6.04E-12
BOX15_Mlig026601g1	984	321.4544	112.4042	-1.51592	2.83E-28	Down	3.27E-31
BOX15_Mlig001653g2	1097	2848.497	996.3465	-1.51548	7.13E-31	Down	7.04E-34
BOX15_Mlig011934g3	1058	4131.423	1448.841	-1.51174	1.81E-22	Down	3.50E-25
BOX15_Mlig024037g1	2604	54.09101	19.00559	-1.50897	3.38E-05	Down	1.20E-06
BOX15_Mlig024181g2	995	10163.69	3580.974	-1.505	3.58E-25	Down	5.63E-28
BOX15_Mlig004961g1	897	66.0424	23.28628	-1.50391	3.70E-07	Down	8.54E-09
BOX15_Mlig031339g1	969	2584.909	913.5697	-1.50053	4.49E-27	Down	6.04E-30
BOX15_Mlig016109g1	3243	105.9005	37.44838	-1.49973	4.15E-08	Down	8.04E-10
BOX15_Mlig012024g2	3431	283.9001	100.4205	-1.49933	4.76E-10	Down	6.35E-12
BOX15_Mlig024117g2	1736	554.7408	196.7419	-1.49551	1.05E-16	Down	4.09E-19
BOX15_Mlig011681g2	4511	249.8953	88.69518	-1.4944	7.36E-15	Down	4.08E-17
BOX15_Mlig003972g2	1034	284.4067	100.9782	-1.49391	1.19E-16	Down	4.74E-19
BOX15_Mlig020751g1	1047	2192.79	779.6091	-1.49194	2.23E-21	Down	5.11E-24
BOX15_Mlig014329g3	1293	98.11147	34.88388	-1.49186	4.62E-05	Down	1.69E-06
BOX15_Mlig027242g3	1128	1616.123	574.7522	-1.49152	4.97E-36	Down	3.13E-39
BOX15_Mlig019716g1	860	300.1255	106.7384	-1.49149	1.77E-21	Down	3.94E-24

BOX15_Mlig004092g1	818	530.4871	189.4508	-1.48549	2.30E-29	Down	2.42E-32
BOX15_Mlig019404g1	1211	251.3175	90.38738	-1.47532	3.02E-08	Down	5.70E-10
BOX15_Mlig024609g1	1143	305.8597	110.0177	-1.47513	4.48E-09	Down	7.15E-11
BOX15_Mlig010446g2	1632	20.52445	7.384137	-1.47484	0.0017545	Down	0.0001023
BOX15_Mlig033396g1	1469	1238.871	447.3104	-1.46968	1.28E-28	Down	1.43E-31
BOX15_Mlig029265g3	1511	266.3407	96.29971	-1.46767	7.52E-09	Down	1.26E-10
BOX15_Mlig011106g1	475	520.9215	188.3951	-1.4673	5.33E-42	Down	1.90E-45
BOX15_Mlig002920g1	5846	1362.961	493.9075	-1.46443	6.75E-31	Down	6.52E-34
BOX15_Mlig012675g1	739	266.6998	96.70099	-1.46361	5.09E-06	Down	1.49E-07
BOX15_Mlig012890g2	1061	11309.9	4105.084	-1.4621	7.92E-19	Down	2.46E-21
BOX15_Mlig021751g2	5917	773.3391	280.9603	-1.46073	4.23E-05	Down	1.54E-06
BOX15_Mlig017920g2	1069	563.2634	205.3928	-1.45542	4.21E-19	Down	1.23E-21
BOX15_Mlig034300g1	2048	464.556	170.0846	-1.4496	4.48E-13	Down	3.50E-15
BOX15_Mlig011934g4	974	10702.14	3919.422	-1.44919	4.05E-28	Down	4.76E-31
BOX15_Mlig005727g3	1254	1478.619	542.0179	-1.44784	0.0005717	Down	2.81E-05
BOX15_Mlig012476g2	1908	690.6057	253.5881	-1.44538	1.19E-27	Down	1.50E-30
BOX15_Mlig025406g3	815	29.32698	10.77425	-1.44464	0.0023929	Down	0.0001465
BOX15_Mlig029560g4	1897	263.0334	96.64736	-1.44444	1.35E-05	Down	4.40E-07
BOX15_Mlig021664g2	2339	46.93793	17.3753	-1.43372	0.0001683	Down	7.05E-06
BOX15_Mlig010915g2	3653	27.80052	10.31735	-1.43004	0.0029701	Down	0.0001886
BOX15_Mlig028371g1	2750	327.2125	121.5242	-1.42898	8.22E-07	Down	2.03E-08
BOX15_Mlig015608g1	1183	1064.282	396.8968	-1.42305	2.21E-28	Down	2.50E-31

BOX15_Mlig001594g18	1171	363.0099	135.4693	-1.42204	1.32E-11	Down	1.37E-13
BOX15_Mlig031361g1	875	19.63406	7.333612	-1.42076	0.0039304	Down	0.0002617
BOX15_Mlig014133g1	1401	2919.424	1091.789	-1.41899	1.32E-31	Down	1.19E-34
BOX15_Mlig001322g6	1511	247.6205	92.76592	-1.41646	1.53E-15	Down	6.99E-18
BOX15_Mlig023297g2	654	94.64418	35.49147	-1.41504	1.83E-06	Down	4.84E-08
BOX15_Mlig008305g1	2892	1526.316	572.4763	-1.41477	3.87E-15	Down	2.02E-17
BOX15_Mlig030509g1	5365	85.97967	32.2731	-1.41366	3.72E-06	Down	1.06E-07
BOX15_Mlig027274g1	4983	421.9963	158.4215	-1.41346	5.32E-11	Down	6.05E-13
BOX15_Mlig028573g1	1879	100.3922	37.69892	-1.41305	0.0012056	Down	6.61E-05
BOX15_Mlig014767g2	2035	484.8048	182.1645	-1.41216	0.002469	Down	0.0001521
BOX15_Mlig021782g1	419	29.15252	10.95638	-1.41185	0.0022891	Down	0.0001395
BOX15_Mlig001203g4	1842	64.88388	24.51334	-1.40429	6.08E-06	Down	1.82E-07
BOX15_Mlig019523g2	1418	16.07596	6.100516	-1.3979	0.0018469	Down	0.0001088
BOX15_Mlig031325g1	2619	332.1975	126.7489	-1.39007	3.22E-10	Down	4.21E-12
BOX15_Mlig031540g4	2035	353.1564	134.7724	-1.38978	9.08E-10	Down	1.28E-11
BOX15_Mlig009825g1	568	30.83391	11.80321	-1.38534	0.0006808	Down	3.42E-05
BOX15_Mlig006166g1	700	64.09763	24.55778	-1.38409	0.0002942	Down	1.33E-05
BOX15_Mlig005059g2	862	311.002	119.7262	-1.37719	1.77E-11	Down	1.88E-13
BOX15_Mlig009185g1	1942	48.89668	18.89834	-1.37148	3.16E-05	Down	1.12E-06
BOX15_Mlig032537g3	2640	14.86278	5.751581	-1.36967	0.0041945	Down	0.0002817
BOX15_Mlig019159g1	525	101.404	39.24533	-1.36952	0.0060153	Down	0.0004321
BOX15_Mlig020308g1	1040	916.6132	354.9376	-1.36875	1.09E-24	Down	1.78E-27

BOX15_Mlig000613g4	760	27.43459	10.62853	-1.36805	0.0029054	Down	0.0001839
BOX15_Mlig025084g2	1070	32.48345	12.61347	-1.36474	0.0008447	Down	4.36E-05
BOX15_Mlig009359g2	1125	44.00726	17.15005	-1.35953	6.80E-06	Down	2.06E-07
BOX15_Mlig005977g2	994	51.40344	20.09686	-1.35489	7.54E-05	Down	2.87E-06
BOX15_Mlig004261g3	1458	318.5822	124.6318	-1.35399	9.35E-19	Down	2.92E-21
BOX15_Mlig028934g1	3389	80.71876	31.6085	-1.35259	7.11E-07	Down	1.74E-08
BOX15_Mlig013683g1	2072	20.26968	7.958245	-1.3488	0.0058407	Down	0.0004159
BOX15_Mlig014088g1	842	108.3011	42.52784	-1.34857	9.32E-10	Down	1.31E-11
BOX15_Mlig007195g2	2708	87.77622	34.57494	-1.3441	5.79E-09	Down	9.38E-11
BOX15_Mlig010193g1	5035	33.80312	13.32552	-1.34296	0.0009381	Down	4.94E-05
BOX15_Mlig017636g4	728	44.49278	17.5727	-1.34024	0.0008086	Down	4.15E-05
BOX15_Mlig031543g1	590	39.02621	15.48635	-1.33345	5.71E-05	Down	2.12E-06
BOX15_Mlig014329g2	1265	60.37906	24.01075	-1.33037	0.0002206	Down	9.62E-06
BOX15_Mlig011383g1	1684	855.8685	340.7654	-1.32861	1.46E-08	Down	2.59E-10
BOX15_Mlig008010g2	760	29.32626	11.68016	-1.32813	0.0008873	Down	4.63E-05
BOX15_Mlig018543g4	656	23.59773	9.400578	-1.32783	0.0039667	Down	0.0002647
BOX15_Mlig033396g2	1022	2287.781	911.9944	-1.32685	3.72E-27	Down	4.92E-30
BOX15_Mlig031156g1	3544	125.0985	49.94037	-1.32479	7.44E-12	Down	7.29E-14
BOX15_Mlig023503g4	1708	267.7752	107.1907	-1.32084	4.44E-13	Down	3.46E-15
BOX15_Mlig008406g1	3067	52.42056	20.99844	-1.31985	1.03E-05	Down	3.26E-07
BOX15_Mlig010193g4	5105	43.07016	17.28495	-1.31717	0.0050237	Down	0.0003469
BOX15_Mlig006391g1	1437	52.49808	21.11412	-1.31406	3.06E-05	Down	1.07E-06

BOX15_Mlig018928g1	1120	139.4121	56.32216	-1.30758	1.59E-08	Down	2.85E-10
BOX15_Mlig006720g1	1176	47.78861	19.35539	-1.30393	0.0017545	Down	0.0001023
BOX15_Mlig003467g1	1781	48.68367	19.80485	-1.29758	2.06E-05	Down	6.99E-07
BOX15_Mlig006166g2	696	32.79739	13.37041	-1.29454	0.0034489	Down	0.0002251
BOX15_Mlig014259g3	513	170.2147	69.44768	-1.29336	2.12E-08	Down	3.92E-10
BOX15_Mlig011654g2	4025	450.6693	184.1263	-1.29137	2.41E-15	Down	1.18E-17
BOX15_Mlig002147g2	3007	31.03724	12.68174	-1.29125	0.0011094	Down	5.98E-05
BOX15_Mlig019960g2	944	32.36933	13.2382	-1.28992	0.0081577	Down	0.0006226
BOX15_Mlig015896g1	1407	313.2009	128.4858	-1.28548	0.001432	Down	8.08E-05
BOX15_Mlig032862g1	1778	18.09256	7.432054	-1.28356	0.0094165	Down	0.0007353
BOX15_Mlig016455g2	930	888.183	365.3504	-1.28158	3.89E-22	Down	8.00E-25
BOX15_Mlig031960g1	989	59.52903	24.50679	-1.28041	2.98E-05	Down	1.04E-06
BOX15_Mlig007253g2	648	25.76229	10.63523	-1.27641	0.0033549	Down	0.0002174
BOX15_Mlig033431g2	1151	149.5297	61.77274	-1.27539	1.67E-15	Down	7.74E-18
BOX15_Mlig031586g1	1976	2041.184	845.5505	-1.27144	0.0011379	Down	6.17E-05
BOX15_Mlig002429g2	2556	21.04205	8.723827	-1.27024	0.0060453	Down	0.000435
BOX15_Mlig015609g3	3219	33.76134	14.01773	-1.26812	0.0001644	Down	6.86E-06
BOX15_Mlig003431g3	788	249.839	103.7452	-1.26795	4.65E-10	Down	6.21E-12
BOX15_Mlig033514g3	807	75.44168	31.36785	-1.26608	0.000344	Down	1.59E-05
BOX15_Mlig009735g2	2652	59.87063	24.9871	-1.26066	0.0002889	Down	1.30E-05
BOX15_Mlig019960g1	932	19.90855	8.357005	-1.25233	0.0068715	Down	0.0005053
BOX15_Mlig025972g2	14256	3394.29	1426.162	-1.25097	3.78E-19	Down	1.09E-21

BOX15_Mlig028461g1	982	24.88257	10.47175	-1.24863	0.0033666	Down	0.0002184
BOX15_Mlig013587g3	778	20.49918	8.633298	-1.24758	0.013568	Down	0.0011558
BOX15_Mlig008306g1	1029	89.5727	37.73016	-1.24734	8.75E-07	Down	2.17E-08
BOX15_Mlig031280g2	1221	119.6101	50.41302	-1.24647	1.54E-08	Down	2.75E-10
BOX15_Mlig020976g1	1716	284.9647	120.5102	-1.24163	4.62E-06	Down	1.34E-07
BOX15_Mlig033498g1	3100	224.1506	94.85017	-1.24075	1.11E-08	Down	1.93E-10
BOX15_Mlig031902g1	3071	28.51358	12.07792	-1.23928	0.0129311	Down	0.0010855
BOX15_Mlig030330g2	694	54.54863	23.12116	-1.23833	7.42E-05	Down	2.83E-06
BOX15_Mlig025699g1	1592	41.5369	17.61356	-1.23771	0.0019308	Down	0.0001146
BOX15_Mlig006099g2	2233	217.4238	92.54872	-1.23222	3.43E-07	Down	7.86E-09
BOX15_Mlig009359g1	1643	64.56862	27.57988	-1.22722	6.98E-05	Down	2.64E-06
BOX15_Mlig031325g2	2618	1143.099	488.7775	-1.2257	1.36E-11	Down	1.41E-13
BOX15_Mlig005034g1	2191	1549.377	663.9172	-1.22261	1.24E-06	Down	3.17E-08
BOX15_Mlig031029g2	1699	768.6267	329.6072	-1.22154	2.49E-34	Down	1.83E-37
BOX15_Mlig028933g1	786	112.7768	48.51523	-1.21696	1.36E-06	Down	3.50E-08
BOX15_Mlig024253g1	1749	113.3875	48.83651	-1.21523	4.03E-08	Down	7.76E-10
BOX15_Mlig015255g1	1481	72.50195	31.22882	-1.21514	0.0010454	Down	5.60E-05
BOX15_Mlig030040g1	2363	893.9139	385.4959	-1.21342	7.85E-07	Down	1.94E-08
BOX15_Mlig005666g1	1038	125.1957	54.07975	-1.21102	6.11E-05	Down	2.29E-06
BOX15_Mlig005666g2	1038	125.1957	54.07975	-1.21102	6.11E-05	Down	2.29E-06
BOX15_Mlig005080g1	1916	219.4353	94.93532	-1.20878	5.64E-05	Down	2.10E-06
BOX15_Mlig011360g4	1519	228.654	99.0303	-1.20722	2.45E-09	Down	3.69E-11

BOX15_Mlig011360g2	1519	228.654	99.0303	-1.20722	2.45E-09	Down	3.69E-11
BOX15_Mlig032615g1	1391	107.935	46.81729	-1.20505	0.0037183	Down	0.0002456
BOX15_Mlig003730g1	1275	315.3889	137.1442	-1.20144	7.42E-05	Down	2.83E-06
BOX15_Mlig013697g1	1765	189.0087	82.37007	-1.19826	1.50E-06	Down	3.94E-08
BOX15_Mlig018679g4	842	227.4717	99.16561	-1.19778	2.84E-10	Down	3.66E-12
BOX15_Mlig022348g3	1163	122.3825	53.35358	-1.19774	7.34E-06	Down	2.25E-07
BOX15_Mlig001203g5	1737	242.5867	105.778	-1.19746	9.61E-06	Down	3.04E-07
BOX15_Mlig005382g1	1998	849.8028	370.5963	-1.19728	0.0014156	Down	7.97E-05
BOX15_Mlig016334g4	2333	486.3973	212.426	-1.19517	2.30E-05	Down	7.84E-07
BOX15_Mlig005727g2	1251	1721.352	752.2251	-1.19431	0.000682	Down	3.43E-05
BOX15_Mlig020027g2	702	41.31513	18.05737	-1.19408	0.008006	Down	0.0006085
BOX15_Mlig027878g1	589	99.81489	43.7221	-1.19089	3.54E-09	Down	5.50E-11
BOX15_Mlig023503g3	1529	332.1935	145.5344	-1.19066	5.45E-19	Down	1.63E-21
BOX15_Mlig006322g4	1927	271.2655	119.0023	-1.18872	0.000119	Down	4.79E-06
BOX15_Mlig027754g1	1337	16.76449	7.37102	-1.18547	0.010891	Down	0.0008795
BOX15_Mlig017921g3	6566	112.7332	49.60593	-1.18433	5.78E-06	Down	1.72E-07
BOX15_Mlig003757g3	2974	19.05117	8.385538	-1.1839	0.0213934	Down	0.0020004
BOX15_Mlig034010g2	1330	100.4814	44.23711	-1.1836	0.0010094	Down	5.38E-05
BOX15_Mlig033902g1	1188	36.6349	16.13036	-1.18344	0.0074822	Down	0.0005618
BOX15_Mlig020211g2	1275	31.66085	13.94417	-1.18304	0.0157532	Down	0.0013793
BOX15_Mlig014555g3	742	102.1459	45.0008	-1.18261	8.78E-05	Down	3.42E-06
BOX15_Mlig004549g1	2725	69.25813	30.51397	-1.18251	0.000506	Down	2.44E-05

BOX15_Mlig026025g1	2203	41.18871	18.18361	-1.17961	0.0015005	Down	8.54E-05
BOX15_Mlig030733g1	3908	213.7543	94.39812	-1.17912	1.69E-07	Down	3.66E-09
BOX15_Mlig020103g1	2054	275.8785	121.8916	-1.17843	9.86E-07	Down	2.46E-08
BOX15_Mlig009706g3	1534	51.50937	22.78991	-1.17644	0.0220863	Down	0.0020806
BOX15_Mlig031196g2	1396	456.9477	202.2126	-1.17616	3.35E-15	Down	1.72E-17
BOX15_Mlig002441g1	2174	59.33815	26.26814	-1.17565	4.85E-06	Down	1.42E-07
BOX15_Mlig000825g2	3153	30.32809	13.42714	-1.1755	0.0053952	Down	0.0003786
BOX15_Mlig009597g3	1778	469.1845	207.8461	-1.17464	2.67E-25	Down	4.14E-28
BOX15_Mlig023709g1	4093	325.5332	144.2421	-1.17431	3.31E-05	Down	1.17E-06
BOX15_Mlig012594g4	405	281.9958	125.0804	-1.17282	3.29E-06	Down	9.20E-08
BOX15_Mlig033443g1	1386	398.7578	177.0035	-1.17173	0.0028221	Down	0.0001779
BOX15_Mlig014360g1	782	129.5626	57.58232	-1.16995	3.87E-05	Down	1.40E-06
BOX15_Mlig006099g3	2230	88.30224	39.27484	-1.16884	1.45E-07	Down	3.10E-09
BOX15_Mlig024282g3	2253	94.20929	42.05681	-1.16353	6.85E-05	Down	2.59E-06
BOX15_Mlig014098g1	3807	58.96569	26.32807	-1.16327	0.0002236	Down	9.76E-06
BOX15_Mlig003431g1	928	132.1103	59.00071	-1.16294	0.0001179	Down	4.74E-06
BOX15_Mlig025426g2	2534	43.07142	19.27356	-1.16011	0.0007342	Down	3.73E-05
BOX15_Mlig016455g1	929	1025.312	459.823	-1.15691	2.49E-12	Down	2.18E-14
BOX15_Mlig010462g1	1234	180.0092	80.80032	-1.15564	4.13E-08	Down	7.96E-10
BOX15_Mlig024489g1	2977	593.0922	266.2513	-1.15547	0.0025945	Down	0.0001618
BOX15_Mlig024555g1	866	389.5656	174.8992	-1.15534	4.48E-12	Down	4.21E-14
BOX15_Mlig005666g3	1038	170.86	76.72115	-1.15512	0.00276	Down	0.0001735

BOX15_Mlig014529g1	1473	57.1609	25.68723	-1.15398	0.0003596	Down	1.66E-05
BOX15_Mlig011999g3	715	231.348	104.0233	-1.15316	9.56E-09	Down	1.63E-10
BOX15_Mlig029047g1	1092	79.15437	35.63858	-1.15123	2.59E-05	Down	8.98E-07
BOX15_Mlig028573g2	1882	183.9281	82.87701	-1.1501	0.0025348	Down	0.0001572
BOX15_Mlig005293g3	1716	440.4451	198.6788	-1.14852	2.71E-22	Down	5.41E-25
BOX15_Mlig011922g1	1263	96.17768	43.41111	-1.14764	4.86E-05	Down	1.79E-06
BOX15_Mlig027209g1	1920	73.45505	33.1582	-1.1475	1.87E-05	Down	6.25E-07
BOX15_Mlig013428g2	954	167.3458	75.55177	-1.14729	4.78E-10	Down	6.40E-12
BOX15_Mlig014518g4	1476	23.86058	10.78127	-1.1461	0.0245005	Down	0.0023706
BOX15_Mlig009735g1	2653	58.52766	26.46862	-1.14484	2.35E-05	Down	8.04E-07
BOX15_Mlig027602g2	2522	423.512	191.5938	-1.14435	1.49E-22	Down	2.82E-25
BOX15_Mlig015295g3	842	1531.452	693.8072	-1.14229	0.0099572	Down	0.0007878
BOX15_Mlig008469g2	2132	6641.243	3013.578	-1.13998	1.96E-11	Down	2.09E-13
BOX15_Mlig018360g1	771	35.56347	16.14569	-1.13925	0.0298999	Down	0.0030432
BOX15_Mlig003877g2	470	288.3646	130.9302	-1.1391	4.06E-06	Down	1.17E-07
BOX15_Mlig003877g3	470	288.3646	130.9302	-1.1391	4.06E-06	Down	1.17E-07
BOX15_Mlig029110g1	881	237.8294	107.9974	-1.13893	1.33E-07	Down	2.83E-09
BOX15_Mlig022685g1	1460	565.3542	256.9425	-1.13771	0.0118036	Down	0.0009691
BOX15_Mlig029249g1	1417	30.65116	13.93965	-1.13675	0.0226428	Down	0.0021457
BOX15_Mlig007063g1	2594	48.80708	22.23852	-1.13403	0.0005768	Down	2.84E-05
BOX15_Mlig024884g2	808	101.4741	46.2605	-1.13326	0.0047431	Down	0.0003242
BOX15_Mlig030139g1	1712	398.9397	182.0177	-1.13209	8.54E-08	Down	1.77E-09

BOX15_Mlig026047g3	3923	34.94666	15.95002	-1.1316	0.0185829	Down	0.001688
BOX15_Mlig009393g3	681	132.7753	60.61908	-1.13114	9.16E-05	Down	3.59E-06
BOX15_Mlig032034g1	1977	117.3777	53.61882	-1.13035	6.28E-06	Down	1.89E-07
BOX15_Mlig019823g3	1718	382.5178	175.119	-1.12719	1.52E-11	Down	1.58E-13
BOX15_Mlig007411g2	1103	161.2562	73.82553	-1.12716	5.70E-10	Down	7.74E-12
BOX15_Mlig000897g4	702	55.38119	25.39005	-1.12513	0.0012546	Down	6.92E-05
BOX15_Mlig033410g1	761	43.19276	19.84509	-1.12201	0.0030333	Down	0.000193
BOX15_Mlig019549g1	1035	1784.693	820.1361	-1.12174	4.84E-20	Down	1.27E-22
BOX15_Mlig032388g3	1510	172.4267	79.27298	-1.12108	4.09E-06	Down	1.18E-07
BOX15_Mlig002734g2	498	294.8777	135.6702	-1.12001	0.0115317	Down	0.0009417
BOX15_Mlig008101g1	2569	143.7318	66.14189	-1.11974	0.002979	Down	0.0001893
BOX15_Mlig017246g2	699	6.570138	3.026906	-1.11808	0.0217582	Down	0.0020432
BOX15_Mlig026142g3	1232	270.8319	124.7965	-1.11782	1.49E-11	Down	1.56E-13
BOX15_Mlig008586g2	723	31.899	14.70701	-1.11701	0.0074758	Down	0.0005608
BOX15_Mlig012325g4	2125	647.7952	298.7024	-1.11683	8.69E-10	Down	1.22E-11
BOX15_Mlig030015g1	459	838.5496	386.9048	-1.11592	1.93E-14	Down	1.19E-16
BOX15_Mlig025406g1	808	20.87574	9.649183	-1.11335	0.03283	Down	0.0034214
BOX15_Mlig030931g2	1441	219.4043	101.521	-1.11181	3.51E-09	Down	5.44E-11
BOX15_Mlig030931g1	1441	219.4043	101.521	-1.11181	3.51E-09	Down	5.44E-11
BOX15_Mlig008436g1	1533	84.66882	39.18766	-1.11143	0.0031138	Down	0.0001995
BOX15_Mlig023202g1	1416	189.1356	87.57276	-1.11087	1.12E-06	Down	2.82E-08
BOX15_Mlig019161g2	2170	14.40565	6.672069	-1.11043	0.0176208	Down	0.0015825

BOX15_Mlig012543g1	1959	57.8835	26.81377	-1.11018	0.0349166	Down	0.0037129
BOX15_Mlig023851g3	741	47.30461	21.92966	-1.1091	0.0008122	Down	4.18E-05
BOX15_Mlig023851g2	741	47.30461	21.92966	-1.1091	0.0008122	Down	4.18E-05
BOX15_Mlig023527g1	968	96.29707	44.6662	-1.10831	0.0014878	Down	8.46E-05
BOX15_Mlig000041g5	1619	210.6368	97.71413	-1.10812	5.56E-08	Down	1.11E-09
BOX15_Mlig032530g3	473	86.2968	40.11487	-1.10517	1.88E-05	Down	6.32E-07
BOX15_Mlig034405g3	1740	300.6308	139.9112	-1.10348	2.02E-12	Down	1.75E-14
BOX15_Mlig004113g4	809	354.5183	165.1401	-1.10217	8.81E-06	Down	2.75E-07
BOX15_Mlig016567g1	5095	1069.735	498.5077	-1.10157	5.63E-07	Down	1.36E-08
BOX15_Mlig005107g2	898	516.4185	240.7398	-1.10107	2.09E-14	Down	1.32E-16
BOX15_Mlig010624g1	3042	243.1957	113.4084	-1.10059	4.36E-06	Down	1.26E-07
BOX15_Mlig008300g1	2275	251.5345	117.3104	-1.10043	1.12E-12	Down	9.23E-15
BOX15_Mlig022408g2	546	1209.597	565.0718	-1.09802	2.62E-15	Down	1.31E-17
BOX15_Mlig033085g1	2029	64.64509	30.2037	-1.09782	0.0106052	Down	0.000852
BOX15_Mlig031517g2	1843	505.1633	236.4464	-1.09524	9.13E-22	Down	1.99E-24
BOX15_Mlig020711g1	3241	80.97382	37.9136	-1.09474	0.0006503	Down	3.25E-05
BOX15_Mlig028548g2	2967	32.90945	15.42128	-1.09358	0.006952	Down	0.0005135
BOX15_Mlig018396g2	1942	145.3453	68.15562	-1.09258	9.84E-06	Down	3.12E-07
BOX15_Mlig008217g2	1818	38.5994	18.12014	-1.09098	0.0365293	Down	0.0039342
BOX15_Mlig021596g1	1654	409.748	192.7318	-1.08814	0.0098505	Down	0.0007773
BOX15_Mlig004487g1	5597	96.29146	45.32764	-1.08702	0.0001465	Down	6.02E-06
BOX15_Mlig026807g3	1339	494.3194	232.8822	-1.08584	1.14E-20	Down	2.70E-23

BOX15_Mlig033765g1	1601	216.7798	102.1461	-1.0856	2.97E-12	Down	2.64E-14
BOX15_Mlig005293g2	1681	298.0659	140.5269	-1.08479	3.27E-12	Down	2.93E-14
BOX15_Mlig011681g1	4012	463.2354	218.4005	-1.08477	3.80E-13	Down	2.93E-15
BOX15_Mlig026382g3	1385	348.3592	164.4177	-1.08321	5.65E-13	Down	4.50E-15
BOX15_Mlig028066g2	1253	484.3436	228.618	-1.08309	1.16E-25	Down	1.73E-28
BOX15_Mlig028931g1	2276	164.412	77.65879	-1.08209	0.0030986	Down	0.0001984
BOX15_Mlig019589g1	3393	236.7236	111.8681	-1.0814	0.0001655	Down	6.91E-06
BOX15_Mlig009779g1	616	6.85148	3.239722	-1.08055	0.0431974	Down	0.0048849
BOX15_Mlig013168g3	824	277.7294	131.3726	-1.08002	7.49E-18	Down	2.56E-20
BOX15_Mlig027653g1	804	102.8608	48.6886	-1.07904	4.93E-07	Down	1.18E-08
BOX15_Mlig014754g2	1305	677.8545	320.9663	-1.07855	2.63E-08	Down	4.90E-10
BOX15_Mlig034033g2	5722	143.9062	68.15378	-1.07826	0.0012319	Down	6.80E-05
BOX15_Mlig033381g1	1297	799.142	378.5834	-1.07784	2.20E-15	Down	1.06E-17
BOX15_Mlig034252g2	1536	505.1165	239.3702	-1.07737	2.40E-15	Down	1.17E-17
BOX15_Mlig017689g3	1484	148.2838	70.35218	-1.07569	0.0001464	Down	6.01E-06
BOX15_Mlig020960g1	1837	38.73188	18.40522	-1.07341	0.0013665	Down	7.65E-05
BOX15_Mlig030040g3	2383	783.0672	372.2855	-1.07273	2.92E-06	Down	8.10E-08
BOX15_Mlig020767g1	4661	119.5656	56.88677	-1.07164	5.20E-06	Down	1.53E-07
BOX15_Mlig012151g3	1096	394.0266	187.5325	-1.07115	2.16E-07	Down	4.77E-09
BOX15_Mlig017119g2	1094	104.2906	49.68031	-1.06986	0.0047161	Down	0.000322
BOX15_Mlig006480g2	1420	639.899	305.3378	-1.06744	3.75E-05	Down	1.35E-06
BOX15_Mlig015519g1	650	60.77142	29.00234	-1.06722	0.000342	Down	1.57E-05

BOX15_Mlig013456g1	1145	44.4914	21.24518	-1.06639	0.0158306	Down	0.0013875
BOX15_Mlig029804g2	1550	959.3007	458.3036	-1.06568	3.88E-20	Down	9.94E-23
BOX15_Mlig010865g2	931	120.8905	57.82933	-1.06383	1.39E-05	Down	4.53E-07
BOX15_Mlig007323g1	2766	151.0224	72.32324	-1.06223	3.34E-08	Down	6.35E-10
BOX15_Mlig027394g1	1933	1090.958	522.5368	-1.06199	6.08E-23	Down	1.10E-25
BOX15_Mlig021515g1	1648	7372.973	3531.998	-1.06176	3.81E-17	Down	1.40E-19
BOX15_Mlig019603g1	1300	11.41828	5.475718	-1.06023	0.0241831	Down	0.0023318
BOX15_Mlig012493g1	1570	25.7519	12.35718	-1.05933	0.0098989	Down	0.0007824
BOX15_Mlig018571g1	1257	172.7419	82.90211	-1.05914	2.88E-06	Down	7.97E-08
BOX15_Mlig022958g3	1798	13.07853	6.278273	-1.05876	0.0464484	Down	0.005374
BOX15_Mlig010245g2	2253	48.56056	23.31926	-1.05826	0.0059285	Down	0.0004246
BOX15_Mlig029107g1	1491	373.5441	179.5091	-1.05722	3.99E-09	Down	6.28E-11
BOX15_Mlig029306g2	946	104.8865	50.42766	-1.05654	1.47E-06	Down	3.84E-08
BOX15_Mlig019823g2	1700	466.7781	224.4286	-1.05648	6.10E-28	Down	7.31E-31
BOX15_Mlig031029g1	1699	928.4512	446.6719	-1.05561	4.85E-12	Down	4.57E-14
BOX15_Mlig027033g2	1199	474.0363	228.0729	-1.0555	4.67E-11	Down	5.25E-13
BOX15_Mlig009049g1	1196	36.79157	17.70874	-1.05491	0.0083957	Down	0.0006436
BOX15_Mlig012766g1	941	63.26428	30.4789	-1.05358	0.0001813	Down	7.67E-06
BOX15_Mlig019791g2	3649	93.62909	45.1476	-1.05231	0.0025945	Down	0.0001618
BOX15_Mlig029861g1	868	2691.84	1298.134	-1.05215	3.30E-18	Down	1.09E-20
BOX15_Mlig004085g3	1440	529.6452	255.4426	-1.05203	1.15E-18	Down	3.64E-21
BOX15_Mlig031196g1	1963	532.3133	256.7499	-1.05191	2.08E-16	Down	8.46E-19

BOX15_Mlig004316g1	1788	294.0627	141.9034	-1.05121	1.74E-14	Down	1.06E-16
BOX15_Mlig011240g2	1197	127.1343	61.36853	-1.05078	0.011736	Down	0.0009619
BOX15_Mlig027405g1	494	62.86252	30.34867	-1.05057	0.0028934	Down	0.0001829
BOX15_Mlig006188g1	1021	244.1079	117.8659	-1.05037	3.60E-15	Down	1.86E-17
BOX15_Mlig016679g1	2302	1017.49	491.2891	-1.05037	2.80E-09	Down	4.25E-11
BOX15_Mlig030398g1	1386	370.0455	178.7594	-1.04968	7.27E-16	Down	3.22E-18
BOX15_Mlig024254g2	1419	345.0646	166.7466	-1.04921	0.0001005	Down	3.97E-06
BOX15_Mlig031325g3	2625	585.3872	282.8792	-1.04921	7.27E-08	Down	1.49E-09
BOX15_Mlig002237g1	2006	188.0149	90.91802	-1.04821	2.91E-06	Down	8.07E-08
BOX15_Mlig026318g2	2102	61.09173	29.54385	-1.04812	0.0022012	Down	0.0001332
BOX15_Mlig016838g1	2021	399.2059	193.0803	-1.04793	2.40E-05	Down	8.24E-07
BOX15_Mlig013426g1	1369	121.8538	58.94918	-1.04761	6.89E-05	Down	2.60E-06
BOX15_Mlig027303g1	1209	226.8918	109.7672	-1.04756	8.91E-05	Down	3.48E-06
BOX15_Mlig031249g1	3067	73.48368	35.56482	-1.04697	0.006293	Down	0.0004563
BOX15_Mlig016002g1	2128	298.1411	144.3736	-1.04619	3.49E-11	Down	3.86E-13
BOX15_Mlig008349g1	847	72.73654	35.23366	-1.04573	0.0025318	Down	0.0001569
BOX15_Mlig034034g1	1455	421.206	204.0592	-1.04554	4.69E-18	Down	1.60E-20
BOX15_Mlig009467g2	1536	942.3759	456.6723	-1.04514	9.59E-20	Down	2.56E-22
BOX15_Mlig003887g3	1712	163.8381	79.44264	-1.04429	5.42E-12	Down	5.16E-14
BOX15_Mlig003887g2	1712	163.8381	79.44264	-1.04429	5.42E-12	Down	5.16E-14
BOX15_Mlig027771g2	2423	209.0355	101.3653	-1.04418	4.25E-08	Down	8.26E-10
BOX15_Mlig011360g1	1520	478.3092	231.9587	-1.04408	7.34E-10	Down	1.01E-11

BOX15_Mlig003428g1	1340	80.83702	39.20956	-1.04381	0.0025025	Down	0.0001547
BOX15_Mlig009492g1	1373	59.25205	28.75354	-1.04313	0.0002606	Down	1.16E-05
BOX15_Mlig019480g1	820	37.39883	18.1503	-1.043	0.0029162	Down	0.0001847
BOX15_Mlig005967g1	1919	37.40933	18.16692	-1.04208	0.0315958	Down	0.0032589
BOX15_Mlig000897g5	875	37.12848	18.04941	-1.04057	0.0063396	Down	0.0004606
BOX15_Mlig033473g1	1159	229.232	111.4468	-1.04045	5.18E-08	Down	1.02E-09
BOX15_Mlig017079g2	1443	543.3381	264.2774	-1.0398	7.04E-14	Down	4.78E-16
BOX15_Mlig012596g3	1991	90.53541	44.05339	-1.03923	2.79E-05	Down	9.74E-07
BOX15_Mlig016326g1	3679	402.1699	195.6911	-1.03923	2.54E-08	Down	4.73E-10
BOX15_Mlig013936g3	973	4.885436	2.377959	-1.03876	0.0364288	Down	0.0039204
BOX15_Mlig018393g1	959	121.2706	59.03239	-1.03865	0.00103	Down	5.51E-05
BOX15_Mlig012607g3	924	397.7612	193.6663	-1.03833	7.54E-12	Down	7.43E-14
BOX15_Mlig026085g2	707	16.16228	7.881727	-1.03605	0.0272624	Down	0.0027042
BOX15_Mlig015032g1	523	102.9557	50.21833	-1.03574	0.0006115	Down	3.03E-05
BOX15_Mlig021664g3	2403	53.86525	26.27961	-1.03541	0.0035548	Down	0.000233
BOX15_Mlig004811g1	1267	211.6751	103.2726	-1.03539	4.90E-10	Down	6.57E-12
BOX15_Mlig009684g3	685	62.87649	30.67641	-1.03539	0.0066492	Down	0.0004865
BOX15_Mlig009433g2	1966	622.8124	303.9704	-1.03487	0.0260814	Down	0.0025598
BOX15_Mlig022355g1	2591	350.7941	171.4675	-1.03269	7.58E-17	Down	2.90E-19
BOX15_Mlig026284g1	985	99.2945	48.54145	-1.0325	7.04E-08	Down	1.44E-09
BOX15_Mlig027762g1	700	62.97026	30.78543	-1.03242	0.0022349	Down	0.0001357
BOX15_Mlig033027g3	815	351.5408	171.9527	-1.03168	5.99E-15	Down	3.26E-17

BOX15_Mlig029107g3	1574	338.4704	165.7129	-1.03034	8.81E-10	Down	1.23E-11
BOX15_Mlig027161g3	1594	1105.04	541.2447	-1.02974	0.0436192	Down	0.0049533
BOX15_Mlig012102g1	3992	82.9676	40.63751	-1.02974	0.000284	Down	1.28E-05
BOX15_Mlig026611g2	1526	185.1949	90.71507	-1.02963	0.0003425	Down	1.58E-05
BOX15_Mlig034146g2	1595	795.2343	389.5755	-1.02948	2.23E-21	Down	5.10E-24
BOX15_Mlig009211g1	4466	369.5552	181.1118	-1.02891	4.10E-14	Down	2.71E-16
BOX15_Mlig024817g1	2146	61.07842	29.95784	-1.02773	0.0011942	Down	6.53E-05
BOX15_Mlig032070g1	1328	142.3923	69.84345	-1.02767	2.22E-06	Down	5.96E-08
BOX15_Mlig001155g2	1520	346.5754	170.036	-1.02733	6.14E-09	Down	1.00E-10
BOX15_Mlig005755g5	4329	88.13124	43.25226	-1.02688	3.16E-05	Down	1.12E-06
BOX15_Mlig022954g2	818	51.51627	25.29872	-1.02596	0.0004835	Down	2.32E-05
BOX15_Mlig007397g2	1212	705.0918	346.6899	-1.02417	4.64E-16	Down	1.99E-18
BOX15_Mlig007397g1	1212	705.0918	346.6899	-1.02417	4.64E-16	Down	1.99E-18
BOX15_Mlig015825g2	1150	80.25879	39.46318	-1.02415	0.0150133	Down	0.0013048
BOX15_Mlig003657g2	1296	313.2987	154.1725	-1.02299	1.99E-09	Down	2.95E-11
BOX15_Mlig031517g3	1117	242.854	119.5165	-1.02288	6.79E-11	Down	8.02E-13
BOX15_Mlig019823g1	1718	314.334	154.7072	-1.02276	7.83E-07	Down	1.93E-08
BOX15_Mlig003162g1	1144	195.5829	96.27498	-1.02255	3.84E-07	Down	8.92E-09
BOX15_Mlig008923g5	1820	115.8998	57.11045	-1.02105	0.0011927	Down	6.52E-05
BOX15_Mlig010171g2	2009	355.7867	175.3544	-1.02074	3.97E-07	Down	9.28E-09
BOX15_Mlig006907g1	1195	226.4375	111.6703	-1.01987	3.22E-05	Down	1.13E-06
BOX15_Mlig020446g1	3439	146.3786	72.19725	-1.01969	1.52E-05	Down	5.00E-07

BOX15_Mlig028030g2	8160	1101.915	543.5785	-1.01945	2.61E-11	Down	2.85E-13
BOX15_Mlig000727g2	2070	103.1993	50.94464	-1.01843	2.82E-05	Down	9.86E-07
BOX15_Mlig012260g2	1524	80.79802	39.90501	-1.01775	2.64E-05	Down	9.15E-07
BOX15_Mlig008746g4	7026	24427.28	12065.48	-1.01761	3.17E-07	Down	7.25E-09
BOX15_Mlig013321g3	650	644.975	318.608	-1.01746	3.84E-13	Down	2.97E-15
BOX15_Mlig015746g2	1737	153.3977	75.78144	-1.01736	0.0008614	Down	4.47E-05
BOX15_Mlig030802g1	2950	1530.036	756.0816	-1.01695	1.74E-19	Down	4.86E-22
BOX15_Mlig011255g1	2120	2211.327	1092.813	-1.01687	2.93E-27	Down	3.82E-30
BOX15_Mlig017616g3	625	69.89917	34.55203	-1.0165	0.0003693	Down	1.71E-05
BOX15_Mlig028187g2	1532	289.3663	143.0526	-1.01635	3.81E-12	Down	3.46E-14
BOX15_Mlig001756g3	1005	140.2102	69.32146	-1.01622	1.34E-06	Down	3.45E-08
BOX15_Mlig026055g2	1146	2371.215	1173.552	-1.01474	1.55E-14	Down	9.34E-17
BOX15_Mlig012607g1	924	377.0831	186.6297	-1.0147	9.48E-12	Down	9.58E-14
BOX15_Mlig019399g1	6057	237.3147	117.4991	-1.01415	0.0477221	Down	0.0055704
BOX15_Mlig027370g1	2726	959.9594	475.3944	-1.01385	2.70E-26	Down	3.86E-29
BOX15_Mlig033303g3	2372	519.6705	257.4327	-1.0134	5.13E-16	Down	2.22E-18
BOX15_Mlig033303g4	2372	519.6705	257.4327	-1.0134	5.13E-16	Down	2.22E-18
BOX15_Mlig013757g3	1470	478.0263	236.8341	-1.01321	8.63E-06	Down	2.69E-07
BOX15_Mlig022954g1	817	160.7721	79.67484	-1.01282	3.39E-06	Down	9.54E-08
BOX15_Mlig015518g1	1914	601.6394	298.1786	-1.01272	8.22E-23	Down	1.50E-25
BOX15_Mlig034135g3	1146	323.7794	160.553	-1.01196	8.87E-12	Down	8.91E-14
BOX15_Mlig006969g1	708	53.151	26.37072	-1.01116	0.018954	Down	0.0017273

BOX15_Mlig031679g2	1659	339.1251	168.2639	-1.01109	1.95E-13	Down	1.45E-15
BOX15_Mlig003105g1	1673	646.4266	320.8309	-1.01067	8.38E-06	Down	2.61E-07
BOX15_Mlig008126g1	1439	41.57288	20.64922	-1.00956	0.0009156	Down	4.80E-05
BOX15_Mlig012053g1	2409	121.3602	60.30379	-1.00897	1.68E-08	Down	3.04E-10
BOX15_Mlig004811g2	1221	137.741	68.44522	-1.00894	8.23E-06	Down	2.55E-07
BOX15_Mlig021472g1	2513	48.90702	24.30735	-1.00865	0.0129151	Down	0.0010839
BOX15_Mlig031548g2	1217	434.5053	216.4647	-1.00524	8.08E-17	Down	3.10E-19
BOX15_Mlig000041g1	5518	954.0535	475.6301	-1.00423	7.46E-15	Down	4.15E-17
BOX15_Mlig032245g1	1439	1089.093	542.9658	-1.00419	4.63E-34	Down	3.50E-37
BOX15_Mlig032375g2	2008	165.5255	82.52404	-1.00417	0.0077416	Down	0.0005865
BOX15_Mlig007379g2	2204	468.0365	233.3774	-1.00396	2.18E-07	Down	4.84E-09
BOX15_Mlig025490g4	626	74.0549	36.95793	-1.00271	0.0005319	Down	2.58E-05
BOX15_Mlig009355g1	1019	469.1973	234.3179	-1.00173	1.10E-16	Down	4.31E-19
BOX15_Mlig027033g1	1194	553.7177	276.5366	-1.00168	3.64E-18	Down	1.22E-20
BOX15_Mlig034542g2	1611	2321.484	1159.644	-1.00136	1.56E-11	Down	1.63E-13
BOX15_Mlig003907g1	962	94.52423	47.23789	-1.00074	7.06E-05	Down	2.67E-06
BOX15_Mlig013341g1	1237	124.0307	61.9901	-1.00059	0.0013985	Down	7.85E-05
BOX15_Mlig004447g1	1657	83.92102	41.94881	-1.0004	0.0497439	Down	0.005883

Table 19 Differential expressed genes of pathogenic confronted animals (LPV_Cut vs. Ctr_Cut)

GeneID	Length	Ctr_cut -Expression	LPV_mix -Expression	log2 Fold Change (LPV_mix / Ctr_cut)	Padj	Up / Down	P value
BOX15_Mlig003757g1	2934	4.435697	893.3949	7.653993	2.28E-103	Up	1.24E-106
BOX15_Mlig003757g3	2974	9.419308	1659.863	7.461227	2.99E-160	Up	1.88E-164
BOX15_Mlig018319g2	3382	32.28586	2643.089	6.355179	1.07E-282	Up	2.24E-287
BOX15_Mlig003757g2	3075	9.025373	607.1214	6.071855	6.21E-110	Up	2.61E-113
BOX15_Mlig018319g1	3383	256.8913	9005.297	5.131544	4.59E-50	Up	1.22E-52
BOX15_Mlig016899g3	678	5.34977	143.3114	4.743533	2.16E-35	Up	1.28E-37
BOX15_Mlig020156g3	2673	26.86507	682.8718	4.667811	6.02E-153	Up	5.05E-157
BOX15_Mlig002307g1	723	63.70079	1298.714	4.349629	4.06E-84	Up	3.75E-87
BOX15_Mlig000982g3	3060	45.77952	918.9456	4.327205	6.65E-145	Up	6.98E-149
BOX15_Mlig012849g2	4549	2.094503	41.43623	4.306213	5.32E-19	Up	8.39E-21
BOX15_Mlig012089g1	3129	2.135561	42.24465	4.306082	6.10E-19	Up	9.68E-21
BOX15_Mlig018012g1	3025	42.65151	817.2796	4.260161	1.51E-100	Up	9.83E-104
BOX15_Mlig025388g1	1359	71.92793	1366.19	4.247462	1.28E-114	Up	4.29E-118
BOX15_Mlig005128g3	1159	20.16063	325.9644	4.015102	2.70E-59	Up	5.38E-62
BOX15_Mlig005128g2	1159	20.16063	325.9644	4.015102	2.70E-59	Up	5.38E-62
BOX15_Mlig005128g1	1159	20.16063	325.9644	4.015102	2.70E-59	Up	5.38E-62
BOX15_Mlig013576g6	3227	5.336632	80.02853	3.906513	4.50E-18	Up	7.69E-20
BOX15_Mlig020156g2	2663	79.7337	1192.041	3.9021	1.78E-107	Up	8.62E-111
BOX15_Mlig008663g1	2683	20.39759	300.4723	3.880761	9.51E-62	Up	1.58E-64
BOX15_Mlig031296g1	1578	84.39087	1223.017	3.857214	5.84E-73	Up	6.50E-76
BOX15_Mlig031515g1	1448	100.99	1449.369	3.843141	6.10E-36	Up	3.47E-38
BOX15_Mlig010203g1	1725	120.721	1713.901	3.827536	5.62E-20	Up	8.33E-22
BOX15_Mlig020156g1	2649	52.50615	738.0237	3.813109	1.24E-61	Up	2.08E-64
BOX15_Mlig004619g1	7231	3.881844	54.31505	3.806538	2.83E-19	Up	4.41E-21
BOX15_Mlig032649g1	1550	26.38432	359.2948	3.767415	7.01E-63	Up	1.12E-65
BOX15_Mlig031413g1	2158	5.43644	73.80958	3.763074	1.82E-21	Up	2.39E-23
BOX15_Mlig019960g2	944	10.8038	146.5901	3.762176	2.44E-42	Up	1.01E-44
BOX15_Mlig025962g1	1233	175.5947	2359.174	3.747961	1.60E-22	Up	1.97E-24
BOX15_Mlig002074g3	1773	25.21579	332.2994	3.720085	2.99E-60	Up	5.51E-63
BOX15_Mlig030732g1	1405	28.40167	351.3345	3.628798	9.30E-61	Up	1.64E-63
BOX15_Mlig000982g1	2771	64.60355	768.9698	3.573242	9.97E-56	Up	2.11E-58
BOX15_Mlig004921g1	1482	12.10842	140.563	3.537134	2.31E-36	Up	1.29E-38
BOX15_Mlig023248g3	3568	31.82512	353.9475	3.475298	1.95E-59	Up	3.76E-62
BOX15_Mlig031296g3	1574	150.1536	1611.357	3.423765	3.38E-24	Up	3.68E-26
BOX15_Mlig025727g1	3379	243.3622	2587.122	3.410171	1.36E-132	Up	3.15E-136
BOX15_Mlig014899g2	2609	251.7061	2673.14	3.408723	7.00E-20	Up	1.05E-21
BOX15_Mlig032170g4	4614	12.71819	133.2845	3.389543	5.66E-40	Up	2.67E-42

BOX15_Mlig022805g3	1050	56.46875	590.159	3.385579	9.15E-40	Up	4.42E-42
BOX15_Mlig011792g2	2281	132.7407	1336.773	3.332072	1.46E-22	Up	1.79E-24
BOX15_Mlig006668g1	2079	576.7145	5754.827	3.318843	1.97E-26	Up	1.87E-28
BOX15_Mlig013277g1	2817	324.2846	3207.045	3.305912	1.89E-19	Up	2.91E-21
BOX15_Mlig019960g1	932	9.353959	91.64343	3.292382	2.15E-18	Up	3.60E-20
BOX15_Mlig032649g2	1523	22.981	218.7176	3.250556	2.58E-45	Up	9.31E-48
BOX15_Mlig006668g3	2159	426.1417	4013.055	3.235296	8.08E-49	Up	2.29E-51
BOX15_Mlig017915g1	1492	62.23226	577.5803	3.214287	1.11E-18	Up	1.81E-20
BOX15_Mlig028263g2	1147	22.15046	205.2768	3.212162	6.85E-31	Up	5.16E-33
BOX15_Mlig006668g2	2158	476.0648	4338.11	3.187837	4.00E-16	Up	7.91E-18
BOX15_Mlig026167g1	1458	34.06099	300.6504	3.141895	7.17E-40	Up	3.43E-42
BOX15_Mlig022805g1	1458	34.06099	300.6504	3.141895	7.17E-40	Up	3.43E-42
BOX15_Mlig011792g1	2893	211.7396	1844.545	3.122902	4.06E-141	Up	6.82E-145
BOX15_Mlig017125g2	22842	862.88	7464.898	3.112891	3.40E-74	Up	3.64E-77
BOX15_Mlig014599g1	13436	8.35398	71.30574	3.093483	5.31E-13	Up	1.40E-14
BOX15_Mlig034147g2	1663	125.0736	1050.688	3.070484	1.44E-38	Up	7.17E-41
BOX15_Mlig014899g1	2489	247.4627	2060.434	3.057665	4.42E-14	Up	1.04E-15
BOX15_Mlig019325g1	659	102.0115	847.5404	3.054551	1.38E-137	Up	2.89E-141
BOX15_Mlig007799g2	1160	35.66191	295.5332	3.050864	4.61E-31	Up	3.45E-33
BOX15_Mlig007799g4	1160	35.66191	295.5332	3.050864	4.61E-31	Up	3.45E-33
BOX15_Mlig009056g3	4809	7.126436	58.45616	3.036102	3.87E-12	Up	1.12E-13
BOX15_Mlig030733g1	3908	98.23237	800.6239	3.026854	4.41E-66	Up	6.30E-69
BOX15_Mlig011722g2	1483	68.81448	560.2699	3.025338	1.18E-47	Up	3.50E-50
BOX15_Mlig005979g1	7527	99.15118	788.1283	2.990729	2.14E-108	Up	9.89E-112
BOX15_Mlig024829g2	2466	54.49874	433.1611	2.990609	2.50E-39	Up	1.22E-41
BOX15_Mlig014438g2	2420	94.94365	742.2887	2.966837	3.58E-40	Up	1.66E-42
BOX15_Mlig007224g1	4651	65.57377	509.1019	2.956764	1.49E-52	Up	3.62E-55
BOX15_Mlig030948g3	1300	22.87054	177.1913	2.953745	1.45E-27	Up	1.32E-29
BOX15_Mlig010283g2	1918	75.96689	586.2016	2.947954	1.92E-93	Up	1.53E-96
BOX15_Mlig010283g1	1919	67.96394	523.4593	2.945236	6.24E-76	Up	6.42E-79
BOX15_Mlig021751g2	5917	257.7512	1981.231	2.942346	2.37E-53	Up	5.52E-56
BOX15_Mlig006713g1	895	33.78108	259.3301	2.940502	1.36E-27	Up	1.22E-29
BOX15_Mlig009539g1	2450	307.5621	2359.471	2.939514	4.19E-08	Up	2.03E-09
BOX15_Mlig031296g2	1573	72.04303	541.725	2.91063	1.03E-15	Up	2.09E-17
BOX15_Mlig028547g1	1058	35.42885	265.9365	2.908085	9.72E-11	Up	3.25E-12
BOX15_Mlig005034g1	2191	704.5252	5139.876	2.86701	7.92E-37	Up	4.32E-39
BOX15_Mlig030817g1	6022	84.43584	615.0427	2.864759	5.14E-38	Up	2.63E-40
BOX15_Mlig000053g3	2593	430.8093	3126.93	2.859626	1.07E-20	Up	1.49E-22
BOX15_Mlig022960g2	6808	56.45279	404.6726	2.841638	1.92E-23	Up	2.23E-25
BOX15_Mlig009539g2	2467	517.9745	3707.564	2.839519	3.12E-07	Up	1.76E-08
BOX15_Mlig017377g1	1461	26.64315	188.3353	2.821467	2.41E-33	Up	1.62E-35
BOX15_Mlig008551g2	1125	26.57313	186.7087	2.812749	1.92E-14	Up	4.36E-16

BOX15_Mlig014438g1	1589	362.6965	2535.402	2.80538	4.22E-57	Up	8.68E-60
BOX15_Mlig012942g1	4042	77.16105	538.2543	2.802343	5.20E-46	Up	1.79E-48
BOX15_Mlig028646g2	1479	51.78735	354.4533	2.774924	2.57E-34	Up	1.62E-36
BOX15_Mlig001422g1	621	20.36837	138.8968	2.76961	1.82E-25	Up	1.79E-27
BOX15_Mlig030509g1	5365	32.22953	218.8517	2.763499	5.80E-34	Up	3.76E-36
BOX15_Mlig032648g1	607	34.13215	231.5868	2.76235	1.82E-25	Up	1.80E-27
BOX15_Mlig027746g1	708	4.828642	32.61466	2.755831	5.00E-09	Up	2.12E-10
BOX15_Mlig007902g2	387	9.449535	63.24939	2.742736	1.23E-07	Up	6.47E-09
BOX15_Mlig024254g1	1241	102.4732	684.2542	2.739285	7.00E-43	Up	2.79E-45
BOX15_Mlig004384g1	1319	85.54042	570.4176	2.73734	5.22E-95	Up	3.83E-98
BOX15_Mlig010283g3	1916	99.57636	660.4796	2.729639	2.74E-47	Up	8.52E-50
BOX15_Mlig032170g1	4395	13.77547	91.28183	2.728226	2.02E-10	Up	6.99E-12
BOX15_Mlig009539g3	2465	296.5303	1957.324	2.722631	1.25E-06	Up	7.81E-08
BOX15_Mlig006741g2	3738	233.0416	1512.646	2.698415	1.19E-144	Up	1.50E-148
BOX15_Mlig001422g2	2068	64.34472	417.1804	2.696778	1.22E-49	Up	3.32E-52
BOX15_Mlig001422g4	2068	64.34472	417.1804	2.696778	1.22E-49	Up	3.32E-52
BOX15_Mlig030874g1	1799	138.1995	887.8562	2.683574	1.72E-31	Up	1.25E-33
BOX15_Mlig019791g2	3649	47.77579	306.218	2.680208	1.97E-24	Up	2.11E-26
BOX15_Mlig015977g1	3411	109.5413	699.8906	2.675655	1.33E-90	Up	1.12E-93
BOX15_Mlig033269g1	1681	1245.592	7927.398	2.670016	4.44E-09	Up	1.87E-10
BOX15_Mlig024829g1	2470	89.62259	568.2574	2.66461	4.65E-10	Up	1.70E-11
BOX15_Mlig028277g3	1581	36.1934	228.3075	2.65718	6.31E-35	Up	3.84E-37
BOX15_Mlig030932g2	1043	107.5118	676.0369	2.652607	2.67E-44	Up	9.93E-47
BOX15_Mlig031394g3	762	52.22768	324.4382	2.635057	1.86E-60	Up	3.34E-63
BOX15_Mlig028263g1	1116	16.24518	100.4446	2.628316	4.32E-23	Up	5.11E-25
BOX15_Mlig008551g1	1123	22.94095	141.6235	2.626064	2.58E-19	Up	4.01E-21
BOX15_Mlig013931g1	2451	71.80774	436.8176	2.60482	4.77E-10	Up	1.74E-11
BOX15_Mlig002318g1	1059	11.6047	70.39551	2.600775	9.53E-08	Up	4.92E-09
BOX15_Mlig019325g2	659	123.4329	733.8524	2.571764	8.60E-66	Up	1.25E-68
BOX15_Mlig002597g1	564	33.22819	197.2542	2.569576	1.11E-50	Up	2.88E-53
BOX15_Mlig002447g2	3871	497.0707	2945.785	2.567129	3.40E-11	Up	1.08E-12
BOX15_Mlig011879g14	9138	164.1786	971.2891	2.564635	1.88E-69	Up	2.33E-72
BOX15_Mlig034147g3	1680	703.0883	4149.438	2.561138	1.67E-94	Up	1.26E-97
BOX15_Mlig022156g1	1184	7.600724	44.64588	2.554318	1.27E-08	Up	5.70E-10
BOX15_Mlig027367g1	1175	188.6814	1108.286	2.554307	8.90E-47	Up	2.88E-49
BOX15_Mlig030948g2	1299	26.42006	154.9493	2.55209	7.21E-31	Up	5.47E-33
BOX15_Mlig014999g2	1836	79.38543	461.7974	2.540314	2.08E-89	Up	1.84E-92
BOX15_Mlig013000g1	5293	430.9299	2504.332	2.5389	2.23E-11	Up	6.95E-13
BOX15_Mlig007760g1	1204	45.01117	261.1947	2.536771	2.52E-45	Up	9.03E-48
BOX15_Mlig026453g2	3236	237.7006	1370.042	2.527003	3.29E-138	Up	6.22E-142
BOX15_Mlig029811g1	1049	61.4017	353.1441	2.523906	1.27E-46	Up	4.13E-49
BOX15_Mlig022912g1	2293	289.854	1659.928	2.517722	2.72E-116	Up	8.56E-120

BOX15_Mlig030932g3	931	59.31844	338.4261	2.512288	3.36E-43	Up	1.33E-45
BOX15_Mlig025363g1	2256	36.62524	208.6257	2.510007	2.99E-28	Up	2.60E-30
BOX15_Mlig015691g1	3078	94.68252	538.9798	2.509061	1.28E-08	Up	5.73E-10
BOX15_Mlig010446g2	1632	5.968892	33.81745	2.502233	9.29E-10	Up	3.51E-11
BOX15_Mlig001698g1	802	384.1424	2167.541	2.496346	1.01E-54	Up	2.23E-57
BOX15_Mlig020288g1	2814	172.1621	970.4059	2.494821	6.93E-38	Up	3.56E-40
BOX15_Mlig005353g2	1602	42.77872	241.1188	2.494779	2.23E-15	Up	4.71E-17
BOX15_Mlig020151g2	3121	93.65128	520.2113	2.473727	2.08E-26	Up	1.97E-28
BOX15_Mlig033701g3	2254	2.935469	16.22079	2.466181	7.98E-06	Up	5.90E-07
BOX15_Mlig031394g2	735	52.93488	292.3258	2.465287	1.26E-71	Up	1.48E-74
BOX15_Mlig009130g1	1704	98.61481	544.5096	2.465081	8.76E-06	Up	6.52E-07
BOX15_Mlig029494g3	2237	15.71316	86.64431	2.463132	3.85E-21	Up	5.18E-23
BOX15_Mlig025338g2	4115	797.742	4393.958	2.461527	8.84E-64	Up	1.35E-66
BOX15_Mlig016001g1	2969	90.89302	497.7104	2.453065	1.50E-06	Up	9.57E-08
BOX15_Mlig021149g2	1187	27.1927	148.6965	2.451079	1.90E-22	Up	2.35E-24
BOX15_Mlig009092g1	1772	85.76322	466.105	2.442224	2.57E-50	Up	6.75E-53
BOX15_Mlig013995g1	566	28.18212	152.6575	2.437447	6.60E-23	Up	7.97E-25
BOX15_Mlig014584g1	15959	54.78403	296.6823	2.437091	2.43E-25	Up	2.43E-27
BOX15_Mlig030035g3	1227	6.826312	36.7487	2.428515	4.75E-06	Up	3.34E-07
BOX15_Mlig030035g2	1227	6.826312	36.7487	2.428515	4.75E-06	Up	3.34E-07
BOX15_Mlig015959g2	2388	397.48	2126.502	2.419528	1.97E-09	Up	7.84E-11
BOX15_Mlig011722g1	1611	115.624	618.495	2.419321	7.60E-39	Up	3.76E-41
BOX15_Mlig021149g1	6795	169.7094	901.3844	2.409076	9.90E-40	Up	4.80E-42
BOX15_Mlig028371g1	2750	117.4779	623.837	2.40878	6.54E-41	Up	2.95E-43
BOX15_Mlig027116g1	4805	386.4201	2051.443	2.408397	2.84E-11	Up	8.95E-13
BOX15_Mlig015691g3	2815	113.9022	604.225	2.40729	3.73E-09	Up	1.55E-10
BOX15_Mlig030948g1	1303	24.23063	128.2998	2.404615	2.01E-18	Up	3.34E-20
BOX15_Mlig000053g1	2587	263.5934	1391.219	2.399964	7.14E-08	Up	3.61E-09
BOX15_Mlig007658g1	1146	22.16443	116.3703	2.392404	6.37E-21	Up	8.72E-23
BOX15_Mlig033269g2	1696	728.8396	3797.529	2.381388	1.53E-06	Up	9.79E-08
BOX15_Mlig019547g1	2645	153.6817	800.1338	2.380296	7.95E-09	Up	3.47E-10
BOX15_Mlig020288g3	3220	220.1052	1142.531	2.375969	3.25E-79	Up	3.21E-82
BOX15_Mlig020288g2	3220	220.1052	1142.531	2.375969	3.25E-79	Up	3.21E-82
BOX15_Mlig029501g1	4221	882.508	4577.563	2.374899	3.05E-111	Up	1.15E-114
BOX15_Mlig029661g1	2318	45.89974	238.0505	2.37471	3.54E-25	Up	3.59E-27
BOX15_Mlig030932g1	976	75.18037	389.5575	2.373408	5.92E-22	Up	7.53E-24
BOX15_Mlig017608g1	1003	22.72244	117.4623	2.370008	4.86E-24	Up	5.38E-26
BOX15_Mlig005382g1	1998	384.9578	1984.809	2.366228	1.15E-13	Up	2.80E-15
BOX15_Mlig012673g1	1792	22.51492	115.4855	2.358759	3.80E-10	Up	1.36E-11
BOX15_Mlig025303g3	8831	164.0366	841.1531	2.358351	3.02E-34	Up	1.92E-36
BOX15_Mlig031198g5	9375	927.0238	4733.954	2.352367	2.69E-102	Up	1.64E-105
BOX15_Mlig016899g1	690	34.44862	175.8582	2.351895	2.31E-13	Up	5.83E-15

BOX15_Mlig020640g1	1848	111.3891	568.4023	2.351304	5.08E-07	Up	2.97E-08
BOX15_Mlig007236g1	6667	427.4032	2180.807	2.351193	7.86E-144	Up	1.16E-147
BOX15_Mlig032801g2	3921	113.9062	578.3211	2.344024	7.65E-30	Up	6.08E-32
BOX15_Mlig010308g1	3106	73.05273	370.5526	2.342668	9.58E-54	Up	2.21E-56
BOX15_Mlig025900g2	3200	13.92513	70.59627	2.341901	2.59E-06	Up	1.73E-07
BOX15_Mlig022742g1	907	379.7058	1922.533	2.340054	8.71E-29	Up	7.37E-31
BOX15_Mlig003788g3	1279	154.7223	778.9165	2.331787	2.60E-34	Up	1.64E-36
BOX15_Mlig019434g3	1509	156.109	785.4495	2.330965	1.55E-112	Up	5.51E-116
BOX15_Mlig019791g1	3652	99.14438	498.805	2.330873	7.33E-36	Up	4.22E-38
BOX15_Mlig020395g1	1750	48.01643	238.4039	2.311808	7.41E-22	Up	9.51E-24
BOX15_Mlig005456g1	1123	127.1808	630.2364	2.309012	7.90E-74	Up	8.62E-77
BOX15_Mlig031198g6	9342	497.7589	2461.325	2.305916	2.40E-87	Up	2.17E-90
BOX15_Mlig019051g1	11352	93.25143	460.2095	2.303093	4.96E-29	Up	4.12E-31
BOX15_Mlig027007g1	706	126.1644	622.1715	2.302007	3.11E-20	Up	4.48E-22
BOX15_Mlig013091g1	1517	18.44651	90.83795	2.299947	2.39E-15	Up	5.07E-17
BOX15_Mlig003838g5	1050	26.49397	130.4416	2.299668	4.35E-10	Up	1.58E-11
BOX15_Mlig002074g2	3255	28.9782	142.4816	2.297735	2.13E-18	Up	3.57E-20
BOX15_Mlig007744g2	993	149.8261	733.2578	2.291032	2.14E-05	Up	1.73E-06
BOX15_Mlig008101g1	2569	78.60035	383.3193	2.285939	2.56E-08	Up	1.20E-09
BOX15_Mlig025303g1	8771	281.5525	1364.473	2.276867	1.47E-23	Up	1.70E-25
BOX15_Mlig002214g1	1752	119.4727	578.8036	2.276393	7.73E-24	Up	8.72E-26
BOX15_Mlig005493g1	1660	841.6214	4062.159	2.271003	1.03E-24	Up	1.09E-26
BOX15_Mlig004882g1	2195	58.49901	281.1099	2.26465	3.87E-24	Up	4.24E-26
BOX15_Mlig000441g3	2849	64.07431	307.427	2.262426	2.03E-22	Up	2.52E-24
BOX15_Mlig016452g5	4631	2.08574	9.991676	2.260167	8.71E-05	Up	8.24E-06
BOX15_Mlig029647g1	1539	458.1883	2191.816	2.258114	6.69E-51	Up	1.69E-53
BOX15_Mlig025363g2	2146	9.620017	45.9332	2.255426	2.86E-10	Up	1.01E-11
BOX15_Mlig010660g1	2229	253.6611	1206.961	2.250405	1.77E-28	Up	1.52E-30
BOX15_Mlig005456g3	1121	75.60212	357.6144	2.241906	1.37E-30	Up	1.06E-32
BOX15_Mlig009154g1	1077	55.36449	261.6173	2.240425	5.29E-25	Up	5.47E-27
BOX15_Mlig014338g1	8051	1.895614	8.953925	2.239855	0.00011	Up	1.07E-05
BOX15_Mlig007799g1	1154	46.86405	220.4006	2.233574	1.55E-06	Up	9.92E-08
BOX15_Mlig022297g4	1101	57.27454	268.1321	2.226978	3.47E-07	Up	1.97E-08
BOX15_Mlig001303g3	1947	120.3558	561.7628	2.222655	2.44E-42	Up	1.01E-44
BOX15_Mlig027017g1	2585	207.6995	967.0572	2.219104	1.30E-117	Up	3.83E-121
BOX15_Mlig031394g1	762	64.48028	299.7482	2.216821	1.24E-41	Up	5.35E-44
BOX15_Mlig018015g2	7273	10.19026	47.30706	2.214865	3.04E-05	Up	2.54E-06
BOX15_Mlig007002g3	16773	195.3238	901.0218	2.205694	4.21E-59	Up	8.48E-62
BOX15_Mlig014470g1	4126	69.33949	319.7205	2.205062	6.92E-16	Up	1.39E-17
BOX15_Mlig011786g1	2352	286.8833	1319.943	2.20194	8.05E-07	Up	4.90E-08
BOX15_Mlig026025g1	2203	17.91632	82.39278	2.201243	6.40E-17	Up	1.17E-18
BOX15_Mlig021787g1	5123	141.0698	647.8098	2.199161	1.82E-27	Up	1.66E-29

BOX15_Mlig015026g1	1154	56.77889	260.2482	2.196461	4.89E-27	Up	4.51E-29
BOX15_Mlig006682g1	3033	50.79864	232.4746	2.194211	5.20E-45	Up	1.91E-47
BOX15_Mlig019592g1	1387	222.7457	1017.852	2.192058	4.63E-09	Up	1.95E-10
BOX15_Mlig003318g1	1704	63.28593	288.6755	2.189492	1.85E-36	Up	1.03E-38
BOX15_Mlig001698g3	386	594.1481	2697.06	2.182493	3.82E-45	Up	1.40E-47
BOX15_Mlig003730g1	1275	140.5478	637.6261	2.18165	1.74E-17	Up	3.10E-19
BOX15_Mlig005498g2	1038	161.2695	726.9856	2.172454	8.92E-130	Up	2.25E-133
BOX15_Mlig033618g2	2292	62.7631	282.7021	2.171294	9.84E-55	Up	2.15E-57
BOX15_Mlig016175g1	1791	66.7826	299.8644	2.166766	6.28E-42	Up	2.65E-44
BOX15_Mlig004487g1	5597	46.49437	208.4429	2.164525	9.79E-22	Up	1.27E-23
BOX15_Mlig017197g3	1421	105.4506	471.2005	2.159774	8.33E-25	Up	8.71E-27
BOX15_Mlig008539g1	1510	100.1693	447.5967	2.159759	6.76E-46	Up	2.34E-48
BOX15_Mlig031586g1	1976	855.3794	3816.389	2.157572	4.71E-10	Up	1.72E-11
BOX15_Mlig006006g2	2688	437.3137	1949.414	2.1563	2.90E-29	Up	2.36E-31
BOX15_Mlig007104g2	885	52.81202	234.9476	2.153401	1.05E-10	Up	3.54E-12
BOX15_Mlig031198g3	3651	152.6766	674.9057	2.144207	2.78E-46	Up	9.32E-49
BOX15_Mlig026274g1	4844	414.6992	1828.081	2.140193	7.01E-26	Up	6.78E-28
BOX15_Mlig019434g1	1521	182.8151	804.6337	2.137947	2.65E-31	Up	1.94E-33
BOX15_Mlig023709g1	4093	147.6017	649.1159	2.136767	1.21E-19	Up	1.82E-21
BOX15_Mlig003788g6	1287	139.0498	610.0119	2.133236	1.39E-08	Up	6.26E-10
BOX15_Mlig007744g1	1050	69.3227	304.0832	2.133067	0.000113	Up	1.10E-05
BOX15_Mlig001164g1	2559	81.15875	355.7885	2.132202	2.91E-07	Up	1.63E-08
BOX15_Mlig011681g2	4511	89.61211	392.8235	2.132115	5.74E-41	Up	2.58E-43
BOX15_Mlig004203g4	7608	38.04386	166.3158	2.12819	2.60E-33	Up	1.75E-35
BOX15_Mlig012464g1	2593	369.3168	1613.729	2.127468	9.65E-69	Up	1.22E-71
BOX15_Mlig006317g2	919	109.031	475.6956	2.125301	2.84E-20	Up	4.07E-22
BOX15_Mlig020773g1	2420	683.1742	2979.827	2.124903	7.81E-54	Up	1.79E-56
BOX15_Mlig021119g2	711	166.716	726.2866	2.123147	4.70E-46	Up	1.60E-48
BOX15_Mlig017915g2	1986	110.472	481.1481	2.122801	3.12E-24	Up	3.38E-26
BOX15_Mlig010656g2	4233	137.846	599.3242	2.120279	1.40E-35	Up	8.22E-38
BOX15_Mlig019932g2	2260	19.33555	83.84884	2.116535	1.61E-06	Up	1.03E-07
BOX15_Mlig024254g2	1419	169.3268	733.8545	2.115684	7.82E-30	Up	6.23E-32
BOX15_Mlig005321g1	2874	30.351	131.2656	2.112672	5.35E-23	Up	6.39E-25
BOX15_Mlig025091g1	2710	297.4128	1286.276	2.112662	4.18E-26	Up	4.02E-28
BOX15_Mlig028277g1	1595	55.55387	240.2461	2.112554	3.08E-24	Up	3.33E-26
BOX15_Mlig001890g2	6306	202.0427	869.7732	2.105979	1.36E-07	Up	7.19E-09
BOX15_Mlig000487g1	3936	165.3273	709.7218	2.101928	7.08E-34	Up	4.61E-36
BOX15_Mlig030403g1	4889	420.3849	1797.006	2.095812	1.06E-24	Up	1.12E-26
BOX15_Mlig024611g3	2847	78.63973	334.911	2.090447	1.66E-50	Up	4.31E-53
BOX15_Mlig025634g2	669	7.206004	30.63646	2.087978	4.73E-06	Up	3.33E-07
BOX15_Mlig011400g2	1510	32.42255	137.5788	2.085188	1.75E-23	Up	2.04E-25
BOX15_Mlig000706g2	2599	26.78202	113.6023	2.084655	5.86E-13	Up	1.55E-14

BOX15_Mlig009232g2	2869	115.7179	490.4629	2.083532	6.99E-35	Up	4.28E-37
BOX15_Mlig027028g1	2350	106.8209	452.5797	2.082978	6.47E-35	Up	3.95E-37
BOX15_Mlig027853g1	792	16.07501	67.99361	2.080579	1.53E-12	Up	4.26E-14
BOX15_Mlig008988g1	4125	369.7423	1562.412	2.079183	5.01E-103	Up	2.84E-106
BOX15_Mlig000995g3	6495	99.46764	419.9276	2.077842	2.67E-32	Up	1.84E-34
BOX15_Mlig022628g2	1689	339.7421	1425.825	2.069285	1.60E-54	Up	3.55E-57
BOX15_Mlig026130g3	847	729.1561	3059.291	2.068898	3.57E-79	Up	3.59E-82
BOX15_Mlig000846g4	2990	38.7056	162.3877	2.068828	4.80E-08	Up	2.35E-09
BOX15_Mlig000846g3	2981	119.4215	499.6106	2.064741	4.38E-39	Up	2.16E-41
BOX15_Mlig008615g1	1621	86.83098	363.1872	2.064432	1.63E-24	Up	1.74E-26
BOX15_Mlig007002g2	4239	4.062982	16.93832	2.05968	0.000226	Up	2.38E-05
BOX15_Mlig033865g1	3236	367.0182	1529.816	2.059435	2.28E-10	Up	7.93E-12
BOX15_Mlig011129g1	3179	22.23592	92.5852	2.057889	1.91E-12	Up	5.38E-14
BOX15_Mlig017526g1	1703	6.951126	28.88919	2.055211	6.95E-05	Up	6.41E-06
BOX15_Mlig033322g1	1497	68.58777	284.4179	2.051989	9.65E-19	Up	1.56E-20
BOX15_Mlig022297g1	1100	73.16285	302.8915	2.049618	1.47E-06	Up	9.35E-08
BOX15_Mlig011580g1	979	623.6325	2578.234	2.047615	2.21E-60	Up	4.04E-63
BOX15_Mlig021892g1	2599	356.1613	1469.747	2.044966	1.06E-43	Up	4.15E-46
BOX15_Mlig033701g1	18393	1949.191	8018.307	2.040423	6.53E-42	Up	2.77E-44
BOX15_Mlig006383g1	1958	32.86416	134.9052	2.037359	1.27E-19	Up	1.93E-21
BOX15_Mlig012383g2	344	2.003122	8.219822	2.036857	0.000511	Up	5.96E-05
BOX15_Mlig017761g1	5147	729.747	2994.455	2.036825	4.06E-06	Up	2.81E-07
BOX15_Mlig019026g1	1033	130.9731	537.0383	2.035754	2.47E-67	Up	3.31E-70
BOX15_Mlig028464g2	811	156.9237	642.912	2.034558	4.29E-111	Up	1.71E-114
BOX15_Mlig030651g2	1427	47.56871	193.6935	2.025691	3.80E-15	Up	8.15E-17
BOX15_Mlig020009g1	3226	227.9343	927.7579	2.02513	8.44E-11	Up	2.79E-12
BOX15_Mlig020678g2	545	21.73361	88.35233	2.023341	1.13E-10	Up	3.80E-12
BOX15_Mlig014786g1	1743	45.96462	186.749	2.022505	8.90E-23	Up	1.08E-24
BOX15_Mlig010092g4	5853	186.0503	755.5666	2.021866	1.24E-18	Up	2.02E-20
BOX15_Mlig013263g8	9116	150.6062	609.1185	2.015942	3.24E-28	Up	2.83E-30
BOX15_Mlig009568g1	716	30.85403	124.7659	2.015693	1.98E-22	Up	2.46E-24
BOX15_Mlig029665g1	3316	183.049	740.0708	2.015433	7.74E-60	Up	1.46E-62
BOX15_Mlig010170g3	921	71.7866	290.0621	2.014575	1.88E-28	Up	1.62E-30
BOX15_Mlig011400g1	1664	54.09167	217.8884	2.010111	1.00E-23	Up	1.14E-25
BOX15_Mlig023248g2	3568	56.76146	228.3843	2.00848	1.15E-17	Up	2.03E-19
BOX15_Mlig028381g1	1664	8.764295	35.23125	2.007146	0.000497	Up	5.79E-05
BOX15_Mlig024044g1	2936	49.67156	199.6317	2.006849	2.19E-17	Up	3.91E-19
BOX15_Mlig023709g2	5187	346.2607	1385.717	2.000702	1.06E-10	Up	3.55E-12
BOX15_Mlig026500g4	1161	128.944	515.3045	1.99868	3.71E-18	Up	6.30E-20
BOX15_Mlig020745g1	2403	173.1884	691.4179	1.997216	5.22E-09	Up	2.22E-10
BOX15_Mlig027388g2	3072	458.1801	1828.674	1.996811	1.36E-09	Up	5.26E-11
BOX15_Mlig034205g7	4498	12.10565	48.30291	1.99643	3.58E-07	Up	2.04E-08

BOX15_Mlig008867g1	2063	11.15792	44.46988	1.99476	4.34E-09	Up	1.82E-10
BOX15_Mlig024044g2	2759	728.8601	2902.298	1.993482	2.75E-31	Up	2.02E-33
BOX15_Mlig032170g10	4389	3.44165	13.68575	1.991502	0.00074	Up	9.05E-05
BOX15_Mlig028564g1	5345	30.38357	120.5905	1.988753	1.65E-19	Up	2.53E-21
BOX15_Mlig014943g2	846	432.0372	1714.578	1.988626	3.18E-32	Up	2.20E-34
BOX15_Mlig000846g1	3292	365.8838	1444.327	1.98094	7.55E-50	Up	2.03E-52
BOX15_Mlig000722g3	3135	130.6166	514.4954	1.97782	3.34E-06	Up	2.28E-07
BOX15_Mlig025573g1	4928	472.3141	1860.385	1.977783	1.56E-66	Up	2.17E-69
BOX15_Mlig007104g1	804	36.7233	143.5538	1.966824	1.52E-15	Up	3.17E-17
BOX15_Mlig027053g1	3653	632.7316	2466.112	1.962573	3.41E-97	Up	2.29E-100
BOX15_Mlig009056g4	4447	9.322122	36.29922	1.961208	0.000443	Up	5.10E-05
BOX15_Mlig013859g1	3573	8.520298	33.1591	1.960429	3.13E-07	Up	1.77E-08
BOX15_Mlig033860g1	2763	67.25556	261.3748	1.958395	2.89E-25	Up	2.90E-27
BOX15_Mlig000724g2	1885	36.80955	143.0414	1.958281	1.16E-14	Up	2.59E-16
BOX15_Mlig017490g1	4122	70.94158	275.1839	1.955693	4.29E-29	Up	3.54E-31
BOX15_Mlig032633g2	746	87.64611	339.8613	1.955184	2.77E-16	Up	5.38E-18
BOX15_Mlig005493g2	1756	788.4187	3052.676	1.953041	1.99E-17	Up	3.56E-19
BOX15_Mlig003944g1	3544	305.7975	1183.37	1.952253	3.29E-63	Up	5.18E-66
BOX15_Mlig014351g3	5607	333.1513	1288.926	1.95192	9.76E-58	Up	1.99E-60
BOX15_Mlig001622g3	1930	11.24525	43.49675	1.951592	1.72E-06	Up	1.11E-07
BOX15_Mlig019757g1	1592	217.3283	839.2991	1.949309	1.28E-41	Up	5.57E-44
BOX15_Mlig010092g3	4678	138.2247	532.5472	1.945894	1.90E-49	Up	5.27E-52
BOX15_Mlig005456g2	1124	108.0496	415.3172	1.94252	4.00E-28	Up	3.50E-30
BOX15_Mlig010054g1	12499	34.29379	131.4711	1.938727	3.09E-12	Up	8.89E-14
BOX15_Mlig001546g1	6325	415.7756	1592.337	1.937268	4.81E-06	Up	3.40E-07
BOX15_Mlig025033g1	1737	89.19826	341.2566	1.93577	1.98E-25	Up	1.96E-27
BOX15_Mlig029642g1	2455	5.756182	22.02108	1.935701	0.000914	Up	0.000115
BOX15_Mlig007910g2	1526	33.11934	126.6671	1.935296	1.10E-12	Up	2.99E-14
BOX15_Mlig026867g1	2925	44.62743	170.1918	1.931159	2.11E-14	Up	4.82E-16
BOX15_Mlig001052g5	3718	3.407256	12.9772	1.929296	0.000733	Up	8.93E-05
BOX15_Mlig005389g2	2380	277.1437	1051.714	1.924036	5.98E-57	Up	1.24E-59
BOX15_Mlig033696g1	4791	186.3637	703.5117	1.916454	7.05E-35	Up	4.34E-37
BOX15_Mlig006760g2	1931	155.1203	585.4624	1.916189	2.38E-47	Up	7.31E-50
BOX15_Mlig002447g1	3816	287.2382	1080.964	1.911998	4.87E-05	Up	4.29E-06
BOX15_Mlig023102g4	2370	5.42695	20.41037	1.911089	0.001074	Up	0.000138
BOX15_Mlig003340g1	2036	47.71019	179.4345	1.911088	6.29E-30	Up	4.97E-32
BOX15_Mlig004860g5	575	4.986747	18.74993	1.910715	0.000992	Up	0.000126
BOX15_Mlig027017g2	2590	233.0987	874.077	1.906819	2.78E-43	Up	1.10E-45
BOX15_Mlig027367g2	1173	163.3184	612.1015	1.906083	5.84E-44	Up	2.22E-46
BOX15_Mlig033514g1	558	20.79805	77.89368	1.905058	2.61E-14	Up	6.03E-16
BOX15_Mlig031851g1	862	336.0425	1256.889	1.903142	4.57E-50	Up	1.21E-52
BOX15_Mlig022628g1	1663	255.0113	953.7991	1.903124	3.89E-46	Up	1.31E-48

BOX15_Mlig017963g1	2715	229.4381	855.9501	1.899422	1.73E-06	Up	1.12E-07
BOX15_Mlig020745g2	2428	144.162	537.5454	1.898696	1.63E-18	Up	2.71E-20
BOX15_Mlig001063g2	5581	1064.697	3967.229	1.897689	1.99E-05	Up	1.59E-06
BOX15_Mlig014630g1	5161	21.64835	80.59954	1.896515	7.58E-08	Up	3.85E-09
BOX15_Mlig023964g2	982	58.77495	218.6641	1.895443	9.64E-12	Up	2.91E-13
BOX15_Mlig003349g1	2879	485.1494	1792.512	1.885482	1.02E-81	Up	9.62E-85
BOX15_Mlig001164g2	1435	29.93839	110.5849	1.885086	2.59E-13	Up	6.59E-15
BOX15_Mlig012961g3	1919	15.70832	57.8908	1.881805	0.000538	Up	6.31E-05
BOX15_Mlig033892g1	3807	235.9784	868.8988	1.880533	9.16E-62	Up	1.50E-64
BOX15_Mlig028542g3	1317	76.30297	280.787	1.879665	1.34E-05	Up	1.04E-06
BOX15_Mlig010517g1	7836	192.707	708.4297	1.878216	1.25E-15	Up	2.57E-17
BOX15_Mlig008647g1	3344	58.00542	213.2236	1.878108	1.27E-37	Up	6.59E-40
BOX15_Mlig027017g3	2582	239.0135	876.8916	1.875307	7.21E-30	Up	5.73E-32
BOX15_Mlig031699g1	3516	16.31631	59.84837	1.874997	7.88E-08	Up	4.01E-09
BOX15_Mlig017952g1	2285	76.27342	279.3999	1.873079	2.38E-33	Up	1.59E-35
BOX15_Mlig014351g1	5585	457.1112	1670.611	1.869759	1.59E-18	Up	2.62E-20
BOX15_Mlig011164g2	12570	451.8447	1650.247	1.868783	5.51E-16	Up	1.10E-17
BOX15_Mlig031198g1	1226	38.65815	141.1603	1.86849	0.001481	Up	0.0002
BOX15_Mlig001549g6	910	43.52065	158.7457	1.866946	1.39E-20	Up	1.96E-22
BOX15_Mlig001549g2	910	43.52065	158.7457	1.866946	1.39E-20	Up	1.96E-22
BOX15_Mlig001549g3	910	43.52065	158.7457	1.866946	1.39E-20	Up	1.96E-22
BOX15_Mlig029683g1	1664	175.3583	637.588	1.862319	3.24E-30	Up	2.53E-32
BOX15_Mlig007002g4	8307	896.431	3242.073	1.854652	2.27E-61	Up	3.90E-64
BOX15_Mlig006368g3	4473	2015.279	7287.16	1.854377	5.83E-21	Up	7.97E-23
BOX15_Mlig008077g1	2832	297.8598	1077.002	1.854316	6.08E-53	Up	1.44E-55
BOX15_Mlig008075g1	1995	531.9631	1923.278	1.854169	1.82E-38	Up	9.19E-41
BOX15_Mlig029384g1	4668	173.2833	626.384	1.853915	7.56E-37	Up	4.11E-39
BOX15_Mlig002542g1	2303	76.27647	275.2625	1.851498	0.000504	Up	5.88E-05
BOX15_Mlig033701g2	9725	6760.671	24396.26	1.851422	3.47E-27	Up	3.19E-29
BOX15_Mlig006317g1	908	78.29256	282.0679	1.849095	1.51E-12	Up	4.20E-14
BOX15_Mlig017915g3	1552	113.9802	409.4143	1.844778	3.97E-15	Up	8.54E-17
BOX15_Mlig000150g1	4889	60.14734	215.9493	1.844119	2.72E-37	Up	1.43E-39
BOX15_Mlig015809g2	9326	72.49559	259.4224	1.839338	3.20E-17	Up	5.75E-19
BOX15_Mlig005545g2	2093	7.618722	27.24217	1.838221	2.58E-05	Up	2.12E-06
BOX15_Mlig003838g2	1640	2.314836	8.266983	1.836451	0.002155	Up	0.000306
BOX15_Mlig033618g1	2132	67.20074	239.8758	1.835739	3.01E-29	Up	2.45E-31
BOX15_Mlig008561g1	1152	93.61708	333.4134	1.832468	2.21E-15	Up	4.68E-17
BOX15_Mlig017571g1	1152	93.61708	333.4134	1.832468	2.21E-15	Up	4.68E-17
BOX15_Mlig014351g2	5573	160.1994	570.3669	1.832022	4.10E-28	Up	3.60E-30
BOX15_Mlig017608g2	977	20.82007	74.06605	1.830838	0.00034	Up	3.79E-05
BOX15_Mlig027376g1	3427	29.62514	105.318	1.829858	5.74E-06	Up	4.11E-07
BOX15_Mlig013322g1	4052	22.65463	80.50034	1.829189	2.66E-10	Up	9.33E-12

BOX15_Mlig020864g1	2193	26.35497	93.50183	1.82692	2.92E-06	Up	1.97E-07
BOX15_Mlig013564g1	1998	41.5803	147.3987	1.825752	6.89E-15	Up	1.51E-16
BOX15_Mlig002901g2	1034	18.88547	66.81981	1.823	5.63E-10	Up	2.08E-11
BOX15_Mlig010986g1	2640	74.42539	263.2146	1.822373	8.31E-10	Up	3.13E-11
BOX15_Mlig034147g1	1679	723.6614	2558.81	1.822086	1.43E-47	Up	4.27E-50
BOX15_Mlig011383g1	1684	342.0696	1208.746	1.821149	1.67E-21	Up	2.18E-23
BOX15_Mlig002901g1	1343	33.16714	117.1729	1.820812	2.09E-18	Up	3.50E-20
BOX15_Mlig026218g1	3233	131.3832	463.3722	1.81839	6.59E-53	Up	1.58E-55
BOX15_Mlig028081g1	3232	140.7078	495.9268	1.817425	1.44E-39	Up	7.03E-42
BOX15_Mlig034277g2	600	166.0471	584.3114	1.815145	3.93E-67	Up	5.37E-70
BOX15_Mlig030149g1	624	32.2437	113.2815	1.812823	6.20E-14	Up	1.48E-15
BOX15_Mlig001154g2	2665	18.70833	65.63284	1.810737	4.55E-09	Up	1.92E-10
BOX15_Mlig012461g1	10009	348.3929	1220.912	1.809172	4.05E-08	Up	1.96E-09
BOX15_Mlig031699g3	2259	6.461365	22.42018	1.794887	6.03E-05	Up	5.46E-06
BOX15_Mlig030447g1	2126	34.41565	119.3874	1.794514	1.19E-16	Up	2.24E-18
BOX15_Mlig032900g1	784	6.66323	23.10285	1.793777	0.000334	Up	3.71E-05
BOX15_Mlig007314g1	2039	367.1673	1273.015	1.79374	1.98E-45	Up	7.06E-48
BOX15_Mlig030604g1	2346	183.9227	637.5159	1.793362	2.85E-21	Up	3.80E-23
BOX15_Mlig028573g1	1879	33.88999	116.8595	1.785844	1.79E-05	Up	1.41E-06
BOX15_Mlig010354g1	1651	6.129183	21.12642	1.785282	0.000182	Up	1.87E-05
BOX15_Mlig020762g2	5247	464.4414	1597.437	1.78219	1.63E-41	Up	7.17E-44
BOX15_Mlig022951g1	847	8.175255	28.08746	1.78059	0.002616	Up	0.000382
BOX15_Mlig029436g1	1906	14.38546	49.33028	1.777863	6.58E-07	Up	3.94E-08
BOX15_Mlig027552g2	1589	221.0655	757.3081	1.776407	3.50E-60	Up	6.54E-63
BOX15_Mlig008822g1	2093	143.6412	491.5059	1.774739	2.21E-41	Up	9.79E-44
BOX15_Mlig033906g2	3628	683.109	2329.351	1.76974	2.64E-46	Up	8.82E-49
BOX15_Mlig002169g1	1782	326.6958	1113.95	1.769665	4.15E-70	Up	5.06E-73
BOX15_Mlig016420g3	1437	104.1795	355.1925	1.76953	6.16E-49	Up	1.73E-51
BOX15_Mlig017608g3	1166	778.3797	2651.25	1.768127	1.06E-33	Up	6.91E-36
BOX15_Mlig016420g2	1434	75.79105	257.515	1.764557	4.67E-22	Up	5.89E-24
BOX15_Mlig017553g2	1099	16.49911	56.01221	1.763353	1.05E-08	Up	4.64E-10
BOX15_Mlig028277g2	1581	51.14347	173.3645	1.761186	4.85E-16	Up	9.62E-18
BOX15_Mlig021312g1	1641	86.20342	292.1555	1.760919	7.79E-16	Up	1.57E-17
BOX15_Mlig032875g1	1160	43.63183	147.7826	1.760023	2.76E-11	Up	8.66E-13
BOX15_Mlig016319g1	1315	34.14255	115.3256	1.756071	4.51E-11	Up	1.45E-12
BOX15_Mlig011512g1	3192	55.21179	186.1236	1.753213	8.16E-18	Up	1.42E-19
BOX15_Mlig029371g1	1507	7.006409	23.56541	1.749924	0.002549	Up	0.000371
BOX15_Mlig025161g1	1516	59.01368	198.3947	1.749252	1.56E-13	Up	3.85E-15
BOX15_Mlig022060g1	1585	458.9424	1541.913	1.748337	1.89E-44	Up	6.98E-47
BOX15_Mlig005353g1	1602	33.90315	113.729	1.746109	0.003618	Up	0.000558
BOX15_Mlig001598g13	310	7.484711	25.1031	1.745847	0.00323	Up	0.000488
BOX15_Mlig006368g1	5357	2451.992	8216.776	1.744618	1.95E-17	Up	3.47E-19

BOX15_Mlig021724g2	1492	46.89361	156.9109	1.742482	1.23E-12	Up	3.38E-14
BOX15_Mlig001484g2	1593	197.9659	662.2345	1.74209	6.15E-54	Up	1.39E-56
BOX15_Mlig006920g3	2596	142.5037	475.1882	1.7375	0.000631	Up	7.55E-05
BOX15_Mlig000722g1	3026	248.4026	827.536	1.736142	0.000133	Up	1.31E-05
BOX15_Mlig034537g1	1026	298.3824	993.4678	1.735311	5.82E-20	Up	8.66E-22
BOX15_Mlig026136g3	5187	385.0822	1281.148	1.734199	5.00E-48	Up	1.45E-50
BOX15_Mlig012322g2	1503	28.42607	94.49199	1.732977	6.08E-08	Up	3.04E-09
BOX15_Mlig026841g1	2183	64.78531	215.2691	1.732402	1.95E-26	Up	1.84E-28
BOX15_Mlig021611g1	2395	79.33509	263.0607	1.729365	2.03E-32	Up	1.40E-34
BOX15_Mlig031877g1	3112	20.33971	67.41237	1.728714	5.57E-06	Up	3.97E-07
BOX15_Mlig004058g1	3049	283.738	939.9865	1.72808	2.60E-05	Up	2.14E-06
BOX15_Mlig019846g1	3147	155.8106	515.9845	1.727534	6.99E-37	Up	3.77E-39
BOX15_Mlig018761g1	1996	151.3	500.6865	1.726496	1.27E-41	Up	5.53E-44
BOX15_Mlig012636g1	6219	156.8986	518.564	1.72469	1.17E-17	Up	2.05E-19
BOX15_Mlig021879g1	4184	24.26355	80.04498	1.722021	3.10E-11	Up	9.82E-13
BOX15_Mlig016278g3	3206	181.3265	596.3402	1.717546	9.61E-18	Up	1.68E-19
BOX15_Mlig005308g2	1684	127.1486	418.0942	1.717312	1.53E-21	Up	2.00E-23
BOX15_Mlig001894g2	6274	85.21776	280.0481	1.716449	0.001213	Up	0.000159
BOX15_Mlig029118g1	4321	839.7339	2755.464	1.714291	0.000152	Up	1.53E-05
BOX15_Mlig029840g1	2193	116.8678	383.2393	1.713368	5.74E-22	Up	7.28E-24
BOX15_Mlig008077g2	2832	371.4279	1217.684	1.712986	1.29E-95	Up	9.22E-99
BOX15_Mlig013931g2	2415	112.7951	368.9929	1.709889	0.003877	Up	0.000604
BOX15_Mlig019404g1	1211	88.45648	289.0009	1.708034	8.62E-15	Up	1.91E-16
BOX15_Mlig028464g1	850	256.5841	837.7151	1.707028	2.57E-64	Up	3.89E-67
BOX15_Mlig030307g2	3419	4.001423	13.05663	1.706198	0.004126	Up	0.000649
BOX15_Mlig034555g1	2235	62.96143	205.4213	1.706046	5.22E-34	Up	3.37E-36
BOX15_Mlig008075g2	1594	259.1342	845.1658	1.705535	5.58E-29	Up	4.68E-31
BOX15_Mlig020762g1	5259	556.4255	1813.867	1.704808	9.66E-36	Up	5.60E-38
BOX15_Mlig009209g2	3186	111.2409	362.491	1.704258	0.000199	Up	2.07E-05
BOX15_Mlig026049g1	2095	57.77635	188.1852	1.703603	4.66E-08	Up	2.28E-09
BOX15_Mlig003944g2	3553	655.3935	2133.687	1.702915	1.51E-100	Up	9.67E-104
BOX15_Mlig020035g2	1428	478.0758	1555.504	1.702071	6.00E-37	Up	3.20E-39
BOX15_Mlig034040g1	741	37.48839	121.8728	1.70086	1.85E-08	Up	8.48E-10
BOX15_Mlig025563g1	2839	722.6972	2348.314	1.700162	1.15E-27	Up	1.02E-29
BOX15_Mlig017843g1	2561	172.0497	558.9086	1.699787	3.61E-06	Up	2.48E-07
BOX15_Mlig034443g1	1591	105.5313	342.7123	1.699327	3.10E-16	Up	6.07E-18
BOX15_Mlig030943g1	1347	41.303	134.0064	1.697984	3.71E-11	Up	1.18E-12
BOX15_Mlig012180g5	4710	687.2775	2229.054	1.697467	5.29E-24	Up	5.87E-26
BOX15_Mlig017032g1	2387	4.40222	14.27545	1.697233	0.003941	Up	0.000616
BOX15_Mlig010170g1	922	119.6881	387.8768	1.696319	7.10E-12	Up	2.12E-13
BOX15_Mlig000487g3	3936	225.5897	728.3089	1.690849	3.82E-13	Up	9.88E-15
BOX15_Mlig019932g1	2266	28.57388	92.22034	1.690388	4.93E-08	Up	2.42E-09

BOX15_Mlig019701g1	2863	84.60643	272.663	1.68828	5.39E-29	Up	4.50E-31
BOX15_Mlig028547g2	983	53.74347	173.1174	1.687589	0.004804	Up	0.000774
BOX15_Mlig032615g1	1391	42.68185	137.3624	1.686292	1.45E-09	Up	5.64E-11
BOX15_Mlig021744g1	1800	101.7583	327.1284	1.68471	9.63E-31	Up	7.38E-33
BOX15_Mlig013175g3	1962	182.6971	586.1549	1.681828	1.28E-40	Up	5.81E-43
BOX15_Mlig034132g1	5386	421.7031	1352.065	1.680865	1.18E-42	Up	4.80E-45
BOX15_Mlig013265g1	931	115.0098	368.6433	1.680469	7.73E-11	Up	2.54E-12
BOX15_Mlig031956g1	538	25.00382	80.01519	1.678125	3.14E-05	Up	2.64E-06
BOX15_Mlig004040g1	2692	318.6769	1019.766	1.678072	9.35E-29	Up	7.95E-31
BOX15_Mlig010351g1	7169	124.9631	399.4641	1.676563	2.15E-11	Up	6.69E-13
BOX15_Mlig027001g1	2445	93.21575	297.5567	1.674519	4.37E-35	Up	2.63E-37
BOX15_Mlig022669g1	1410	59.93527	191.127	1.673055	5.88E-10	Up	2.17E-11
BOX15_Mlig002514g1	1646	58.31047	185.9083	1.672764	5.52E-15	Up	1.20E-16
BOX15_Mlig007002g1	6628	1570.364	5000.995	1.671116	5.05E-119	Up	1.38E-122
BOX15_Mlig027525g6	3251	2607.537	8278.59	1.666698	0.0019	Up	0.000264
BOX15_Mlig019444g1	2580	216.8425	688.2049	1.66619	4.28E-20	Up	6.27E-22
BOX15_Mlig015234g1	988	16.46608	52.24274	1.665734	1.58E-05	Up	1.24E-06
BOX15_Mlig026261g2	846	6935.453	22002.06	1.665577	0.002163	Up	0.000307
BOX15_Mlig009479g3	13873	6.023135	19.08459	1.663822	0.006302	Up	0.001063
BOX15_Mlig003152g1	504	13.38752	42.35016	1.661478	1.62E-07	Up	8.72E-09
BOX15_Mlig006748g1	1247	85.09534	268.4468	1.657484	3.72E-32	Up	2.62E-34
BOX15_Mlig006748g2	1247	85.09534	268.4468	1.657484	3.72E-32	Up	2.62E-34
BOX15_Mlig023248g1	3570	79.04838	249.1583	1.656255	3.68E-26	Up	3.53E-28
BOX15_Mlig021821g1	2535	391.3637	1233.515	1.656194	1.04E-06	Up	6.43E-08
BOX15_Mlig018856g1	5029	117.2722	369.1168	1.654216	1.44E-24	Up	1.53E-26
BOX15_Mlig033514g3	807	29.32906	92.21948	1.652741	8.70E-13	Up	2.35E-14
BOX15_Mlig029678g3	2254	18.3046	57.51123	1.651638	9.12E-07	Up	5.60E-08
BOX15_Mlig020035g3	1418	1683.324	5287.197	1.65119	7.01E-24	Up	7.84E-26
BOX15_Mlig018001g1	2891	2502.569	7855.053	1.650211	0.000571	Up	6.75E-05
BOX15_Mlig007181g3	2841	142.7291	447.6607	1.649127	3.87E-29	Up	3.17E-31
BOX15_Mlig025935g2	3948	316.1811	990.6172	1.647577	8.00E-06	Up	5.92E-07
BOX15_Mlig006971g1	519	42.3294	132.5816	1.647148	0.006916	Up	0.001183
BOX15_Mlig010193g4	5105	16.18378	50.61702	1.645074	0.000917	Up	0.000115
BOX15_Mlig009793g1	3023	88.17557	275.2959	1.642532	8.93E-24	Up	1.01E-25
BOX15_Mlig019714g1	3191	59.74118	186.2879	1.640736	0.003147	Up	0.000473
BOX15_Mlig005493g3	1706	622.5697	1936.122	1.636863	1.51E-12	Up	4.20E-14
BOX15_Mlig009209g1	3158	94.42406	293.1372	1.634349	0.000431	Up	4.94E-05
BOX15_Mlig001590g2	1577	12.95633	40.14428	1.631538	0.003012	Up	0.00045
BOX15_Mlig015884g1	1760	690.0933	2137.812	1.631271	1.55E-35	Up	9.13E-38
BOX15_Mlig015884g3	1760	690.0933	2137.812	1.631271	1.55E-35	Up	9.13E-38
BOX15_Mlig007322g2	654	12.19099	37.71478	1.629315	0.000107	Up	1.03E-05
BOX15_Mlig032633g1	3086	553.8149	1712.743	1.628833	7.71E-56	Up	1.62E-58

BOX15_Mlig000572g5	10782	272.8371	842.1001	1.625952	9.07E-16	Up	1.84E-17
BOX15_Mlig000729g2	3602	8.185027	25.22528	1.623811	0.001648	Up	0.000225
BOX15_Mlig032801g1	3892	280.7306	864.8951	1.623339	2.22E-46	Up	7.36E-49
BOX15_Mlig000935g1	17778	35.45464	109.1869	1.622754	4.39E-05	Up	3.82E-06
BOX15_Mlig025026g2	2146	5.901993	18.15958	1.621457	0.000735	Up	8.97E-05
BOX15_Mlig022693g3	2186	71.41948	219.603	1.620508	6.93E-08	Up	3.49E-09
BOX15_Mlig007181g1	2853	189.0905	581.2462	1.620073	0.006064	Up	0.001015
BOX15_Mlig018677g1	1589	90.69716	278.7289	1.619733	1.96E-33	Up	1.31E-35
BOX15_Mlig021751g1	3374	101.0648	310.4857	1.619246	9.48E-21	Up	1.31E-22
BOX15_Mlig032123g2	3127	219.2368	672.8943	1.61789	1.28E-31	Up	9.25E-34
BOX15_Mlig002752g1	5793	268.2732	823.3716	1.617841	1.27E-48	Up	3.62E-51
BOX15_Mlig024351g3	1730	4.070377	12.49135	1.617695	0.006131	Up	0.001028
BOX15_Mlig000724g3	3546	85.02614	260.6939	1.616378	2.39E-14	Up	5.48E-16
BOX15_Mlig024051g2	383	7.654951	23.46084	1.61579	0.005942	Up	0.000991
BOX15_Mlig016889g2	832	31.6381	96.91946	1.615123	2.79E-09	Up	1.14E-10
BOX15_Mlig018180g1	2309	287.8608	880.6556	1.613207	6.09E-13	Up	1.62E-14
BOX15_Mlig030447g2	2210	18.9292	57.74603	1.609108	1.85E-06	Up	1.20E-07
BOX15_Mlig029320g1	737	62.66429	190.7923	1.606287	0.008477	Up	0.001505
BOX15_Mlig025156g1	1689	84.32978	256.2905	1.603666	1.61E-11	Up	4.95E-13
BOX15_Mlig019119g1	4764	197.4332	599.9732	1.603533	6.90E-18	Up	1.20E-19
BOX15_Mlig015915g1	2764	18.27739	55.52813	1.603159	2.59E-08	Up	1.22E-09
BOX15_Mlig031142g1	6017	113.7805	345.505	1.602453	5.31E-40	Up	2.49E-42
BOX15_Mlig016165g3	3886	516.8176	1569.012	1.602129	9.46E-39	Up	4.71E-41
BOX15_Mlig014588g3	1894	117.8203	357.6221	1.601848	1.05E-19	Up	1.58E-21
BOX15_Mlig026500g1	1393	415.4837	1259.665	1.600176	3.33E-20	Up	4.81E-22
BOX15_Mlig027789g1	1552	50.05691	151.7436	1.599994	9.99E-15	Up	2.22E-16
BOX15_Mlig021440g2	4360	65.7337	199.1947	1.599474	2.50E-21	Up	3.33E-23
BOX15_Mlig009932g1	2031	59.91869	181.4387	1.598404	5.76E-21	Up	7.85E-23
BOX15_Mlig022499g2	1233	22.54438	68.22145	1.597458	1.64E-07	Up	8.85E-09
BOX15_Mlig022499g3	1233	22.54438	68.22145	1.597458	1.64E-07	Up	8.85E-09
BOX15_Mlig002784g1	1986	39.38045	119.1621	1.597374	8.44E-14	Up	2.04E-15
BOX15_Mlig002358g1	6527	120.6138	364.3593	1.594967	7.43E-26	Up	7.20E-28
BOX15_Mlig011527g1	801	6.57804	19.87082	1.594922	0.000979	Up	0.000124
BOX15_Mlig003191g1	3067	178.2348	538.3185	1.594681	1.86E-60	Up	3.36E-63
BOX15_Mlig002508g1	1305	117.945	355.8833	1.59329	7.44E-44	Up	2.86E-46
BOX15_Mlig007098g1	2430	134.1252	404.5463	1.592724	9.35E-18	Up	1.63E-19
BOX15_Mlig027369g1	11401	129.7344	391.1861	1.592294	4.14E-27	Up	3.81E-29
BOX15_Mlig018045g1	1664	232.0005	699.0286	1.591224	4.32E-42	Up	1.81E-44
BOX15_Mlig022620g1	4024	54.19957	163.1811	1.59012	2.61E-09	Up	1.06E-10
BOX15_Mlig032207g1	2109	40.3354	121.4227	1.58992	8.15E-12	Up	2.44E-13
BOX15_Mlig026999g2	1120	3.070843	9.241115	1.589432	0.009238	Up	0.001666
BOX15_Mlig010542g3	3326	200.085	601.911	1.588937	7.67E-23	Up	9.28E-25

BOX15_Mlig027552g3	1607	616.1975	1853.554	1.588829	1.24E-74	Up	1.30E-77
BOX15_Mlig006006g1	2689	153.6972	462.2361	1.588539	3.75E-16	Up	7.39E-18
BOX15_Mlig019757g2	1558	253.0934	761.1273	1.588468	7.16E-11	Up	2.35E-12
BOX15_Mlig014464g1	2382	48.73898	146.5561	1.588306	1.96E-13	Up	4.92E-15
BOX15_Mlig000724g1	1906	19.47662	58.53204	1.587483	0.000188	Up	1.95E-05
BOX15_Mlig009479g4	13164	4.32907	13.00542	1.586984	0.007166	Up	0.001235
BOX15_Mlig017197g2	1391	143.0029	429.4739	1.586526	4.42E-05	Up	3.84E-06
BOX15_Mlig031235g3	3638	61.5383	184.5611	1.584542	0.007055	Up	0.001211
BOX15_Mlig016602g3	3159	30.61371	91.81314	1.584523	8.39E-12	Up	2.52E-13
BOX15_Mlig018543g4	656	7.101633	21.2733	1.582821	0.007098	Up	0.00122
BOX15_Mlig029626g2	1474	169.9715	508.9073	1.58211	6.83E-05	Up	6.29E-06
BOX15_Mlig034277g1	619	125.5088	375.4243	1.580733	4.99E-13	Up	1.31E-14
BOX15_Mlig015026g2	1154	99.80248	298.3888	1.580046	2.83E-13	Up	7.24E-15
BOX15_Mlig018052g1	4956	594.9333	1777.682	1.579197	6.31E-05	Up	5.75E-06
BOX15_Mlig006368g4	5196	3014.72	9000.972	1.578057	5.36E-21	Up	7.27E-23
BOX15_Mlig015884g2	1914	478.7253	1429.033	1.577769	2.87E-16	Up	5.59E-18
BOX15_Mlig016186g5	1388	16.89746	50.4297	1.577467	2.59E-06	Up	1.73E-07
BOX15_Mlig007780g1	1512	68.66932	204.7384	1.576044	2.83E-13	Up	7.24E-15
BOX15_Mlig029935g1	7623	175.3257	522.2513	1.574707	2.19E-16	Up	4.20E-18
BOX15_Mlig001839g3	2400	8.139248	24.2011	1.572105	0.003117	Up	0.000467
BOX15_Mlig002169g3	1692	362.474	1077.651	1.571941	2.65E-102	Up	1.56E-105
BOX15_Mlig030447g3	2144	18.97868	56.40178	1.571361	0.002368	Up	0.00034
BOX15_Mlig026505g1	2234	34.23015	101.6719	1.570581	3.74E-10	Up	1.34E-11
BOX15_Mlig012961g2	1926	16.29004	48.37446	1.570255	0.004872	Up	0.000787
BOX15_Mlig008728g4	2017	426.4001	1265.433	1.569351	3.18E-25	Up	3.21E-27
BOX15_Mlig008728g3	2017	426.4001	1265.433	1.569351	3.18E-25	Up	3.21E-27
BOX15_Mlig001264g1	2418	335.6846	992.6905	1.564238	7.32E-36	Up	4.20E-38
BOX15_Mlig012068g1	1496	23.29228	68.84766	1.563556	0.003569	Up	0.000549
BOX15_Mlig033041g1	4300	92.35159	272.9186	1.563262	7.11E-12	Up	2.12E-13
BOX15_Mlig026425g1	2907	50.48677	149.1611	1.562894	6.98E-15	Up	1.53E-16
BOX15_Mlig017553g1	1060	23.60588	69.62893	1.560541	1.94E-09	Up	7.69E-11
BOX15_Mlig000706g3	2244	41.79185	123.2239	1.559988	3.80E-08	Up	1.83E-09
BOX15_Mlig006143g2	2834	105.1691	309.6745	1.558042	5.79E-14	Up	1.37E-15
BOX15_Mlig021821g2	2535	434.1809	1278.37	1.557938	1.31E-06	Up	8.27E-08
BOX15_Mlig031432g4	2691	3.570661	10.50923	1.557393	0.009457	Up	0.001714
BOX15_Mlig031142g2	5446	123.6456	363.7183	1.556611	6.79E-27	Up	6.29E-29
BOX15_Mlig000668g18	3790	7.051381	20.73541	1.556119	0.008144	Up	0.001435
BOX15_Mlig019093g1	2386	77.99236	229.1042	1.554599	6.87E-14	Up	1.64E-15
BOX15_Mlig017107g3	4170	49.94178	146.5722	1.553293	3.05E-11	Up	9.65E-13
BOX15_Mlig027757g2	2320	19.27151	56.49358	1.551618	6.90E-05	Up	6.37E-06
BOX15_Mlig001616g2	1426	106.6924	312.7149	1.551391	3.22E-09	Up	1.32E-10
BOX15_Mlig028966g9	2155	446.9259	1309.572	1.550988	4.59E-21	Up	6.20E-23

BOX15_Mlig007168g2	3715	7.150188	20.92155	1.548936	0.009495	Up	0.001723
BOX15_Mlig000371g2	2797	4.65087	13.60316	1.548369	0.009884	Up	0.001807
BOX15_Mlig029317g3	2150	66.50947	194.48	1.54799	2.84E-06	Up	1.91E-07
BOX15_Mlig016852g2	5035	13.88064	40.5063	1.545072	5.36E-06	Up	3.81E-07
BOX15_Mlig000049g2	5577	195.8706	571.15	1.543969	9.63E-13	Up	2.61E-14
BOX15_Mlig005545g4	3331	8.157596	23.77293	1.543104	0.004528	Up	0.000723
BOX15_Mlig025303g2	4404	32.01373	93.28507	1.542956	0.011134	Up	0.002079
BOX15_Mlig002897g3	6516	131.6438	383.4177	1.542277	5.66E-28	Up	4.98E-30
BOX15_Mlig004587g3	1547	57.20371	166.6021	1.542226	1.72E-07	Up	9.25E-09
BOX15_Mlig029876g1	4330	312.4987	909.2046	1.540755	7.81E-36	Up	4.51E-38
BOX15_Mlig010354g3	1650	422.9928	1227.401	1.536902	3.32E-32	Up	2.31E-34
BOX15_Mlig031275g1	3612	83.51607	242.2635	1.536451	5.63E-12	Up	1.66E-13
BOX15_Mlig021739g1	1383	59.99731	173.8557	1.53492	0.002109	Up	0.000298
BOX15_Mlig025935g1	4053	124.6222	361.0367	1.534584	1.29E-21	Up	1.67E-23
BOX15_Mlig030395g2	1586	225.5829	653.3279	1.53415	2.93E-20	Up	4.20E-22
BOX15_Mlig007264g1	3004	30.76601	89.07254	1.533644	0.000125	Up	1.23E-05
BOX15_Mlig014836g1	1338	10.45277	30.25049	1.533074	0.000479	Up	5.55E-05
BOX15_Mlig023442g1	4114	198.9245	575.5366	1.532687	3.82E-35	Up	2.29E-37
BOX15_Mlig020395g2	1778	74.26975	214.8525	1.5325	6.61E-06	Up	4.79E-07
BOX15_Mlig032561g1	1096	7145.817	20588.55	1.526672	0.006012	Up	0.001005
BOX15_Mlig008240g2	1980	111.9588	322.4948	1.526308	1.48E-21	Up	1.93E-23
BOX15_Mlig022693g1	2185	59.00815	169.9018	1.525715	2.06E-14	Up	4.69E-16
BOX15_Mlig031877g2	4283	58.8693	169.4284	1.525088	2.20E-18	Up	3.70E-20
BOX15_Mlig029371g2	5784	192.3356	553.5365	1.525053	4.92E-25	Up	5.05E-27
BOX15_Mlig012661g2	2442	4.245209	12.21571	1.52483	0.009825	Up	0.001794
BOX15_Mlig014999g1	1713	83.99758	241.3331	1.522606	1.39E-19	Up	2.11E-21
BOX15_Mlig028238g1	2221	7.787912	22.36113	1.521685	0.008736	Up	0.001558
BOX15_Mlig006568g1	804	41.47971	119.0705	1.521339	1.52E-15	Up	3.17E-17
BOX15_Mlig017756g2	2076	17.6781	50.73922	1.521138	9.47E-05	Up	9.01E-06
BOX15_Mlig024152g2	1390	17.19901	49.34823	1.520673	0.000314	Up	3.46E-05
BOX15_Mlig013843g2	1607	54.0973	155.2038	1.520535	5.92E-05	Up	5.35E-06
BOX15_Mlig019660g1	4462	81.66317	234.2531	1.520311	0.000585	Up	6.94E-05
BOX15_Mlig014829g9	8239	23.0418	66.08033	1.519968	5.28E-09	Up	2.25E-10
BOX15_Mlig011681g1	4012	226.6894	648.9716	1.517438	2.47E-15	Up	5.25E-17
BOX15_Mlig026130g2	837	2006.158	5739.906	1.516592	0.000187	Up	1.93E-05
BOX15_Mlig026435g1	2437	78.04466	223.1186	1.515439	1.25E-28	Up	1.07E-30
BOX15_Mlig012180g6	4708	779.1575	2225.306	1.514017	2.76E-14	Up	6.38E-16
BOX15_Mlig008158g1	781	49.15368	140.2437	1.512565	1.13E-09	Up	4.34E-11
BOX15_Mlig020232g1	4145	113.4442	322.911	1.509154	1.07E-16	Up	1.99E-18
BOX15_Mlig034435g2	2010	203.8859	580.0881	1.50851	7.77E-22	Up	9.98E-24
BOX15_Mlig018234g1	3211	240.3694	681.6951	1.503874	8.82E-25	Up	9.25E-27
BOX15_Mlig011617g2	2498	457.924	1298.601	1.503779	6.12E-06	Up	4.41E-07

BOX15_Mlig030557g1	4598	67.43641	190.9236	1.501396	1.28E-09	Up	4.96E-11
BOX15_Mlig029489g1	1465	17.33579	49.04642	1.500394	2.08E-05	Up	1.67E-06
BOX15_Mlig033322g2	2914	737.7233	2086.669	1.50005	5.36E-06	Up	3.82E-07
BOX15_Mlig028238g2	4123	323.4054	914.6835	1.499929	2.71E-06	Up	1.82E-07
BOX15_Mlig007253g2	648	10.18117	28.79102	1.499716	0.000919	Up	0.000116
BOX15_Mlig030657g1	4853	360.7921	1020.269	1.499711	0.000115	Up	1.12E-05
BOX15_Mlig025889g1	1204	70.7768	200.1359	1.499632	1.47E-23	Up	1.71E-25
BOX15_Mlig007346g1	5932	19.14696	54.08872	1.498213	5.74E-06	Up	4.12E-07
BOX15_Mlig025655g3	2344	69.17193	194.826	1.493928	5.16E-08	Up	2.54E-09
BOX15_Mlig028542g2	1263	71.02673	200.0077	1.493621	0.002526	Up	0.000367
BOX15_Mlig023527g6	7336	317.0937	891.7237	1.491688	1.64E-27	Up	1.49E-29
BOX15_Mlig028175g2	9285	4.44945	12.50333	1.490613	0.007432	Up	0.001289
BOX15_Mlig022864g2	2469	75.40868	211.8985	1.490571	5.55E-18	Up	9.55E-20
BOX15_Mlig016357g1	1489	84.33071	236.8693	1.489961	5.82E-08	Up	2.90E-09
BOX15_Mlig011617g1	1517	183.1394	514.3375	1.489773	0.000747	Up	9.14E-05
BOX15_Mlig016326g1	3679	201.0426	564.5385	1.489571	7.85E-16	Up	1.59E-17
BOX15_Mlig028869g1	1945	6.281504	17.63689	1.489414	0.014992	Up	0.002969
BOX15_Mlig001549g5	1428	224.0762	629.1091	1.489321	2.87E-10	Up	1.01E-11
BOX15_Mlig020571g1	3896	202.7197	567.8554	1.486037	2.52E-29	Up	2.05E-31
BOX15_Mlig000572g3	9648	275.7286	771.5459	1.484503	2.51E-18	Up	4.23E-20
BOX15_Mlig027974g2	8095	130.4696	364.994	1.484159	5.38E-24	Up	5.99E-26
BOX15_Mlig027525g3	6483	8302.811	23226.94	1.484127	0.013508	Up	0.002621
BOX15_Mlig007046g1	4397	183.206	511.9366	1.482498	2.88E-26	Up	2.74E-28
BOX15_Mlig019714g2	3194	264.2075	738.1578	1.482258	0.014353	Up	0.002816
BOX15_Mlig012911g1	3910	226.5376	632.3732	1.481026	1.59E-38	Up	7.97E-41
BOX15_Mlig028966g4	2137	616.533	1720.343	1.480446	5.89E-28	Up	5.20E-30
BOX15_Mlig021945g1	5779	9.843951	27.45162	1.479582	0.017217	Up	0.003506
BOX15_Mlig033370g2	10378	115.5037	321.9558	1.478924	7.43E-35	Up	4.59E-37
BOX15_Mlig017197g1	1389	192.2907	534.3406	1.474471	9.53E-11	Up	3.18E-12
BOX15_Mlig004499g1	2268	141.5355	392.928	1.473101	6.34E-14	Up	1.51E-15
BOX15_Mlig013187g1	3546	32.20125	89.36706	1.472627	0.000178	Up	1.83E-05
BOX15_Mlig001484g3	1981	177.5008	492.181	1.471364	4.75E-14	Up	1.12E-15
BOX15_Mlig031977g1	2480	466.8402	1293.391	1.470158	1.08E-68	Up	1.39E-71
BOX15_Mlig009516g1	1555	312.0559	864.4907	1.470046	0.004388	Up	0.000697
BOX15_Mlig001833g1	4420	104.9006	290.1379	1.467717	2.64E-23	Up	3.08E-25
BOX15_Mlig032170g3	5042	20.45973	56.55373	1.466835	1.86E-06	Up	1.20E-07
BOX15_Mlig027525g2	3105	6036.136	16680.81	1.466492	0.014774	Up	0.002916
BOX15_Mlig023726g1	3193	160.5855	443.7277	1.466333	4.96E-44	Up	1.87E-46
BOX15_Mlig001067g1	2085	4.099338	11.31393	1.464637	0.013926	Up	0.002719
BOX15_Mlig002278g1	3596	158.2182	435.7885	1.461712	1.93E-09	Up	7.68E-11
BOX15_Mlig012940g1	2866	23.68023	65.159	1.460282	4.25E-06	Up	2.96E-07
BOX15_Mlig011669g1	6986	169.7356	466.5565	1.458763	1.84E-07	Up	1.00E-08

BOX15_Mlig018315g1	2853	320.4989	880.6456	1.458242	1.82E-40	Up	8.32E-43
BOX15_Mlig028253g1	7245	290.0046	795.7572	1.456253	1.02E-72	Up	1.16E-75
BOX15_Mlig000191g1	3641	365.4413	1001.18	1.453989	4.61E-29	Up	3.82E-31
BOX15_Mlig006550g2	1413	77.09417	210.943	1.45216	5.88E-23	Up	7.05E-25
BOX15_Mlig015540g3	3296	66.581	182.0668	1.451286	1.90E-17	Up	3.38E-19
BOX15_Mlig005389g1	6942	122.2423	334.2506	1.451186	9.56E-14	Up	2.32E-15
BOX15_Mlig034537g4	1025	265.0256	723.3155	1.448493	4.93E-17	Up	8.96E-19
BOX15_Mlig021316g1	8053	148.6572	405.6101	1.448104	3.05E-26	Up	2.92E-28
BOX15_Mlig022376g2	2137	177.6026	483.9939	1.446336	0.000793	Up	9.79E-05
BOX15_Mlig020486g1	4194	60.01159	163.3875	1.444984	1.83E-10	Up	6.30E-12
BOX15_Mlig006278g1	1052	336.4137	915.0903	1.443678	9.50E-32	Up	6.78E-34
BOX15_Mlig004619g2	7447	2.204145	5.989123	1.442125	0.018183	Up	0.003746
BOX15_Mlig002220g1	6105	508.2306	1378.326	1.439362	2.94E-24	Up	3.17E-26
BOX15_Mlig022672g1	3052	17.32382	46.98052	1.439306	1.78E-05	Up	1.41E-06
BOX15_Mlig031142g3	5449	189.067	512.6342	1.439032	6.44E-22	Up	8.22E-24
BOX15_Mlig006317g3	905	101.1473	274.2416	1.43899	1.84E-13	Up	4.60E-15
BOX15_Mlig010092g1	370	4.768733	12.92924	1.438959	0.021748	Up	0.004658
BOX15_Mlig004686g1	3451	149.6866	405.1591	1.436544	2.00E-25	Up	1.98E-27
BOX15_Mlig024423g2	2165	65.4613	176.7473	1.432974	9.05E-09	Up	3.98E-10
BOX15_Mlig032458g1	2342	102.8485	277.5679	1.43232	8.13E-25	Up	8.48E-27
BOX15_Mlig002858g1	960	26.44151	71.2952	1.431	0.002997	Up	0.000447
BOX15_Mlig030557g5	3661	47.02679	126.7739	1.430703	1.96E-07	Up	1.07E-08
BOX15_Mlig032942g1	2243	76.9637	207.4202	1.430307	3.14E-15	Up	6.73E-17
BOX15_Mlig006278g2	1029	492.1471	1325.777	1.429677	1.25E-31	Up	9.00E-34
BOX15_Mlig030072g3	2807	119.4383	321.6455	1.429206	1.10E-13	Up	2.68E-15
BOX15_Mlig008360g1	1426	3.556637	9.572605	1.428398	0.015798	Up	0.003162
BOX15_Mlig019680g2	2405	14.03386	37.76657	1.428197	0.000182	Up	1.88E-05
BOX15_Mlig033236g1	556	5.940326	15.97662	1.427348	0.010147	Up	0.001865
BOX15_Mlig010532g1	3277	24.54626	65.99816	1.426923	9.65E-06	Up	7.24E-07
BOX15_Mlig023997g1	2059	155.609	418.3129	1.426657	7.57E-17	Up	1.39E-18
BOX15_Mlig030122g2	8515	98.57009	264.8864	1.426152	1.06E-17	Up	1.85E-19
BOX15_Mlig021984g3	4362	8.687675	23.3334	1.425354	0.004165	Up	0.000657
BOX15_Mlig020035g1	1443	957.3849	2568.92	1.423991	9.86E-16	Up	2.00E-17
BOX15_Mlig028913g1	2242	142.9024	383.0339	1.422442	1.41E-23	Up	1.63E-25
BOX15_Mlig030437g1	5821	7.791999	20.87414	1.421651	0.004152	Up	0.000654
BOX15_Mlig014392g2	860	74.15423	198.6058	1.421307	3.67E-21	Up	4.92E-23
BOX15_Mlig005102g1	1692	66.61295	178.3678	1.420981	3.81E-10	Up	1.36E-11
BOX15_Mlig001225g4	1393	1010.552	2705.895	1.420963	1.90E-30	Up	1.47E-32
BOX15_Mlig021912g1	3696	185.0632	495.0998	1.419701	1.36E-15	Up	2.80E-17
BOX15_Mlig006291g3	4021	2352.049	6289.302	1.418982	1.83E-41	Up	8.07E-44
BOX15_Mlig003707g2	3199	31.58663	84.42584	1.418371	0.007572	Up	0.001317
BOX15_Mlig006328g1	2331	66.85317	178.6778	1.418293	0.000169	Up	1.73E-05

BOX15_Mlig000636g1	3781	522.3798	1395.289	1.417393	4.25E-94	Up	3.30E-97
BOX15_Mlig000534g4	1706	34.19289	91.3156	1.417165	5.46E-06	Up	3.89E-07
BOX15_Mlig034022g1	669	33.71752	90.02181	1.416776	4.12E-06	Up	2.86E-07
BOX15_Mlig026762g1	2596	55.55969	148.1431	1.414881	8.10E-09	Up	3.54E-10
BOX15_Mlig028966g6	2128	158.8387	423.2877	1.414076	2.70E-18	Up	4.56E-20
BOX15_Mlig012180g2	4659	328.0961	874.1279	1.413726	0.008011	Up	0.001408
BOX15_Mlig002256g1	4990	13.26973	35.35306	1.413696	0.003824	Up	0.000595
BOX15_Mlig027467g2	1694	710.504	1891.744	1.412802	6.22E-13	Up	1.66E-14
BOX15_Mlig032303g4	555	5.309279	14.13257	1.412436	0.023386	Up	0.005085
BOX15_Mlig032303g3	555	5.309279	14.13257	1.412436	0.023386	Up	0.005085
BOX15_Mlig032303g2	555	5.309279	14.13257	1.412436	0.023386	Up	0.005085
BOX15_Mlig005209g2	1627	185.8033	493.5531	1.409429	1.81E-21	Up	2.37E-23
BOX15_Mlig027552g1	2146	51.84828	137.6679	1.408825	2.12E-17	Up	3.79E-19
BOX15_Mlig014584g2	7284	880.3949	2336.688	1.408243	4.67E-14	Up	1.10E-15
BOX15_Mlig013331g1	2901	28.4793	75.57669	1.408028	9.74E-06	Up	7.32E-07
BOX15_Mlig004587g2	1548	34.37437	91.17698	1.407336	2.48E-08	Up	1.16E-09
BOX15_Mlig030358g2	2223	103.124	273.4838	1.407076	8.60E-22	Up	1.11E-23
BOX15_Mlig013175g5	2125	58.95726	156.1709	1.405384	9.91E-05	Up	9.49E-06
BOX15_Mlig014176g1	862	63.70434	168.7439	1.405372	4.70E-15	Up	1.01E-16
BOX15_Mlig018122g4	5489	585.974	1551.977	1.405199	3.17E-35	Up	1.89E-37
BOX15_Mlig030597g1	1465	624.1709	1651.731	1.403966	1.76E-47	Up	5.36E-50
BOX15_Mlig013175g4	2145	170.3258	450.4754	1.403151	1.03E-23	Up	1.17E-25
BOX15_Mlig013523g1	4636	256.1997	677.5689	1.403099	1.94E-27	Up	1.77E-29
BOX15_Mlig010092g2	3947	182.3572	481.9251	1.402042	1.88E-21	Up	2.47E-23
BOX15_Mlig001059g2	2889	14.40973	38.06809	1.401539	0.006223	Up	0.001047
BOX15_Mlig011327g1	1560	10.04955	26.5413	1.401108	0.004111	Up	0.000646
BOX15_Mlig019469g3	2122	123.2998	325.4297	1.400176	4.85E-32	Up	3.42E-34
BOX15_Mlig006524g1	1385	718.0165	1893.887	1.399261	4.12E-71	Up	4.93E-74
BOX15_Mlig020678g1	776	17.18474	45.2932	1.398166	2.27E-05	Up	1.84E-06
BOX15_Mlig021912g2	3481	205.4722	541.5015	1.398022	1.54E-13	Up	3.82E-15
BOX15_Mlig013995g4	719	48.03891	126.5449	1.397374	4.15E-07	Up	2.39E-08
BOX15_Mlig011820g3	4267	557.2058	1467.34	1.396921	6.57E-44	Up	2.51E-46
BOX15_Mlig000856g1	3064	47.83461	125.9083	1.396247	2.00E-06	Up	1.30E-07
BOX15_Mlig003030g1	2541	469.0294	1233.914	1.395491	2.55E-49	Up	7.12E-52
BOX15_Mlig030791g2	4259	364.7185	957.3755	1.392301	8.02E-51	Up	2.04E-53
BOX15_Mlig015234g2	3156	192.28	504.2791	1.391013	2.26E-34	Up	1.42E-36
BOX15_Mlig019194g1	2417	209.7401	550.0563	1.390977	1.64E-45	Up	5.74E-48
BOX15_Mlig014288g3	3779	7.397714	19.39551	1.390571	0.021949	Up	0.004712
BOX15_Mlig008982g1	3203	541.3311	1417.164	1.388424	3.52E-92	Up	2.88E-95
BOX15_Mlig018538g1	3387	433.3754	1133.575	1.387191	6.13E-22	Up	7.81E-24
BOX15_Mlig013425g1	3395	111.7957	292.4105	1.387131	3.76E-09	Up	1.56E-10
BOX15_Mlig000644g4	1684	210.5833	550.6741	1.386808	0.007948	Up	0.001395

BOX15_Mlig012180g4	1961	208.287	544.5711	1.386548	0.001515	Up	0.000205
BOX15_Mlig033406g1	2000	114.2435	298.3211	1.384754	4.46E-25	Up	4.56E-27
BOX15_Mlig010354g2	1632	321.1243	838.4383	1.384573	6.61E-19	Up	1.05E-20
BOX15_Mlig012038g1	1885	44.52901	116.2439	1.384337	1.13E-06	Up	7.02E-08
BOX15_Mlig003291g2	12095	142.635	372.194	1.383727	1.19E-16	Up	2.24E-18
BOX15_Mlig016904g1	2387	26.28855	68.59424	1.383653	0.000241	Up	2.57E-05
BOX15_Mlig033296g1	3041	88.61606	231.1982	1.38349	1.65E-13	Up	4.10E-15
BOX15_Mlig017224g3	1980	315.5384	823.2095	1.383444	5.94E-48	Up	1.73E-50
BOX15_Mlig000860g1	3326	184.5522	481.3989	1.383204	1.50E-18	Up	2.47E-20
BOX15_Mlig013263g7	2763	16.35543	42.65867	1.38307	1.95E-05	Up	1.56E-06
BOX15_Mlig016769g2	1907	2.036859	5.309955	1.382354	0.027584	Up	0.006185
BOX15_Mlig027184g4	4574	95.84014	249.6165	1.381011	3.43E-20	Up	4.96E-22
BOX15_Mlig022332g1	2894	133.484	347.3603	1.379765	1.07E-22	Up	1.30E-24
BOX15_Mlig017311g1	3980	325.2156	846.196	1.379596	3.88E-33	Up	2.64E-35
BOX15_Mlig005321g2	2879	38.81875	100.9395	1.378665	1.46E-11	Up	4.48E-13
BOX15_Mlig016602g2	3122	17.13451	44.51354	1.37734	0.000833	Up	0.000104
BOX15_Mlig006713g2	4036	148.4949	385.7552	1.377272	7.49E-37	Up	4.06E-39
BOX15_Mlig031702g1	1088	31.24114	81.15535	1.377239	7.07E-08	Up	3.57E-09
BOX15_Mlig029219g1	3010	96.33179	250.1693	1.376821	2.35E-17	Up	4.21E-19
BOX15_Mlig009192g1	2841	12.57324	32.64437	1.376478	0.007868	Up	0.001378
BOX15_Mlig030395g1	2294	551.3266	1431.301	1.376348	8.92E-23	Up	1.08E-24
BOX15_Mlig001067g4	2395	13.93253	36.16416	1.376104	0.003044	Up	0.000455
BOX15_Mlig007942g1	1702	60.39709	156.7416	1.375837	3.12E-09	Up	1.28E-10
BOX15_Mlig016602g1	3120	32.25108	83.69339	1.375766	9.78E-08	Up	5.06E-09
BOX15_Mlig008992g1	1093	173.9457	451.3627	1.37565	3.95E-11	Up	1.26E-12
BOX15_Mlig034460g2	3557	416.1541	1079.762	1.375523	2.52E-39	Up	1.24E-41
BOX15_Mlig026004g1	2184	58.1937	150.9234	1.374882	1.37E-15	Up	2.82E-17
BOX15_Mlig033771g2	323	2.705731	7.01401	1.374221	0.029239	Up	0.006647
BOX15_Mlig033771g4	323	2.705731	7.01401	1.374221	0.029239	Up	0.006647
BOX15_Mlig033771g3	323	2.705731	7.01401	1.374221	0.029239	Up	0.006647
BOX15_Mlig027525g8	6530	9959.159	25812.08	1.373951	0.021098	Up	0.004486
BOX15_Mlig021119g3	2998	143.3331	371.4197	1.373679	1.19E-18	Up	1.94E-20
BOX15_Mlig030606g1	744	51.62306	133.631	1.372167	7.98E-07	Up	4.85E-08
BOX15_Mlig022970g1	1532	84.86605	219.6648	1.372044	3.02E-07	Up	1.70E-08
BOX15_Mlig006227g2	1819	23.38408	60.51738	1.371823	2.07E-07	Up	1.14E-08
BOX15_Mlig017224g2	1952	291.7326	754.8459	1.371535	1.65E-29	Up	1.33E-31
BOX15_Mlig020229g1	2606	186.8396	483.3601	1.371298	9.91E-08	Up	5.13E-09
BOX15_Mlig019188g2	1713	142.0617	367.3815	1.370761	2.32E-13	Up	5.88E-15
BOX15_Mlig003878g3	7442	286.2386	739.5777	1.369484	4.08E-17	Up	7.38E-19
BOX15_Mlig012322g3	1530	69.06546	178.338	1.368578	1.13E-12	Up	3.08E-14
BOX15_Mlig028140g1	2895	224.009	577.5508	1.366391	5.76E-21	Up	7.87E-23
BOX15_Mlig025686g1	3666	39.35982	101.397	1.365219	1.57E-07	Up	8.43E-09

BOX15_Mlig000081g15	4051	6.302348	16.22919	1.36463	0.030217	Up	0.006929
BOX15_Mlig018315g2	2867	271.2432	698.1765	1.364005	1.41E-28	Up	1.21E-30
BOX15_Mlig004853g1	1633	18.46984	47.51997	1.363363	0.002071	Up	0.000292
BOX15_Mlig022201g4	3127	532.3703	1368.596	1.362195	1.62E-43	Up	6.35E-46
BOX15_Mlig034537g2	1284	708.6575	1820.59	1.361245	2.02E-37	Up	1.06E-39
BOX15_Mlig022908g2	2344	3.861571	9.919837	1.361129	0.021257	Up	0.004527
BOX15_Mlig024024g1	993	92.40031	237.1475	1.359815	2.47E-13	Up	6.27E-15
BOX15_Mlig013187g2	3537	46.74961	119.9785	1.35975	6.55E-07	Up	3.91E-08
BOX15_Mlig020251g1	3484	6.221797	15.96134	1.359179	0.016388	Up	0.003305
BOX15_Mlig021189g1	2381	123.827	317.4491	1.3582	1.95E-08	Up	8.97E-10
BOX15_Mlig023081g2	1779	4.263932	10.91831	1.356493	0.02526	Up	0.005582
BOX15_Mlig030586g1	5456	16.38701	41.95891	1.356424	6.12E-05	Up	5.55E-06
BOX15_Mlig001330g1	2315	136.6105	349.7401	1.356215	2.70E-20	Up	3.86E-22
BOX15_Mlig016420g1	1438	178.1109	455.9443	1.356082	1.65E-36	Up	9.13E-39
BOX15_Mlig028014g1	2861	321.9415	824.044	1.355923	9.85E-29	Up	8.40E-31
BOX15_Mlig004569g1	3743	177.8845	455.0254	1.355007	4.56E-08	Up	2.22E-09
BOX15_Mlig006308g1	2272	50.61501	129.4101	1.354313	5.41E-13	Up	1.43E-14
BOX15_Mlig000866g1	3310	70.95591	181.3798	1.35402	9.99E-09	Up	4.42E-10
BOX15_Mlig008781g4	2580	40.19075	102.6467	1.352751	0.004215	Up	0.000666
BOX15_Mlig008937g2	3341	236.2447	603.1046	1.352126	8.24E-14	Up	1.99E-15
BOX15_Mlig011785g2	8546	17.44315	44.52199	1.351857	0.01507	Up	0.002988
BOX15_Mlig004044g2	1808	71.12699	181.1119	1.348412	2.74E-05	Up	2.27E-06
BOX15_Mlig024024g2	985	76.08284	193.673	1.34798	1.84E-06	Up	1.20E-07
BOX15_Mlig025671g5	2417	1545.63	3933.514	1.347624	2.93E-53	Up	6.89E-56
BOX15_Mlig020155g1	2823	107.9859	274.7502	1.347277	5.77E-10	Up	2.13E-11
BOX15_Mlig018577g1	3089	114.8435	292.1095	1.34684	7.62E-07	Up	4.61E-08
BOX15_Mlig001829g3	553	3.691326	9.388992	1.346831	0.0227	Up	0.004902
BOX15_Mlig005820g1	2067	153.4928	390.2354	1.346174	0.034352	Up	0.008109
BOX15_Mlig014518g4	1476	8.873341	22.54382	1.345183	0.003136	Up	0.000471
BOX15_Mlig032788g1	2045	111.222	282.4593	1.344601	3.67E-08	Up	1.76E-09
BOX15_Mlig003030g3	2538	783.8097	1989.88	1.344106	2.14E-108	Up	9.62E-112
BOX15_Mlig022951g3	842	7.870744	19.9811	1.344064	0.032307	Up	0.007508
BOX15_Mlig008240g1	1979	175.2831	444.939	1.343921	4.09E-24	Up	4.49E-26
BOX15_Mlig025598g1	1047	7.703934	19.54945	1.343461	0.002928	Up	0.000435
BOX15_Mlig000547g2	3696	118.5396	300.7278	1.343089	0.002131	Up	0.000302
BOX15_Mlig023357g2	2061	16.75102	42.47969	1.342524	0.003875	Up	0.000604
BOX15_Mlig013997g1	2128	21.73108	55.0935	1.342122	0.000106	Up	1.02E-05
BOX15_Mlig018924g1	4455	208.0547	527.4606	1.342101	6.68E-28	Up	5.95E-30
BOX15_Mlig012543g1	1959	24.49806	61.97908	1.339114	0.01768	Up	0.00362
BOX15_Mlig011240g2	1197	58.51527	147.8616	1.337362	3.30E-05	Up	2.78E-06
BOX15_Mlig011017g6	4761	2.955915	7.464217	1.336386	0.024148	Up	0.005281
BOX15_Mlig001881g4	2132	7.379575	18.6254	1.335662	0.034837	Up	0.008244

BOX15_Mlig006920g1	2598	145.71	367.6414	1.335199	5.36E-07	Up	3.15E-08
BOX15_Mlig021316g3	8014	257.5052	648.7403	1.333039	3.98E-20	Up	5.81E-22
BOX15_Mlig000425g3	1155	270.148	680.5285	1.332906	2.17E-14	Up	4.96E-16
BOX15_Mlig015047g1	2513	104.7965	263.9909	1.332898	4.04E-12	Up	1.17E-13
BOX15_Mlig032089g1	1256	166.8096	420.1106	1.332567	1.25E-06	Up	7.82E-08
BOX15_Mlig000644g6	2821	90.75881	228.5475	1.332385	0.00851	Up	0.001512
BOX15_Mlig016504g5	3969	4.043825	10.17731	1.331564	0.036757	Up	0.008792
BOX15_Mlig006202g2	4414	177.2923	445.8802	1.330526	1.21E-07	Up	6.38E-09
BOX15_Mlig030225g2	2902	49.81424	125.1283	1.328778	8.55E-11	Up	2.83E-12
BOX15_Mlig001059g3	2519	28.12987	70.59903	1.327545	0.000388	Up	4.39E-05
BOX15_Mlig031471g1	2469	257.9229	646.3903	1.325466	8.34E-08	Up	4.26E-09
BOX15_Mlig034225g2	6033	80.80691	202.4514	1.325025	3.78E-17	Up	6.81E-19
BOX15_Mlig011767g1	2287	50.21337	125.7094	1.323948	4.17E-09	Up	1.75E-10
BOX15_Mlig017662g3	770	6.193732	15.50053	1.323437	0.00831	Up	0.00147
BOX15_Mlig018407g2	1796	143.8499	359.614	1.321885	4.88E-23	Up	5.81E-25
BOX15_Mlig013265g3	926	55.80312	139.502	1.321868	4.24E-10	Up	1.53E-11
BOX15_Mlig021063g3	2372	154.9216	386.8497	1.320234	3.19E-19	Up	4.99E-21
BOX15_Mlig032547g1	3586	7.341922	18.33161	1.320104	0.034845	Up	0.008247
BOX15_Mlig034245g1	3916	57.8371	144.256	1.318564	4.89E-11	Up	1.58E-12
BOX15_Mlig006365g2	7159	63.28182	157.6598	1.316952	8.02E-05	Up	7.52E-06
BOX15_Mlig016115g2	1668	273.9797	682.0642	1.315838	6.78E-21	Up	9.30E-23
BOX15_Mlig032346g1	2449	153.4043	381.4628	1.314204	5.08E-29	Up	4.23E-31
BOX15_Mlig026261g1	892	1660.135	4121.081	1.311723	0.025308	Up	0.005595
BOX15_Mlig000191g2	4839	139.0616	345.0173	1.310945	4.05E-11	Up	1.30E-12
BOX15_Mlig014942g1	1731	355.7226	882.3908	1.310665	4.37E-30	Up	3.42E-32
BOX15_Mlig010601g1	1351	94.70215	234.9103	1.310641	3.08E-11	Up	9.77E-13
BOX15_Mlig019338g1	2057	163.9509	406.3902	1.309601	1.98E-21	Up	2.62E-23
BOX15_Mlig005947g3	817	301.0822	745.9897	1.308998	0.017543	Up	0.003588
BOX15_Mlig009524g1	5693	43.96535	108.8394	1.307761	6.16E-07	Up	3.66E-08
BOX15_Mlig031416g2	2156	414.7747	1026.784	1.307733	9.88E-19	Up	1.61E-20
BOX15_Mlig005876g1	15645	708.3674	1753.447	1.307624	9.29E-23	Up	1.13E-24
BOX15_Mlig032089g3	1232	144.6925	357.9988	1.306964	0.001108	Up	0.000143
BOX15_Mlig017439g1	5041	22.85032	56.49659	1.30595	4.40E-06	Up	3.07E-07
BOX15_Mlig026668g1	4605	59.00876	145.8339	1.305325	2.45E-05	Up	2.00E-06
BOX15_Mlig030358g1	2213	68.43366	168.9662	1.303957	1.01E-11	Up	3.06E-13
BOX15_Mlig023464g1	4981	198.6222	490.3175	1.303689	1.32E-15	Up	2.73E-17
BOX15_Mlig032929g1	1489	831.2285	2050.863	1.302914	2.99E-34	Up	1.90E-36
BOX15_Mlig006964g1	1995	263.1753	649.0555	1.302317	0.003429	Up	0.000523
BOX15_Mlig028573g2	1882	80.72566	199.0877	1.302305	0.000311	Up	3.43E-05
BOX15_Mlig006080g1	4169	401.4159	989.8352	1.302091	9.79E-19	Up	1.59E-20
BOX15_Mlig014147g1	1820	255.4486	628.9409	1.299892	9.11E-10	Up	3.44E-11
BOX15_Mlig022951g2	853	11.54675	28.42407	1.299626	0.003109	Up	0.000466

BOX15_Mlig006964g3	1935	395.6745	973.335	1.298622	0.001863	Up	0.000259
BOX15_Mlig027292g2	2672	8.649519	21.2645	1.297755	0.016912	Up	0.003431
BOX15_Mlig022715g1	3729	68.15205	167.5378	1.297658	9.18E-07	Up	5.64E-08
BOX15_Mlig028776g3	964	103.0679	253.2895	1.297192	4.92E-09	Up	2.08E-10
BOX15_Mlig027518g1	3206	48.54188	119.1957	1.296031	3.39E-13	Up	8.73E-15
BOX15_Mlig003009g1	1788	105.815	259.7573	1.29562	1.04E-05	Up	7.83E-07
BOX15_Mlig030651g1	1430	28.49043	69.92841	1.295401	3.20E-06	Up	2.18E-07
BOX15_Mlig032089g2	1227	62.89465	154.312	1.294842	0.000124	Up	1.22E-05
BOX15_Mlig010885g1	2092	81.98441	201.1395	1.294775	9.12E-17	Up	1.69E-18
BOX15_Mlig012940g3	2675	34.24452	83.92394	1.293209	4.68E-05	Up	4.11E-06
BOX15_Mlig000402g1	3668	170.3852	417.4248	1.292717	2.02E-16	Up	3.85E-18
BOX15_Mlig014424g1	4856	82.82873	202.8855	1.292463	1.02E-10	Up	3.42E-12
BOX15_Mlig006484g2	4097	14.75311	36.08111	1.290225	0.00195	Up	0.000272
BOX15_Mlig024565g2	1916	13.25045	32.33968	1.287264	0.004367	Up	0.000693
BOX15_Mlig002473g2	1671	42.93785	104.7461	1.286574	4.76E-06	Up	3.35E-07
BOX15_Mlig010927g2	2435	107.4474	262.0935	1.286451	1.86E-12	Up	5.22E-14
BOX15_Mlig019457g1	3470	37.8871	92.37413	1.285782	5.81E-08	Up	2.89E-09
BOX15_Mlig005255g1	775	212.7568	518.7062	1.285712	0.015541	Up	0.003098
BOX15_Mlig000537g2	8137	40.69386	99.20963	1.285669	8.27E-07	Up	5.04E-08
BOX15_Mlig015094g3	3073	73.2659	178.5934	1.285465	4.22E-12	Up	1.23E-13
BOX15_Mlig009479g1	14346	7.444831	18.12463	1.283641	0.045731	Up	0.011463
BOX15_Mlig028838g3	1111	41.74127	101.5698	1.282925	3.39E-09	Up	1.40E-10
BOX15_Mlig028838g1	1111	41.74127	101.5698	1.282925	3.39E-09	Up	1.40E-10
BOX15_Mlig009578g1	1467	86.38309	210.1544	1.282629	1.46E-20	Up	2.06E-22
BOX15_Mlig009578g2	1467	86.38309	210.1544	1.282629	1.46E-20	Up	2.06E-22
BOX15_Mlig027034g1	1484	3.884832	9.445718	1.281808	0.044031	Up	0.010962
BOX15_Mlig020494g1	2312	156.806	381.2587	1.28179	1.63E-25	Up	1.60E-27
BOX15_Mlig004095g4	4722	821.6769	1997.457	1.281522	2.96E-13	Up	7.59E-15
BOX15_Mlig001932g3	3679	2.148764	5.223363	1.281472	0.041825	Up	0.010302
BOX15_Mlig017326g1	3203	61.78589	150.1811	1.281354	6.73E-10	Up	2.50E-11
BOX15_Mlig010542g2	3328	166.9925	405.7342	1.280751	7.20E-17	Up	1.32E-18
BOX15_Mlig011241g1	2671	102.4655	248.8361	1.280057	0.005601	Up	0.000924
BOX15_Mlig013722g1	3721	75.85253	184.1192	1.279371	6.36E-09	Up	2.73E-10
BOX15_Mlig005206g1	3302	174.6316	423.8169	1.279126	8.81E-07	Up	5.40E-08
BOX15_Mlig030316g1	3937	57.20694	138.706	1.277768	3.23E-10	Up	1.15E-11
BOX15_Mlig030827g2	2810	103.5073	250.8802	1.277266	1.32E-10	Up	4.49E-12
BOX15_Mlig010907g1	2834	37.84424	91.59836	1.275248	0.041205	Up	0.010112
BOX15_Mlig002769g1	3468	24.65466	59.66164	1.274943	2.07E-05	Up	1.67E-06
BOX15_Mlig003409g1	1542	193.2765	467.4908	1.274272	1.04E-14	Up	2.32E-16
BOX15_Mlig030606g2	746	10.84253	26.21409	1.27364	0.003803	Up	0.000591
BOX15_Mlig018407g1	1862	133.6491	323.0243	1.273193	4.77E-20	Up	7.04E-22
BOX15_Mlig029907g1	2313	63.08916	152.4665	1.273028	5.40E-05	Up	4.82E-06

BOX15_Mlig011654g2	4025	187.1857	452.2966	1.272799	2.03E-15	Up	4.27E-17
BOX15_Mlig026852g1	1884	32.25734	77.94246	1.272782	3.74E-08	Up	1.80E-09
BOX15_Mlig016278g1	2912	180.0565	434.9586	1.272429	4.65E-15	Up	1.00E-16
BOX15_Mlig013910g1	2244	342.2343	826.4334	1.271914	7.18E-36	Up	4.10E-38
BOX15_Mlig005321g3	2101	10.50005	25.3312	1.27052	0.01507	Up	0.002988
BOX15_Mlig005066g1	2382	212.907	513.6293	1.270504	5.07E-12	Up	1.49E-13
BOX15_Mlig024333g1	1662	2.889458	6.969766	1.270311	0.032009	Up	0.007427
BOX15_Mlig017692g3	1637	44.15666	106.3899	1.268659	2.60E-10	Up	9.09E-12
BOX15_Mlig029714g2	673	10.60516	25.54511	1.268281	0.007582	Up	0.001319
BOX15_Mlig013843g1	1831	114.1644	274.8988	1.267788	2.25E-07	Up	1.25E-08
BOX15_Mlig013859g2	3589	34.42976	82.87673	1.267311	0.000294	Up	3.22E-05
BOX15_Mlig002073g1	2789	51.21064	123.258	1.267166	1.77E-12	Up	4.97E-14
BOX15_Mlig023511g1	4315	25.4814	61.27457	1.265844	0.001243	Up	0.000164
BOX15_Mlig027634g1	3352	55.50094	133.3745	1.264899	1.66E-13	Up	4.11E-15
BOX15_Mlig032862g1	1778	4.798907	11.52803	1.264368	0.048608	Up	0.01237
BOX15_Mlig004095g1	4611	1888.72	4535.902	1.26398	1.12E-24	Up	1.18E-26
BOX15_Mlig015656g1	4225	64.93994	155.918	1.263609	3.39E-14	Up	7.90E-16
BOX15_Mlig029213g2	1487	7.074496	16.98473	1.263539	0.049301	Up	0.012587
BOX15_Mlig018795g4	715	6.49944	15.58416	1.261693	0.017773	Up	0.003642
BOX15_Mlig008077g3	2840	310.4231	744.0596	1.261182	4.57E-48	Up	1.31E-50
BOX15_Mlig029129g1	1791	171.8837	411.9869	1.261165	1.73E-31	Up	1.26E-33
BOX15_Mlig012684g2	1704	124.7988	298.9156	1.260134	1.29E-21	Up	1.68E-23
BOX15_Mlig012684g1	1704	124.7988	298.9156	1.260134	1.29E-21	Up	1.68E-23
BOX15_Mlig004095g2	4722	665.8782	1594.269	1.259565	5.01E-11	Up	1.62E-12
BOX15_Mlig033488g2	7298	108.6535	260.1377	1.259541	9.85E-12	Up	2.98E-13
BOX15_Mlig001616g4	1431	70.95018	169.6836	1.257969	0.001039	Up	0.000133
BOX15_Mlig018315g3	2865	304.9434	729.2719	1.257915	2.69E-38	Up	1.37E-40
BOX15_Mlig031416g3	2332	246.2	587.9804	1.255937	1.39E-27	Up	1.25E-29
BOX15_Mlig030072g1	2860	166.1147	396.7126	1.255914	1.10E-10	Up	3.71E-12
BOX15_Mlig025693g2	1832	402.2424	960.1863	1.255249	4.91E-47	Up	1.55E-49
BOX15_Mlig011500g2	10687	36.78489	87.78011	1.254781	4.36E-06	Up	3.04E-07
BOX15_Mlig006143g3	1834	66.55791	158.7878	1.254418	1.33E-05	Up	1.03E-06
BOX15_Mlig004587g1	1544	92.53636	220.4864	1.252598	1.31E-13	Up	3.22E-15
BOX15_Mlig027304g1	3502	271.6847	646.2563	1.250173	9.11E-14	Up	2.20E-15
BOX15_Mlig020864g2	2197	113.8639	270.4041	1.247807	1.86E-13	Up	4.65E-15
BOX15_Mlig008497g1	7055	303.2973	720.1944	1.247654	0.000479	Up	5.55E-05
BOX15_Mlig003879g2	2323	2001.519	4750.206	1.246895	0.036173	Up	0.008628
BOX15_Mlig015542g3	1234	15.54256	36.88091	1.24665	0.002591	Up	0.000378
BOX15_Mlig004105g2	966	27.22214	64.53162	1.245226	0.000153	Up	1.54E-05
BOX15_Mlig005947g5	828	818.707	1940.769	1.245209	0.011831	Up	0.002237
BOX15_Mlig034290g1	1226	59.56027	141.1412	1.244717	2.51E-06	Up	1.67E-07
BOX15_Mlig005467g2	4191	101.7355	241.0212	1.244337	1.45E-18	Up	2.38E-20

BOX15_Mlig023431g2	3075	204.086	483.1679	1.243347	2.10E-12	Up	5.96E-14
BOX15_Mlig005977g1	994	16.79033	39.73907	1.242927	0.000197	Up	2.05E-05
BOX15_Mlig005977g3	994	16.79033	39.73907	1.242927	0.000197	Up	2.05E-05
BOX15_Mlig003400g1	12241	10.3004	24.36899	1.242346	0.003474	Up	0.000531
BOX15_Mlig008333g2	2990	56.83421	134.4548	1.242289	3.88E-06	Up	2.68E-07
BOX15_Mlig008878g1	2068	97.56084	230.7342	1.241858	2.24E-18	Up	3.76E-20
BOX15_Mlig032975g2	2832	11.57998	27.37361	1.241153	0.024764	Up	0.005449
BOX15_Mlig002622g2	16379	34.44022	81.36138	1.24025	0.003935	Up	0.000615
BOX15_Mlig027184g3	4577	73.83124	174.2497	1.238853	3.59E-14	Up	8.38E-16
BOX15_Mlig006365g1	8689	161.8929	381.9035	1.238168	1.57E-14	Up	3.53E-16
BOX15_Mlig026695g1	3622	159.6104	376.3766	1.237622	2.08E-08	Up	9.60E-10
BOX15_Mlig018484g1	16494	57.47281	135.51	1.237448	6.66E-06	Up	4.83E-07
BOX15_Mlig028619g2	3792	512.8596	1208.165	1.236181	2.59E-47	Up	7.99E-50
BOX15_Mlig024988g3	1594	349.9008	824.1483	1.235958	1.72E-09	Up	6.77E-11
BOX15_Mlig010375g2	2056	25.07464	59.06009	1.235955	3.29E-06	Up	2.24E-07
BOX15_Mlig019946g1	2486	21.02309	49.50894	1.235714	0.001335	Up	0.000177
BOX15_Mlig026467g1	5408	31.37013	73.85227	1.235251	4.73E-06	Up	3.33E-07
BOX15_Mlig034555g2	2226	120.4806	282.9915	1.231958	3.67E-20	Up	5.34E-22
BOX15_Mlig015234g3	3151	111.0742	260.4673	1.229578	6.24E-11	Up	2.04E-12
BOX15_Mlig017224g1	1970	284.5306	666.9775	1.229054	3.85E-10	Up	1.38E-11
BOX15_Mlig019302g1	4141	69.72025	163.4167	1.228906	6.13E-10	Up	2.27E-11
BOX15_Mlig013841g2	2758	203.6987	477.4252	1.228838	7.09E-14	Up	1.70E-15
BOX15_Mlig020676g3	931	79.65338	186.625	1.228335	6.18E-06	Up	4.45E-07
BOX15_Mlig011371g5	3467	22.02009	51.58747	1.2282	0.002225	Up	0.000317
BOX15_Mlig007286g3	4251	96.62628	226.3561	1.228107	4.68E-18	Up	8.01E-20
BOX15_Mlig017611g1	3101	22.99994	53.86199	1.227637	1.49E-05	Up	1.16E-06
BOX15_Mlig002622g1	4458	16.05943	37.59926	1.227284	0.001287	Up	0.00017
BOX15_Mlig030837g1	4500	25.80051	60.37227	1.226487	0.000971	Up	0.000123
BOX15_Mlig023507g3	3766	563.6977	1318.726	1.226151	5.28E-31	Up	3.97E-33
BOX15_Mlig003708g2	8254	417.6229	975.0191	1.22323	9.16E-20	Up	1.38E-21
BOX15_Mlig003901g1	1756	65.77384	153.535	1.222982	3.57E-08	Up	1.71E-09
BOX15_Mlig020467g1	3874	220.0095	513.4583	1.222681	1.64E-15	Up	3.42E-17
BOX15_Mlig015973g1	3686	56.03509	130.7377	1.222273	1.91E-09	Up	7.59E-11
BOX15_Mlig005081g1	2175	45.40435	105.8078	1.220544	1.25E-06	Up	7.81E-08
BOX15_Mlig026130g1	850	403.4064	939.4237	1.219542	0.008819	Up	0.001576
BOX15_Mlig001489g2	1855	836.8885	1948.731	1.219428	3.54E-44	Up	1.32E-46
BOX15_Mlig028452g3	4767	7.018632	16.32227	1.21758	0.018378	Up	0.003795
BOX15_Mlig020368g1	16186	1638.835	3809.386	1.216888	8.49E-18	Up	1.48E-19
BOX15_Mlig033102g1	3188	49.48611	115.0196	1.216785	0.000152	Up	1.53E-05
BOX15_Mlig010986g2	3784	466.3064	1083.741	1.21667	0.003496	Up	0.000535
BOX15_Mlig010346g1	1062	30.07776	69.76211	1.213746	1.72E-06	Up	1.11E-07
BOX15_Mlig030197g2	2729	215.0276	497.59	1.210436	3.97E-17	Up	7.17E-19

BOX15_Mlig007652g1	1981	36.26776	83.87509	1.209555	1.13E-06	Up	7.02E-08
BOX15_Mlig018884g2	3454	60.10559	138.971	1.209213	5.40E-08	Up	2.67E-09
BOX15_Mlig011719g5	3025	14.87459	34.38325	1.208856	0.008734	Up	0.001558
BOX15_Mlig019251g2	975	374.9994	865.9827	1.20745	4.09E-12	Up	1.19E-13
BOX15_Mlig004757g1	2314	78.22251	180.5002	1.206344	4.93E-07	Up	2.88E-08
BOX15_Mlig014039g1	1634	35.7069	82.38723	1.206218	6.17E-05	Up	5.61E-06
BOX15_Mlig001875g3	4036	99.54997	229.5889	1.20556	1.38E-17	Up	2.44E-19
BOX15_Mlig006291g2	3954	1864.844	4300.624	1.205491	4.14E-31	Up	3.08E-33
BOX15_Mlig026026g1	1720	212.3691	489.6896	1.205294	3.09E-06	Up	2.10E-07
BOX15_Mlig025967g2	3054	148.3471	342.0598	1.205272	1.49E-06	Up	9.48E-08
BOX15_Mlig002476g1	1809	20.08504	46.26852	1.20391	0.000208	Up	2.18E-05
BOX15_Mlig005288g1	4579	214.4216	493.8466	1.203613	2.77E-30	Up	2.15E-32
BOX15_Mlig011816g1	2369	101.8237	234.142	1.201311	0.023478	Up	0.005109
BOX15_Mlig013513g1	2408	211.6108	486.3224	1.2005	6.99E-26	Up	6.75E-28
BOX15_Mlig009793g2	2988	149.8361	344.0942	1.199418	5.55E-17	Up	1.01E-18
BOX15_Mlig030072g2	2860	172.8108	396.8167	1.199279	1.97E-15	Up	4.15E-17
BOX15_Mlig033058g1	3501	118.6534	272.4231	1.199095	9.17E-09	Up	4.04E-10
BOX15_Mlig027397g2	2555	99.96892	229.5232	1.199089	6.79E-10	Up	2.53E-11
BOX15_Mlig019373g1	1484	219.682	504.2392	1.198691	5.72E-28	Up	5.05E-30
BOX15_Mlig006354g1	4265	295.9055	678.7123	1.197664	4.61E-23	Up	5.48E-25
BOX15_Mlig029596g1	13031	131.6247	301.2299	1.194435	4.73E-09	Up	2.00E-10
BOX15_Mlig015255g1	1481	29.25702	66.93803	1.194043	7.85E-05	Up	7.34E-06
BOX15_Mlig011126g1	2456	237.7153	543.839	1.193945	8.17E-07	Up	4.98E-08
BOX15_Mlig028556g1	3586	29.2529	66.91616	1.193775	4.35E-06	Up	3.04E-07
BOX15_Mlig006395g2	11508	63.60898	145.4731	1.19345	8.02E-14	Up	1.93E-15
BOX15_Mlig030723g1	1109	43.97621	100.5152	1.192618	3.38E-08	Up	1.61E-09
BOX15_Mlig007719g2	1192	123.2305	281.5587	1.192076	1.36E-05	Up	1.05E-06
BOX15_Mlig004697g1	995	16.32961	37.28543	1.191122	0.041029	Up	0.010061
BOX15_Mlig010387g1	983	54.62527	124.7043	1.190871	0.000113	Up	1.10E-05
BOX15_Mlig021912g3	3516	127.6473	291.3479	1.19058	0.000134	Up	1.33E-05
BOX15_Mlig014926g1	2460	139.7017	318.8261	1.19042	0.004983	Up	0.000807
BOX15_Mlig002220g3	6010	607.8077	1386.55	1.189812	5.22E-34	Up	3.35E-36
BOX15_Mlig030241g2	1562	19.4026	44.26174	1.18981	0.007408	Up	0.001283
BOX15_Mlig033444g2	1560	19.64975	44.81276	1.189398	0.011007	Up	0.00205
BOX15_Mlig003221g1	1886	71.99695	164.1534	1.189037	1.07E-06	Up	6.62E-08
BOX15_Mlig031902g1	3071	10.33712	23.54594	1.187644	0.04047	Up	0.00989
BOX15_Mlig029661g2	2318	105.5795	240.4199	1.187227	4.06E-07	Up	2.33E-08
BOX15_Mlig009161g1	224	6.651582	15.11963	1.184653	0.032796	Up	0.007652
BOX15_Mlig008937g1	3341	185.3682	421.2946	1.184436	2.21E-08	Up	1.02E-09
BOX15_Mlig002020g10	909	26.38716	59.92818	1.183398	3.71E-05	Up	3.17E-06
BOX15_Mlig029351g4	2425	114.1394	259.0382	1.182368	8.87E-13	Up	2.40E-14
BOX15_Mlig018465g2	2332	176.5	400.5294	1.18224	3.70E-12	Up	1.07E-13

BOX15_Mlig004794g8	4209	28.35649	64.33532	1.181932	7.83E-07	Up	4.75E-08
BOX15_Mlig005947g2	1078	907.9461	2059.227	1.181424	0.002122	Up	0.0003
BOX15_Mlig006166g2	696	11.91151	27.00261	1.180742	0.012708	Up	0.002437
BOX15_Mlig005396g1	976	386.7082	876.1131	1.179872	2.12E-25	Up	2.11E-27
BOX15_Mlig014467g3	4075	882.4664	1996.61	1.177939	2.59E-16	Up	5.01E-18
BOX15_Mlig013453g2	1730	21.19888	47.90955	1.176325	0.00034	Up	3.80E-05
BOX15_Mlig019049g3	648	102.6727	231.945	1.17573	4.71E-05	Up	4.14E-06
BOX15_Mlig002516g1	2688	372.9814	842.424	1.175443	2.04E-11	Up	6.34E-13
BOX15_Mlig029607g2	2351	107.9354	243.7205	1.175059	9.63E-21	Up	1.34E-22
BOX15_Mlig025713g2	3134	268.59	606.1522	1.174275	1.63E-51	Up	4.00E-54
BOX15_Mlig024988g2	1595	333.7478	753.1982	1.174271	0.001387	Up	0.000185
BOX15_Mlig024024g3	976	169.1532	380.6783	1.170242	1.72E-07	Up	9.25E-09
BOX15_Mlig030197g4	2677	450.0196	1011.763	1.168812	3.13E-10	Up	1.11E-11
BOX15_Mlig023083g2	1667	60.35632	135.6821	1.168654	1.19E-07	Up	6.26E-09
BOX15_Mlig022732g1	1867	75.32074	169.322	1.16865	1.14E-08	Up	5.07E-10
BOX15_Mlig003153g1	1482	187.5086	421.0268	1.166955	0.023085	Up	0.005003
BOX15_Mlig026833g1	4174	473.3766	1061.661	1.165263	2.68E-15	Up	5.73E-17
BOX15_Mlig025671g1	2435	1714.167	3842.759	1.164635	1.26E-68	Up	1.63E-71
BOX15_Mlig008084g3	2251	19.61628	43.95808	1.164077	0.004483	Up	0.000715
BOX15_Mlig026668g2	4600	107.3954	240.6329	1.163902	1.95E-07	Up	1.07E-08
BOX15_Mlig010387g2	985	92.33145	206.8342	1.163581	2.52E-14	Up	5.82E-16
BOX15_Mlig033328g1	1703	63.11101	141.2042	1.16182	3.58E-06	Up	2.46E-07
BOX15_Mlig018244g1	7094	409.7084	916.5383	1.161598	1.18E-37	Up	6.07E-40
BOX15_Mlig016460g2	7200	8.822629	19.73046	1.161144	0.010141	Up	0.001863
BOX15_Mlig018198g1	4243	261.5248	584.3744	1.159945	1.07E-36	Up	5.87E-39
BOX15_Mlig010823g3	6054	28.13225	62.84268	1.15952	6.89E-05	Up	6.35E-06
BOX15_Mlig009708g1	2740	89.35928	199.6132	1.159518	1.72E-08	Up	7.84E-10
BOX15_Mlig000049g1	5591	275.435	615.2423	1.159443	5.68E-19	Up	8.98E-21
BOX15_Mlig018827g1	2307	50.94054	113.7722	1.159262	1.16E-10	Up	3.92E-12
BOX15_Mlig019733g3	2491	267.8937	598.0346	1.158568	1.03E-15	Up	2.11E-17
BOX15_Mlig008661g1	1851	156.5334	349.4285	1.158527	5.07E-16	Up	1.01E-17
BOX15_Mlig007866g1	1933	364.7975	813.7222	1.15744	2.57E-20	Up	3.67E-22
BOX15_Mlig025293g1	5711	447.9841	999.1844	1.157304	9.46E-15	Up	2.09E-16
BOX15_Mlig014943g1	2450	88.64426	197.6924	1.157158	1.44E-06	Up	9.11E-08
BOX15_Mlig022079g1	2897	89.03404	198.4991	1.156704	1.50E-08	Up	6.76E-10
BOX15_Mlig021016g3	1671	252.9194	563.345	1.155341	7.16E-06	Up	5.23E-07
BOX15_Mlig011062g3	717	18.84487	41.96554	1.155034	0.019957	Up	0.004195
BOX15_Mlig009419g1	3187	228.103	507.8538	1.154728	3.92E-22	Up	4.91E-24
BOX15_Mlig022034g1	3769	152.3462	339.0569	1.154174	2.07E-18	Up	3.46E-20
BOX15_Mlig015603g1	2150	93.55159	208.0656	1.153204	5.44E-08	Up	2.69E-09
BOX15_Mlig005308g3	1805	149.8708	333.2762	1.152999	7.12E-13	Up	1.91E-14
BOX15_Mlig021365g2	2596	138.0167	306.8628	1.15275	4.95E-09	Up	2.10E-10

BOX15_Mlig010820g1	2501	199.7175	443.8616	1.152149	4.88E-12	Up	1.43E-13
BOX15_Mlig003123g2	3698	321.6306	714.582	1.151695	1.57E-47	Up	4.70E-50
BOX15_Mlig022818g3	2116	50.80729	112.876	1.151631	7.02E-06	Up	5.12E-07
BOX15_Mlig019584g1	1251	32.07399	71.25472	1.151582	0.000302	Up	3.32E-05
BOX15_Mlig029219g2	3037	129.8745	288.5148	1.151527	2.97E-06	Up	2.01E-07
BOX15_Mlig028140g3	2900	309.9044	688.3461	1.151311	1.30E-33	Up	8.57E-36
BOX15_Mlig017052g1	2433	111.9564	248.5203	1.150426	3.28E-09	Up	1.35E-10
BOX15_Mlig017636g4	728	16.10203	35.73829	1.150228	0.006949	Up	0.00119
BOX15_Mlig022945g1	5103	20.4874	45.45444	1.149684	0.000279	Up	3.03E-05
BOX15_Mlig014588g1	1326	59.28216	131.5242	1.149658	2.41E-11	Up	7.54E-13
BOX15_Mlig001276g4	2383	169.0384	374.6114	1.148044	3.43E-12	Up	9.89E-14
BOX15_Mlig003549g1	27101	2710.152	6004.041	1.14756	2.58E-15	Up	5.50E-17
BOX15_Mlig011493g1	2905	120.4483	266.75	1.147074	1.92E-15	Up	4.04E-17
BOX15_Mlig022723g1	5566	35.46005	78.52743	1.147002	0.001154	Up	0.000151
BOX15_Mlig005814g1	1966	551.4417	1221.16	1.146973	6.84E-15	Up	1.50E-16
BOX15_Mlig020676g2	900	101.3247	224.3617	1.14684	7.22E-07	Up	4.35E-08
BOX15_Mlig018134g1	4039	2380.067	5266.802	1.145925	1.58E-15	Up	3.28E-17
BOX15_Mlig017118g2	6644	87.63457	193.9088	1.145806	1.18E-09	Up	4.56E-11
BOX15_Mlig011447g2	2309	97.75594	216.2613	1.145519	0.000146	Up	1.46E-05
BOX15_Mlig021993g6	2046	39.56846	87.49897	1.144915	1.37E-05	Up	1.06E-06
BOX15_Mlig014551g2	2007	62.12711	137.3577	1.144643	6.07E-10	Up	2.25E-11
BOX15_Mlig010841g2	1109	11.86378	26.22972	1.144639	0.040956	Up	0.010035
BOX15_Mlig012262g1	1842	41.1132	90.8746	1.144275	1.49E-06	Up	9.51E-08
BOX15_Mlig019049g1	647	232.5028	513.8154	1.144002	0.006054	Up	0.001013
BOX15_Mlig004960g1	2574	40.94027	90.44732	1.143557	3.63E-06	Up	2.49E-07
BOX15_Mlig023073g1	2478	21.39094	47.24822	1.14326	0.0005	Up	5.82E-05
BOX15_Mlig017633g1	1625	197.1099	435.157	1.142536	6.83E-20	Up	1.02E-21
BOX15_Mlig003531g1	3308	115.696	255.4196	1.142531	0.02385	Up	0.005204
BOX15_Mlig005162g1	10107	123.8612	273.3987	1.142283	0.000307	Up	3.37E-05
BOX15_Mlig002220g2	5116	424.7129	937.2705	1.141978	7.98E-25	Up	8.31E-27
BOX15_Mlig032022g1	2638	88.21967	194.4836	1.140476	7.13E-13	Up	1.92E-14
BOX15_Mlig015476g1	3087	87.69275	193.1713	1.139352	6.52E-16	Up	1.31E-17
BOX15_Mlig024423g1	2172	60.97972	134.2581	1.138607	6.63E-05	Up	6.08E-06
BOX15_Mlig008391g3	13147	12.48082	27.44264	1.136707	0.021005	Up	0.004461
BOX15_Mlig027363g3	1228	55.96489	123.0134	1.136222	0.000218	Up	2.29E-05
BOX15_Mlig018122g5	5453	594.7599	1307.185	1.136084	8.04E-32	Up	5.71E-34
BOX15_Mlig018615g1	2423	62.12475	136.4409	1.135036	1.42E-07	Up	7.54E-09
BOX15_Mlig034435g1	2017	213.5211	468.778	1.134526	1.96E-10	Up	6.76E-12
BOX15_Mlig029238g1	3017	156.5801	343.603	1.133841	1.08E-09	Up	4.14E-11
BOX15_Mlig021935g2	3628	18.65736	40.93909	1.133734	0.002029	Up	0.000285
BOX15_Mlig002934g1	2811	218.8565	479.967	1.13295	3.74E-10	Up	1.34E-11
BOX15_Mlig007719g1	1183	89.10456	195.3492	1.132484	1.66E-05	Up	1.31E-06

BOX15_Mlig022009g4	2040	99.23501	217.4955	1.132065	9.83E-15	Up	2.18E-16
BOX15_Mlig001947g6	6981	98.9178	216.793	1.132016	3.73E-10	Up	1.33E-11
BOX15_Mlig015529g1	1245	35.89073	78.65623	1.13195	9.23E-05	Up	8.76E-06
BOX15_Mlig026804g1	4104	56.63529	124.1145	1.131898	0.000214	Up	2.25E-05
BOX15_Mlig025890g1	940	1575.297	3451.874	1.131756	0.001552	Up	0.00021
BOX15_Mlig023357g4	2135	42.68731	93.52606	1.131561	0.00177	Up	0.000244
BOX15_Mlig026523g4	1724	35.21001	77.14014	1.131496	0.032642	Up	0.007605
BOX15_Mlig009450g3	1028	43.90754	96.1427	1.130709	9.03E-07	Up	5.54E-08
BOX15_Mlig015349g2	1257	342.2195	749.2782	1.13058	9.81E-43	Up	3.95E-45
BOX15_Mlig006291g1	4019	1580.828	3461.088	1.130545	2.90E-26	Up	2.77E-28
BOX15_Mlig019702g1	2339	52.17066	114.1003	1.128992	8.19E-08	Up	4.18E-09
BOX15_Mlig031078g1	2990	80.83658	176.7913	1.128967	1.78E-08	Up	8.12E-10
BOX15_Mlig010573g2	1358	29.74191	65.02259	1.128444	0.001623	Up	0.000221
BOX15_Mlig032906g3	3048	17.5879	38.39342	1.126276	0.00466	Up	0.000747
BOX15_Mlig001276g6	2428	122.6956	267.8059	1.126105	1.94E-07	Up	1.06E-08
BOX15_Mlig008937g3	3338	183.7737	400.9304	1.125421	3.21E-09	Up	1.32E-10
BOX15_Mlig017046g1	1956	34.98584	76.24203	1.123815	1.61E-06	Up	1.03E-07
BOX15_Mlig009071g1	3162	166.53	362.7676	1.123264	0.005648	Up	0.000934
BOX15_Mlig034375g1	3189	46.05945	100.3287	1.123165	1.80E-06	Up	1.16E-07
BOX15_Mlig007219g1	4371	451.1515	982.1544	1.122338	2.58E-41	Up	1.15E-43
BOX15_Mlig002153g8	3989	509.7201	1109.276	1.121841	2.21E-29	Up	1.79E-31
BOX15_Mlig023151g1	1306	65.79279	143.1809	1.121838	8.30E-10	Up	3.12E-11
BOX15_Mlig022012g1	5073	22.85911	49.73963	1.121626	0.04706	Up	0.011875
BOX15_Mlig006420g1	3205	7.125036	15.48538	1.119937	0.035995	Up	0.008578
BOX15_Mlig017637g2	3858	255.4198	555.114	1.119914	7.01E-09	Up	3.03E-10
BOX15_Mlig031246g1	1133	7.055796	15.32966	1.119445	0.036759	Up	0.008794
BOX15_Mlig014642g1	1604	79.0151	171.5548	1.118469	7.84E-05	Up	7.33E-06
BOX15_Mlig029607g3	2212	28.07171	60.92564	1.117932	0.000288	Up	3.14E-05
BOX15_Mlig015667g1	1938	143.2992	310.7961	1.116938	3.77E-16	Up	7.44E-18
BOX15_Mlig023897g3	1842	87.90908	190.5059	1.115752	0.002571	Up	0.000374
BOX15_Mlig030680g1	1709	967.0458	2094.809	1.115163	0.024538	Up	0.005389
BOX15_Mlig022065g1	2883	34.1154	73.88595	1.114877	5.70E-05	Up	5.11E-06
BOX15_Mlig003079g5	2102	15.96444	34.55856	1.114182	0.047603	Up	0.012048
BOX15_Mlig003079g6	2102	15.96444	34.55856	1.114182	0.047603	Up	0.012048
BOX15_Mlig006367g1	6815	643.2111	1392.116	1.113915	5.71E-09	Up	2.44E-10
BOX15_Mlig029626g1	1475	219.1227	473.7021	1.112241	0.005964	Up	0.000994
BOX15_Mlig028548g2	2967	15.64665	33.8138	1.111758	0.022795	Up	0.004925
BOX15_Mlig031867g3	3996	54.61051	117.9812	1.111306	1.27E-06	Up	7.97E-08
BOX15_Mlig030616g2	2454	23.83952	51.4874	1.110864	0.000178	Up	1.83E-05
BOX15_Mlig024116g1	2273	226.9996	490.0309	1.110183	6.79E-10	Up	2.53E-11
BOX15_Mlig018513g1	3695	13.24922	28.59838	1.110026	0.010541	Up	0.00195
BOX15_Mlig014772g2	2366	343.3005	740.5923	1.109208	5.25E-07	Up	3.08E-08

BOX15_Mlig024828g5	3655	48.17792	103.901	1.108766	0.001484	Up	0.0002
BOX15_Mlig016524g1	2778	128.5685	277.2611	1.108708	1.81E-15	Up	3.79E-17
BOX15_Mlig027489g2	4455	95.65845	206.2474	1.108412	1.44E-10	Up	4.92E-12
BOX15_Mlig016146g2	5178	136.5945	294.4243	1.107997	1.19E-12	Up	3.28E-14
BOX15_Mlig001638g5	970	172.3273	371.1838	1.106982	8.68E-11	Up	2.88E-12
BOX15_Mlig021993g2	1885	85.96765	185.0936	1.106389	6.10E-11	Up	1.99E-12
BOX15_Mlig012082g1	3223	26.5453	57.1526	1.106363	0.000119	Up	1.17E-05
BOX15_Mlig016904g2	3091	112.2005	241.3353	1.10496	6.58E-09	Up	2.83E-10
BOX15_Mlig019284g2	2758	133.024	285.9547	1.104101	5.55E-10	Up	2.04E-11
BOX15_Mlig004757g3	2317	79.27329	170.1346	1.10177	0.031578	Up	0.007309
BOX15_Mlig014424g2	4858	79.68506	170.9296	1.101021	7.47E-06	Up	5.47E-07
BOX15_Mlig005308g1	1804	141.0287	302.3976	1.100457	4.98E-08	Up	2.45E-09
BOX15_Mlig014544g2	2019	146.5521	314.1874	1.100212	0.00028	Up	3.05E-05
BOX15_Mlig006964g2	1983	228.1931	488.9504	1.099433	0.018057	Up	0.003715
BOX15_Mlig007529g1	2639	67.69091	144.9721	1.098741	0.001721	Up	0.000236
BOX15_Mlig021785g1	1277	73.02091	156.1724	1.096758	1.67E-08	Up	7.61E-10
BOX15_Mlig030083g3	9403	63.13458	135.0165	1.096634	4.88E-06	Up	3.45E-07
BOX15_Mlig021461g1	3891	92.43215	197.5	1.095386	7.14E-11	Up	2.34E-12
BOX15_Mlig003190g1	2703	396.0205	845.7876	1.09472	3.44E-12	Up	9.92E-14
BOX15_Mlig023302g3	4002	566.8996	1210.394	1.094312	1.32E-24	Up	1.40E-26
BOX15_Mlig004935g1	1630	150.6224	321.5738	1.094214	0.01919	Up	0.004001
BOX15_Mlig021027g1	5995	413.0233	881.5875	1.093881	1.47E-21	Up	1.92E-23
BOX15_Mlig019810g2	4383	70.70428	150.9091	1.09381	3.00E-11	Up	9.50E-13
BOX15_Mlig021365g1	2691	93.90778	200.41	1.093638	0.000225	Up	2.37E-05
BOX15_Mlig026500g2	1693	213.072	454.6202	1.093321	4.61E-11	Up	1.49E-12
BOX15_Mlig001339g1	2253	37.06039	79.06675	1.093193	0.003085	Up	0.000462
BOX15_Mlig018021g1	2962	27.63376	58.94615	1.092966	5.41E-05	Up	4.84E-06
BOX15_Mlig020467g2	3985	127.2139	271.3115	1.092694	4.30E-10	Up	1.56E-11
BOX15_Mlig017118g1	2179	68.0746	145.1123	1.091981	2.46E-06	Up	1.63E-07
BOX15_Mlig027034g2	1489	23.40342	49.85696	1.091076	0.000423	Up	4.84E-05
BOX15_Mlig033274g3	1204	58.19677	123.9523	1.090774	2.04E-06	Up	1.33E-07
BOX15_Mlig014460g2	1384	17.92661	38.172	1.090412	0.001225	Up	0.000161
BOX15_Mlig000951g1	2068	163.6521	348.4052	1.090134	4.93E-08	Up	2.42E-09
BOX15_Mlig021593g2	3254	406.8792	866.0563	1.08986	3.35E-13	Up	8.60E-15
BOX15_Mlig000289g1	3586	109.898	233.7263	1.088655	8.67E-09	Up	3.81E-10
BOX15_Mlig006405g1	1381	17.96117	38.17292	1.087669	0.006512	Up	0.001104
BOX15_Mlig012100g1	2002	177.4771	377.1776	1.087611	1.36E-15	Up	2.81E-17
BOX15_Mlig014467g2	2039	351.5287	747.0172	1.087499	9.00E-21	Up	1.24E-22
BOX15_Mlig030864g1	2922	154.7568	328.7988	1.087202	1.87E-12	Up	5.27E-14
BOX15_Mlig002873g1	2348	33.95679	72.13715	1.087042	0.000366	Up	4.12E-05
BOX15_Mlig018518g1	3214	349.9447	743.3295	1.086875	1.48E-13	Up	3.66E-15
BOX15_Mlig029766g2	2416	56.60673	120.2297	1.086748	1.60E-07	Up	8.58E-09

BOX15_Mlig012838g10	4735	188.4656	400.2577	1.086628	1.22E-05	Up	9.35E-07
BOX15_Mlig034005g2	3314	151.0521	320.7676	1.086482	4.39E-11	Up	1.41E-12
BOX15_Mlig026754g1	2250	459.5842	975.7951	1.086249	5.03E-23	Up	6.00E-25
BOX15_Mlig033488g3	8770	258.6327	548.9399	1.085743	2.68E-16	Up	5.20E-18
BOX15_Mlig025647g1	5911	190.4668	404.178	1.085452	9.03E-21	Up	1.25E-22
BOX15_Mlig024764g3	6528	526.1194	1116.329	1.0853	2.32E-13	Up	5.88E-15
BOX15_Mlig022376g1	2132	227.827	482.8741	1.083708	9.85E-15	Up	2.19E-16
BOX15_Mlig024448g1	2886	111.7317	236.7632	1.083406	6.25E-12	Up	1.85E-13
BOX15_Mlig003980g1	3484	16.20341	34.31781	1.08266	0.003608	Up	0.000556
BOX15_Mlig025396g2	1343	216.0968	457.5275	1.082181	5.05E-06	Up	3.58E-07
BOX15_Mlig033014g1	5374	233.2965	493.5833	1.081129	6.19E-10	Up	2.29E-11
BOX15_Mlig019728g1	3895	379.8206	803.365	1.080738	7.62E-09	Up	3.31E-10
BOX15_Mlig033056g5	1396	109.9819	232.5618	1.080348	6.65E-19	Up	1.06E-20
BOX15_Mlig015105g6	4118	14.21766	30.06042	1.080181	0.006099	Up	0.001022
BOX15_Mlig017571g2	4700	206.1185	435.6224	1.079604	1.12E-24	Up	1.19E-26
BOX15_Mlig022233g1	2016	98.06819	207.208	1.079222	1.35E-13	Up	3.31E-15
BOX15_Mlig014250g1	2945	155.8792	329.2764	1.07887	5.05E-16	Up	1.01E-17
BOX15_Mlig004757g2	2341	84.81222	179.0811	1.078269	4.81E-07	Up	2.80E-08
BOX15_Mlig008209g2	1934	24.29521	51.29548	1.07816	0.025463	Up	0.005638
BOX15_Mlig013502g1	1632	13.98011	29.51105	1.077879	0.015713	Up	0.00314
BOX15_Mlig032168g1	1166	35.73496	75.42278	1.077664	0.000289	Up	3.16E-05
BOX15_Mlig023673g2	2243	126.0429	266.0065	1.077547	3.57E-05	Up	3.04E-06
BOX15_Mlig024864g2	1646	94.57299	199.5846	1.077501	1.31E-15	Up	2.69E-17
BOX15_Mlig024864g1	1646	94.57299	199.5846	1.077501	1.31E-15	Up	2.69E-17
BOX15_Mlig002869g2	1712	57.6882	121.7063	1.077055	5.73E-05	Up	5.14E-06
BOX15_Mlig025351g1	1901	366.6203	773.4097	1.076946	2.95E-12	Up	8.48E-14
BOX15_Mlig021091g4	2251	58.338	123.0638	1.076898	0.005468	Up	0.000899
BOX15_Mlig032346g2	1071	98.74653	208.3019	1.076874	2.38E-10	Up	8.28E-12
BOX15_Mlig008488g4	1434	16.28254	34.34348	1.07671	0.010571	Up	0.001958
BOX15_Mlig022429g2	2096	63.78382	134.5242	1.076603	1.04E-05	Up	7.85E-07
BOX15_Mlig030628g1	3785	45.32323	95.49591	1.075188	1.57E-07	Up	8.38E-09
BOX15_Mlig025564g1	960	526.341	1107.518	1.07326	4.92E-15	Up	1.07E-16
BOX15_Mlig014270g3	5999	14.76678	31.07052	1.073191	0.009469	Up	0.001716
BOX15_Mlig016455g3	929	322.8828	679.3643	1.073175	3.81E-16	Up	7.52E-18
BOX15_Mlig011506g3	2039	59.07901	124.2772	1.072844	2.19E-09	Up	8.80E-11
BOX15_Mlig021091g3	2255	68.01199	143.0399	1.072557	2.67E-07	Up	1.49E-08
BOX15_Mlig032303g1	5419	191.5116	402.5195	1.071627	0.000103	Up	9.94E-06
BOX15_Mlig009760g1	1722	116.1331	244.044	1.071362	1.83E-05	Up	1.45E-06
BOX15_Mlig007205g1	2648	78.16014	164.1764	1.070742	2.00E-07	Up	1.10E-08
BOX15_Mlig023527g5	7037	306.1562	642.4962	1.06942	4.30E-18	Up	7.34E-20
BOX15_Mlig024764g4	6455	765.273	1605.693	1.069149	1.25E-25	Up	1.22E-27
BOX15_Mlig031910g1	4075	42.6155	89.40697	1.069009	2.26E-06	Up	1.49E-07

BOX15_Mlig013239g1	1395	973.8652	2041.99	1.068182	0.039711	Up	0.009656
BOX15_Mlig027532g1	758	36.6357	76.74248	1.066775	0.000191	Up	1.98E-05
BOX15_Mlig027802g1	3983	32.80246	68.7105	1.066727	0.003925	Up	0.000613
BOX15_Mlig015394g1	4398	44.87051	93.97594	1.066524	2.71E-05	Up	2.24E-06
BOX15_Mlig024222g1	6420	24.52625	51.32666	1.065382	0.001027	Up	0.000131
BOX15_Mlig033672g1	2067	66.1244	138.3732	1.06531	4.57E-11	Up	1.47E-12
BOX15_Mlig006684g1	1931	83.19992	174.0295	1.064678	1.18E-06	Up	7.38E-08
BOX15_Mlig016222g2	2075	409.8668	857.1311	1.064361	2.23E-10	Up	7.75E-12
BOX15_Mlig011752g3	8138	610.5581	1276.349	1.063822	8.99E-12	Up	2.71E-13
BOX15_Mlig007505g1	3742	328.4123	686.3277	1.063389	6.08E-28	Up	5.39E-30
BOX15_Mlig023507g2	3767	576.7623	1205.061	1.063057	4.23E-13	Up	1.10E-14
BOX15_Mlig029743g2	3032	71.16792	148.6694	1.062809	0.005888	Up	0.00098
BOX15_Mlig014762g2	2542	13.84153	28.90524	1.062328	0.041288	Up	0.010139
BOX15_Mlig028452g1	4614	11.70817	24.44444	1.061991	0.036259	Up	0.008652
BOX15_Mlig026074g1	1260	20.16212	42.09406	1.061969	0.003019	Up	0.000451
BOX15_Mlig018201g2	2870	106.2869	221.8485	1.061611	3.15E-10	Up	1.12E-11
BOX15_Mlig031546g1	7811	114.8193	239.6363	1.061481	7.62E-09	Up	3.31E-10
BOX15_Mlig027184g1	4574	99.83136	208.347	1.061424	2.53E-06	Up	1.68E-07
BOX15_Mlig023664g3	5220	77.13696	160.9822	1.061407	3.04E-05	Up	2.54E-06
BOX15_Mlig025655g2	2357	222.6695	464.6455	1.061227	2.04E-18	Up	3.41E-20
BOX15_Mlig022272g1	2391	49.2677	102.7849	1.060915	9.16E-09	Up	4.04E-10
BOX15_Mlig030197g3	2649	443.8374	925.6478	1.060432	6.76E-19	Up	1.08E-20
BOX15_Mlig011197g1	2357	436.7883	910.6805	1.060011	2.45E-21	Up	3.25E-23
BOX15_Mlig003811g1	2993	117.4076	244.7777	1.059946	1.25E-10	Up	4.26E-12
BOX15_Mlig007719g3	1186	129.5953	269.8909	1.058363	0.000104	Up	9.96E-06
BOX15_Mlig024946g1	7172	82.89201	172.5244	1.057495	0.000707	Up	8.57E-05
BOX15_Mlig028548g1	2745	15.13022	31.48971	1.057448	0.007961	Up	0.001398
BOX15_Mlig018004g1	4035	44.30582	92.07018	1.055238	8.48E-05	Up	8.00E-06
BOX15_Mlig028309g1	1716	117.6457	244.4362	1.055009	5.34E-10	Up	1.96E-11
BOX15_Mlig029494g1	2240	32.68629	67.9059	1.054852	0.025561	Up	0.005664
BOX15_Mlig024827g2	3462	762.1999	1581.907	1.053423	4.51E-06	Up	3.16E-07
BOX15_Mlig022864g1	2418	66.85282	138.7238	1.053155	0.013366	Up	0.002587
BOX15_Mlig011579g1	486	272.2181	564.8421	1.053085	2.47E-31	Up	1.80E-33
BOX15_Mlig000843g4	2903	123.2402	255.7032	1.052997	9.86E-17	Up	1.83E-18
BOX15_Mlig015936g5	3859	234.8947	487.3606	1.052975	2.37E-16	Up	4.57E-18
BOX15_Mlig013806g2	4354	154.7169	320.8946	1.052469	1.02E-13	Up	2.48E-15
BOX15_Mlig001933g2	4204	1334.483	2765.613	1.051318	6.75E-10	Up	2.51E-11
BOX15_Mlig011721g1	1565	37.4515	77.58116	1.050683	0.003176	Up	0.000478
BOX15_Mlig001622g1	5115	40.94276	84.80289	1.050505	0.000413	Up	4.71E-05
BOX15_Mlig032780g1	2644	342.2709	708.8345	1.05031	8.24E-18	Up	1.43E-19
BOX15_Mlig031616g1	3009	429.8268	889.7896	1.049709	1.21E-45	Up	4.23E-48
BOX15_Mlig012832g1	2090	33.11684	68.51875	1.048934	0.000664	Up	7.99E-05

BOX15_Mlig012588g2	2265	23.53819	48.6989	1.048886	0.016934	Up	0.003437
BOX15_Mlig011852g1	2460	102.4305	211.8824	1.048618	5.42E-09	Up	2.31E-10
BOX15_Mlig027209g1	1920	32.82024	67.86192	1.048016	1.33E-05	Up	1.03E-06
BOX15_Mlig005782g1	2222	86.17977	178.1484	1.047659	1.55E-12	Up	4.33E-14
BOX15_Mlig034354g2	1658	41.12961	84.9807	1.046958	0.000115	Up	1.12E-05
BOX15_Mlig018884g1	3448	60.88118	125.7269	1.046226	1.56E-06	Up	9.96E-08
BOX15_Mlig005716g1	1890	18.23349	37.62542	1.045117	0.004182	Up	0.00066
BOX15_Mlig008110g3	1813	146.6522	302.4634	1.044362	5.70E-07	Up	3.36E-08
BOX15_Mlig017994g1	2405	218.0387	449.5015	1.043742	1.51E-12	Up	4.20E-14
BOX15_Mlig032113g2	4392	919.3509	1894.116	1.042837	8.82E-47	Up	2.83E-49
BOX15_Mlig028575g1	3258	105.51	217.3356	1.042544	1.34E-13	Up	3.30E-15
BOX15_Mlig031246g3	863	14.17364	29.15929	1.040745	0.009442	Up	0.00171
BOX15_Mlig014302g1	6601	205.1436	421.8298	1.040027	1.44E-07	Up	7.64E-09
BOX15_Mlig014424g4	4906	68.11613	139.9706	1.039055	9.01E-06	Up	6.73E-07
BOX15_Mlig014588g2	2534	90.13262	185.1654	1.038693	1.09E-08	Up	4.85E-10
BOX15_Mlig017972g3	4373	499.9377	1026.408	1.037785	9.22E-20	Up	1.39E-21
BOX15_Mlig022639g1	1412	66.58033	136.6514	1.037333	0.003957	Up	0.000619
BOX15_Mlig012789g4	2984	62.04611	127.339	1.037261	1.07E-05	Up	8.09E-07
BOX15_Mlig033932g2	4999	541.6655	1110.843	1.03618	2.52E-36	Up	1.42E-38
BOX15_Mlig029614g2	2363	40.97294	83.98521	1.035464	1.17E-05	Up	8.92E-07
BOX15_Mlig023435g1	5570	9.136291	18.71762	1.034716	0.04894	Up	0.012474
BOX15_Mlig005694g1	2190	191.1353	391.5647	1.034657	2.91E-07	Up	1.63E-08
BOX15_Mlig010543g1	2852	451.5792	925.045	1.034545	7.70E-43	Up	3.09E-45
BOX15_Mlig006979g1	2233	54.60267	111.8512	1.034538	0.000279	Up	3.02E-05
BOX15_Mlig000742g1	3550	96.20787	196.9498	1.033601	4.90E-11	Up	1.58E-12
BOX15_Mlig019303g2	3341	48.13638	98.46638	1.032504	7.12E-06	Up	5.19E-07
BOX15_Mlig028662g1	2864	147.2428	300.7542	1.030388	1.73E-10	Up	5.95E-12
BOX15_Mlig008110g4	2267	152.2681	310.9513	1.030075	1.14E-15	Up	2.32E-17
BOX15_Mlig028619g1	3780	559.3016	1141.678	1.029458	2.26E-19	Up	3.50E-21
BOX15_Mlig017637g3	3853	301.4145	615.0692	1.029	0.00602	Up	0.001006
BOX15_Mlig029351g2	2430	85.96707	175.3989	1.028784	4.61E-09	Up	1.95E-10
BOX15_Mlig007658g2	492	43.10608	87.94763	1.028753	0.001185	Up	0.000155
BOX15_Mlig003377g1	3449	182.2299	371.7417	1.028541	1.81E-10	Up	6.23E-12
BOX15_Mlig007863g4	3188	291.8001	595.039	1.028004	2.38E-10	Up	8.30E-12
BOX15_Mlig011169g1	1090	70.11883	142.9642	1.02778	9.19E-08	Up	4.73E-09
BOX15_Mlig028362g1	1837	78.8546	160.7552	1.027598	3.46E-09	Up	1.43E-10
BOX15_Mlig023455g1	2772	216.6782	441.7202	1.027579	1.69E-10	Up	5.78E-12
BOX15_Mlig025215g2	2506	104.3608	212.5211	1.026026	6.27E-07	Up	3.73E-08
BOX15_Mlig002093g11	8355	214.4219	436.5352	1.025645	8.74E-08	Up	4.48E-09
BOX15_Mlig004342g2	2749	285.0526	580.321	1.025623	4.02E-07	Up	2.30E-08
BOX15_Mlig026583g1	1044	81.43905	165.7495	1.025212	8.12E-11	Up	2.68E-12
BOX15_Mlig033781g1	5014	279.675	568.8297	1.024245	2.33E-26	Up	2.22E-28

BOX15_Mlig027769g2	691	112.8658	229.5355	1.024108	2.33E-11	Up	7.27E-13
BOX15_Mlig006562g2	1822	244.5654	497.2513	1.023755	1.41E-23	Up	1.63E-25
BOX15_Mlig013428g2	954	76.53312	155.4758	1.022534	2.75E-09	Up	1.12E-10
BOX15_Mlig033399g2	5340	470.0479	954.6879	1.022221	1.36E-25	Up	1.34E-27
BOX15_Mlig003517g1	6341	42.6663	86.64007	1.021937	1.41E-05	Up	1.09E-06
BOX15_Mlig016200g3	3636	244.0042	495.4028	1.021696	4.10E-12	Up	1.19E-13
BOX15_Mlig003689g1	2953	523.6473	1061.847	1.019909	5.34E-33	Up	3.66E-35
BOX15_Mlig003493g1	1497	25.41214	51.51902	1.019587	0.000812	Up	0.000101
BOX15_Mlig034212g2	2475	162.6029	329.5591	1.019184	3.94E-05	Up	3.39E-06
BOX15_Mlig020874g1	4357	200.3094	405.9654	1.019127	4.33E-13	Up	1.13E-14
BOX15_Mlig003811g2	3155	216.7049	439.0476	1.018646	2.44E-15	Up	5.19E-17
BOX15_Mlig004041g2	2648	147.3846	298.5321	1.0183	2.05E-16	Up	3.90E-18
BOX15_Mlig025396g1	1798	151.5464	306.9048	1.018032	9.04E-06	Up	6.76E-07
BOX15_Mlig025564g2	971	215.483	436.3589	1.017941	4.20E-08	Up	2.04E-09
BOX15_Mlig008333g1	2983	36.22694	73.32856	1.017312	6.81E-05	Up	6.27E-06
BOX15_Mlig000615g1	3716	20.452	41.35811	1.015929	0.009556	Up	0.001736
BOX15_Mlig024197g1	3325	28.70901	58.04729	1.015725	0.006882	Up	0.001176
BOX15_Mlig003483g1	2080	75.04124	151.7168	1.015626	0.000286	Up	3.12E-05
BOX15_Mlig002898g1	1834	18.9431	38.28814	1.015225	0.005547	Up	0.000914
BOX15_Mlig018615g3	2425	43.82791	88.52036	1.01416	0.000437	Up	5.02E-05
BOX15_Mlig002073g2	2816	88.87788	179.4352	1.013566	7.11E-10	Up	2.66E-11
BOX15_Mlig008362g1	4063	377.4844	762.0451	1.013459	5.60E-11	Up	1.82E-12
BOX15_Mlig019450g1	2561	90.118	181.8818	1.013114	2.42E-08	Up	1.13E-09
BOX15_Mlig034453g1	2769	40.47621	81.68083	1.012923	0.000357	Up	4.01E-05
BOX15_Mlig017538g1	2181	328.4284	662.6767	1.012726	5.18E-25	Up	5.34E-27
BOX15_Mlig002367g1	861	309.9422	625.3524	1.01267	4.48E-24	Up	4.93E-26
BOX15_Mlig028619g9	3780	468.1733	944.2002	1.01205	2.93E-31	Up	2.16E-33
BOX15_Mlig029434g3	2731	103.1497	207.868	1.010927	3.53E-09	Up	1.46E-10
BOX15_Mlig024937g2	3592	377.1211	759.9249	1.010829	2.75E-17	Up	4.93E-19
BOX15_Mlig007135g1	3332	52.05584	104.7789	1.009216	1.22E-06	Up	7.63E-08
BOX15_Mlig026365g1	2525	121.726	245.0012	1.009151	6.14E-14	Up	1.46E-15
BOX15_Mlig028998g1	2732	60.78291	122.3206	1.00893	0.00049	Up	5.69E-05
BOX15_Mlig030791g1	4253	359.6369	722.9989	1.007453	4.89E-16	Up	9.73E-18
BOX15_Mlig011284g1	8775	139.9387	281.3165	1.0074	8.12E-12	Up	2.43E-13
BOX15_Mlig017756g3	2401	49.70192	99.87469	1.006817	0.000109	Up	1.06E-05
BOX15_Mlig012219g1	1940	69.53611	139.6544	1.006026	2.92E-05	Up	2.43E-06
BOX15_Mlig026026g2	1584	210.1474	421.9919	1.005814	7.58E-25	Up	7.88E-27
BOX15_Mlig005468g1	10437	333.1533	668.9244	1.005657	4.43E-20	Up	6.54E-22
BOX15_Mlig032526g3	3350	2634.909	5287.887	1.004938	4.99E-31	Up	3.74E-33
BOX15_Mlig007371g1	2352	419.3355	841.529	1.004908	4.28E-18	Up	7.28E-20
BOX15_Mlig021174g1	6958	238.0359	477.642	1.004751	2.78E-06	Up	1.87E-07
BOX15_Mlig034331g4	1884	38.9637	78.17294	1.004539	2.91E-05	Up	2.42E-06

BOX15_Mlig014068g1	2637	238.654	478.7228	1.00427	1.58E-17	Up	2.80E-19
BOX15_Mlig017972g1	4371	601.0221	1205.374	1.003991	1.68E-19	Up	2.59E-21
BOX15_Mlig024827g1	3223	1296.374	2599.166	1.003567	1.08E-08	Up	4.81E-10
BOX15_Mlig013806g1	4370	462.6728	927.3799	1.003168	3.24E-29	Up	2.65E-31
BOX15_Mlig032985g2	2285	664.2426	1330.695	1.002398	3.88E-10	Up	1.40E-11
BOX15_Mlig029779g1	1440	132.8074	265.9232	1.001674	1.84E-15	Up	3.85E-17
BOX15_Mlig022903g3	28266	496.0995	992.5947	1.000575	5.54E-24	Up	6.17E-26
BOX15_Mlig014609g2	4012	88.20038	176.448	1.000386	5.04E-10	Up	1.85E-11
BOX15_Mlig007703g1	5955	132.3978	66.17935	-1.000426	1.04E-08	Down	4.63E-10
BOX15_Mlig031752g3	1502	125.5713	62.75604	-1.000681	9.38E-06	Down	7.03E-07
BOX15_Mlig016558g1	1920	94.00686	46.97995	-1.000721	0.000108	Down	1.04E-05
BOX15_Mlig026070g1	6142	324.6697	162.2514	-1.000741	7.59E-08	Down	3.86E-09
BOX15_Mlig006456g1	3279	135.2558	67.57905	-1.001042	0.002855	Down	0.000422
BOX15_Mlig001527g1	1311	113.1967	56.54801	-1.001284	6.19E-05	Down	5.63E-06
BOX15_Mlig026767g2	2099	87.59676	43.75826	-1.001322	0.000928	Down	0.000117
BOX15_Mlig005938g3	929	20.75408	10.3668	-1.001425	0.048435	Down	0.012316
BOX15_Mlig020397g1	4845	293.5525	146.6239	-1.001499	3.77E-12	Down	1.09E-13
BOX15_Mlig017303g1	2170	229.8507	114.7046	-1.002774	3.40E-05	Down	2.87E-06
BOX15_Mlig019522g3	4245	302.4218	150.9076	-1.002897	3.16E-09	Down	1.30E-10
BOX15_Mlig014701g1	1522	60.59104	30.21259	-1.003955	0.000737	Down	9.00E-05
BOX15_Mlig029592g1	771	138.7477	69.18159	-1.004004	2.39E-06	Down	1.58E-07
BOX15_Mlig007461g2	4211	44.11283	21.99108	-1.00428	0.004657	Down	0.000747
BOX15_Mlig021431g1	1596	99.32543	49.50395	-1.004619	0.005723	Down	0.000948
BOX15_Mlig015604g3	1471	96.51342	48.07281	-1.005508	0.00629	Down	0.001061
BOX15_Mlig031755g2	2130	1023.071	509.4525	-1.005887	5.38E-34	Down	3.48E-36
BOX15_Mlig013365g1	1124	32.99483	16.42041	-1.00675	0.005399	Down	0.000886
BOX15_Mlig020479g1	894	6953.839	3458.985	-1.007461	2.39E-25	Down	2.39E-27
BOX15_Mlig025862g1	1944	311.808	154.9927	-1.008457	7.00E-10	Down	2.61E-11
BOX15_Mlig013020g1	1892	2479.768	1232.44	-1.008687	4.07E-42	Down	1.69E-44
BOX15_Mlig024873g1	2231	72.8588	36.18893	-1.009555	6.90E-05	Down	6.37E-06
BOX15_Mlig002330g5	1396	182.0781	90.37991	-1.010483	4.78E-06	Down	3.37E-07
BOX15_Mlig030927g1	937	39.52365	19.61859	-1.010495	0.020048	Down	0.004217
BOX15_Mlig002886g1	1484	226.1263	112.1702	-1.01144	1.09E-09	Down	4.17E-11
BOX15_Mlig008387g1	2557	2491.544	1235.773	-1.011626	5.19E-46	Down	1.77E-48
BOX15_Mlig032862g2	1791	46.81016	23.21626	-1.011686	0.025445	Down	0.005631
BOX15_Mlig028647g9	2370	525.1177	260.4252	-1.011772	4.24E-11	Down	1.36E-12
BOX15_Mlig003773g3	1358	318.4984	157.8245	-1.012965	4.56E-11	Down	1.47E-12
BOX15_Mlig012700g1	860	231.5097	114.699	-1.01322	0.001054	Down	0.000135
BOX15_Mlig032068g4	466	391.7611	194.0763	-1.01335	7.06E-13	Down	1.89E-14
BOX15_Mlig026681g1	781	195.8446	96.99644	-1.013706	1.00E-06	Down	6.21E-08
BOX15_Mlig016804g3	2326	1869.676	925.8752	-1.013899	4.79E-40	Down	2.24E-42
BOX15_Mlig021137g1	2984	1305.715	646.3728	-1.014402	6.29E-10	Down	2.33E-11

BOX15_Mlig028497g1	687	312.9795	154.9261	-1.014488	2.26E-19	Down	3.51E-21
BOX15_Mlig024275g2	2770	53.42933	26.44472	-1.014652	0.004879	Down	0.000788
BOX15_Mlig029702g1	4980	1633.051	808.1441	-1.014885	0.002142	Down	0.000304
BOX15_Mlig022761g1	7009	90.41123	44.7167	-1.015688	0.000883	Down	0.00011
BOX15_Mlig030280g1	2451	74.23337	36.6958	-1.016453	4.08E-06	Down	2.83E-07
BOX15_Mlig011554g1	1192	52.01564	25.71095	-1.016562	0.001477	Down	0.000199
BOX15_Mlig016970g1	2691	1628.04	804.0838	-1.017718	3.19E-40	Down	1.47E-42
BOX15_Mlig004668g2	2363	31.16499	15.38796	-1.018125	0.018183	Down	0.003746
BOX15_Mlig030146g3	1964	64.99491	32.08813	-1.018287	0.002514	Down	0.000365
BOX15_Mlig009593g1	430	1061.1	523.8552	-1.01832	2.66E-05	Down	2.19E-06
BOX15_Mlig029451g1	2182	644.0417	317.8576	-1.018774	4.43E-06	Down	3.09E-07
BOX15_Mlig000583g11	2559	292.5652	144.3514	-1.019173	5.28E-14	Down	1.25E-15
BOX15_Mlig020806g1	1193	347.6978	171.5304	-1.01937	3.72E-08	Down	1.79E-09
BOX15_Mlig002585g1	2084	76.88073	37.91726	-1.019767	0.000283	Down	3.08E-05
BOX15_Mlig032142g1	790	71.26361	35.14026	-1.020041	0.004676	Down	0.00075
BOX15_Mlig032899g1	2088	98.66046	48.6446	-1.020192	0.000202	Down	2.11E-05
BOX15_Mlig030980g1	1812	370.1869	182.4132	-1.021044	1.03E-05	Down	7.74E-07
BOX15_Mlig020696g1	1180	34.06648	16.77996	-1.021614	0.008593	Down	0.001529
BOX15_Mlig034188g1	1114	321.0147	158.082	-1.021967	1.09E-09	Down	4.17E-11
BOX15_Mlig005044g1	5283	255.8588	125.9785	-1.02217	7.09E-09	Down	3.07E-10
BOX15_Mlig029545g1	2669	3092.166	1521.704	-1.02293	1.40E-40	Down	6.36E-43
BOX15_Mlig005197g2	1781	77.93164	38.34159	-1.023299	0.021693	Down	0.004645
BOX15_Mlig010329g4	2562	740.5663	364.3276	-1.023393	2.13E-12	Down	6.03E-14
BOX15_Mlig025383g2	3416	447.4618	220.0616	-1.023857	2.55E-12	Down	7.28E-14
BOX15_Mlig021280g2	1315	26.64778	13.10324	-1.024092	0.033823	Down	0.007955
BOX15_Mlig015876g3	2584	35.5506	17.47704	-1.024413	0.014866	Down	0.002937
BOX15_Mlig031752g1	1516	86.39146	42.46715	-1.024541	0.002945	Down	0.000438
BOX15_Mlig014564g2	1241	65.7196	32.29851	-1.024856	0.000711	Down	8.63E-05
BOX15_Mlig020221g2	478	540.7902	265.701	-1.025265	0.0002	Down	2.08E-05
BOX15_Mlig015396g1	1113	90.53111	44.46544	-1.025729	5.29E-05	Down	4.71E-06
BOX15_Mlig012489g3	1017	965.4465	474.14	-1.025883	1.57E-08	Down	7.14E-10
BOX15_Mlig029424g2	1458	196.4856	96.47736	-1.026161	1.40E-08	Down	6.33E-10
BOX15_Mlig017435g1	2412	461.2974	226.4861	-1.026274	7.36E-09	Down	3.20E-10
BOX15_Mlig005390g3	2766	163.9235	80.45782	-1.026718	9.92E-10	Down	3.77E-11
BOX15_Mlig028147g2	1923	130.3505	63.96157	-1.027119	0.004155	Down	0.000655
BOX15_Mlig008500g1	1428	25.43071	12.47337	-1.02772	0.017918	Down	0.003679
BOX15_Mlig022496g1	1332	23.36427	11.45699	-1.028075	0.014082	Down	0.002754
BOX15_Mlig013227g1	1245	102.3551	50.16591	-1.028804	2.53E-07	Down	1.41E-08
BOX15_Mlig004012g2	3229	117.9506	57.80403	-1.028941	1.89E-08	Down	8.67E-10
BOX15_Mlig029040g1	5079	495.0674	242.6112	-1.028979	1.94E-08	Down	8.91E-10
BOX15_Mlig030184g1	3010	121.9478	59.7385	-1.029531	1.03E-05	Down	7.79E-07
BOX15_Mlig018047g1	1624	42.68602	20.90865	-1.029663	0.019623	Down	0.004109

BOX15_Mlig028724g2	1474	51.21525	25.08357	-1.029831	0.020268	Down	0.004274
BOX15_Mlig003720g1	3064	62.58731	30.64447	-1.030243	0.000292	Down	3.19E-05
BOX15_Mlig029931g1	2451	1241.959	608.0972	-1.030244	0.021927	Down	0.004704
BOX15_Mlig018970g1	3021	292.1699	142.9689	-1.031106	1.92E-06	Down	1.25E-07
BOX15_Mlig009645g2	2765	48.84888	23.90314	-1.031125	0.004115	Down	0.000647
BOX15_Mlig024012g1	1440	620.9065	303.7895	-1.031304	4.69E-06	Down	3.29E-07
BOX15_Mlig031613g1	1105	109.9405	53.77758	-1.031646	0.000238	Down	2.53E-05
BOX15_Mlig025916g1	2465	370.0327	180.9965	-1.031691	3.19E-13	Down	8.19E-15
BOX15_Mlig003975g1	1965	157.8608	77.19021	-1.032163	0.002442	Down	0.000352
BOX15_Mlig010693g4	1038	145.7001	71.24217	-1.032199	2.59E-06	Down	1.73E-07
BOX15_Mlig026388g1	1705	112.9823	55.21123	-1.033063	6.08E-05	Down	5.51E-06
BOX15_Mlig015185g2	1312	133.2044	65.08201	-1.033311	1.51E-09	Down	5.89E-11
BOX15_Mlig026732g2	2970	65.76533	32.12899	-1.033452	3.48E-05	Down	2.96E-06
BOX15_Mlig010335g4	2569	827.0352	403.9645	-1.03372	1.93E-07	Down	1.06E-08
BOX15_Mlig006242g1	1086	188.2351	91.93748	-1.033811	1.47E-07	Down	7.86E-09
BOX15_Mlig009261g2	686	111.4855	54.44204	-1.034063	5.54E-05	Down	4.97E-06
BOX15_Mlig011797g1	1075	38.54926	18.82461	-1.034083	0.003278	Down	0.000496
BOX15_Mlig027771g1	2422	66.21187	32.3124	-1.035002	0.000192	Down	1.99E-05
BOX15_Mlig017770g1	1532	21.41628	10.4486	-1.035398	0.033471	Down	0.007848
BOX15_Mlig006970g2	1308	72.34715	35.2826	-1.035979	9.03E-05	Down	8.55E-06
BOX15_Mlig022973g1	658	80.31318	39.16751	-1.03598	5.38E-07	Down	3.17E-08
BOX15_Mlig033498g1	3100	92.41086	45.05915	-1.036242	3.96E-05	Down	3.41E-06
BOX15_Mlig013855g1	5384	1100.181	536.1916	-1.03692	1.31E-08	Down	5.87E-10
BOX15_Mlig016089g1	741	1294.25	630.6865	-1.037121	2.73E-06	Down	1.84E-07
BOX15_Mlig025142g3	1571	1160.364	565.2924	-1.037509	1.17E-22	Down	1.43E-24
BOX15_Mlig020207g2	945	63.2284	30.79884	-1.037697	0.000991	Down	0.000126
BOX15_Mlig011372g2	1502	244.3725	119.0058	-1.03805	1.01E-14	Down	2.24E-16
BOX15_Mlig034188g2	1121	258.77	126.0165	-1.038057	1.61E-11	Down	4.98E-13
BOX15_Mlig032487g1	2124	2155.626	1049.454	-1.038468	0.029166	Down	0.006629
BOX15_Mlig029881g1	2940	41.50887	20.19912	-1.039127	0.033512	Down	0.007862
BOX15_Mlig021889g3	1298	55.49115	26.99671	-1.039474	0.00791	Down	0.001387
BOX15_Mlig002313g1	2949	30.14124	14.66116	-1.03974	0.008749	Down	0.001561
BOX15_Mlig025801g1	3024	69.50865	33.80883	-1.039792	0.001321	Down	0.000176
BOX15_Mlig012147g1	918	123.9653	60.28061	-1.04017	1.09E-06	Down	6.74E-08
BOX15_Mlig007568g1	2377	96.41728	46.85375	-1.041127	0.013945	Down	0.002724
BOX15_Mlig030686g1	3678	81.1363	39.4236	-1.041288	0.000318	Down	3.51E-05
BOX15_Mlig016330g1	909	38.23981	18.57733	-1.041532	0.012679	Down	0.00243
BOX15_Mlig029578g3	811	60.7733	29.52393	-1.041553	0.00156	Down	0.000212
BOX15_Mlig006599g1	1283	134.0106	65.07916	-1.042079	0.000206	Down	2.16E-05
BOX15_Mlig029333g1	2755	217.8063	105.7715	-1.042095	2.41E-10	Down	8.42E-12
BOX15_Mlig008343g1	2391	257.281	124.9329	-1.042191	3.47E-07	Down	1.97E-08
BOX15_Mlig013211g1	2159	132.8702	64.45819	-1.043582	2.55E-07	Down	1.42E-08

BOX15_Mlig009511g1	1796	142.5597	69.15057	-1.043753	1.39E-07	Down	7.37E-09
BOX15_Mlig018792g3	2793	122.1115	59.18332	-1.044936	0.0001	Down	9.59E-06
BOX15_Mlig009876g2	3142	127.4898	61.7771	-1.045238	6.14E-07	Down	3.64E-08
BOX15_Mlig010914g1	1178	414.1963	200.6426	-1.045687	6.52E-22	Down	8.34E-24
BOX15_Mlig022255g1	1963	192.3141	93.10468	-1.046539	2.59E-08	Down	1.22E-09
BOX15_Mlig002888g2	1360	1160.011	561.2684	-1.047376	8.34E-07	Down	5.09E-08
BOX15_Mlig009754g1	4698	68.02729	32.91158	-1.047518	0.000113	Down	1.10E-05
BOX15_Mlig007520g2	2962	26.09278	12.62355	-1.047533	0.044319	Down	0.011046
BOX15_Mlig005808g1	3292	460.5796	222.7533	-1.048003	3.84E-06	Down	2.65E-07
BOX15_Mlig007251g1	1103	127.2446	61.53411	-1.048146	4.17E-08	Down	2.02E-09
BOX15_Mlig025669g2	1498	55.10004	26.62851	-1.049082	0.003331	Down	0.000506
BOX15_Mlig029442g1	610	56.43659	27.27383	-1.049113	0.000424	Down	4.85E-05
BOX15_Mlig012454g1	1218	75.08155	36.27762	-1.049379	1.90E-05	Down	1.51E-06
BOX15_Mlig012508g1	2882	165.9658	80.18879	-1.049414	1.52E-08	Down	6.89E-10
BOX15_Mlig026600g1	2074	785.9299	379.6444	-1.049752	5.26E-16	Down	1.05E-17
BOX15_Mlig015889g1	4378	63.62349	30.72757	-1.050026	0.000106	Down	1.02E-05
BOX15_Mlig034149g1	2189	106.9825	51.66339	-1.050161	2.49E-08	Down	1.17E-09
BOX15_Mlig027095g2	676	94.14638	45.45221	-1.050555	0.007129	Down	0.001227
BOX15_Mlig003525g2	1708	106.979	51.55443	-1.053159	7.82E-09	Down	3.41E-10
BOX15_Mlig027713g1	1942	79.81582	38.46171	-1.053252	0.004508	Down	0.000719
BOX15_Mlig029176g1	1939	127.6475	61.4991	-1.053528	2.70E-08	Down	1.27E-09
BOX15_Mlig000653g5	3228	76.29871	36.69958	-1.055895	0.000574	Down	6.79E-05
BOX15_Mlig030431g2	1908	52.91912	25.45208	-1.056006	0.005343	Down	0.000875
BOX15_Mlig015604g1	1269	249.4422	119.9035	-1.056832	6.70E-17	Down	1.23E-18
BOX15_Mlig025630g1	2221	98.78794	47.46716	-1.057405	6.00E-06	Down	4.32E-07
BOX15_Mlig026783g1	1336	69.68402	33.47812	-1.057609	0.031377	Down	0.007253
BOX15_Mlig033606g2	1003	19.17247	9.210405	-1.0577	0.023971	Down	0.005238
BOX15_Mlig033606g1	1003	19.17247	9.210405	-1.0577	0.023971	Down	0.005238
BOX15_Mlig017709g1	966	215.8823	103.7039	-1.057775	1.69E-07	Down	9.11E-09
BOX15_Mlig004458g1	4364	123.3076	59.22667	-1.057943	5.41E-06	Down	3.85E-07
BOX15_Mlig001780g2	790	24.46307	11.74807	-1.058182	0.018995	Down	0.003953
BOX15_Mlig011172g3	739	63.74213	30.58453	-1.059445	1.13E-05	Down	8.65E-07
BOX15_Mlig011172g1	739	63.74213	30.58453	-1.059445	1.13E-05	Down	8.65E-07
BOX15_Mlig013667g1	4241	173.9929	83.46694	-1.059752	0.001058	Down	0.000136
BOX15_Mlig021015g1	1628	531.1265	254.5028	-1.061374	5.88E-09	Down	2.52E-10
BOX15_Mlig024646g3	2909	86.88141	41.62844	-1.061478	6.12E-06	Down	4.41E-07
BOX15_Mlig016492g2	2284	67.21669	32.18391	-1.06248	0.006608	Down	0.001122
BOX15_Mlig021980g1	3833	4393.763	2103.118	-1.062927	1.24E-71	Down	1.43E-74
BOX15_Mlig017824g2	4975	64.16895	30.71373	-1.062992	0.007468	Down	0.001296
BOX15_Mlig019270g1	1486	54.08256	25.87638	-1.063528	0.004958	Down	0.000803
BOX15_Mlig022826g2	2559	178.8053	85.49566	-1.064466	1.14E-12	Down	3.13E-14
BOX15_Mlig021901g3	745	4088.708	1954.674	-1.064717	1.01E-09	Down	3.85E-11

BOX15_Mlig000939g3	1829	440.9602	210.7806	-1.064907	4.15E-07	Down	2.39E-08
BOX15_Mlig027553g1	816	63.39722	30.30053	-1.065077	0.025424	Down	0.005626
BOX15_Mlig033673g1	2166	55.94455	26.72686	-1.065707	0.002877	Down	0.000426
BOX15_Mlig019754g1	1764	41.29495	19.72515	-1.065929	0.002508	Down	0.000363
BOX15_Mlig018970g2	3005	108.7889	51.9264	-1.066992	6.71E-05	Down	6.16E-06
BOX15_Mlig018560g1	2887	52.42707	25.01716	-1.067394	0.001423	Down	0.000191
BOX15_Mlig012538g1	2525	1750.37	835.0988	-1.067641	0.039955	Down	0.009728
BOX15_Mlig025609g1	3126	33.69931	16.07529	-1.067874	0.011656	Down	0.002197
BOX15_Mlig008601g1	874	4080.905	1946.574	-1.067952	1.68E-59	Down	3.21E-62
BOX15_Mlig028821g4	1043	292.5118	139.4451	-1.068798	4.39E-13	Down	1.14E-14
BOX15_Mlig019794g1	2849	76.76712	36.58888	-1.069083	4.51E-06	Down	3.16E-07
BOX15_Mlig016493g1	1163	60.93246	29.02662	-1.069835	0.009993	Down	0.00183
BOX15_Mlig012538g2	2267	1688.256	803.9969	-1.070271	0.03758	Down	0.009033
BOX15_Mlig001410g2	947	56.34085	26.82961	-1.070355	0.000586	Down	6.95E-05
BOX15_Mlig002485g1	4625	59.94928	28.52743	-1.071392	0.000689	Down	8.34E-05
BOX15_Mlig016859g1	3624	208.2753	99.0431	-1.072363	1.74E-09	Down	6.84E-11
BOX15_Mlig030000g3	1942	117.9478	56.05082	-1.073341	4.10E-05	Down	3.54E-06
BOX15_Mlig032425g2	4915	123.0415	58.43126	-1.074333	0.002376	Down	0.000342
BOX15_Mlig005433g2	1699	212.2869	100.8068	-1.074423	3.85E-09	Down	1.60E-10
BOX15_Mlig028868g1	2112	393.6371	186.8717	-1.074818	9.92E-15	Down	2.21E-16
BOX15_Mlig008161g2	2154	522.0855	247.8477	-1.074832	7.68E-31	Down	5.84E-33
BOX15_Mlig012279g3	959	78.79031	37.34854	-1.076966	1.59E-05	Down	1.25E-06
BOX15_Mlig018622g4	2830	221.2795	104.8735	-1.07722	2.47E-08	Down	1.16E-09
BOX15_Mlig002888g1	1344	900.2031	426.537	-1.07758	1.03E-08	Down	4.54E-10
BOX15_Mlig001660g1	581	10487.41	4968.615	-1.077742	6.11E-12	Down	1.81E-13
BOX15_Mlig012248g2	1586	56.71305	26.86376	-1.078019	0.002962	Down	0.000441
BOX15_Mlig030894g2	2094	122.4341	57.91644	-1.07996	4.65E-05	Down	4.08E-06
BOX15_Mlig028906g1	2406	37.99982	17.97134	-1.080295	0.020526	Down	0.004338
BOX15_Mlig024794g1	1410	52.81078	24.97566	-1.08031	0.00967	Down	0.00176
BOX15_Mlig032068g3	1389	72.38099	34.22913	-1.080386	2.86E-05	Down	2.37E-06
BOX15_Mlig003548g2	2434	55.39538	26.19615	-1.080411	0.01572	Down	0.003142
BOX15_Mlig024813g1	2367	295.8827	139.9173	-1.080451	1.31E-05	Down	1.01E-06
BOX15_Mlig016886g2	1843	24.63641	11.64801	-1.080708	0.01272	Down	0.00244
BOX15_Mlig021407g2	1539	83.66423	39.55259	-1.080839	1.19E-05	Down	9.12E-07
BOX15_Mlig032486g3	2306	1252.505	591.8508	-1.081511	2.86E-23	Down	3.35E-25
BOX15_Mlig023494g1	16517	1900.827	898.0365	-1.081781	3.76E-12	Down	1.09E-13
BOX15_Mlig020105g3	1498	274.6846	129.7256	-1.082313	3.33E-05	Down	2.81E-06
BOX15_Mlig012736g2	3153	83.82191	39.55181	-1.083584	0.00598	Down	0.000998
BOX15_Mlig026257g2	412	162.7035	76.71915	-1.084587	0.000635	Down	7.61E-05
BOX15_Mlig019467g1	1264	115.7963	54.57865	-1.085181	5.26E-05	Down	4.68E-06
BOX15_Mlig015156g2	1599	84.02389	39.58347	-1.085901	4.36E-05	Down	3.79E-06
BOX15_Mlig034181g2	2531	146.9594	69.21106	-1.086343	7.33E-08	Down	3.71E-09

BOX15_Mlig025281g2	1950	223.9581	105.4698	-1.086399	1.26E-08	Down	5.67E-10
BOX15_Mlig008455g2	2137	99.99587	47.04394	-1.08786	0.000449	Down	5.17E-05
BOX15_Mlig017435g2	2405	355.6024	167.2846	-1.08796	1.04E-07	Down	5.40E-09
BOX15_Mlig032560g1	1314	15.93746	7.487694	-1.089828	0.041057	Down	0.010072
BOX15_Mlig004709g2	1054	43.18959	20.28235	-1.090459	0.003342	Down	0.000508
BOX15_Mlig011670g3	2890	390.7003	183.4422	-1.090737	1.93E-05	Down	1.54E-06
BOX15_Mlig009020g2	3597	170.2047	79.90442	-1.090924	7.09E-07	Down	4.26E-08
BOX15_Mlig003691g1	3229	222.1088	104.27	-1.090943	4.03E-08	Down	1.95E-09
BOX15_Mlig031313g1	1183	132.2651	62.06247	-1.091639	1.33E-05	Down	1.03E-06
BOX15_Mlig028714g2	1484	57.05248	26.76653	-1.091859	0.000309	Down	3.41E-05
BOX15_Mlig025907g1	2231	317.2893	148.8577	-1.091864	0.047485	Down	0.012011
BOX15_Mlig028821g1	1029	284.985	133.6026	-1.092938	6.08E-18	Down	1.05E-19
BOX15_Mlig008926g1	3057	163.9935	76.86648	-1.093212	1.56E-08	Down	7.05E-10
BOX15_Mlig005602g2	3343	63.89737	29.93016	-1.094156	0.004391	Down	0.000698
BOX15_Mlig029097g1	2063	161.6402	75.69747	-1.094469	1.98E-05	Down	1.58E-06
BOX15_Mlig023623g3	2100	57.05154	26.69985	-1.095434	0.007863	Down	0.001376
BOX15_Mlig002045g2	5566	46.52135	21.7647	-1.095903	0.049424	Down	0.012627
BOX15_Mlig033280g1	1649	651.0903	304.3948	-1.096914	4.56E-11	Down	1.47E-12
BOX15_Mlig029609g1	955	26.32686	12.30644	-1.097122	0.019072	Down	0.003971
BOX15_Mlig011678g3	1987	97.97433	45.79692	-1.097153	0.001122	Down	0.000146
BOX15_Mlig004347g1	3883	278.8949	130.2074	-1.098911	0.000245	Down	2.62E-05
BOX15_Mlig010008g1	2254	67.07448	31.31481	-1.098919	0.000535	Down	6.28E-05
BOX15_Mlig021003g1	2110	91.26836	42.60903	-1.098955	0.00129	Down	0.000171
BOX15_Mlig031613g2	1091	114.6782	53.52928	-1.099191	6.85E-05	Down	6.31E-06
BOX15_Mlig013672g2	2594	84.82588	39.5941	-1.099219	6.61E-07	Down	3.95E-08
BOX15_Mlig010750g1	3546	199.883	93.29358	-1.099306	4.19E-11	Down	1.34E-12
BOX15_Mlig032285g1	2268	176.0556	82.16399	-1.099453	2.72E-06	Down	1.82E-07
BOX15_Mlig023536g1	405	399.8708	186.6151	-1.099468	6.74E-07	Down	4.03E-08
BOX15_Mlig002339g5	16406	52.81231	24.63091	-1.100404	0.000438	Down	5.03E-05
BOX15_Mlig024391g2	1197	71.57934	33.37063	-1.100964	4.09E-05	Down	3.53E-06
BOX15_Mlig008995g3	6354	53.59312	24.97768	-1.101408	0.000126	Down	1.25E-05
BOX15_Mlig030523g1	2503	86.7687	40.37736	-1.103628	0.04504	Down	0.011265
BOX15_Mlig013820g2	1658	144.3783	67.18212	-1.103704	0.003287	Down	0.000498
BOX15_Mlig001719g2	763	190.9395	88.71372	-1.105887	1.07E-13	Down	2.59E-15
BOX15_Mlig020299g1	1735	321.2618	149.1799	-1.106697	2.22E-12	Down	6.32E-14
BOX15_Mlig025426g1	2796	36.10711	16.76309	-1.106995	0.001284	Down	0.00017
BOX15_Mlig031786g3	1476	538.6272	249.9229	-1.107804	4.09E-08	Down	1.98E-09
BOX15_Mlig020673g1	1940	174.9411	81.10876	-1.10894	9.18E-07	Down	5.64E-08
BOX15_Mlig010100g2	1208	520.9964	241.4967	-1.10927	1.71E-12	Down	4.79E-14
BOX15_Mlig031511g1	1971	213.8645	99.11404	-1.109536	2.19E-05	Down	1.77E-06
BOX15_Mlig032217g5	4435	62.44608	28.92772	-1.110158	0.000904	Down	0.000113
BOX15_Mlig001692g3	914	87.6367	40.59652	-1.110179	2.63E-05	Down	2.17E-06

BOX15_Mlig003606g3	3728	909.2978	421.1013	-1.110586	9.39E-10	Down	3.55E-11
BOX15_Mlig028673g2	1300	251.5442	116.3566	-1.112259	3.41E-16	Down	6.68E-18
BOX15_Mlig026600g2	2002	978.8095	452.3233	-1.113674	1.17E-20	Down	1.64E-22
BOX15_Mlig011694g2	2553	23.1629	10.69984	-1.114227	0.049847	Down	0.012772
BOX15_Mlig015731g1	3416	58.49701	27.01254	-1.114734	0.00489	Down	0.00079
BOX15_Mlig032748g1	2260	182.161	84.01452	-1.116503	1.06E-14	Down	2.38E-16
BOX15_Mlig008310g1	1531	80.79661	37.2563	-1.116811	0.010113	Down	0.001856
BOX15_Mlig032079g1	939	8375.555	3860.671	-1.117333	1.52E-26	Down	1.43E-28
BOX15_Mlig013450g2	1505	44.33375	20.42153	-1.118314	0.00277	Down	0.000408
BOX15_Mlig029894g3	1177	424.343	195.3673	-1.119042	5.52E-21	Down	7.50E-23
BOX15_Mlig032217g3	4540	33.90015	15.60683	-1.119115	0.009583	Down	0.001742
BOX15_Mlig027095g1	2232	47.96205	22.0793	-1.119199	0.003756	Down	0.000583
BOX15_Mlig019845g1	1282	239.8883	110.341	-1.120394	9.03E-10	Down	3.41E-11
BOX15_Mlig033116g3	1711	62.31685	28.66363	-1.120401	0.018462	Down	0.003817
BOX15_Mlig025843g1	2095	659.7854	303.3932	-1.120808	9.23E-29	Down	7.83E-31
BOX15_Mlig030000g1	2101	133.1608	61.16275	-1.122445	0.003485	Down	0.000533
BOX15_Mlig007811g2	842	16.45715	7.554178	-1.123368	0.027852	Down	0.006259
BOX15_Mlig029747g3	1162	36.58096	16.78929	-1.123552	0.002589	Down	0.000377
BOX15_Mlig031786g1	1477	356.9356	163.7288	-1.124356	2.62E-09	Down	1.06E-10
BOX15_Mlig010110g1	2548	267.9772	122.9107	-1.1245	3.45E-06	Down	2.36E-07
BOX15_Mlig020808g1	2613	136.7667	62.72084	-1.1247	0.000235	Down	2.50E-05
BOX15_Mlig030746g1	1812	124.0699	56.85323	-1.125839	4.27E-05	Down	3.71E-06
BOX15_Mlig017783g1	2460	98.78907	45.25016	-1.126429	4.44E-08	Down	2.17E-09
BOX15_Mlig023012g2	3057	75.75685	34.67997	-1.127274	5.30E-05	Down	4.73E-06
BOX15_Mlig001180g3	2611	177.0154	81.01566	-1.127602	2.74E-05	Down	2.27E-06
BOX15_Mlig004952g3	679	407.4339	186.4623	-1.127682	3.11E-09	Down	1.27E-10
BOX15_Mlig001582g3	1703	295.9301	135.4196	-1.12782	4.17E-06	Down	2.90E-07
BOX15_Mlig025724g1	1089	98.56806	45.07699	-1.128729	1.89E-05	Down	1.51E-06
BOX15_Mlig006735g1	6608	78.98711	36.11205	-1.129137	0.005373	Down	0.00088
BOX15_Mlig031546g2	6938	55.01428	25.14828	-1.129346	0.0102	Down	0.001876
BOX15_Mlig004956g1	2892	113.1031	51.69888	-1.129433	1.84E-05	Down	1.46E-06
BOX15_Mlig002643g1	438	115.0172	52.55146	-1.130046	0.008749	Down	0.001561
BOX15_Mlig016147g1	2820	501.3033	228.9676	-1.13054	1.57E-06	Down	1.00E-07
BOX15_Mlig002973g1	2086	860.8961	392.9362	-1.131544	2.36E-34	Down	1.48E-36
BOX15_Mlig010364g10	1118	50.27348	22.93611	-1.132177	4.04E-05	Down	3.49E-06
BOX15_Mlig010364g8	1118	50.27348	22.93611	-1.132177	4.04E-05	Down	3.49E-06
BOX15_Mlig024785g1	4765	101.9266	46.47824	-1.132903	5.19E-07	Down	3.04E-08
BOX15_Mlig023934g1	1987	189.7281	86.49004	-1.133327	1.32E-10	Down	4.50E-12
BOX15_Mlig033713g1	2060	175.3303	79.92663	-1.133327	0.000307	Down	3.38E-05
BOX15_Mlig012785g3	821	47.77749	21.7794	-1.133367	0.00093	Down	0.000117
BOX15_Mlig005207g1	1234	193.8909	88.37883	-1.133472	5.89E-13	Down	1.56E-14
BOX15_Mlig032486g2	2224	1997.813	910.6038	-1.133526	5.56E-65	Down	8.29E-68

BOX15_Mlig005322g1	787	450.1651	205.1853	-1.133527	3.09E-05	Down	2.59E-06
BOX15_Mlig032145g1	1699	509.1222	231.9313	-1.134315	5.14E-14	Down	1.21E-15
BOX15_Mlig018087g4	2028	81.36439	37.02442	-1.13592	5.63E-06	Down	4.02E-07
BOX15_Mlig032854g1	5435	128.0454	58.21429	-1.137211	6.12E-08	Down	3.06E-09
BOX15_Mlig031793g4	3640	33.80707	15.36913	-1.137289	0.00301	Down	0.000449
BOX15_Mlig016716g2	6757	58.72557	26.68971	-1.137705	0.00071	Down	8.61E-05
BOX15_Mlig031143g1	906	46.4187	21.06535	-1.139835	0.000244	Down	2.60E-05
BOX15_Mlig018784g2	1974	47.58528	21.59011	-1.140145	0.000195	Down	2.02E-05
BOX15_Mlig034105g1	1458	252.0364	114.3297	-1.140432	3.57E-08	Down	1.71E-09
BOX15_Mlig001101g1	2168	26.22896	11.89158	-1.14122	0.042841	Down	0.010603
BOX15_Mlig014861g1	1360	56.86542	25.78004	-1.141297	0.001839	Down	0.000255
BOX15_Mlig015277g1	1554	64.49603	29.2328	-1.141623	2.00E-06	Down	1.31E-07
BOX15_Mlig028449g3	4463	2244.741	1016.513	-1.142921	7.87E-11	Down	2.59E-12
BOX15_Mlig026936g2	1391	643.8466	291.556	-1.142944	6.42E-14	Down	1.53E-15
BOX15_Mlig006036g3	1916	39.41728	17.83688	-1.143965	0.007584	Down	0.001319
BOX15_Mlig010168g1	1315	81.78709	36.98739	-1.14484	0.004839	Down	0.000781
BOX15_Mlig001719g7	766	139.5191	63.02942	-1.146365	1.47E-06	Down	9.33E-08
BOX15_Mlig011299g3	1510	50.28452	22.7065	-1.147009	0.00018	Down	1.86E-05
BOX15_Mlig022653g4	1254	262.6433	118.463	-1.148669	0.000334	Down	3.71E-05
BOX15_Mlig014918g2	1656	46.11054	20.795	-1.14886	0.000341	Down	3.80E-05
BOX15_Mlig014364g1	832	50.45382	22.73453	-1.150079	8.67E-05	Down	8.20E-06
BOX15_Mlig011080g2	697	269.9518	121.5988	-1.150573	6.80E-07	Down	4.07E-08
BOX15_Mlig027742g1	992	5367.151	2415.562	-1.151798	3.13E-07	Down	1.77E-08
BOX15_Mlig002765g2	1974	626.3715	281.6572	-1.153078	2.17E-12	Down	6.16E-14
BOX15_Mlig006678g1	1013	65.29268	29.35249	-1.153438	9.49E-05	Down	9.04E-06
BOX15_Mlig027913g4	1177	72.25318	32.47331	-1.153807	5.22E-07	Down	3.06E-08
BOX15_Mlig012121g1	3271	999.6596	449.2202	-1.154014	1.58E-11	Down	4.86E-13
BOX15_Mlig007587g1	992	16.38145	7.35947	-1.154389	0.015974	Down	0.003206
BOX15_Mlig007587g2	992	16.38145	7.35947	-1.154389	0.015974	Down	0.003206
BOX15_Mlig028889g1	1733	79.96419	35.92182	-1.154494	0.000523	Down	6.12E-05
BOX15_Mlig021439g1	2550	45.04696	20.22885	-1.155015	0.003439	Down	0.000525
BOX15_Mlig019641g2	7303	426.0145	191.3036	-1.155038	1.84E-16	Down	3.50E-18
BOX15_Mlig010763g1	3121	30.85783	13.85472	-1.155259	0.011269	Down	0.002111
BOX15_Mlig006988g1	3242	56.07425	25.14599	-1.15701	0.014691	Down	0.002896
BOX15_Mlig020459g1	2532	124.6891	55.90801	-1.157209	2.84E-07	Down	1.59E-08
BOX15_Mlig011678g1	1998	260.0695	116.5123	-1.158415	0.000101	Down	9.74E-06
BOX15_Mlig012027g1	1884	104.7093	46.88642	-1.159148	3.67E-05	Down	3.14E-06
BOX15_Mlig026897g1	3523	117.2427	52.49293	-1.159303	9.19E-07	Down	5.65E-08
BOX15_Mlig023942g2	1944	10152.52	4544.217	-1.159734	3.28E-22	Down	4.09E-24
BOX15_Mlig032440g1	4158	36.00222	16.10132	-1.160907	0.009229	Down	0.001664
BOX15_Mlig014638g1	4817	968.1017	432.8337	-1.161346	0.000999	Down	0.000127
BOX15_Mlig026366g3	1773	28.29535	12.6431	-1.162214	0.004086	Down	0.000642

BOX15_Mlig029463g2	1651	30.24898	13.49626	-1.164326	0.003711	Down	0.000574
BOX15_Mlig032913g1	1814	47.77363	21.29665	-1.165588	0.007268	Down	0.001255
BOX15_Mlig010314g2	3379	403.8599	179.9966	-1.165886	2.05E-34	Down	1.28E-36
BOX15_Mlig006965g1	1077	18.52592	8.249305	-1.167201	0.026188	Down	0.005828
BOX15_Mlig008926g2	3050	257.5186	114.6353	-1.167625	3.45E-13	Down	8.89E-15
BOX15_Mlig012389g1	3948	273.8975	121.8929	-1.168022	6.28E-05	Down	5.72E-06
BOX15_Mlig007295g1	2003	156.6537	69.70878	-1.168167	1.60E-07	Down	8.60E-09
BOX15_Mlig031483g1	2204	1996.539	887.5452	-1.169609	1.10E-09	Down	4.22E-11
BOX15_Mlig005966g3	1055	38.47518	17.09051	-1.170733	0.008216	Down	0.001451
BOX15_Mlig032138g1	1588	17.13538	7.60925	-1.171152	0.012929	Down	0.002487
BOX15_Mlig026403g5	7045	167.576	74.41124	-1.171223	5.17E-05	Down	4.59E-06
BOX15_Mlig008233g1	2537	160.8219	71.38343	-1.171803	8.34E-09	Down	3.65E-10
BOX15_Mlig016804g2	2872	515.7261	228.9004	-1.171885	1.26E-09	Down	4.85E-11
BOX15_Mlig021901g1	720	3791.201	1682.253	-1.172261	7.16E-19	Down	1.15E-20
BOX15_Mlig006675g2	2257	98.85556	43.85769	-1.172492	1.90E-08	Down	8.71E-10
BOX15_Mlig004981g1	773	109.3119	48.47862	-1.17303	1.40E-06	Down	8.86E-08
BOX15_Mlig032507g1	1239	82.57964	36.6156	-1.173328	5.67E-05	Down	5.08E-06
BOX15_Mlig017709g3	962	268.3933	118.9933	-1.173469	5.59E-23	Down	6.68E-25
BOX15_Mlig020068g3	2662	168.3175	74.54802	-1.174943	2.04E-05	Down	1.64E-06
BOX15_Mlig023623g2	2079	35.19308	15.57756	-1.175823	0.011739	Down	0.002216
BOX15_Mlig009015g2	2049	702.9815	311.1285	-1.175976	5.05E-16	Down	1.01E-17
BOX15_Mlig020068g1	2660	143.6957	63.54356	-1.177199	3.76E-06	Down	2.59E-07
BOX15_Mlig023260g1	1184	362.0026	159.7937	-1.179789	1.57E-24	Down	1.67E-26
BOX15_Mlig031965g2	1272	125.0715	55.16549	-1.180915	1.80E-06	Down	1.17E-07
BOX15_Mlig028006g2	974	21.51293	9.488622	-1.180933	0.034906	Down	0.008262
BOX15_Mlig029802g2	1405	74.44853	32.7873	-1.183106	0.001789	Down	0.000247
BOX15_Mlig031071g1	1647	61.86833	27.21823	-1.184628	0.040401	Down	0.009868
BOX15_Mlig015780g4	6056	157.6959	69.34693	-1.185241	0.000412	Down	4.69E-05
BOX15_Mlig004952g2	692	596.5136	262.1777	-1.18601	1.48E-09	Down	5.77E-11
BOX15_Mlig003075g1	1495	48.28623	21.21972	-1.186206	0.000524	Down	6.14E-05
BOX15_Mlig011670g2	2887	359.8211	158.068	-1.186734	4.41E-07	Down	2.55E-08
BOX15_Mlig003096g3	2431	865.134	379.8902	-1.187341	1.64E-25	Down	1.61E-27
BOX15_Mlig016672g2	1122	36.32908	15.94894	-1.187664	0.004477	Down	0.000714
BOX15_Mlig003999g1	827	3121.879	1368.264	-1.190068	6.15E-08	Down	3.08E-09
BOX15_Mlig031154g2	3231	83.34074	36.51756	-1.190432	8.03E-05	Down	7.54E-06
BOX15_Mlig003740g1	3101	67.55863	29.57635	-1.191696	0.001823	Down	0.000252
BOX15_Mlig022973g3	662	84.38774	36.92166	-1.192566	8.85E-06	Down	6.60E-07
BOX15_Mlig017292g2	1970	94.87657	41.49089	-1.193257	1.50E-07	Down	8.03E-09
BOX15_Mlig008786g1	4662	75.05686	32.8169	-1.193545	5.83E-07	Down	3.44E-08
BOX15_Mlig028915g2	2337	640.1717	279.685	-1.194656	2.02E-24	Down	2.16E-26
BOX15_Mlig033902g1	1188	12.20577	5.331546	-1.194937	0.033323	Down	0.007804
BOX15_Mlig000899g2	776	71.0863	31.03927	-1.195477	1.87E-07	Down	1.02E-08

BOX15_Mlig010263g3	1087	16.01002	6.980945	-1.197481	0.043048	Down	0.010666
BOX15_Mlig033612g5	2877	59.88622	26.09366	-1.198525	0.001998	Down	0.00028
BOX15_Mlig033612g6	2877	59.88622	26.09366	-1.198525	0.001998	Down	0.00028
BOX15_Mlig000681g2	3757	42.54035	18.5354	-1.198549	0.004078	Down	0.00064
BOX15_Mlig030980g3	1806	298.8333	130.1627	-1.199025	1.17E-05	Down	8.96E-07
BOX15_Mlig010026g1	1897	183.4552	79.79745	-1.201013	4.25E-14	Down	9.95E-16
BOX15_Mlig012389g3	3949	398.964	173.5252	-1.201113	4.23E-07	Down	2.44E-08
BOX15_Mlig031669g1	823	11.15556	4.844767	-1.203263	0.045126	Down	0.011288
BOX15_Mlig033190g3	1809	61.13911	26.54667	-1.203565	0.000786	Down	9.69E-05
BOX15_Mlig005967g2	1915	29.50401	12.80966	-1.203679	0.024708	Down	0.005435
BOX15_Mlig028286g1	6216	98.70385	42.84949	-1.203828	3.56E-08	Down	1.70E-09
BOX15_Mlig005298g1	428	227.7977	98.84664	-1.204489	3.85E-10	Down	1.38E-11
BOX15_Mlig027228g2	2768	104.8277	45.48556	-1.204539	4.11E-05	Down	3.55E-06
BOX15_Mlig000887g2	1212	159.9538	69.40464	-1.204551	3.71E-09	Down	1.54E-10
BOX15_Mlig024756g2	1962	117.2093	50.8272	-1.205414	1.17E-06	Down	7.33E-08
BOX15_Mlig001692g2	871	98.95931	42.88724	-1.206287	8.04E-08	Down	4.10E-09
BOX15_Mlig010259g2	685	78.39302	33.95485	-1.207108	3.23E-06	Down	2.20E-07
BOX15_Mlig005664g1	3255	396.2746	171.5784	-1.207632	0.003225	Down	0.000487
BOX15_Mlig020963g2	1705	34.38739	14.88594	-1.207929	0.004777	Down	0.000769
BOX15_Mlig029386g6	627	251.7539	108.9483	-1.208371	1.52E-15	Down	3.16E-17
BOX15_Mlig029386g2	627	251.7539	108.9483	-1.208371	1.52E-15	Down	3.16E-17
BOX15_Mlig029578g2	3797	221.3796	95.78305	-1.20868	1.72E-12	Down	4.82E-14
BOX15_Mlig001354g1	1963	11465.12	4956.208	-1.209943	0.00579	Down	0.000961
BOX15_Mlig032070g3	1328	91.77397	39.66113	-1.210359	0.000376	Down	4.24E-05
BOX15_Mlig009671g1	1191	82.67056	35.68889	-1.211898	1.83E-06	Down	1.19E-07
BOX15_Mlig001296g4	2199	65.39688	28.23161	-1.21191	9.16E-07	Down	5.63E-08
BOX15_Mlig031202g1	5462	264.7567	114.2719	-1.212196	2.18E-08	Down	1.01E-09
BOX15_Mlig003023g1	1581	285.0977	123.0068	-1.212719	0.007646	Down	0.001333
BOX15_Mlig032252g1	1486	89.11085	38.43947	-1.213013	7.87E-07	Down	4.77E-08
BOX15_Mlig024007g2	3019	1258.079	542.4085	-1.213771	7.03E-31	Down	5.31E-33
BOX15_Mlig020314g2	6174	141.649	61.06773	-1.213838	4.85E-06	Down	3.43E-07
BOX15_Mlig013715g1	2453	59.06245	25.45714	-1.214171	0.000131	Down	1.29E-05
BOX15_Mlig004708g1	1973	40.58313	17.49119	-1.214251	0.000299	Down	3.28E-05
BOX15_Mlig006259g1	939	46.4476	20.01255	-1.214699	0.001516	Down	0.000205
BOX15_Mlig008155g2	2749	191.7367	82.56144	-1.215587	0.020948	Down	0.004447
BOX15_Mlig013820g3	2907	396.9467	170.8971	-1.215818	2.03E-05	Down	1.63E-06
BOX15_Mlig021043g1	875	241.371	103.9012	-1.21604	8.82E-19	Down	1.42E-20
BOX15_Mlig029750g1	3504	143.1774	61.56804	-1.21755	7.45E-13	Down	2.01E-14
BOX15_Mlig013622g1	1941	50.57966	21.74171	-1.218092	1.51E-05	Down	1.18E-06
BOX15_Mlig013622g2	1941	50.57966	21.74171	-1.218092	1.51E-05	Down	1.18E-06
BOX15_Mlig016804g1	2334	1137.423	488.5297	-1.21925	6.25E-29	Down	5.26E-31
BOX15_Mlig019543g1	1027	26.3853	11.33192	-1.219342	0.017803	Down	0.00365

BOX15_Mlig009114g2	1735	37.75999	16.21695	-1.219356	0.003696	Down	0.000572
BOX15_Mlig027269g1	3072	228.4344	98.09859	-1.219475	5.44E-08	Down	2.70E-09
BOX15_Mlig010100g1	1231	704.6064	302.5832	-1.219486	6.23E-23	Down	7.51E-25
BOX15_Mlig003352g1	1686	73.87283	31.69342	-1.220861	0.005797	Down	0.000962
BOX15_Mlig007778g1	2096	206.6315	88.64846	-1.220893	4.21E-13	Down	1.09E-14
BOX15_Mlig011833g3	2708	117.3641	50.31697	-1.221874	1.46E-12	Down	4.05E-14
BOX15_Mlig013387g2	3125	521.7002	223.3042	-1.22421	2.88E-06	Down	1.94E-07
BOX15_Mlig001790g1	6280	50.23459	21.5019	-1.224217	0.00022	Down	2.32E-05
BOX15_Mlig011147g1	956	15.47358	6.620081	-1.224886	0.022042	Down	0.004735
BOX15_Mlig004214g5	4465	24.02175	10.27703	-1.224918	0.046263	Down	0.011615
BOX15_Mlig025507g3	1791	23.47722	10.04021	-1.225471	0.037603	Down	0.009043
BOX15_Mlig034488g1	1776	16.46386	7.038977	-1.225865	0.044928	Down	0.011231
BOX15_Mlig006571g1	1947	1048.966	448.3785	-1.226179	1.88E-26	Down	1.77E-28
BOX15_Mlig002262g1	1584	145.4503	62.06386	-1.228701	9.98E-14	Down	2.42E-15
BOX15_Mlig002394g1	4449	136.2502	58.13449	-1.228792	9.71E-06	Down	7.29E-07
BOX15_Mlig012092g1	1296	17.71966	7.557948	-1.229284	0.020666	Down	0.004373
BOX15_Mlig016768g2	1828	20.56332	8.769641	-1.229483	0.015473	Down	0.003082
BOX15_Mlig024312g1	1774	24.6552	10.50963	-1.23018	0.040158	Down	0.009791
BOX15_Mlig025283g1	1360	1561.374	664.9609	-1.231475	2.22E-07	Down	1.23E-08
BOX15_Mlig011074g1	1227	388.901	165.6221	-1.231508	6.91E-20	Down	1.04E-21
BOX15_Mlig013123g2	864	4992.295	2125.517	-1.231889	1.03E-41	Down	4.40E-44
BOX15_Mlig016153g3	1892	19.79271	8.408376	-1.23507	0.029283	Down	0.00666
BOX15_Mlig027825g1	1686	214.3366	90.92783	-1.237084	6.91E-12	Down	2.06E-13
BOX15_Mlig003232g2	2582	62.6297	26.48369	-1.241743	0.027351	Down	0.006121
BOX15_Mlig016183g1	2522	77.50661	32.74049	-1.243244	5.24E-05	Down	4.66E-06
BOX15_Mlig009118g1	1071	161.6232	68.2618	-1.243484	1.32E-11	Down	4.05E-13
BOX15_Mlig000961g3	987	36.42794	15.3738	-1.244572	0.000669	Down	8.07E-05
BOX15_Mlig006672g3	1836	54.59478	23.03651	-1.244841	1.36E-05	Down	1.05E-06
BOX15_Mlig013426g1	1369	56.52978	23.84936	-1.24506	2.79E-05	Down	2.31E-06
BOX15_Mlig021898g2	1449	65.47154	27.61826	-1.245246	4.81E-05	Down	4.24E-06
BOX15_Mlig021166g1	879	262.42	110.6546	-1.245814	9.82E-10	Down	3.73E-11
BOX15_Mlig013665g2	860	19.6725	8.291857	-1.246413	0.010282	Down	0.001895
BOX15_Mlig013665g4	860	19.6725	8.291857	-1.246413	0.010282	Down	0.001895
BOX15_Mlig013665g1	860	19.6725	8.291857	-1.246413	0.010282	Down	0.001895
BOX15_Mlig019717g1	4636	2813.641	1185.557	-1.246873	7.37E-14	Down	1.77E-15
BOX15_Mlig006551g1	1872	1422.093	598.9706	-1.247458	7.95E-24	Down	8.98E-26
BOX15_Mlig019446g1	7598	165.1648	69.51268	-1.248559	1.43E-06	Down	9.06E-08
BOX15_Mlig021075g1	1882	27.7724	11.68696	-1.248751	0.025081	Down	0.005533
BOX15_Mlig030557g4	852	89.57912	37.69033	-1.248968	1.93E-08	Down	8.87E-10
BOX15_Mlig006794g1	3215	99.58766	41.8097	-1.252129	3.46E-07	Down	1.97E-08
BOX15_Mlig011092g3	986	173.9956	73.03765	-1.252339	7.98E-06	Down	5.89E-07
BOX15_Mlig025145g1	1866	87.39173	36.67614	-1.252655	0.000143	Down	1.42E-05

BOX15_Mlig011306g1	2591	430.2014	180.5219	-1.252838	1.13E-23	Down	1.28E-25
BOX15_Mlig011965g1	3249	89.82089	37.68777	-1.252955	0.000188	Down	1.95E-05
BOX15_Mlig011542g1	1530	186.493	78.21285	-1.253644	7.02E-10	Down	2.62E-11
BOX15_Mlig005725g1	3373	71.06967	29.80326	-1.253764	0.003794	Down	0.000589
BOX15_Mlig029225g1	1982	81.094	33.9589	-1.255806	0.047276	Down	0.011946
BOX15_Mlig009376g1	2452	74.41903	31.16319	-1.255829	3.61E-05	Down	3.08E-06
BOX15_Mlig007587g3	979	50.58362	21.17287	-1.256454	3.05E-05	Down	2.55E-06
BOX15_Mlig026890g3	2610	129.564	54.16881	-1.258131	1.38E-06	Down	8.73E-08
BOX15_Mlig027523g1	1035	3756.186	1568.937	-1.259481	1.01E-35	Down	5.90E-38
BOX15_Mlig013568g1	2472	137.5358	57.34232	-1.262135	5.65E-08	Down	2.80E-09
BOX15_Mlig033956g1	3437	197.2435	82.20913	-1.262607	3.31E-05	Down	2.80E-06
BOX15_Mlig012153g1	831	10.99933	4.582225	-1.263295	0.043975	Down	0.010941
BOX15_Mlig004952g1	679	624.0415	259.9205	-1.263572	6.63E-13	Down	1.77E-14
BOX15_Mlig007597g1	1528	28.8635	12.01769	-1.264086	0.008798	Down	0.001572
BOX15_Mlig015059g1	844	15.03443	6.256473	-1.264848	0.011136	Down	0.00208
BOX15_Mlig016142g1	1263	436.915	181.8085	-1.264933	5.79E-14	Down	1.37E-15
BOX15_Mlig024007g3	3028	1324.85	551.2173	-1.265136	4.05E-38	Down	2.07E-40
BOX15_Mlig033352g2	979	116.6059	48.48478	-1.266037	4.67E-09	Down	1.97E-10
BOX15_Mlig028352g2	4018	265.9447	110.5316	-1.266667	4.92E-13	Down	1.30E-14
BOX15_Mlig017730g1	7672	153.8864	63.93043	-1.267291	1.11E-11	Down	3.39E-13
BOX15_Mlig028779g2	1138	393.0674	163.2713	-1.267506	2.65E-10	Down	9.29E-12
BOX15_Mlig023792g2	1623	47.95261	19.91541	-1.267724	0.000103	Down	9.90E-06
BOX15_Mlig027058g1	2135	268.2425	111.3732	-1.268136	1.17E-07	Down	6.12E-09
BOX15_Mlig014299g1	1320	63.53075	26.37182	-1.268458	0.000505	Down	5.88E-05
BOX15_Mlig027523g4	997	3572.437	1482.225	-1.269144	1.87E-35	Down	1.11E-37
BOX15_Mlig017900g1	1458	141.7922	58.82279	-1.269331	0.021644	Down	0.004632
BOX15_Mlig013767g2	826	27.77255	11.51827	-1.269735	0.0076	Down	0.001323
BOX15_Mlig004719g1	649	34.61041	14.33797	-1.271365	0.048356	Down	0.012289
BOX15_Mlig033186g1	8667	1869.14	772.6583	-1.274472	1.76E-47	Down	5.36E-50
BOX15_Mlig030000g2	1064	57.10356	23.60177	-1.274685	3.89E-05	Down	3.34E-06
BOX15_Mlig003158g1	4896	89.86737	37.08194	-1.277081	2.00E-09	Down	7.98E-11
BOX15_Mlig013387g3	3111	494.1508	203.8489	-1.277452	1.74E-07	Down	9.38E-09
BOX15_Mlig021563g1	831	27.94868	11.52683	-1.277785	0.011725	Down	0.002213
BOX15_Mlig022800g2	883	22.10133	9.111107	-1.278435	0.00823	Down	0.001453
BOX15_Mlig031655g3	1166	45.55148	18.77535	-1.278658	0.000963	Down	0.000122
BOX15_Mlig021043g2	1060	110.0333	45.24646	-1.282063	1.96E-12	Down	5.54E-14
BOX15_Mlig029802g1	1403	27.25444	11.20547	-1.282288	0.016891	Down	0.003425
BOX15_Mlig024007g1	3021	1924.67	790.6564	-1.283488	2.56E-40	Down	1.18E-42
BOX15_Mlig022924g1	1853	234.996	96.5234	-1.283685	7.59E-19	Down	1.22E-20
BOX15_Mlig026868g1	1182	238.3412	97.88268	-1.283903	9.80E-05	Down	9.37E-06
BOX15_Mlig021195g1	1695	294.6208	120.7104	-1.28731	4.31E-13	Down	1.12E-14
BOX15_Mlig002692g1	2664	171.9451	70.39071	-1.288491	1.21E-10	Down	4.10E-12

BOX15_Mlig015277g2	1552	59.49519	24.35421	-1.288602	1.09E-05	Down	8.25E-07
BOX15_Mlig026143g4	831	125.7905	51.48426	-1.28882	6.03E-08	Down	3.01E-09
BOX15_Mlig013645g1	668	25.44962	10.41591	-1.288855	0.003546	Down	0.000545
BOX15_Mlig015143g1	2514	48.13743	19.69479	-1.289345	0.01062	Down	0.001968
BOX15_Mlig029988g1	840	2449.259	1002.033	-1.289416	1.47E-90	Down	1.26E-93
BOX15_Mlig033301g1	4741	81.89359	33.42615	-1.292773	1.99E-07	Down	1.09E-08
BOX15_Mlig000939g1	1821	424.6536	173.2711	-1.293256	3.15E-06	Down	2.14E-07
BOX15_Mlig013683g2	2074	11.5343	4.702028	-1.294575	0.040837	Down	0.009997
BOX15_Mlig022535g1	1010	81.78207	33.31845	-1.295463	4.00E-06	Down	2.76E-07
BOX15_Mlig026247g1	2402	31.58194	12.86537	-1.295607	0.007129	Down	0.001227
BOX15_Mlig022847g2	1716	19.26141	7.843737	-1.296101	0.03228	Down	0.007501
BOX15_Mlig004046g5	1281	56.83766	23.12982	-1.297093	2.78E-05	Down	2.31E-06
BOX15_Mlig017323g4	1834	29.55527	12.01714	-1.298322	0.034053	Down	0.008022
BOX15_Mlig031564g3	2811	4.72826	1.922239	-1.298521	0.039689	Down	0.009647
BOX15_Mlig025594g1	4178	209.7178	85.23446	-1.298941	4.14E-13	Down	1.07E-14
BOX15_Mlig015895g1	1756	27.62066	11.21896	-1.299809	0.00206	Down	0.00029
BOX15_Mlig002611g2	1785	120.6344	48.97775	-1.300443	4.23E-07	Down	2.44E-08
BOX15_Mlig001432g1	2078	346.1775	140.4785	-1.301162	8.39E-12	Down	2.52E-13
BOX15_Mlig034025g1	1760	81.05002	32.86726	-1.302161	4.10E-05	Down	3.55E-06
BOX15_Mlig004034g1	4115	361.4326	146.5454	-1.302379	2.26E-11	Down	7.05E-13
BOX15_Mlig003023g3	1578	159.1301	64.51317	-1.302541	1.30E-08	Down	5.83E-10
BOX15_Mlig024006g1	2704	22.05368	8.938452	-1.302923	0.037693	Down	0.009067
BOX15_Mlig024376g2	1351	14.54792	5.895588	-1.303105	0.040792	Down	0.009983
BOX15_Mlig014142g1	613	3423.021	1385.136	-1.305242	2.27E-19	Down	3.52E-21
BOX15_Mlig033476g1	1838	38.65053	15.63915	-1.305326	0.000772	Down	9.50E-05
BOX15_Mlig020671g2	1468	153.4175	62.07344	-1.305415	1.07E-05	Down	8.11E-07
BOX15_Mlig018691g3	1455	34.42357	13.92356	-1.305868	0.011508	Down	0.002162
BOX15_Mlig024180g3	1269	45.62784	18.43516	-1.307454	0.000611	Down	7.29E-05
BOX15_Mlig010802g1	2307	80.17111	32.37507	-1.308199	1.78E-07	Down	9.63E-09
BOX15_Mlig019717g3	4662	2159.055	871.7735	-1.308375	5.05E-21	Down	6.83E-23
BOX15_Mlig017213g1	2704	252.3002	101.8464	-1.308746	3.42E-18	Down	5.80E-20
BOX15_Mlig019918g1	3769	41.31702	16.67831	-1.308763	0.000574	Down	6.79E-05
BOX15_Mlig020808g2	4061	31.36659	12.65849	-1.309123	0.007265	Down	0.001254
BOX15_Mlig009204g1	1330	9.414262	3.798581	-1.309387	0.0342	Down	0.008064
BOX15_Mlig024652g1	1250	145.5717	58.71596	-1.309906	6.14E-07	Down	3.64E-08
BOX15_Mlig033095g3	4688	381.8157	153.9958	-1.309985	1.07E-16	Down	2.00E-18
BOX15_Mlig019375g1	4662	468.0841	188.7714	-1.310128	7.47E-21	Down	1.03E-22
BOX15_Mlig010599g1	2755	57.54046	23.17948	-1.311729	2.71E-05	Down	2.24E-06
BOX15_Mlig002966g1	4198	319.8822	128.8052	-1.31235	1.60E-18	Down	2.65E-20
BOX15_Mlig011222g3	4390	63.09999	25.39663	-1.313003	0.000313	Down	3.45E-05
BOX15_Mlig017228g1	4567	33.5473	13.4841	-1.314938	0.001679	Down	0.00023
BOX15_Mlig026126g1	1935	68.29149	27.44578	-1.315122	2.54E-06	Down	1.69E-07

BOX15_Mlig024961g2	2499	124.9383	50.17312	-1.316229	6.82E-05	Down	6.28E-06
BOX15_Mlig004074g1	3007	37.43445	15.0326	-1.316272	0.028355	Down	0.006402
BOX15_Mlig029483g1	1468	280.4523	112.5914	-1.316658	2.11E-19	Down	3.26E-21
BOX15_Mlig032886g3	1697	80.20983	32.19716	-1.316845	0.000244	Down	2.60E-05
BOX15_Mlig007651g4	1838	52.98526	21.26394	-1.317182	0.000478	Down	5.53E-05
BOX15_Mlig007651g2	1838	52.98526	21.26394	-1.317182	0.000478	Down	5.53E-05
BOX15_Mlig019085g3	2703	61.61527	24.72079	-1.317563	4.73E-05	Down	4.16E-06
BOX15_Mlig033832g1	1102	139.7974	56.08242	-1.317717	6.81E-06	Down	4.95E-07
BOX15_Mlig022826g1	2556	209.0162	83.78837	-1.318793	8.95E-10	Down	3.37E-11
BOX15_Mlig003031g1	4073	120.8716	48.45084	-1.318882	1.79E-13	Down	4.46E-15
BOX15_Mlig004443g1	2457	115.506	46.2956	-1.31902	0.000286	Down	3.12E-05
BOX15_Mlig012347g1	2005	6.775769	2.714551	-1.319671	0.037573	Down	0.00903
BOX15_Mlig019213g1	1457	43.43733	17.39701	-1.320096	0.001828	Down	0.000253
BOX15_Mlig008995g1	2405	32.78554	13.11348	-1.32201	0.034976	Down	0.008282
BOX15_Mlig025898g5	2626	57.74416	23.09255	-1.322248	1.92E-05	Down	1.53E-06
BOX15_Mlig013201g1	1225	200.2319	80.06013	-1.322516	1.22E-12	Down	3.35E-14
BOX15_Mlig014210g2	1360	1310.399	523.4296	-1.323939	3.63E-21	Down	4.86E-23
BOX15_Mlig015443g3	2440	1306.635	521.624	-1.324774	1.76E-11	Down	5.43E-13
BOX15_Mlig007340g1	2895	103.7321	41.39174	-1.325448	3.85E-09	Down	1.61E-10
BOX15_Mlig013622g3	1616	86.37994	34.46562	-1.325539	1.46E-06	Down	9.27E-08
BOX15_Mlig020268g3	897	105.9742	42.27863	-1.325712	5.02E-07	Down	2.94E-08
BOX15_Mlig006735g2	6965	82.21198	32.72271	-1.329056	0.000438	Down	5.03E-05
BOX15_Mlig012489g2	994	1060.656	422.0819	-1.329362	1.51E-22	Down	1.86E-24
BOX15_Mlig032554g4	1266	627.8282	249.5861	-1.330832	0.001903	Down	0.000265
BOX15_Mlig031842g3	2818	154.271	61.27718	-1.332045	0.000796	Down	9.84E-05
BOX15_Mlig030129g1	2563	50.68457	20.12603	-1.332484	0.01638	Down	0.003303
BOX15_Mlig013860g1	1510	49.94858	19.82349	-1.333233	1.40E-05	Down	1.08E-06
BOX15_Mlig016826g1	1474	253.0767	100.401	-1.333802	4.73E-07	Down	2.75E-08
BOX15_Mlig019816g3	1851	42.28625	16.77459	-1.333911	3.50E-05	Down	2.97E-06
BOX15_Mlig006571g2	1945	707.5398	280.639	-1.334096	7.27E-14	Down	1.74E-15
BOX15_Mlig024674g1	1511	367.9454	145.9259	-1.334255	4.06E-23	Down	4.80E-25
BOX15_Mlig027523g2	894	5114.333	2026.733	-1.33539	3.51E-41	Down	1.57E-43
BOX15_Mlig023741g1	2133	109.5757	43.42204	-1.335428	2.01E-09	Down	7.99E-11
BOX15_Mlig013869g1	950	49.28829	19.52862	-1.335655	0.000109	Down	1.05E-05
BOX15_Mlig011900g1	1419	170.8166	67.62486	-1.336822	5.78E-12	Down	1.71E-13
BOX15_Mlig014154g2	1305	68.17824	26.99098	-1.336834	0.035724	Down	0.008501
BOX15_Mlig026113g1	2789	63.40186	25.08469	-1.337718	5.46E-07	Down	3.21E-08
BOX15_Mlig010331g1	3444	531.3129	210.1087	-1.338426	1.49E-16	Down	2.82E-18
BOX15_Mlig013387g1	3124	515.3846	203.7405	-1.338917	4.06E-15	Down	8.74E-17
BOX15_Mlig028320g2	5525	238.3224	94.01192	-1.341999	5.93E-23	Down	7.13E-25
BOX15_Mlig021573g1	1919	26.13528	10.29632	-1.343869	0.020217	Down	0.00426
BOX15_Mlig017475g1	2129	66.42126	26.16665	-1.343916	7.69E-08	Down	3.91E-09

BOX15_Mlig012489g1	989	1392.057	548.3068	-1.344163	1.14E-12	Down	3.13E-14
BOX15_Mlig032589g2	1295	27.01723	10.64063	-1.344297	0.023479	Down	0.005109
BOX15_Mlig017362g1	1607	77.19747	30.37123	-1.345848	1.81E-08	Down	8.30E-10
BOX15_Mlig032835g1	2879	34.25195	13.4582	-1.347701	0.001356	Down	0.000181
BOX15_Mlig032410g3	1574	154.6868	60.76307	-1.348084	0.000387	Down	4.38E-05
BOX15_Mlig032586g1	637	64.11241	25.14359	-1.350413	1.84E-07	Down	9.99E-09
BOX15_Mlig032919g1	1017	35.1967	13.79877	-1.3509	0.000744	Down	9.10E-05
BOX15_Mlig009948g1	1399	988.2483	387.4228	-1.350965	7.17E-55	Down	1.55E-57
BOX15_Mlig011678g2	1777	87.07227	34.12415	-1.35142	0.000636	Down	7.63E-05
BOX15_Mlig018813g1	2063	251.0926	98.33008	-1.352515	4.91E-10	Down	1.80E-11
BOX15_Mlig018813g2	2063	251.0926	98.33008	-1.352515	4.91E-10	Down	1.80E-11
BOX15_Mlig016137g1	2944	180.9859	70.74108	-1.355257	5.28E-14	Down	1.24E-15
BOX15_Mlig031194g1	2747	36.19938	14.14826	-1.355341	0.012856	Down	0.002471
BOX15_Mlig031249g1	3067	30.51455	11.92449	-1.35557	0.008023	Down	0.00141
BOX15_Mlig004603g1	2552	97.9413	38.18348	-1.358969	2.95E-09	Down	1.20E-10
BOX15_Mlig028314g1	6315	820.1967	319.3986	-1.360612	2.15E-13	Down	5.42E-15
BOX15_Mlig000438g13	4509	385.1784	149.9111	-1.36142	6.05E-16	Down	1.21E-17
BOX15_Mlig006865g1	1293	81.97777	31.89579	-1.361867	1.18E-08	Down	5.29E-10
BOX15_Mlig020583g4	806	42.47742	16.51732	-1.362717	0.004831	Down	0.000779
BOX15_Mlig011670g1	2903	274.6036	106.7422	-1.36322	3.84E-08	Down	1.85E-09
BOX15_Mlig016882g1	2588	55.04111	21.39226	-1.363421	1.24E-05	Down	9.53E-07
BOX15_Mlig009645g1	2773	173.4072	67.31469	-1.365171	6.76E-15	Down	1.48E-16
BOX15_Mlig014518g1	2892	19.37288	7.508751	-1.367394	0.006507	Down	0.001102
BOX15_Mlig014518g3	2892	19.37288	7.508751	-1.367394	0.006507	Down	0.001102
BOX15_Mlig011233g1	1160	40.81972	15.81757	-1.367738	7.44E-05	Down	6.90E-06
BOX15_Mlig025470g1	4309	57.29139	22.19503	-1.368082	6.98E-05	Down	6.44E-06
BOX15_Mlig024449g1	8976	1323.436	512.5576	-1.368503	9.52E-11	Down	3.18E-12
BOX15_Mlig000939g5	1824	484.7557	187.567	-1.369851	6.10E-08	Down	3.05E-09
BOX15_Mlig028779g3	1119	446.7112	172.7679	-1.370507	7.41E-22	Down	9.50E-24
BOX15_Mlig016716g1	6758	89.80567	34.71438	-1.371273	7.10E-05	Down	6.56E-06
BOX15_Mlig031972g1	2128	21.45678	8.289709	-1.37204	0.027941	Down	0.006284
BOX15_Mlig004470g1	16371	640.5544	247.2444	-1.373383	1.25E-19	Down	1.90E-21
BOX15_Mlig010314g3	3207	298.9726	115.2881	-1.37477	5.93E-14	Down	1.41E-15
BOX15_Mlig022908g3	2346	14.54408	5.604961	-1.375655	0.028318	Down	0.006388
BOX15_Mlig015343g3	1138	8061.958	3105.402	-1.37635	2.38E-36	Down	1.34E-38
BOX15_Mlig034535g4	2115	70.07715	26.98755	-1.37665	0.000104	Down	1.00E-05
BOX15_Mlig020858g1	1451	148.3827	57.10795	-1.377559	3.81E-09	Down	1.59E-10
BOX15_Mlig023375g3	3280	9.293863	3.576882	-1.377576	0.019668	Down	0.00412
BOX15_Mlig020105g2	1448	382.6096	146.8266	-1.38176	4.96E-08	Down	2.44E-09
BOX15_Mlig021702g1	1134	11.99975	4.604433	-1.381908	0.02856	Down	0.006456
BOX15_Mlig008438g1	4537	64.36227	24.69498	-1.381997	0.000152	Down	1.53E-05
BOX15_Mlig024177g1	2453	32.3848	12.41984	-1.38267	0.000816	Down	0.000101

BOX15_Mlig011189g1	854	172.9445	66.32542	-1.382675	1.13E-13	Down	2.76E-15
BOX15_Mlig006675g1	2263	142.4838	54.6355	-1.382888	1.09E-07	Down	5.68E-09
BOX15_Mlig013541g1	1368	3345.256	1282.411	-1.383258	1.03E-41	Down	4.45E-44
BOX15_Mlig024599g1	1420	1209.836	462.7548	-1.386492	3.03E-16	Down	5.93E-18
BOX15_Mlig030399g1	1536	243.1919	92.99348	-1.386894	1.30E-31	Down	9.41E-34
BOX15_Mlig020703g1	2129	717.7344	274.2894	-1.387751	8.62E-15	Down	1.91E-16
BOX15_Mlig010300g2	1925	155.8336	59.34373	-1.392839	1.95E-18	Down	3.24E-20
BOX15_Mlig013541g3	1369	1508.72	574.367	-1.39328	5.98E-51	Down	1.49E-53
BOX15_Mlig013541g4	1369	1508.72	574.367	-1.39328	5.98E-51	Down	1.49E-53
BOX15_Mlig034281g1	1857	494.1363	187.7214	-1.396316	4.86E-13	Down	1.28E-14
BOX15_Mlig031659g1	2483	87.32881	33.16957	-1.396598	3.54E-09	Down	1.46E-10
BOX15_Mlig030842g1	672	14.34854	5.448221	-1.397047	0.011541	Down	0.002171
BOX15_Mlig003078g1	1018	5.520382	2.09142	-1.400286	0.026343	Down	0.00587
BOX15_Mlig015343g2	1189	7959.882	3013.126	-1.401486	5.33E-104	Down	2.80E-107
BOX15_Mlig014811g1	1038	47.80613	18.09554	-1.401562	0.009778	Down	0.001784
BOX15_Mlig001593g2	8208	202.4779	76.58707	-1.402592	7.67E-05	Down	7.15E-06
BOX15_Mlig010364g6	1171	12.76348	4.8249	-1.403451	0.017214	Down	0.003505
BOX15_Mlig008555g1	2284	84.92799	32.10286	-1.403538	3.79E-10	Down	1.36E-11
BOX15_Mlig015825g1	1118	60.2088	22.7532	-1.403905	4.25E-06	Down	2.96E-07
BOX15_Mlig015754g3	1853	60.6679	22.8958	-1.40585	0.000149	Down	1.49E-05
BOX15_Mlig024225g2	2472	22.84561	8.620287	-1.406109	0.007606	Down	0.001324
BOX15_Mlig030039g1	1451	32.40023	12.22204	-1.406519	0.000136	Down	1.36E-05
BOX15_Mlig019386g2	3920	133.7545	50.41387	-1.407695	7.17E-06	Down	5.24E-07
BOX15_Mlig020770g1	1150	10.9625	4.130521	-1.408182	0.014958	Down	0.00296
BOX15_Mlig029297g1	6278	4627.026	1740.873	-1.410274	5.21E-37	Down	2.76E-39
BOX15_Mlig006672g2	1840	30.68124	11.53764	-1.411008	0.001735	Down	0.000238
BOX15_Mlig011092g2	969	155.5477	58.48193	-1.411294	1.55E-11	Down	4.76E-13
BOX15_Mlig004954g1	2337	534.7956	200.9153	-1.4124	1.81E-46	Down	5.97E-49
BOX15_Mlig010418g1	3693	167.0086	62.70236	-1.413331	1.57E-16	Down	2.98E-18
BOX15_Mlig010572g2	1424	17.90225	6.719852	-1.413639	0.024105	Down	0.00527
BOX15_Mlig030729g1	1502	35.50578	13.31253	-1.415269	6.71E-05	Down	6.15E-06
BOX15_Mlig018672g1	1037	872.5007	327.02	-1.415777	3.87E-23	Down	4.56E-25
BOX15_Mlig019641g1	7076	577.1874	216.0299	-1.417809	3.16E-25	Down	3.18E-27
BOX15_Mlig027029g1	2293	61.1796	22.87907	-1.419022	2.46E-07	Down	1.37E-08
BOX15_Mlig019375g6	3993	674.7329	252.2577	-1.419418	6.43E-26	Down	6.20E-28
BOX15_Mlig023772g1	5075	34.66269	12.95828	-1.41951	0.001724	Down	0.000237
BOX15_Mlig003076g3	1687	21.89754	8.184158	-1.419863	0.023448	Down	0.005101
BOX15_Mlig003076g2	1687	21.89754	8.184158	-1.419863	0.023448	Down	0.005101
BOX15_Mlig014143g1	6169	574.4465	214.6194	-1.420392	1.47E-46	Down	4.80E-49
BOX15_Mlig004233g1	1098	287.9566	107.5005	-1.421508	6.15E-07	Down	3.65E-08
BOX15_Mlig013733g2	2211	21.74854	8.118899	-1.421563	0.012206	Down	0.002322
BOX15_Mlig011092g1	1003	184.1348	68.71278	-1.422112	1.04E-11	Down	3.15E-13

BOX15_Mlig001841g2	3008	47.77156	17.80343	-1.423997	0.000354	Down	3.97E-05
BOX15_Mlig017367g2	5957	384.8003	143.3825	-1.424241	0.001666	Down	0.000228
BOX15_Mlig002945g1	1476	71.85732	26.75906	-1.425108	8.53E-08	Down	4.37E-09
BOX15_Mlig013297g2	6850	99.28514	36.96795	-1.425303	6.18E-12	Down	1.83E-13
BOX15_Mlig020439g2	1933	32.74527	12.19168	-1.425389	0.000803	Down	9.94E-05
BOX15_Mlig019953g1	2290	10.63072	3.957582	-1.425548	0.023332	Down	0.00507
BOX15_Mlig004670g1	1750	105.8506	39.36704	-1.426969	2.07E-05	Down	1.66E-06
BOX15_Mlig008470g1	1667	44.52233	16.5451	-1.428125	0.000306	Down	3.37E-05
BOX15_Mlig013346g2	1413	22.14934	8.228583	-1.428548	0.013908	Down	0.002713
BOX15_Mlig006318g1	1946	250.4632	92.96865	-1.429782	7.83E-15	Down	1.73E-16
BOX15_Mlig010259g1	750	72.03448	26.72321	-1.430594	1.79E-06	Down	1.16E-07
BOX15_Mlig031519g6	841	71.62597	26.57128	-1.430615	2.16E-06	Down	1.42E-07
BOX15_Mlig026705g1	1356	139.0816	51.54308	-1.432081	3.07E-06	Down	2.08E-07
BOX15_Mlig003945g2	4837	61.39098	22.74912	-1.432216	0.011995	Down	0.002275
BOX15_Mlig019427g1	2157	44.29397	16.41	-1.432535	0.00178	Down	0.000245
BOX15_Mlig026902g1	6146	7.139001	2.643859	-1.433077	0.021927	Down	0.004705
BOX15_Mlig019375g5	1057	251.0727	92.88631	-1.434567	2.90E-14	Down	6.73E-16
BOX15_Mlig014048g3	1635	18.86724	6.97314	-1.436003	0.020048	Down	0.004217
BOX15_Mlig010207g1	2076	61.87273	22.8593	-1.436522	1.41E-06	Down	8.96E-08
BOX15_Mlig018300g4	2518	54.24531	20.0289	-1.437415	5.80E-05	Down	5.22E-06
BOX15_Mlig006618g2	1314	50.26227	18.55734	-1.437486	5.75E-05	Down	5.17E-06
BOX15_Mlig020408g1	780	43.94024	16.22027	-1.437745	1.39E-05	Down	1.07E-06
BOX15_Mlig029988g2	842	1995.653	736.0293	-1.439026	3.13E-61	Down	5.46E-64
BOX15_Mlig028352g1	4090	218.4947	80.54289	-1.439769	7.09E-12	Down	2.11E-13
BOX15_Mlig007435g1	2141	1768.639	651.6162	-1.440545	8.48E-18	Down	1.47E-19
BOX15_Mlig032774g1	1504	45.35912	16.71157	-1.440546	8.88E-05	Down	8.41E-06
BOX15_Mlig022393g1	1851	1120.227	412.1398	-1.442586	9.59E-17	Down	1.78E-18
BOX15_Mlig010523g1	1579	78.18775	28.70197	-1.445793	8.45E-08	Down	4.33E-09
BOX15_Mlig019717g2	4707	2253.789	825.8787	-1.448351	1.93E-21	Down	2.55E-23
BOX15_Mlig021791g2	1488	3430.503	1255.462	-1.450202	0.015727	Down	0.003144
BOX15_Mlig001054g1	2666	17.59503	6.436809	-1.45075	0.012233	Down	0.002328
BOX15_Mlig007477g1	1021	40.28205	14.694	-1.45491	0.000146	Down	1.46E-05
BOX15_Mlig023434g3	823	98.69555	35.97278	-1.45608	1.33E-12	Down	3.68E-14
BOX15_Mlig001415g2	895	154.7592	56.39058	-1.456499	1.80E-06	Down	1.16E-07
BOX15_Mlig019508g1	6025	190.9774	69.57605	-1.456739	9.18E-07	Down	5.64E-08
BOX15_Mlig027208g1	2028	105.0034	38.20614	-1.458559	1.05E-09	Down	4.01E-11
BOX15_Mlig026072g2	1223	270.0037	98.16853	-1.459647	0.006368	Down	0.001076
BOX15_Mlig018578g1	1629	35.41992	12.87605	-1.459871	6.03E-05	Down	5.46E-06
BOX15_Mlig021572g1	13372	778.3477	282.6835	-1.461227	0.000337	Down	3.74E-05
BOX15_Mlig032329g1	2520	19.99246	7.258197	-1.461773	0.018305	Down	0.003777
BOX15_Mlig025252g1	4780	36.48948	13.24379	-1.462165	5.36E-05	Down	4.79E-06
BOX15_Mlig027173g3	854	32.78515	11.8967	-1.462481	0.002307	Down	0.00033

BOX15_Mlig021791g1	1489	4302.823	1559.485	-1.464213	0.015674	Down	0.00313
BOX15_Mlig010468g1	14026	12.18709	4.416496	-1.46438	0.016665	Down	0.00337
BOX15_Mlig001718g3	1108	199.0427	72.0543	-1.465922	2.94E-11	Down	9.27E-13
BOX15_Mlig020503g2	3173	34.15616	12.3483	-1.467833	0.008155	Down	0.001437
BOX15_Mlig005939g1	890	62.19612	22.45951	-1.469498	0.00017	Down	1.74E-05
BOX15_Mlig028779g1	1147	678.945	245.1299	-1.469748	8.33E-26	Down	8.11E-28
BOX15_Mlig000583g1	1759	81.88905	29.48813	-1.473536	7.02E-09	Down	3.04E-10
BOX15_Mlig034294g1	4104	127.1332	45.75393	-1.474373	1.62E-14	Down	3.66E-16
BOX15_Mlig015825g3	1048	40.10355	14.41244	-1.476416	2.18E-05	Down	1.76E-06
BOX15_Mlig015343g1	1137	8330.422	2979.737	-1.483204	3.05E-66	Down	4.29E-69
BOX15_Mlig020858g2	1454	82.33796	29.43506	-1.484022	5.75E-05	Down	5.17E-06
BOX15_Mlig014142g2	592	5820.367	2080.505	-1.484176	4.08E-55	Down	8.74E-58
BOX15_Mlig019968g1	7851	246.67	88.1439	-1.484649	1.11E-09	Down	4.25E-11
BOX15_Mlig031477g1	2189	35.46306	12.67055	-1.484838	0.012708	Down	0.002437
BOX15_Mlig016239g2	2132	98.0095	35.01214	-1.485066	4.61E-05	Down	4.04E-06
BOX15_Mlig016317g1	2627	36.70933	13.10605	-1.485914	1.85E-05	Down	1.47E-06
BOX15_Mlig029566g1	1075	47.66242	16.99045	-1.488128	2.95E-05	Down	2.46E-06
BOX15_Mlig029566g2	1075	47.66242	16.99045	-1.488128	2.95E-05	Down	2.46E-06
BOX15_Mlig021334g1	2147	75.70751	26.95504	-1.489881	4.02E-09	Down	1.68E-10
BOX15_Mlig005025g1	988	11.41773	4.060959	-1.491384	0.012874	Down	0.002475
BOX15_Mlig014498g1	2869	101.6988	36.09102	-1.494591	1.85E-08	Down	8.46E-10
BOX15_Mlig003548g1	2443	47.67751	16.91435	-1.495061	0.000567	Down	6.70E-05
BOX15_Mlig033186g3	8649	1593.93	564.9687	-1.496345	1.21E-33	Down	7.98E-36
BOX15_Mlig016838g1	2021	187.6655	66.48058	-1.497158	3.58E-11	Down	1.14E-12
BOX15_Mlig006618g1	1296	72.8849	25.81643	-1.497331	6.85E-06	Down	4.97E-07
BOX15_Mlig008727g1	2049	368.5665	130.3772	-1.499233	5.86E-36	Down	3.32E-38
BOX15_Mlig002473g1	1461	5.271779	1.863588	-1.500207	0.011845	Down	0.002241
BOX15_Mlig002601g1	4647	78.86491	27.8742	-1.500453	4.87E-05	Down	4.29E-06
BOX15_Mlig033801g3	1317	34.47712	12.17897	-1.501247	4.63E-05	Down	4.05E-06
BOX15_Mlig006324g1	2721	62.90525	22.21962	-1.501346	0.00356	Down	0.000547
BOX15_Mlig029592g2	765	184.8406	65.28061	-1.501555	5.24E-21	Down	7.10E-23
BOX15_Mlig003877g2	470	126.8718	44.72757	-1.504135	2.14E-16	Down	4.08E-18
BOX15_Mlig003877g3	470	126.8718	44.72757	-1.504135	2.14E-16	Down	4.08E-18
BOX15_Mlig003175g1	13257	65.88109	23.1783	-1.50709	1.24E-06	Down	7.76E-08
BOX15_Mlig024391g1	1201	127.0834	44.66647	-1.508512	4.56E-11	Down	1.47E-12
BOX15_Mlig024376g1	1288	25.17142	8.84166	-1.509397	0.00205	Down	0.000288
BOX15_Mlig028686g2	1000	40.78106	14.32213	-1.509653	3.68E-05	Down	3.15E-06
BOX15_Mlig007878g2	1976	33.70916	11.82323	-1.511516	0.000771	Down	9.47E-05
BOX15_Mlig006956g1	912	472.3738	165.2946	-1.514889	2.42E-14	Down	5.57E-16
BOX15_Mlig000187g2	11649	4088.397	1430.429	-1.515087	2.00E-09	Down	7.97E-11
BOX15_Mlig021791g3	1482	3738.524	1307.063	-1.51614	0.010263	Down	0.00189
BOX15_Mlig006763g1	2021	25.48287	8.889702	-1.519321	0.012657	Down	0.002425

BOX15_Mlig015143g2	2541	116.5441	40.64006	-1.519902	0.000109	Down	1.06E-05
BOX15_Mlig002175g3	2120	40.6129	14.15506	-1.52062	1.03E-05	Down	7.82E-07
BOX15_Mlig017210g2	586	396.7994	137.9451	-1.524315	4.03E-29	Down	3.32E-31
BOX15_Mlig030975g1	2542	1449.109	503.6477	-1.52468	2.58E-16	Down	4.99E-18
BOX15_Mlig016142g2	1145	261.0637	90.66001	-1.525864	6.02E-11	Down	1.96E-12
BOX15_Mlig019386g1	3918	314.5969	109.1942	-1.526608	1.95E-15	Down	4.10E-17
BOX15_Mlig020349g2	1033	143.8026	49.84481	-1.528574	7.82E-10	Down	2.93E-11
BOX15_Mlig015876g1	2585	17.30247	5.993228	-1.529573	0.013305	Down	0.002573
BOX15_Mlig010463g1	861	27.26809	9.438599	-1.530569	0.003139	Down	0.000471
BOX15_Mlig018460g2	2143	240.8881	83.34696	-1.531162	1.95E-12	Down	5.50E-14
BOX15_Mlig014647g1	4211	239.8919	82.99818	-1.531233	2.68E-10	Down	9.39E-12
BOX15_Mlig014701g2	1525	82.45348	28.52667	-1.531269	2.80E-10	Down	9.85E-12
BOX15_Mlig026058g2	2885	579.2637	200.3637	-1.531599	3.06E-17	Down	5.50E-19
BOX15_Mlig020420g1	462	11.621	4.010267	-1.534964	0.013206	Down	0.00255
BOX15_Mlig005298g2	427	243.0904	83.74186	-1.537472	6.41E-17	Down	1.17E-18
BOX15_Mlig022705g1	1104	3249.746	1118.151	-1.539212	3.26E-104	Down	1.64E-107
BOX15_Mlig001674g1	1324	39.57777	13.60447	-1.54061	0.000245	Down	2.62E-05
BOX15_Mlig018343g1	6083	142.7366	49.02128	-1.541875	1.51E-12	Down	4.21E-14
BOX15_Mlig005298g3	422	268.7404	92.26838	-1.542305	1.57E-09	Down	6.17E-11
BOX15_Mlig015496g1	673	1795.846	616.3073	-1.542942	6.54E-19	Down	1.04E-20
BOX15_Mlig016672g1	1129	27.34456	9.382639	-1.543188	0.000208	Down	2.18E-05
BOX15_Mlig009731g3	1888	22.76194	7.803257	-1.544475	0.00141	Down	0.000189
BOX15_Mlig023467g2	1689	175.9205	60.24777	-1.545944	4.44E-13	Down	1.16E-14
BOX15_Mlig011447g1	2224	40.3975	13.81185	-1.54836	0.001135	Down	0.000148
BOX15_Mlig009332g1	2171	789.8434	269.6313	-1.550579	3.65E-32	Down	2.55E-34
BOX15_Mlig031046g2	2876	29.19742	9.961642	-1.551385	0.011823	Down	0.002235
BOX15_Mlig023460g3	2337	32.19131	10.97664	-1.552234	0.009926	Down	0.001816
BOX15_Mlig002519g1	2214	271.9386	92.71667	-1.55238	1.36E-09	Down	5.28E-11
BOX15_Mlig002844g1	2627	108.9176	37.10804	-1.553433	8.10E-07	Down	4.92E-08
BOX15_Mlig012617g1	8898	305.3506	103.7377	-1.557527	3.49E-21	Down	4.66E-23
BOX15_Mlig019825g4	5513	95.21691	32.31388	-1.559064	0.011433	Down	0.002146
BOX15_Mlig014338g2	8044	9.191497	3.118071	-1.559646	0.011521	Down	0.002166
BOX15_Mlig013541g2	1373	1346.856	454.7728	-1.566378	4.49E-35	Down	2.71E-37
BOX15_Mlig009111g3	4406	26.74248	9.021693	-1.567663	0.004018	Down	0.00063
BOX15_Mlig018025g2	1951	46.08334	15.54588	-1.567713	0.000139	Down	1.39E-05
BOX15_Mlig023461g1	2208	1240.715	417.3884	-1.571709	1.26E-49	Down	3.47E-52
BOX15_Mlig024225g1	2244	57.19232	19.20947	-1.574004	0.000362	Down	4.07E-05
BOX15_Mlig019085g2	2709	74.2464	24.91076	-1.575552	5.18E-09	Down	2.20E-10
BOX15_Mlig024756g1	1962	78.53085	26.29421	-1.578514	3.38E-05	Down	2.86E-06
BOX15_Mlig029030g2	743	117.7085	39.40261	-1.578856	6.70E-08	Down	3.36E-09
BOX15_Mlig018460g1	2147	214.8474	71.90411	-1.579166	4.41E-24	Down	4.86E-26
BOX15_Mlig012279g1	987	70.56503	23.61144	-1.579468	2.57E-09	Down	1.04E-10

BOX15_Mlig023623g1	2094	41.51762	13.8854	-1.580155	0.009619	Down	0.001749
BOX15_Mlig032184g2	2319	148.3213	49.60167	-1.580265	1.44E-12	Down	3.99E-14
BOX15_Mlig028352g3	4117	202.7574	67.71468	-1.582214	1.35E-14	Down	3.03E-16
BOX15_Mlig016442g2	6450	76.08753	25.39488	-1.583123	1.45E-08	Down	6.55E-10
BOX15_Mlig011086g3	724	162.5391	54.24308	-1.583276	4.37E-20	Down	6.43E-22
BOX15_Mlig002686g1	989	11.1117	3.705603	-1.584299	0.008168	Down	0.00144
BOX15_Mlig018597g1	841	36.59696	12.18762	-1.586307	6.86E-06	Down	4.99E-07
BOX15_Mlig003076g1	1605	97.24052	32.2007	-1.594466	2.80E-06	Down	1.89E-07
BOX15_Mlig017261g2	7460	113.8188	37.68174	-1.594801	3.12E-05	Down	2.61E-06
BOX15_Mlig025507g2	1726	13.53688	4.478591	-1.595778	0.005067	Down	0.000824
BOX15_Mlig023332g1	1017	27.13548	8.97731	-1.595825	0.000107	Down	1.03E-05
BOX15_Mlig016089g2	691	349.98	115.3572	-1.601165	1.22E-29	Down	9.78E-32
BOX15_Mlig018040g2	709	21.94555	7.232754	-1.601311	0.000838	Down	0.000104
BOX15_Mlig033612g2	2883	110.1935	36.26007	-1.603586	0.000866	Down	0.000108
BOX15_Mlig025018g1	6934	325.6691	107.0313	-1.605374	1.26E-15	Down	2.59E-17
BOX15_Mlig030652g2	1544	33.49499	11.00165	-1.606225	0.000803	Down	9.95E-05
BOX15_Mlig002592g2	3072	95.08694	31.17881	-1.608681	0.00155	Down	0.00021
BOX15_Mlig029189g1	1433	33.85235	11.07973	-1.611333	0.000745	Down	9.11E-05
BOX15_Mlig024730g1	2399	68.68548	22.47869	-1.611447	1.11E-06	Down	6.91E-08
BOX15_Mlig020712g1	1715	53.03005	17.31373	-1.614894	2.16E-06	Down	1.42E-07
BOX15_Mlig004589g2	3318	85.36464	27.85642	-1.615629	6.16E-06	Down	4.44E-07
BOX15_Mlig027173g1	851	19.11838	6.230376	-1.617569	0.005842	Down	0.00097
BOX15_Mlig032487g2	2169	1730.334	562.8873	-1.620133	0.000738	Down	9.01E-05
BOX15_Mlig001841g3	3011	91.49363	29.69733	-1.623338	8.49E-06	Down	6.30E-07
BOX15_Mlig009645g3	2763	68.47704	22.19922	-1.625111	3.45E-05	Down	2.92E-06
BOX15_Mlig013863g1	822	1233.356	399.5983	-1.625966	1.30E-36	Down	7.18E-39
BOX15_Mlig011876g1	1430	88.59753	28.67918	-1.627263	1.62E-05	Down	1.28E-06
BOX15_Mlig020382g1	2918	18.22631	5.895638	-1.628303	0.002492	Down	0.00036
BOX15_Mlig033863g1	1488	45.01137	14.55325	-1.628948	0.000202	Down	2.11E-05
BOX15_Mlig032522g1	1462	102.8549	33.24693	-1.629317	1.99E-13	Down	5.00E-15
BOX15_Mlig030454g1	992	22.19215	7.169195	-1.630166	0.006201	Down	0.001042
BOX15_Mlig020665g1	5987	1672.903	540.278	-1.63058	2.25E-27	Down	2.06E-29
BOX15_Mlig010873g2	945	2058.294	660.5642	-1.639678	5.85E-40	Down	2.77E-42
BOX15_Mlig011372g1	1504	122.1782	39.1766	-1.640922	4.57E-08	Down	2.23E-09
BOX15_Mlig025292g4	798	521.7575	167.0889	-1.642764	3.26E-13	Down	8.37E-15
BOX15_Mlig025292g2	798	521.7575	167.0889	-1.642764	3.26E-13	Down	8.37E-15
BOX15_Mlig012933g1	812	44.97186	14.30613	-1.652389	0.000199	Down	2.07E-05
BOX15_Mlig027995g1	4974	181.892	57.80099	-1.653916	3.99E-06	Down	2.76E-07
BOX15_Mlig004855g1	4027	39.32789	12.48299	-1.655589	1.30E-05	Down	1.00E-06
BOX15_Mlig004418g1	1965	23.63306	7.485125	-1.658708	0.005861	Down	0.000975
BOX15_Mlig007447g1	1810	878.2934	277.8023	-1.660644	3.30E-27	Down	3.03E-29
BOX15_Mlig014353g1	1058	4269.656	1350.083	-1.661072	1.44E-52	Down	3.47E-55

BOX15_Mlig026687g2	721	9.486676	2.99948	-1.66119	0.005964	Down	0.000994
BOX15_Mlig000012g2	5685	66.82676	21.08487	-1.664218	8.78E-05	Down	8.31E-06
BOX15_Mlig013281g3	1594	20.39578	6.4263	-1.666211	0.004528	Down	0.000723
BOX15_Mlig015496g2	719	520.7562	163.7984	-1.668687	2.93E-31	Down	2.16E-33
BOX15_Mlig000356g2	4404	78.49576	24.66952	-1.669885	6.67E-05	Down	6.12E-06
BOX15_Mlig019691g1	2786	265.4446	83.34234	-1.671289	4.78E-22	Down	6.04E-24
BOX15_Mlig031704g1	3434	95.09968	29.85698	-1.671372	2.19E-06	Down	1.44E-07
BOX15_Mlig020221g3	530	4.838287	1.517825	-1.672491	0.00506	Down	0.000822
BOX15_Mlig028817g1	4240	291.9579	91.53776	-1.673321	5.71E-05	Down	5.12E-06
BOX15_Mlig027468g1	2502	27.54259	8.614727	-1.676787	0.00194	Down	0.000271
BOX15_Mlig025897g2	1372	51.04101	15.95725	-1.677445	3.18E-08	Down	1.51E-09
BOX15_Mlig029030g1	762	314.2102	98.19528	-1.678005	1.40E-19	Down	2.14E-21
BOX15_Mlig031600g1	3584	47.39148	14.80693	-1.678355	8.61E-06	Down	6.39E-07
BOX15_Mlig005367g15	1725	30.60669	9.546716	-1.68077	0.002663	Down	0.00039
BOX15_Mlig000759g2	3537	116.9545	36.39237	-1.684239	8.37E-09	Down	3.66E-10
BOX15_Mlig017210g1	582	434.1339	135.0545	-1.684598	9.83E-23	Down	1.20E-24
BOX15_Mlig000828g1	1539	41.99826	13.05409	-1.685828	1.02E-05	Down	7.72E-07
BOX15_Mlig023028g3	2022	53.89885	16.75052	-1.686049	0.000931	Down	0.000117
BOX15_Mlig002227g1	922	34.8685	10.83317	-1.686469	4.63E-06	Down	3.25E-07
BOX15_Mlig032417g1	1333	18.45637	5.723949	-1.689036	0.00118	Down	0.000154
BOX15_Mlig014210g3	1350	1248.469	387.0163	-1.689693	3.73E-40	Down	1.74E-42
BOX15_Mlig027660g1	1652	334.5853	103.7169	-1.689723	1.05E-42	Down	4.25E-45
BOX15_Mlig015143g3	2531	163.789	50.76969	-1.689799	6.79E-06	Down	4.93E-07
BOX15_Mlig024524g2	567	157.4588	48.74516	-1.691643	7.41E-10	Down	2.78E-11
BOX15_Mlig024524g1	567	157.4588	48.74516	-1.691643	7.41E-10	Down	2.78E-11
BOX15_Mlig003570g1	1860	65.85788	20.33196	-1.695606	1.78E-06	Down	1.15E-07
BOX15_Mlig009609g1	1003	74.7293	23.00985	-1.699422	1.38E-09	Down	5.36E-11
BOX15_Mlig005966g2	1064	56.01542	17.24292	-1.69982	0.000125	Down	1.23E-05
BOX15_Mlig001180g1	2607	219.4696	67.54064	-1.700193	5.62E-10	Down	2.07E-11
BOX15_Mlig013242g1	2333	2721.856	836.5903	-1.701998	7.21E-30	Down	5.71E-32
BOX15_Mlig000828g5	2570	89.32359	27.45224	-1.702117	1.00E-09	Down	3.81E-11
BOX15_Mlig025897g1	1376	61.48716	18.80113	-1.709466	5.25E-05	Down	4.68E-06
BOX15_Mlig002954g3	1877	654.5957	199.531	-1.713991	5.46E-12	Down	1.61E-13
BOX15_Mlig022284g1	831	1622.902	494.2827	-1.715167	4.20E-62	Down	6.79E-65
BOX15_Mlig022482g1	1922	42.35848	12.89497	-1.715843	0.000183	Down	1.88E-05
BOX15_Mlig012903g5	1140	284.6358	86.59967	-1.716683	0.000617	Down	7.36E-05
BOX15_Mlig015594g1	6656	4806.509	1458.639	-1.720366	9.89E-18	Down	1.73E-19
BOX15_Mlig010466g2	1059	13.92837	4.219206	-1.722983	0.003393	Down	0.000517
BOX15_Mlig007464g1	3369	258.5421	78.28645	-1.723565	3.33E-09	Down	1.37E-10
BOX15_Mlig007732g1	2341	171.1677	51.59265	-1.730173	6.62E-09	Down	2.85E-10
BOX15_Mlig014210g1	1221	839.7372	252.9829	-1.730898	1.93E-45	Down	6.82E-48
BOX15_Mlig026357g1	2238	88.40823	26.62212	-1.731555	1.02E-12	Down	2.78E-14

BOX15_Mlig023412g1	1357	19.83052	5.966723	-1.732712	0.003337	Down	0.000507
BOX15_Mlig020186g1	4660	755.0428	227.1001	-1.73323	4.62E-65	Down	6.79E-68
BOX15_Mlig001054g2	2926	88.92458	26.63942	-1.739019	1.85E-08	Down	8.49E-10
BOX15_Mlig030794g1	2860	194.2645	58.15311	-1.740094	8.91E-14	Down	2.15E-15
BOX15_Mlig007110g1	1732	123.406	36.91368	-1.741185	2.99E-20	Down	4.30E-22
BOX15_Mlig010873g1	979	3378.776	1009.259	-1.743204	1.17E-30	Down	8.97E-33
BOX15_Mlig028525g1	6595	286.1925	85.38339	-1.744959	1.23E-16	Down	2.32E-18
BOX15_Mlig024961g1	4086	71.75193	21.38591	-1.746357	0.000778	Down	9.58E-05
BOX15_Mlig023285g1	417	12.66103	3.769342	-1.74801	0.003079	Down	0.000461
BOX15_Mlig023467g1	1686	270.4595	80.4481	-1.749283	3.69E-08	Down	1.77E-09
BOX15_Mlig023467g3	1686	270.4595	80.4481	-1.749283	3.69E-08	Down	1.77E-09
BOX15_Mlig011876g2	1591	171.8306	50.97435	-1.753144	3.31E-22	Down	4.13E-24
BOX15_Mlig019035g1	3388	85.20519	25.21041	-1.756922	1.58E-06	Down	1.01E-07
BOX15_Mlig029973g1	7581	406.7475	120.0255	-1.760793	1.28E-26	Down	1.20E-28
BOX15_Mlig033500g1	1771	156.2521	46.07562	-1.7618	3.99E-25	Down	4.05E-27
BOX15_Mlig025189g1	1755	1180.408	347.9954	-1.762145	8.19E-37	Down	4.49E-39
BOX15_Mlig033186g4	3100	1947.649	572.8895	-1.765405	8.70E-27	Down	8.11E-29
BOX15_Mlig018275g1	2188	73.49561	21.57245	-1.768468	3.68E-09	Down	1.53E-10
BOX15_Mlig001459g3	1957	21.62389	6.337813	-1.770569	0.002511	Down	0.000364
BOX15_Mlig029463g1	2336	77.83917	22.70189	-1.777684	6.25E-13	Down	1.67E-14
BOX15_Mlig010544g1	763	20.88053	6.073224	-1.781624	0.00123	Down	0.000162
BOX15_Mlig016685g2	1811	36.01246	10.46993	-1.782245	0.002496	Down	0.000361
BOX15_Mlig020710g1	5825	65.28378	18.93038	-1.786022	1.11E-06	Down	6.88E-08
BOX15_Mlig019085g1	2542	93.60709	27.08493	-1.789127	2.89E-09	Down	1.18E-10
BOX15_Mlig007208g1	1482	203.3471	58.81288	-1.78974	4.46E-07	Down	2.58E-08
BOX15_Mlig029420g1	789	631.3676	182.5331	-1.790322	5.47E-17	Down	9.96E-19
BOX15_Mlig029944g1	6197	516.6365	149.183	-1.792067	4.35E-20	Down	6.39E-22
BOX15_Mlig017801g3	1567	21.0226	6.033639	-1.800841	0.002258	Down	0.000322
BOX15_Mlig001477g4	868	18502.49	5303.086	-1.802815	5.33E-37	Down	2.83E-39
BOX15_Mlig018641g2	870	46.25589	13.25238	-1.803386	6.91E-06	Down	5.02E-07
BOX15_Mlig032554g5	12427	7529.991	2147.667	-1.809878	2.59E-06	Down	1.73E-07
BOX15_Mlig006345g1	933	39.95722	11.31615	-1.820074	1.17E-06	Down	7.33E-08
BOX15_Mlig017656g3	1164	30.34073	8.589121	-1.820673	0.000236	Down	2.51E-05
BOX15_Mlig009533g2	2621	69.73464	19.73403	-1.82119	8.62E-12	Down	2.60E-13
BOX15_Mlig009533g1	2621	69.73464	19.73403	-1.82119	8.62E-12	Down	2.60E-13
BOX15_Mlig025292g3	804	1106.253	311.7012	-1.827446	1.77E-08	Down	8.06E-10
BOX15_Mlig033190g2	1905	66.54255	18.71874	-1.829794	2.65E-06	Down	1.77E-07
BOX15_Mlig023993g2	1684	15.77355	4.427053	-1.833089	0.001374	Down	0.000184
BOX15_Mlig010347g1	11318	1188.23	333.4596	-1.833231	1.24E-15	Down	2.54E-17
BOX15_Mlig030659g1	1597	73.14383	20.50724	-1.834603	1.01E-06	Down	6.27E-08
BOX15_Mlig003040g2	2438	26.00256	7.287288	-1.835199	9.89E-05	Down	9.47E-06
BOX15_Mlig009114g6	1583	109.365	30.5226	-1.841201	9.29E-09	Down	4.09E-10

BOX15_Mlig017900g2	1097	302.0468	84.20049	-1.842872	1.92E-20	Down	2.74E-22
BOX15_Mlig012886g1	332	13.95801	3.888611	-1.843766	0.001365	Down	0.000182
BOX15_Mlig001415g3	888	181.9564	50.45646	-1.850482	3.19E-20	Down	4.61E-22
BOX15_Mlig018813g3	2063	162.8304	45.07702	-1.852906	3.93E-08	Down	1.90E-09
BOX15_Mlig030729g2	1473	71.52665	19.7775	-1.854621	3.74E-11	Down	1.19E-12
BOX15_Mlig017006g2	2153	52.81365	14.50891	-1.863972	0.000193	Down	2.01E-05
BOX15_Mlig015791g4	2670	125.8738	34.41904	-1.870699	2.18E-08	Down	1.01E-09
BOX15_Mlig014299g2	2093	417.4076	113.8351	-1.874511	7.96E-17	Down	1.47E-18
BOX15_Mlig006672g1	1875	35.57253	9.688775	-1.876377	1.39E-05	Down	1.07E-06
BOX15_Mlig010893g2	2086	24.81876	6.752857	-1.877861	0.00159	Down	0.000216
BOX15_Mlig010463g2	949	63.93424	17.35842	-1.880953	5.01E-07	Down	2.93E-08
BOX15_Mlig005144g1	7132	169917	45827.54	-1.890543	9.45E-14	Down	2.29E-15
BOX15_Mlig017875g1	1619	34.8706	9.395852	-1.891915	1.57E-07	Down	8.39E-09
BOX15_Mlig002349g1	1430	439.7222	118.3154	-1.893955	3.23E-17	Down	5.82E-19
BOX15_Mlig027408g1	2700	346.0754	93.09254	-1.894349	5.16E-06	Down	3.66E-07
BOX15_Mlig026054g2	2335	231.3988	62.14152	-1.896752	6.30E-11	Down	2.06E-12
BOX15_Mlig004262g1	500	47.10391	12.64152	-1.897676	5.13E-08	Down	2.53E-09
BOX15_Mlig020270g1	928	20.0298	5.374866	-1.897847	0.000206	Down	2.15E-05
BOX15_Mlig022697g1	8363	309.1641	82.91657	-1.89864	1.65E-34	Down	1.03E-36
BOX15_Mlig026282g1	815	105.1188	28.05259	-1.905815	2.37E-16	Down	4.57E-18
BOX15_Mlig019637g4	1747	26.09298	6.957898	-1.906938	0.001076	Down	0.000139
BOX15_Mlig021970g1	1916	264.316	70.2867	-1.91094	2.76E-23	Down	3.22E-25
BOX15_Mlig028817g2	4230	264.4848	69.88507	-1.920128	0.000108	Down	1.05E-05
BOX15_Mlig024263g3	1937	108.5149	28.65996	-1.920785	8.80E-14	Down	2.13E-15
BOX15_Mlig014154g1	1304	58.43518	15.39616	-1.924267	0.000357	Down	4.00E-05
BOX15_Mlig004350g1	3538	215.6797	56.80946	-1.924687	2.11E-19	Down	3.25E-21
BOX15_Mlig029578g1	3796	190.4029	50.02799	-1.928248	2.34E-14	Down	5.36E-16
BOX15_Mlig028972g3	1282	4100.551	1077.402	-1.928261	6.42E-28	Down	5.70E-30
BOX15_Mlig020349g3	1018	121.9383	31.96092	-1.931771	3.75E-08	Down	1.81E-09
BOX15_Mlig026605g1	1772	52.09487	13.63932	-1.93337	0.000112	Down	1.09E-05
BOX15_Mlig025063g1	933	4322.383	1128.698	-1.937167	9.39E-48	Down	2.76E-50
BOX15_Mlig034205g1	1026	63.52266	16.58281	-1.937583	5.69E-06	Down	4.07E-07
BOX15_Mlig034366g1	3181	120.8883	31.53545	-1.938628	4.54E-16	Down	9.01E-18
BOX15_Mlig033295g1	2012	367.4543	95.42434	-1.945135	2.14E-16	Down	4.10E-18
BOX15_Mlig019214g1	2649	82.95327	21.52929	-1.945998	8.67E-05	Down	8.19E-06
BOX15_Mlig014353g3	1092	2505.872	646.6727	-1.954205	1.27E-33	Down	8.37E-36
BOX15_Mlig033186g2	8670	1083.543	279.5388	-1.954636	3.10E-45	Down	1.12E-47
BOX15_Mlig021934g1	1865	24.44674	6.289614	-1.958599	0.000896	Down	0.000112
BOX15_Mlig021339g3	1548	95.26775	24.50107	-1.959143	3.44E-08	Down	1.64E-09
BOX15_Mlig021339g4	1548	95.26775	24.50107	-1.959143	3.44E-08	Down	1.64E-09
BOX15_Mlig000828g2	3382	469.0691	120.5052	-1.960705	1.40E-20	Down	1.97E-22
BOX15_Mlig018446g1	1089	61.89811	15.8885	-1.961912	3.08E-11	Down	9.74E-13

BOX15_Mlig021177g3	5252	260.5292	66.73824	-1.96486	9.71E-06	Down	7.29E-07
BOX15_Mlig028041g3	3191	200.7344	51.29805	-1.968312	1.81E-24	Down	1.94E-26
BOX15_Mlig008976g1	1528	67.91551	17.3492	-1.968872	1.17E-10	Down	3.97E-12
BOX15_Mlig028972g1	1029	4720.111	1193.882	-1.98316	1.27E-61	Down	2.15E-64
BOX15_Mlig017980g1	2257	1085.576	274.5196	-1.983479	0.00024	Down	2.56E-05
BOX15_Mlig030850g1	4676	212.8181	53.72806	-1.985873	1.08E-20	Down	1.51E-22
BOX15_Mlig026431g3	2005	34.52228	8.711972	-1.986456	1.56E-05	Down	1.22E-06
BOX15_Mlig001184g3	2561	22.72854	5.733316	-1.987063	0.000645	Down	7.74E-05
BOX15_Mlig023499g2	1817	58.5728	14.71889	-1.992562	2.39E-10	Down	8.35E-12
BOX15_Mlig021488g2	1110	58.83506	14.76344	-1.994648	6.61E-09	Down	2.84E-10
BOX15_Mlig033799g1	1960	121.8479	30.46217	-1.99999	1.89E-20	Down	2.69E-22
BOX15_Mlig033036g1	1221	88.33869	22.06729	-2.001136	3.70E-08	Down	1.78E-09
BOX15_Mlig033036g2	1221	88.33869	22.06729	-2.001136	3.70E-08	Down	1.78E-09
BOX15_Mlig013626g2	1291	65.22525	16.24883	-2.005094	2.05E-07	Down	1.13E-08
BOX15_Mlig003756g1	3651	753.1805	186.9991	-2.009964	1.02E-31	Down	7.32E-34
BOX15_Mlig007058g1	881	4300.242	1064.391	-2.01439	1.23E-35	Down	7.17E-38
BOX15_Mlig023028g1	7239	33.56349	8.297717	-2.016106	0.000116	Down	1.13E-05
BOX15_Mlig020758g1	5338	1221.148	299.765	-2.026334	6.93E-37	Down	3.71E-39
BOX15_Mlig020400g1	528	7.040957	1.727336	-2.027223	0.000549	Down	6.46E-05
BOX15_Mlig026096g1	913	81.4997	19.9095	-2.033337	0.000477	Down	5.52E-05
BOX15_Mlig009131g2	1608	600.0265	145.8005	-2.041031	1.86E-09	Down	7.35E-11
BOX15_Mlig019825g2	5995	187.0251	45.34828	-2.044112	4.78E-05	Down	4.21E-06
BOX15_Mlig010561g1	3072	89.95483	21.80142	-2.044778	4.37E-09	Down	1.84E-10
BOX15_Mlig030687g1	1181	39.39396	9.525057	-2.048175	1.98E-05	Down	1.58E-06
BOX15_Mlig008283g1	960	9532.335	2297.194	-2.052957	8.70E-96	Down	6.02E-99
BOX15_Mlig005629g1	1850	301.2076	72.31968	-2.058298	7.43E-34	Down	4.85E-36
BOX15_Mlig024693g3	817	63.85667	15.30603	-2.060737	4.37E-08	Down	2.13E-09
BOX15_Mlig018300g3	2518	53.43518	12.71858	-2.070852	4.17E-07	Down	2.40E-08
BOX15_Mlig000012g1	5643	61.53592	14.58848	-2.076599	5.41E-09	Down	2.31E-10
BOX15_Mlig033824g1	1093	1007.196	238.3504	-2.079188	7.67E-44	Down	2.98E-46
BOX15_Mlig026804g3	8332	96.97009	22.91035	-2.08154	7.07E-07	Down	4.24E-08
BOX15_Mlig013188g1	887	51.7361	12.2216	-2.081738	6.78E-11	Down	2.22E-12
BOX15_Mlig006077g1	1472	309.4404	72.9991	-2.083711	5.42E-13	Down	1.43E-14
BOX15_Mlig001601g1	1252	29.42877	6.912384	-2.089972	4.88E-05	Down	4.31E-06
BOX15_Mlig031396g2	6038	112.5364	26.29198	-2.097697	3.60E-23	Down	4.23E-25
BOX15_Mlig024693g1	776	83.07619	19.37727	-2.10007	5.48E-15	Down	1.19E-16
BOX15_Mlig009355g2	852	1826.899	425.4026	-2.102496	2.23E-68	Down	2.95E-71
BOX15_Mlig020697g1	608	13.64107	3.158089	-2.110833	0.000188	Down	1.95E-05
BOX15_Mlig020592g1	1285	26.01285	6.016816	-2.112152	0.000267	Down	2.88E-05
BOX15_Mlig020468g1	1874	74.13239	17.14605	-2.112228	2.87E-09	Down	1.17E-10
BOX15_Mlig016941g3	989	60.85674	14.06923	-2.112874	6.83E-05	Down	6.29E-06
BOX15_Mlig001296g1	2341	75.50455	17.34928	-2.121688	1.01E-09	Down	3.85E-11

BOX15_Mlig014587g1	1628	351.9997	80.81628	-2.122856	4.24E-19	Down	6.65E-21
BOX15_Mlig011086g1	745	87.52891	20.09148	-2.123176	1.40E-08	Down	6.34E-10
BOX15_Mlig024693g2	1633	49.55023	11.27535	-2.13572	2.63E-08	Down	1.24E-09
BOX15_Mlig031899g1	5015	48.81021	11.08273	-2.138869	8.33E-10	Down	3.14E-11
BOX15_Mlig019918g2	3822	41.20963	9.344829	-2.140741	0.000166	Down	1.69E-05
BOX15_Mlig032554g2	10010	22619.49	5076.765	-2.155585	4.87E-15	Down	1.06E-16
BOX15_Mlig034071g1	1113	1046.184	234.3103	-2.158644	3.19E-33	Down	2.16E-35
BOX15_Mlig012871g1	774	28.26803	6.317824	-2.161672	0.000173	Down	1.77E-05
BOX15_Mlig019825g3	5926	122.3283	27.30677	-2.163427	0.000189	Down	1.96E-05
BOX15_Mlig000828g6	3313	1254.981	279.6326	-2.166062	4.59E-35	Down	2.79E-37
BOX15_Mlig016746g3	1415	10.79337	2.396464	-2.171167	0.000174	Down	1.78E-05
BOX15_Mlig026054g1	2333	330.082	72.25542	-2.191647	3.02E-16	Down	5.90E-18
BOX15_Mlig030190g1	845	1146.526	250.3247	-2.195397	2.44E-63	Down	3.79E-66
BOX15_Mlig023577g1	1333	133.7536	29.0296	-2.203981	1.51E-07	Down	8.09E-09
BOX15_Mlig028972g2	1291	2890.158	626.4296	-2.205924	2.50E-33	Down	1.68E-35
BOX15_Mlig029317g2	1933	20.63928	4.434997	-2.218387	3.02E-05	Down	2.52E-06
BOX15_Mlig016613g3	1194	39.46377	8.390121	-2.233765	7.27E-05	Down	6.73E-06
BOX15_Mlig007464g2	3369	213.474	44.92261	-2.248546	5.78E-16	Down	1.16E-17
BOX15_Mlig021177g1	5236	84.72029	17.77993	-2.252458	5.29E-07	Down	3.10E-08
BOX15_Mlig012060g1	1201	403.5468	84.61503	-2.25375	3.44E-25	Down	3.48E-27
BOX15_Mlig017599g2	1066	1724.188	355.8679	-2.276503	4.86E-15	Down	1.05E-16
BOX15_Mlig018559g1	5561	45.80892	9.435134	-2.279514	7.16E-07	Down	4.31E-08
BOX15_Mlig025628g1	406	53.03842	10.71077	-2.307975	6.85E-12	Down	2.04E-13
BOX15_Mlig004059g1	1512	70.84493	14.29602	-2.309051	2.02E-13	Down	5.06E-15
BOX15_Mlig025998g3	2022	23.48081	4.718143	-2.315191	5.69E-05	Down	5.10E-06
BOX15_Mlig018025g1	1884	75.97252	15.2419	-2.317435	1.62E-09	Down	6.39E-11
BOX15_Mlig021922g1	1741	347.9403	69.27794	-2.328372	6.47E-29	Down	5.46E-31
BOX15_Mlig031645g1	4376	52.39222	10.42761	-2.328944	2.64E-12	Down	7.54E-14
BOX15_Mlig016239g1	2201	55.88623	11.10038	-2.331884	4.26E-09	Down	1.79E-10
BOX15_Mlig010572g1	1420	39.02537	7.666791	-2.347717	7.22E-09	Down	3.13E-10
BOX15_Mlig012092g3	1331	716.1826	140.1271	-2.353592	2.84E-13	Down	7.26E-15
BOX15_Mlig007058g3	635	190.1217	36.95041	-2.363261	6.28E-20	Down	9.37E-22
BOX15_Mlig007058g2	635	190.1217	36.95041	-2.363261	6.28E-20	Down	9.37E-22
BOX15_Mlig032554g6	1023	3285.567	632.1879	-2.377717	1.91E-14	Down	4.34E-16
BOX15_Mlig013400g1	800	150.767	28.94556	-2.380907	2.72E-06	Down	1.83E-07
BOX15_Mlig017599g1	1075	2011.207	382.3024	-2.395276	2.80E-27	Down	2.56E-29
BOX15_Mlig016613g2	1558	188.4278	35.63484	-2.402651	3.12E-07	Down	1.76E-08
BOX15_Mlig016613g4	1197	127.2488	23.99979	-2.406559	7.08E-10	Down	2.65E-11
BOX15_Mlig033986g1	766	99.72366	18.78933	-2.408022	4.48E-19	Down	7.05E-21
BOX15_Mlig028839g2	1096	379.4311	71.05792	-2.41677	9.83E-19	Down	1.60E-20
BOX15_Mlig029920g1	2225	134.3324	25.1331	-2.418146	2.35E-13	Down	5.96E-15
BOX15_Mlig016941g2	981	61.37785	11.32508	-2.438197	1.34E-06	Down	8.46E-08

BOX15_Mlig009131g1	1631	1107.904	202.8609	-2.44927	6.25E-47	Down	2.00E-49
BOX15_Mlig015976g1	1618	588.9458	105.1014	-2.486353	1.23E-10	Down	4.16E-12
BOX15_Mlig007593g1	1723	87.25295	15.52622	-2.490497	5.62E-21	Down	7.65E-23
BOX15_Mlig010166g1	2534	331.7196	58.60717	-2.500815	4.69E-24	Down	5.18E-26
BOX15_Mlig021177g2	5211	279.1383	48.50358	-2.524817	4.62E-37	Down	2.43E-39
BOX15_Mlig005681g1	966	68.89336	11.91941	-2.531052	2.80E-09	Down	1.14E-10
BOX15_Mlig016613g1	1551	180.2765	31.0626	-2.536961	3.85E-22	Down	4.81E-24
BOX15_Mlig017656g1	1495	69.80414	11.81281	-2.562961	2.48E-08	Down	1.16E-09
BOX15_Mlig029598g3	760	20.61217	3.478724	-2.566866	2.86E-06	Down	1.93E-07
BOX15_Mlig026423g2	1131	15.51684	2.611579	-2.570841	5.09E-06	Down	3.60E-07
BOX15_Mlig026256g1	509	71.61854	11.90261	-2.589056	6.86E-19	Down	1.10E-20
BOX15_Mlig002911g1	3958	657.6113	108.8986	-2.594249	1.09E-10	Down	3.66E-12
BOX15_Mlig022283g1	926	2540.024	417.3758	-2.605423	1.51E-185	Down	6.34E-190
BOX15_Mlig012958g1	1771	58.63544	9.557995	-2.616993	9.13E-13	Down	2.47E-14
BOX15_Mlig025614g1	4998	31.80908	5.171771	-2.620708	1.38E-08	Down	6.22E-10
BOX15_Mlig001055g1	2668	41.69312	6.718878	-2.633517	1.81E-07	Down	9.81E-09
BOX15_Mlig016941g1	1159	305.8618	48.54166	-2.655585	1.26E-18	Down	2.06E-20
BOX15_Mlig008030g1	1590	45.15539	7.025601	-2.684205	2.40E-12	Down	6.83E-14
BOX15_Mlig025175g1	1398	11.71655	1.79916	-2.703152	1.37E-06	Down	8.62E-08
BOX15_Mlig027252g1	1544	160.2862	24.52454	-2.708353	6.93E-37	Down	3.73E-39
BOX15_Mlig013626g1	1280	182.1396	27.28113	-2.739069	5.70E-30	Down	4.47E-32
BOX15_Mlig002051g1	13697	121.1174	17.51089	-2.790081	1.09E-17	Down	1.91E-19
BOX15_Mlig012849g1	4532	12.94221	1.85706	-2.800991	4.57E-07	Down	2.65E-08
BOX15_Mlig008746g5	7210	18200.6	2611.029	-2.801296	3.43E-32	Down	2.39E-34
BOX15_Mlig020370g1	957	1243.875	175.9237	-2.82182	4.28E-47	Down	1.34E-49
BOX15_Mlig028839g1	1154	267.3339	37.06087	-2.850674	4.00E-20	Down	5.85E-22
BOX15_Mlig018655g2	533	13.63627	1.882296	-2.856884	2.36E-07	Down	1.31E-08
BOX15_Mlig002911g2	2249	2279.278	287.2625	-2.988135	2.34E-13	Down	5.93E-15
BOX15_Mlig008746g4	7026	11901.37	1499.772	-2.988313	4.23E-33	Down	2.88E-35
BOX15_Mlig002816g1	9677	132.6355	16.02801	-3.0488	1.14E-20	Down	1.60E-22
BOX15_Mlig002252g3	663	574.2603	68.44789	-3.068627	2.97E-08	Down	1.41E-09
BOX15_Mlig025897g4	1373	18.93106	2.050744	-3.206536	2.50E-09	Down	1.01E-10
BOX15_Mlig020052g1	443	64.04888	6.836755	-3.22779	1.68E-20	Down	2.38E-22
BOX15_Mlig015346g1	5442	86.1447	9.150528	-3.234835	4.19E-11	Down	1.34E-12
BOX15_Mlig002911g3	2949	3994.907	395.4644	-3.336542	4.42E-22	Down	5.55E-24
BOX15_Mlig004729g1	3046	41.23626	3.847498	-3.421921	2.06E-10	Down	7.15E-12
BOX15_Mlig008746g1	7017	7014.726	649.8842	-3.432132	4.86E-24	Down	5.37E-26
BOX15_Mlig011175g3	1679	27.11035	2.410476	-3.491454	3.75E-11	Down	1.20E-12
BOX15_Mlig029288g1	1643	33.53765	2.601442	-3.688398	4.80E-15	Down	1.04E-16
BOX15_Mlig000052g2	1746	32.999	2.324974	-3.827136	7.63E-14	Down	1.84E-15
BOX15_Mlig014754g4	1306	128.5602	3.920295	-5.035338	7.48E-27	Down	6.94E-29